INDC(ARG)-9/G

CNEA NT - 5/82

Progress Report

1980 - 1981

Department of Physics

Comisión Nacional
de Energía Atómica

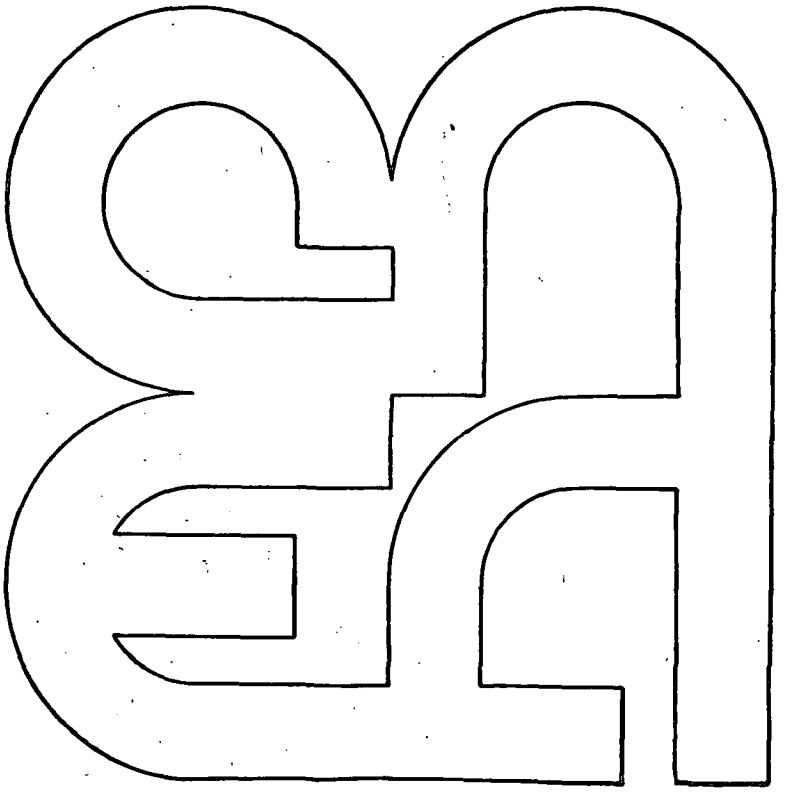

Dirección de
Investigación y Desarrollo

Gerencia de
Investigaciones

Buenos Aires - Argentina
1982

CNEA NT - 5/82

Progress Report

1980 - 1981

Department of Physics

Comisión Nacional
de Energía Atómica

Dirección de
Investigación y Desarrollo

Gerencia de
Investigaciones

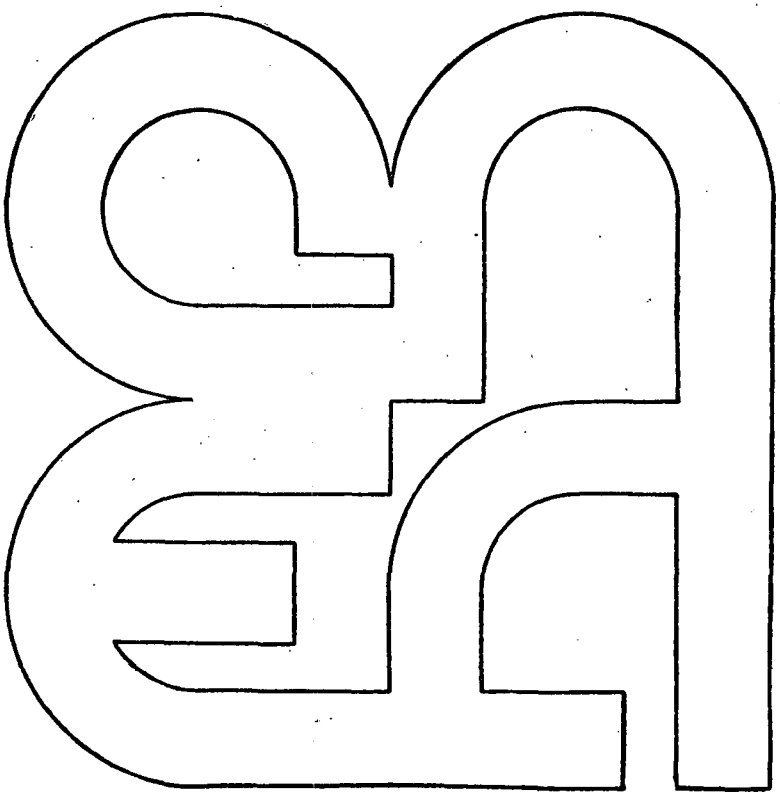

Buenos Aires - Argentina
1982

INTRODUCTION

The period covered by this report is outstanding because of the spectacular progress made in the construction of the TANDAR facility. In January 1980, the excavation work had just started; by December 1981 the column structure was standing in the interior of the 35 m high pressure vessel and the inyector was being readied at its definitive location 56 m above ground.

During 1980 there was a vigorous local drive to meet the schedule for the column installation as agreed with NEC. The main and service towers reached the top at 73 m at a fast pace by using nonstop sliding forms. Previously the pressure tank had been finished and tested to a maximum 18 kg/cm^2 pressure in record time. Shortly afterwards the two spherical storage vessels for the SF_6 gas were completed.

At present, most of the work is being geared to complete the gas handling system and start the high voltage tests.

On the ocassion of the "Third International Conference on Electrostatic Accelerator Technology", we were awarded the distinction of being selected as hosts for the next conference in 1985. We hope that our accelerator will be well ahead in the running stage by then. It is also possible that the adjacent office building originally planned will also be ready for the conference.

The training program which was initiated in 1977 with the purpose of supplementing adequately the research staff needed for an efficient use of the TANDAR is near completion now. This program has involved a dozen young physicists who have finished or are finshing their theses. Most of them have had the opportunity to get experience abroad. Now that the program is almost completed we can be very satisfied with the results. In this connection we wish to acknowledge the collaboration

of those groups abroad which have been willing to host the young graduates in Oxford, München, Göttingen, Heidelberg, Stony Brook, Oak Ridge, Seattle, Berkeley and Rehovot. We keep high expectations on the returns of this program which should start paying off as soon as the first beam becomes usable.

Another aspect of general character which is worth mentioning is that both in 1980 and 1981 the series of nuclear physics workshops, started in 1978, continued with an enlarged audience and distinguished speakers. B.Bayman, S.Bjørnholm, D.Mc. Hyder, M.Macfarlane and F.Stephens contributed with excellent talks.

Within the program for cooperative research managed by the Argentine National Research Council and the U.S. National Science Foundation successful projects were carried out in collaboration with groups of Brookhaven, Ames and Tucson. Other joint efforts were also undertaken with scientists from Rio de Janeiro, Sao Paulo, Santiago de Chile, Tübingen, Washington D.C., Grenoble, Berkeley, Paris, Strassbourg and local universities in Buenos Aires, La Plata and Tandil.

A happy event was the prize awarded by the Academy of Medicine to members of the crystallography group for their work with a medical team dealing with the identification of calcifications of costal cartilage samples in patients with idiopathic familial chondrocalcinosis.

The research output constitutes the main topic of this report and is summarized in the following pages. In general, the activity as a whole has steadily grown in spite of the fact that secondary (but necessary) chores have also multiplied and makes us feel frequently distressed. Adaptation to the new responsabilities ahead is the key. The years of running the old Synchrocyclotron and Cockcroft-Walton accelerator are finished. We now have a very powerful machine becoming operational, which will make possible experiments which up to now were only dreams. It will be our responsability to make them become reality. It is

both a sweet feeling and a heavy burden at the same time, to face this responsability.

The splendid editorial work was this time undertaken by Martha Pérez. Mr. Binda, as in previous years, did his utmost to do the printing work in the shortest time; we are grateful to L.Blanco, M.T.Carmuega and M.Gismondi for typing the manuscript.

Mario A.J. Mariscotti
April 1982

TABLE OF CONTENTS

THE TANDAR PROJECT

NUCLEAR PHYSICS

V. NUCLEAR REACTIONS

VI. INSTRUMENTATION AND DEVELOPMENTS

SOLID STATE PHYSICS

I. VIBRATIONAL SPECTROSCOPY

II. CRYSTAL STRUCTURE AND PHASE TRANSFORMATION

III. MOSSBAUER SPECTROSCOPY

IV. THEORETICAL SOLID STATE PHYSICS

SOLAR ENERGY

APPENDIX

The Tandar Project

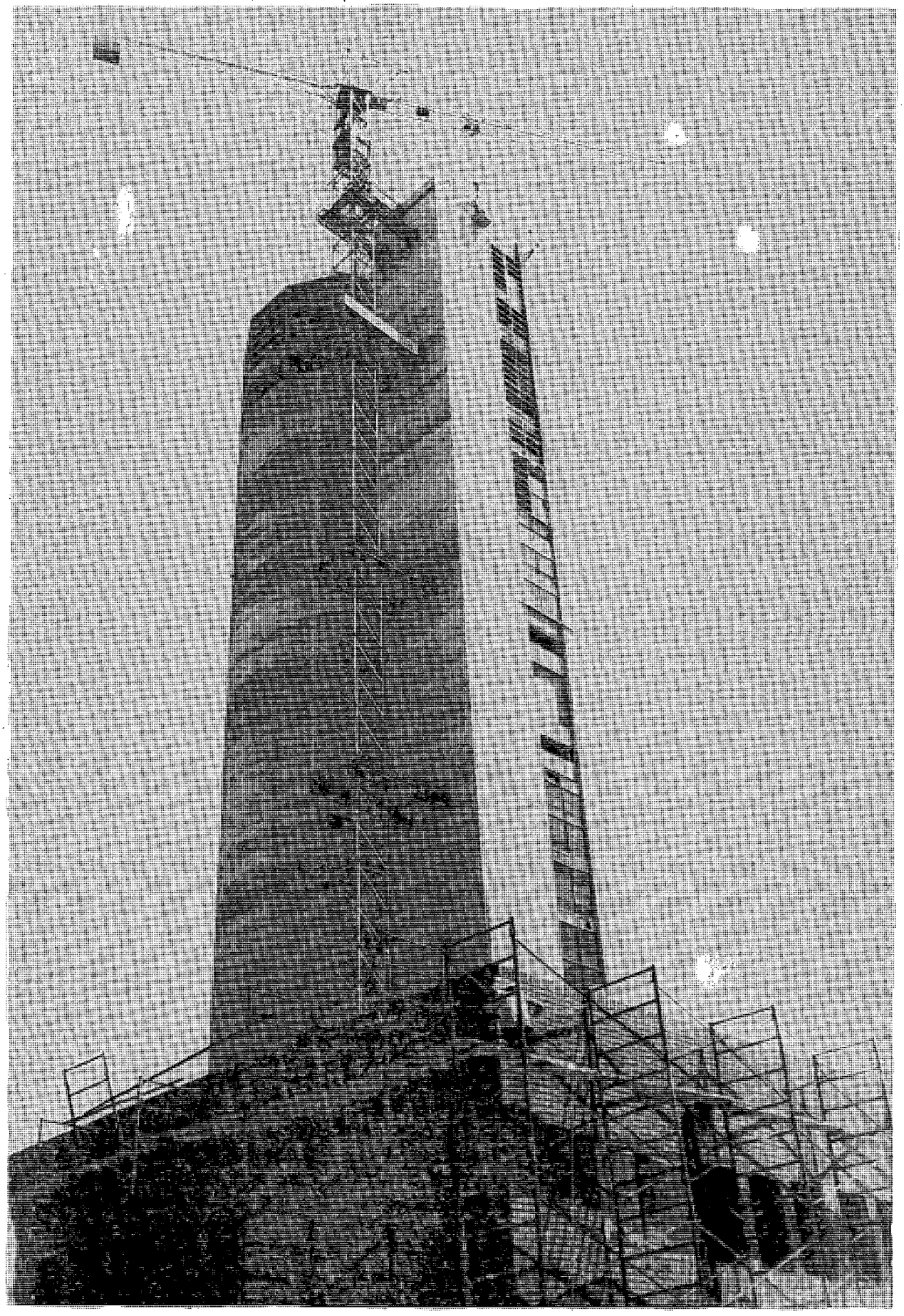

I. THE TANDAR PROJECT

I.1 The Tandar Project: A Personal Overlook

E.Pérez Ferreira and E.Ventura

In December 1977, the Department of Physics of the Atomic Energy Commission (CNEA) of Argentina signed a contract to purchase a large electrostatic Tandem Accelerator which will serve as the base of a new Research Laboratory that includes all the basic research activities currently performed at CNEA, such as nuclear, solid state and atomic physics, reactor chemistry,biology, solar energy;etc.

The activities during the years 1978 and 1979 were accurately described in our previous Progress Report: "...after two years, we should recognize that all of us had a very optimistic idea about the work behind a project of this magnitude".

The work during the years 1980 and 1981 makes even that statement completly obsolete. For little did we all know about the complexities related with activities beyond the normal scope of a physicist; such as dealing with contractors, handling financial problems and going wild with the delays caused by bureaucracy.

How did we cope with it? A theoretical physicist once said that there are two different ways to solve a complicated problem; you either sat patiently thinking about the algorithm that would yield the elegant solution at once, or you used the brute force technique. Needless to say which of the two approaches was used for the Tandar Project, for believe us, there seems to be no room for elegance in the real world.

How did we come out? As an experimental physicist would say, within error bars not so bad. After two years of hard work we have completed 100% of the accelerator tower, gas handling plant and power distribution plant. The experimental areas, support laboratories and offices are more than 80% complete.

After two years of hard work, we have also constructed and assembled the biggest pressure vessel ever made in our country, whose unusual quality deserved encouraging opinions from abroad. Two spherical storage tanks, 10 m in diameter are being filled with succesive shipments of SF_6 gas to reach the inventory of 90 metric tons in time for voltage tests.

We have assembled 100% of the accelerator column and injector in record time and the analyzing magnet has been mounted and aligned with respect to the accelerator and injector.

In the meantime, the data handling system is being completed while construction of a hardware prototype to connect experimental areas with the main system - and the corresponding software - in being developed.

Experimental equipment for six beam lines has been purchased or developed both here and abroad, including a split-pole magnetic spectrometer, an all purpose scattering chamber, a heavy-ion design scattering chamber, a highly sophisticated table for angular correlation measurements and several improvements to the electromagnetic separator to be used for short lived isotopes studies.

Also the training of young physicists has continued in our laboratories and abroad and annual workshops on nuclear physics have continued to ensure updating of accelerator relevant studies.

The following papers show all this work in detail. However this is only part of the story and we are only half way through. There is a lot more to be done and somehow we still have to pull energies from somewhere to acomplish our goal. We are still motivated by the purpose of our work, and the support given to us by the authorities of CNEA constantly reinforces our task.

The encouragement coming from our friends and colleagues here and all over the world keeps us contantly alive. To all of them our deepest thanks.

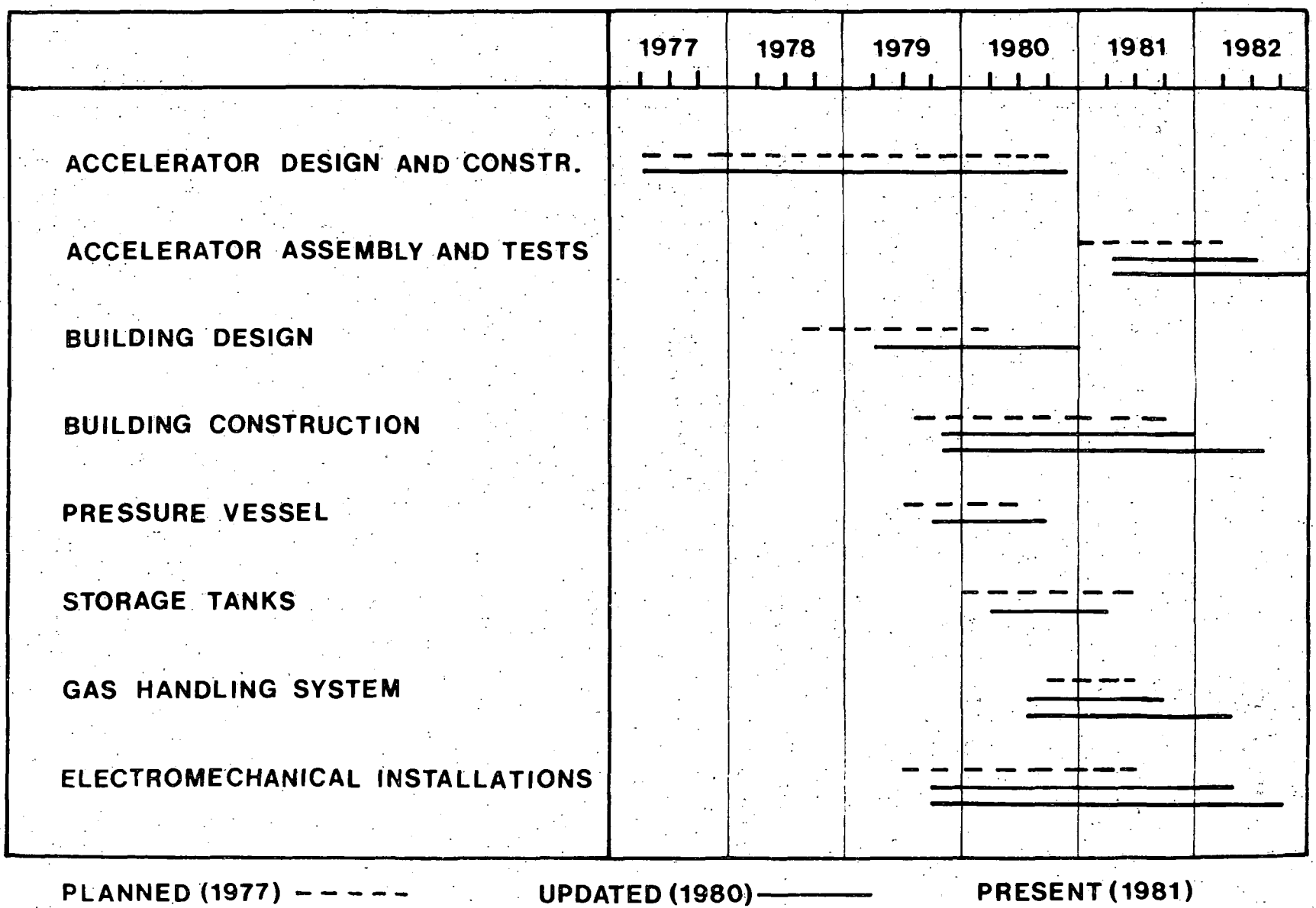

Fig. 1. Schedule for completation of first stage of the TANDAR projet.

I.2. Assembly of the 20 UD Pelletron Accelerator

A.Binda, R.Dieguez, N.Fazzini, E. Garay Ramos, H.Gonzalez, B.Ietri, J.Laffranchi, K.Lochner*, E.Lolago, C.Miguez, C.Palacio, M.Professi, J.C.Rodriguez and J.Vidalle.

The 20 MV straight through Pelletron accelerator built by National Electrostatic Corporation (NEC), Middleton, Wisconsin, U.S.A. according to CNEA specification is shown in Fig. 2.

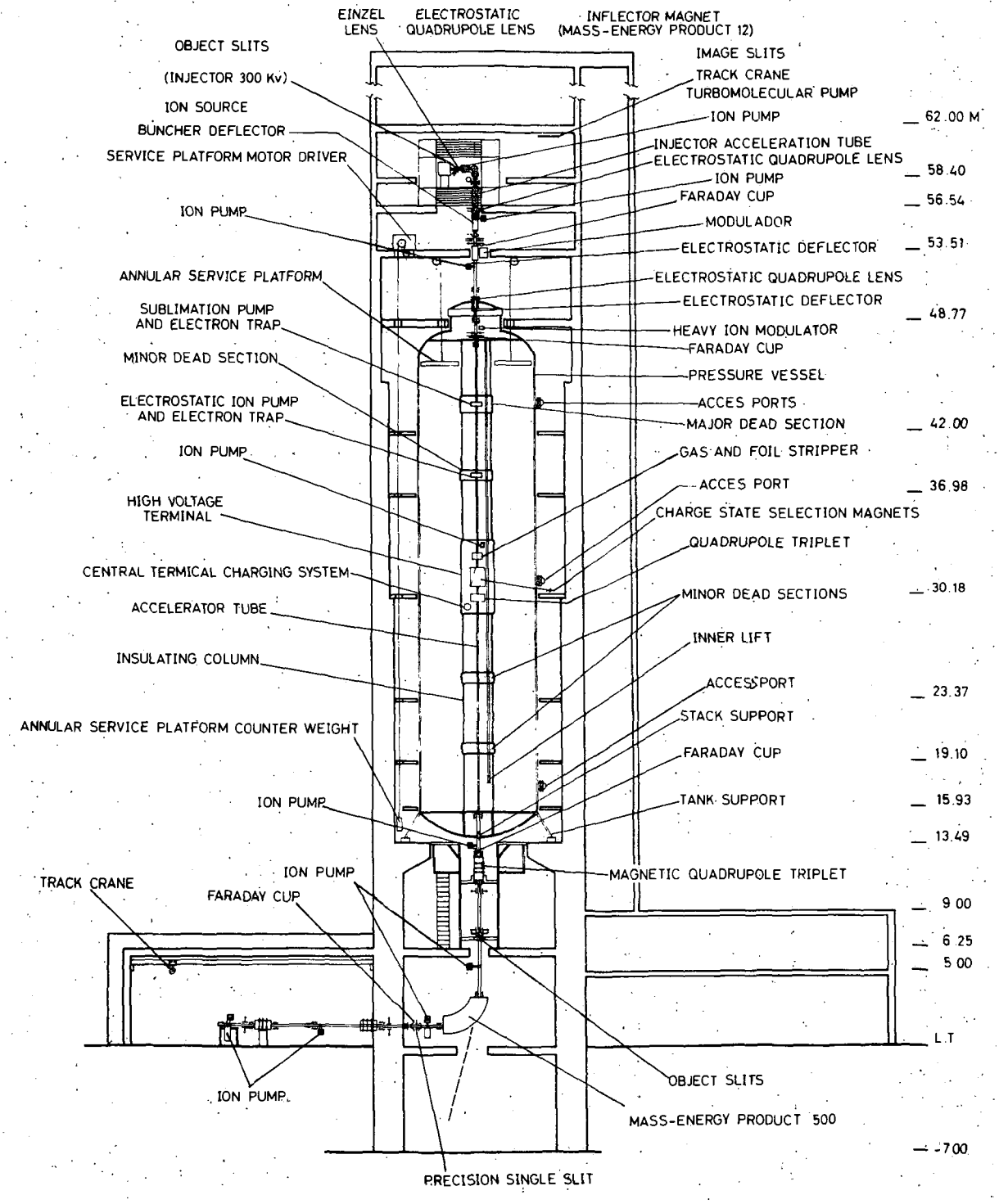

Fig. 2.

It consists basically of a column structure built in 60 cm high modules consisting of 10 cm thick horizontal cast aluminium bulkheads supported by 6 circumferentially located column posts of the type used in previous NEC designs. It has a diameter of 2.15 m and a length of 34.84 m including the high voltage terminal.

One major and three minor dead sections are used in the design. The acceleration tubes are of the standard NEC design. Voltage grading for each acceleration tube and the column structure are provided by two enclosed corona discharge tubes. Two independent groups of two pelletron chains are used to transport 400 μA of charge to the high voltage terminal. Power for various components within the column structure will be provided by two rotating shafts.

The high voltage terminal is 2.44 m in diameter and 4.88 m high. A displaced element electrostatic quadrupole triplet charge selector along with a variable selector aperture and high energy tube matching lens are placed to separate charge states after stripping. Electrostatic steering plates, gas and foil stripping systems and getter-ion pumps are also mounted in the terminal. Focusing elements including a quadrupole triplet lens are also placed in the first dead section. An additional stripping system is located in the first high energy dead section.

In order to increase the reliability keeping at the same time its precision and expansion capabilities, the machine will be controlled by means of a mixed system using light links and control rods. The implementation of the digital control system will use the CAMAC standard. Two PDP-11/23 computers, one acting as backup, will be used to communicate with the system.

Service for the column structure and contents of the high voltage terminal will be performed from two movable service platforms. The large annular platform will be located in the space between the column and pressure vessel. A small platform will move vertically within the column allowing easy access to the interior of the column structure and high voltage terminal.

The shipment of five containers with 90% of the accelerator arrived in Buenos Aires in early February of 1981.

Although completion of the building was not achieved the assembly of

the basic column structure, began in May, after the arrival of the NEC supervisor.

Installation of the annular service platform was completed and succesfully tested.

The basic column structure assembly performed by CNEA personnel with NEC supervision was completed, including equipotential rings, dead section covers, terminal shell, column corona voltage grading system and charging chains. A view of the column assembly is shown in Fig. 3 .

The column will be ready for voltage tests in March 1982.

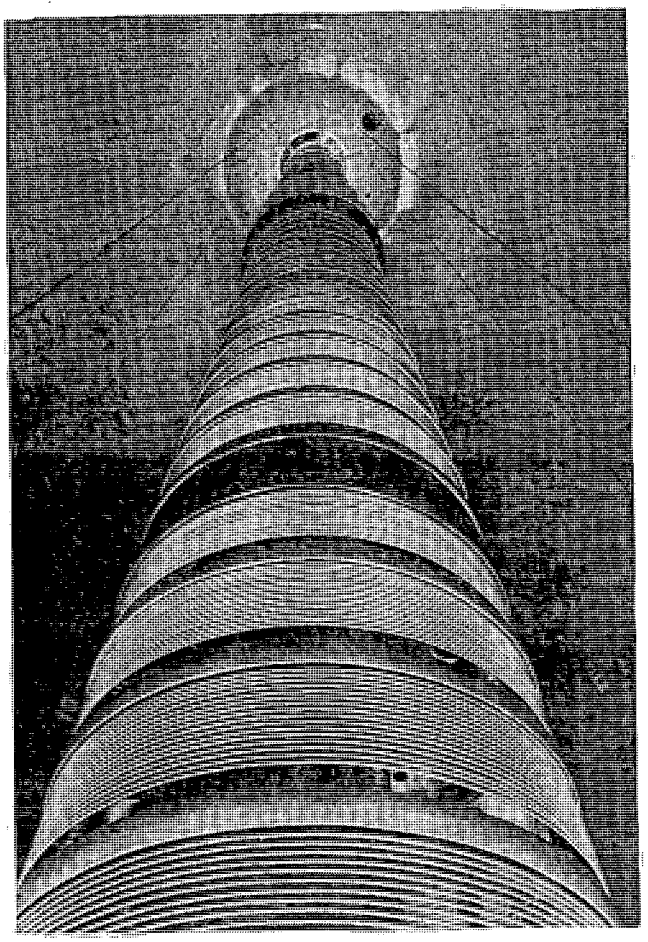

Fig. 3

* National Electrostatics Corporation, Middleton, Wisconsin. U.S.A.

I.3 The Design and Construction of the 20MV Tandem Accelerator Building

F.Antonuccio, N.Fazzini, H.González, M.A.J.Mariscotti, J. Milberg, J.Nicolai, E.Perez Ferreira, R.Requejo, R.Ribarich S.Tau and E.Ventura

The accelerator building constitutes the first and most important stage in the construction plan of the new research laboratory which will be dedicated to CNEA's basic research activities.

Tower Structure

The most prominent feature of this building is the tower structure that houses the accelerator. It consists basically of a dodecagonal base 15 meters in (outer) diameter and 73 meters in height. The design took into consideration the stability of the accelerator during periods of intense wind and solar heat gain. It has been also designed with the appropriate concrete thickness to shield it from radiations originating when beams of protons and deuterons are accelerated to the maximum energy (40 MeV). In addition to the accelerator, space is also provided for the ion sources, injector and 90° analyzer magnet. Finally, a conference room has been included at the top of the structure.

Access to the main tower is through another smaller service tower adjacent to it. One freight elevator and one fast passenger elevator provide the means of convenient transportation of equipment and personnel to the different levels. Fig. 4 shows a vertical cross section of the accelerator building.

The civil construction of this tower is 100% complete. At present work is carried out in two main areas: (1) the installation of the elevators (a temporary freight elevator was installed for the assembly of the accelerator column) and (2) the electromechanical installations that would provide the services for the accelerator.

Experimental areas

Experimental areas were given the utmost importance by the research physicists. The main considerations that when into the design were (1) size and shape, (2) number of rooms and (3) access. The layout has been

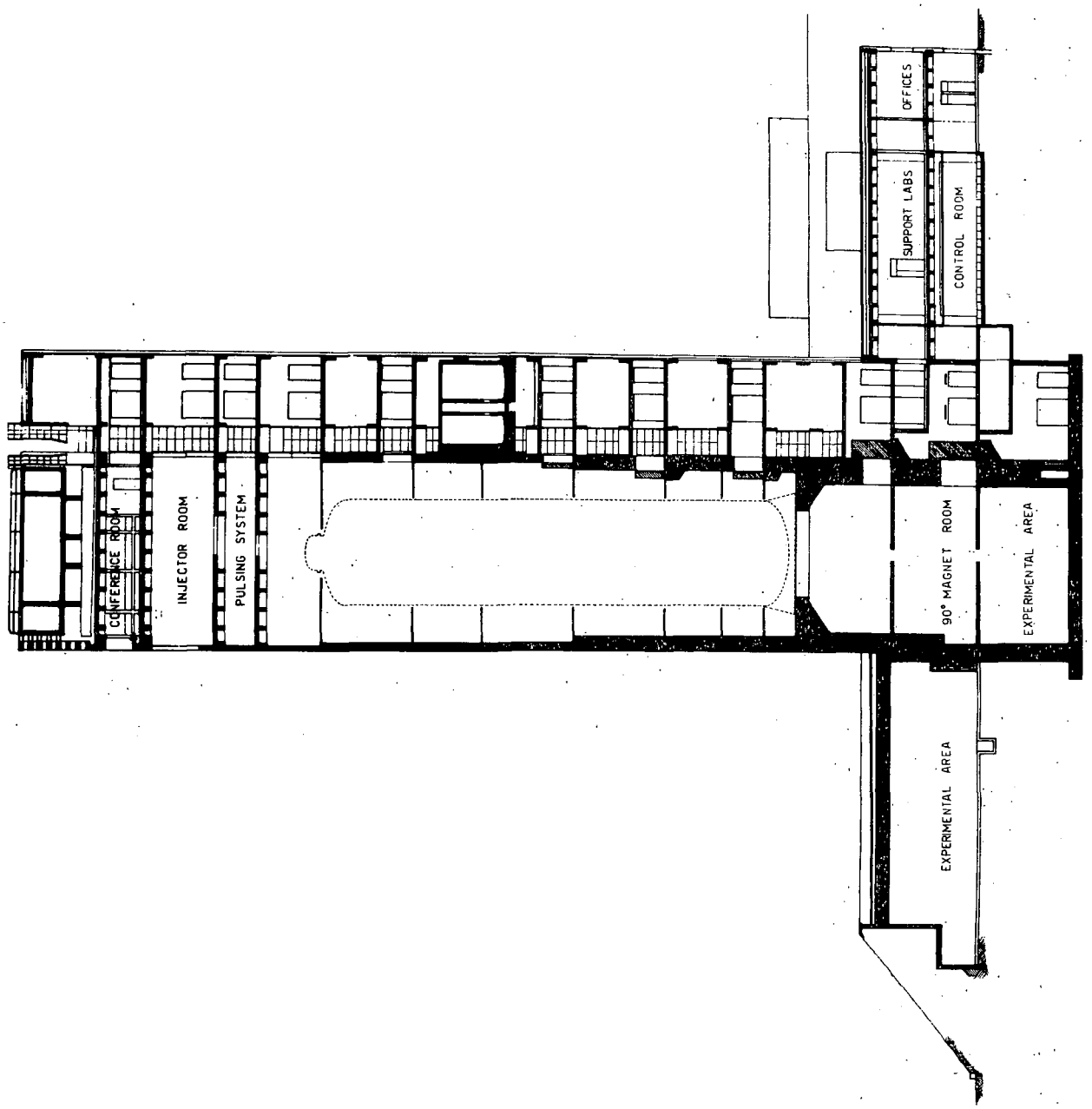
OFFICES
SUPPORT LABS
CONTROL ROOM
CONFERENCE ROOM
INJECTOR ROOM
PULSING SYSTEM
90° MAGNET ROOM
EXPERIMENTAL AREA
EXPERIMENTAL AREA

Fig. 4

arranged in a way to keep as much area as possible available around the base of the accelerator for beam lines, allowing at the same time easy access from the control, data handling and services areas.

The experimental area occupies approximately a 270° sector. The final design, shown in Fig. 5 consists of two, all purpose, shielded (partly by concrete and partly by an earth embankment) rectangular rooms approximately 22 x 23 meters in size, occuping a 180° sector of the floor area. These rooms have the possibility of being equiped with overhead cranes if necessary. Two access doors, with removable concrete blocks, directly connect these areas with an outside road, providing the necessary entrance space for future heavy equipment such as a magnetic spectrometer.

A heavy shielded area for high radiation experiments is also available. This room has been planned to accomodate part of the on line electromagnetic isotope separator facility. In addition there are two unshielded experimental areas for off line use, these can be latter shielded and equipped for on line work.

Finally there is an experimental room in the basement directly below the 90° analyzer magnet. It has been designed for studied with heavy molecular beams focused through the 15° port of the magnet.

One of the two main experimental areas is now ready to start receiving experimental equipment. The other main area will be ready by April 1982.

Plant Areas and Support Laboratories

The control and data handling facilities are located in the ground level with direct access to experimental areas, gas handling plant and tower entrance. It has been designed so that the area can be easily divided into separate functional compartiments.

The gas handling plant is located on two levels (ground and first floor) so as to locate the vaccum pumps as close to the tank as possible. Due to its noisy operation the plant has been acoustically separated from the rest of the building.

The upper floor accomodates the support laboratories needed in connection with the accelerator activities: electronics. ion source development, target preparation, detectors and health physics. Office space is

provided throughout these levels, its destination being mainly for accelerator related personnel. Figs. 5 and 6 shows layouts of these two levels. Finally, a separate building, across the street of the main accelerator building, will house the main shop and storage area.

Services

The installation of the services for the entire accelerator building are proceeding at a rate consistente with the civil works, and with the exception of the air conditioning, they will be completed by April/May 1982. The air conditioning is expected to be completed by July 1982.

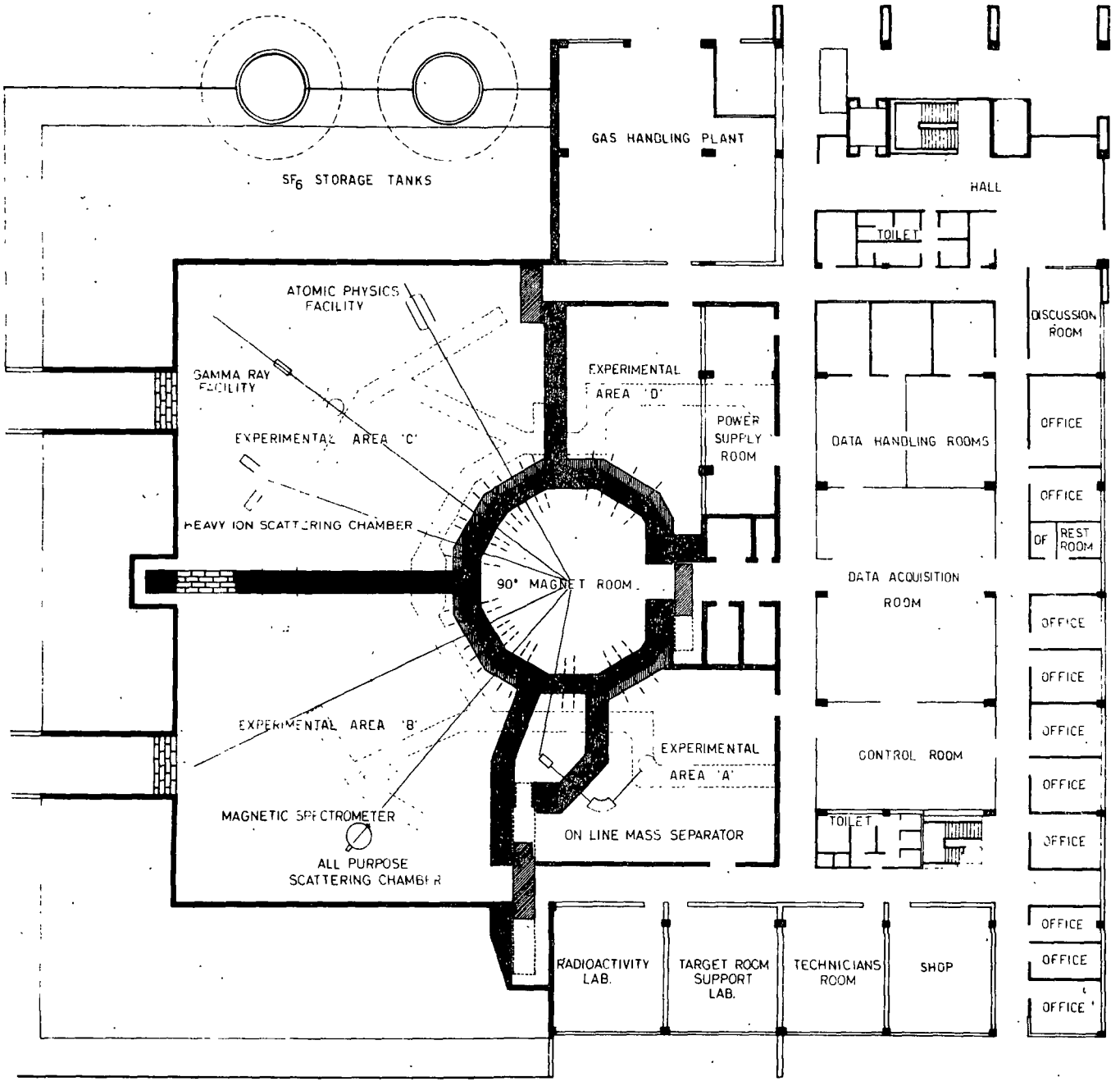

Fig. 5

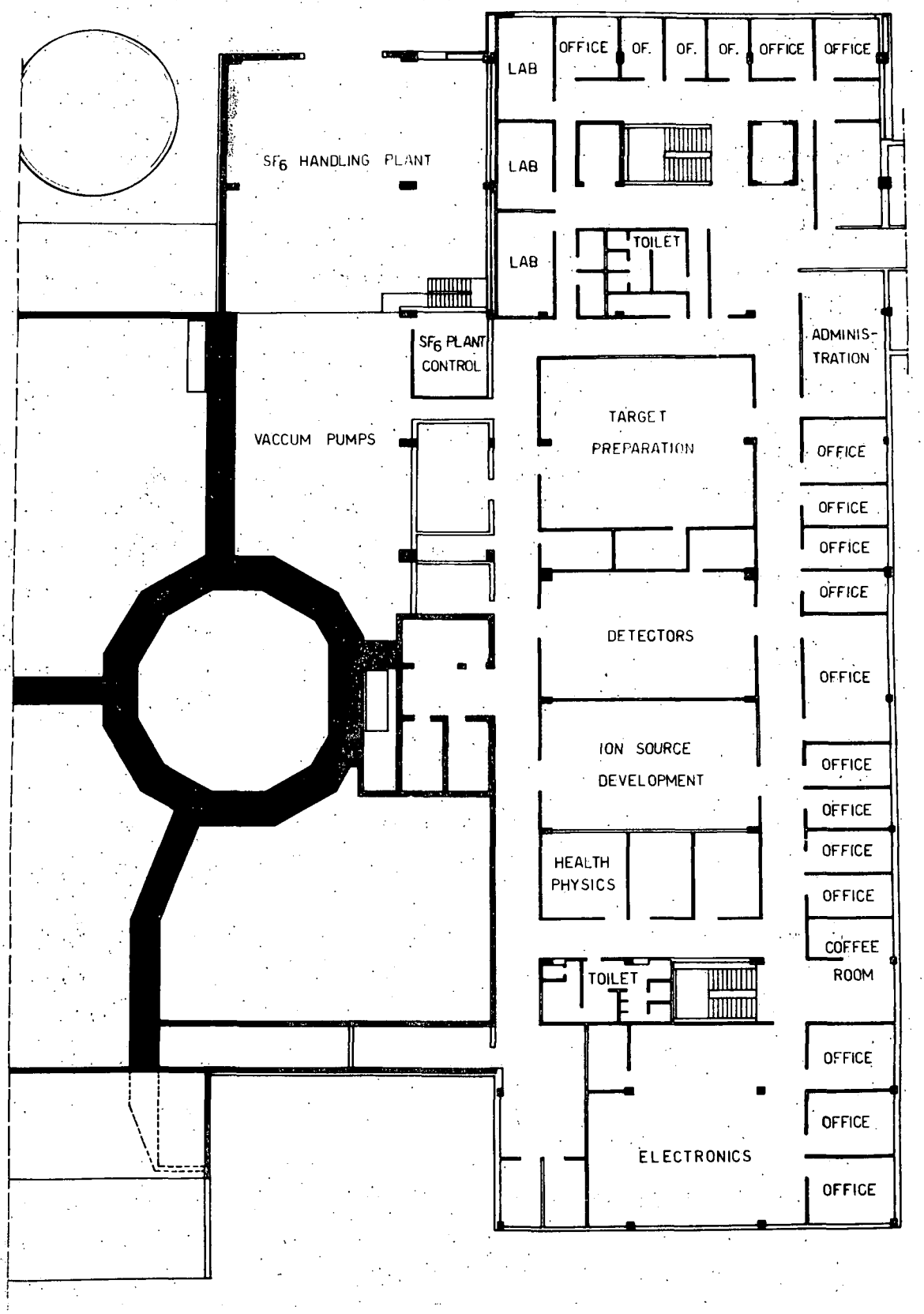
LAB
OFFICE
OF.
OF.
OF.
OFFICE
OFFICE
LAB
LAB
TOILET
SF_6 HANDLING PLANT
SF_6 PLANT CONTROL
ADMINIS-TRATION
TARGET PREPARATION
VACCUM PUMPS
OFFICE
OFFICE
OFFICE
OFFICE
DETECTORS
OFFICE
ION SOURCE DEVELOPMENT
OFFICE
OFFICE
HEALTH PHYSICS
OFFICE
OFFICE
COFFEE ROOM
TOILET
OFFICE
OFFICE
ELECTRONICS
OFFICE

Fig. 6

I.4 The Pressure Vessel and Storage Tanks for the 20UD Accelerator

N.Fazzini, H.González, J.Nicolai and R.Requejo

Pressure Vessel

The accelerator is enclosed in a cylindrically shaped pressure vessel, 7.6 m in diameter and 36.3 m in height filled with 100% pure sulphur hexafluoride (SF_6) as insulating gas. The vessel is made of steel 28 mm thick designed to work at a maximum of 10 Kg/cm^2 absolute pressure. This is 2 kg/cm^2 above the operating pressure specified by NEC to achieve 20MV in the terminal, thus having the advantage of not being severely tank limited in reaching voltages above 20 Megavolts.

Due to its size, the vessel was field fabricated, and one of the features in the choice of its maximum working pressure was the avoidance of a difficult and expensive on site stress-relief treatment. Access for normal accelerator service operations is provided through five ports in the tank. Access to the annular service platform takes place through three side manways. Another port, located on top of the vessel, is used for ventilation (together with bottom port), and for lowering heavy objects to the annular service platform. For assembly of the column structure and major service operations a large port is provided on top of the vessel. In addition there are many smaller openings dealing with the requirements for viewing windows, cable entries, light links, probes, etc.

The tank is supported by a skirt which has the capability of realigning the vessel if necessary. This skirt was designed to carry the weight of the tank plus the weight of 1500 m^3 water during the hidraulic test. The overoll weight of the pressure vessel (without gas) is 310 metric tons.

Storage tanks

Two spherical containers are used for the storage of the SF_6 gas. Each sphere has a diameter of 10 m and a volume of 520 m^3. They are rated for a maximum working pressure of 23 Kg/cm^2 absolute. The spheres were made of

steel 31 mm thick with a design temperature range of 20 - 80°C.

These tanks were also field fabricated by welding several pieces of pre-fabricated steel. They were hydraulically and pneumatically tested according with the standards in use. Forty tons of SF_6 are now stored in one of the tanks. The filling operation had to be done with temporary piping in order to meet the delivery schedule.

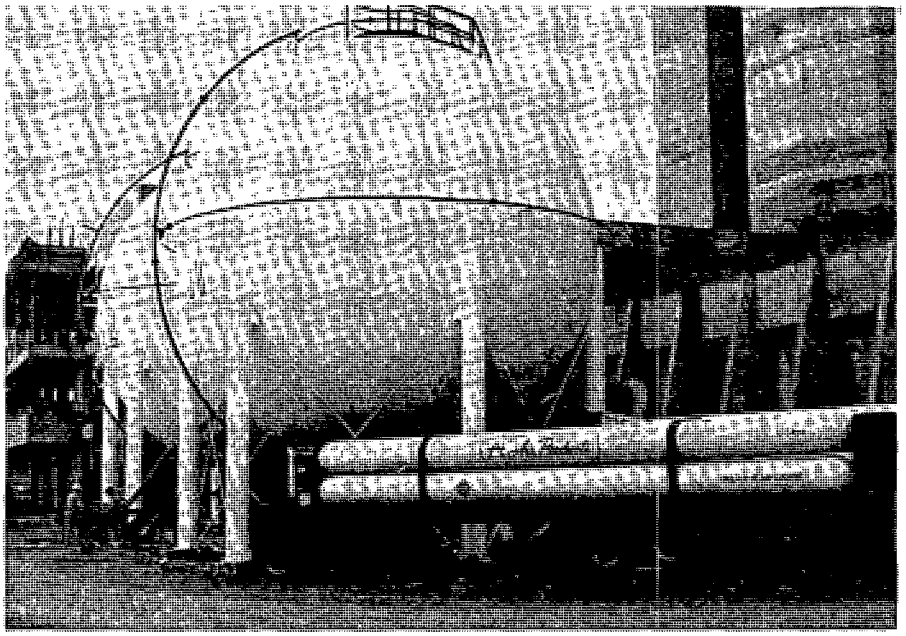

I.5 Design and Construction of the SF_6 Gas Handling System

N.Fazzini, H.González, J.Nicolai and S.Tau

The gas handling system can be divided into two main sections: (1) the SF_6 transfer system and (2) the recirculation and purification system.

SF_6 Transfer System

The main features of this system are that it makes use of gas storage, as oppose to liquid storage for all other plants of this size and that it is an oil free system. A study made by CNEA in this respect showed that both liquid and gas storage systems are equivalent in price when operating costs over a 10 year period are taken into account. Gas storage was chosen since it has the advantages of being a simpler, more reliable and versatile system.

The main components of the system are the vaccum pumps, the compressors the charging system and the storage tanks. A block diagram of the system is shown in Fig. 7.

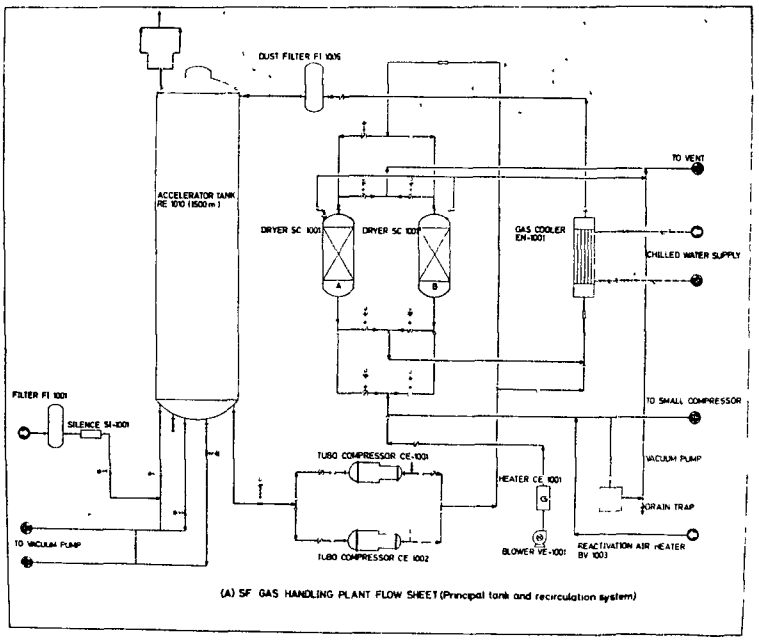

Fig. 7

Vacuum Pumps

There are two groups of pumps. They have been purchased from Leybold-Heraeus, West Germany. Each group is composed of the following five pumps:

2 x WAU	2000	(7,5 Kw)
1 x RAV	1000	(18,5 Kw)
1 x RAV	1000	(15 Kw)
1 x RAV	250G	(7,5 Kw)

All of these are Roots pumps, the RAV ones modified to work against atmospheric pressure. This allows the system to be free from oil contamination. The pumps were supplied with their own control system, and its noise during operation will be reduced to 85 dB using silenciers and acoustic cases. The accelerator pump-down time for SF_6, combining the capabilities of the two groups of pumps, is less than 5 h in order to get from 1 atm to 1 torr inside the tank.

Compressors

Two identical Norwalk compressors with non-lubricated cylinders will be used. They are rated for a maximum discharge pressure of 21 Kg/cm^2, having a variable suction pressure of 1-10 atm, and a piston displacement of 540 CFM. Each compressor requires up to 175 HP of electrical power and 50 GPM of cooling water for the inter and after coolers. Another small compressor will be used to recirculate leaks into the main compressors.

Charging System

It consists of a manifold where the SF_6 containers will be connected. A heater is located between this manifold and the storage tanks in order to compensate the temperature drop caused by the expansion of the gas. In addition, there is a by-pass which connects the charging system with the small "leak compressor" having a maximum discharge pressure of 21 Kg/cm^2 to the storage tanks. The first step of the gas charging procedure can be accomplished without using this compressor. After equalising the pressure between storage tanks and containers, the small compressor is used.

The recirculation and purification system

Drawings and components of the recirculation system for purification and refrigeration of the dielectric gas were contracted from NEC. A block diagram is shown in Fig. 8.

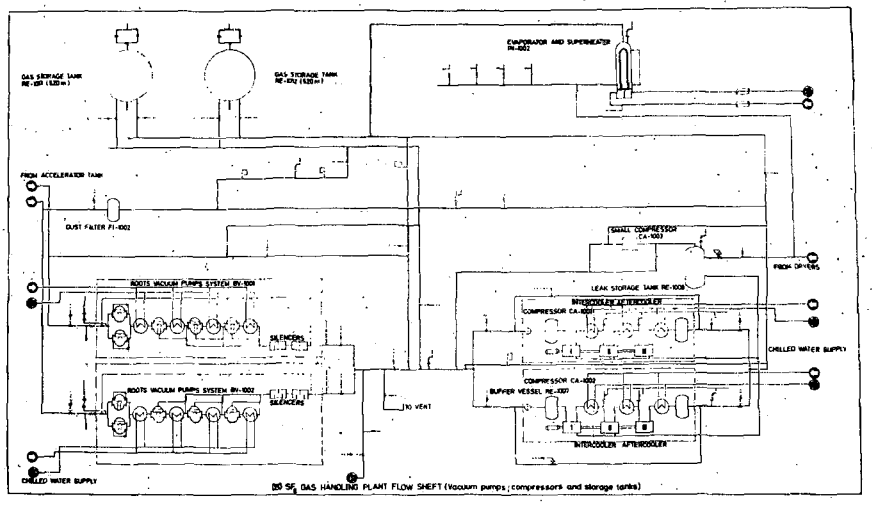

Fig. 8

The system has two turbocompressors, which circulate a continuous amount of gas through alumina absorption beds. These dryers remove the moisture present in the gas in addition to the gas breakdown products.

Before reinjection into the tank, the gas is cooled in a water operated heat exchanger in order to remove the heat produce by the electrical components inside the tank. Finally, the gas is filtered before being passed back into the tank. The system has been designed with two dryers: while one is in operation, the other can be reactivated by a hot air current at 400 °C.

Construction and Assembly

Piping for the system has been installed according to the requirements of the welding standards in use. The contract specified 100% X-rays, hydraulic tests and cleaning procedures. This job is completely finished involving a total of 25 tons of pipes of different sizes.

The two groups of vaccum pumps, the compressors and all the components of the recirculation system have already been positioned and leveled, this was a major job, due in particular to the weight of the components (13 tons for each compressor).

In addition, electrical work is being carried out the installation of trays and conduits for wiring is 90% complete. Panels and console for the plant operation are ready for installation.

I.6 A Micro-computer Based Control System for de 20 UD Pelletron

C.Hinton*, M.Meyers*, C.Pauly*, R.Rathmell* and S.Tau

The 20 UD column, has relatively complex equipment within the terminal and dead sections including electrostatic quadrupoles, electrostatic steerers, and offset quadrupole triplet charge separator, vacuum pumps, electron traps, foil and gas strippers, and other components. Because of its complexity and the length of the column (approx. 16 m from ground to terminal) it was concluded that a digital communication link would be required to provide the smooth, high resolution control needed for the ion-optic components and to provide a reliable system to monitor the large number of parameters. To further ensure reliability, some basic components such as foil stripper and the terminal matching quadrupole have back-up control via control rods to allow limited operation in the event of a failure of the digital system.

Digital communication is implemented through a CAMAC system which is interfaced to a DEC 11/23 microcomputer. CAMAC was specified because it is an international standard for computer interface equipment, and repair, replacement, and additional equipment would be readily available. Another significant reason for choosing CAMAC was the experiencie of the ORNL and JAERI tandems which have demonstrated that CAMAC equipment is reliable in a well shielded enclosure inside the accelerator column.

The computer programs are written using PASCAL with a small amount of assembly language. There are four major programs of which three are utility support and the fourth is the Real Time Accelerator Controller. Central to all software is a database which completely defines each parameter in the system.

Within the accelerator column, the digital system is implemented with a 13 slot half-sized CAMAC crate in the terminal which communicates to the outside via a 5 MHz bi-phase encoded bit serial highway using line-of-sight digital light links.

The individual dead sections are less complex than the terminal and in some cases they contain only electron traps and ion pumps. They did not, therefore, warrant the cost and complexity of individual CAMAC crates.

The external control system consists of a CAMAC crate and interface, operator interaction equipment, and the microcomputer.

The microcomputer has 64K bytes of memory, firmware floating point arithmetic, two .5 Mbyte "floppy" discs, LA 120 line printer, and a VT 100 CRT. The operating system is RT-11.

The operator interaction equipment is a color CRT, keyboard, two assignable digital shaft encoders, 8 assignable analog recording jacks, and a status control "DO-IT" button. The color CRT is an Intercolor 8001 monitor with 64 foreground/background color combinations. It comunicates with the computer via a 19.2 Kbaud RS232 link. The digital encoders have a sixteen bit register which, when assigned, is preset to a parameter's current control value and is incremented and decremented by the corresponding knob on the console. Each encorder has a programable maximum data size of 8-16 bits with under and over flow limits and a four position sensitivity selector. The meters have 1-3-10 Volt scales with over-scale indicators and a two digit range display for autoranging parameters. The analog jacks are digital-to-analog outputs for attachment to external meters or chart recorders. The DO-IT button is used to activate/deactivate toggle or momentary switch type controls.

---

* Electrostatics International, Inc., Middleton, Wisconsin, U.S.A.

I.7 Automation of a Heavy-Ion Scattering Chamber

D.V.Camín, M.E.Satinosky and J.E.Vieiro

One of the experimental facilities of the TANDAR Project is a heavy ion scattering chamber. Inside the chamber there are three concentric plates which are used to hold detectors. In its center an array of eight different targets is located. The plates, targets and the body itself can be moved remotely.

A micro-processor based system controls both all the movements and

the man-machine interface.

In Fig. 9 a brief sketch is shown, The control unit is an Industrial Controller Chassis from INTEL. A floppy disk driver is used as a mass storage.

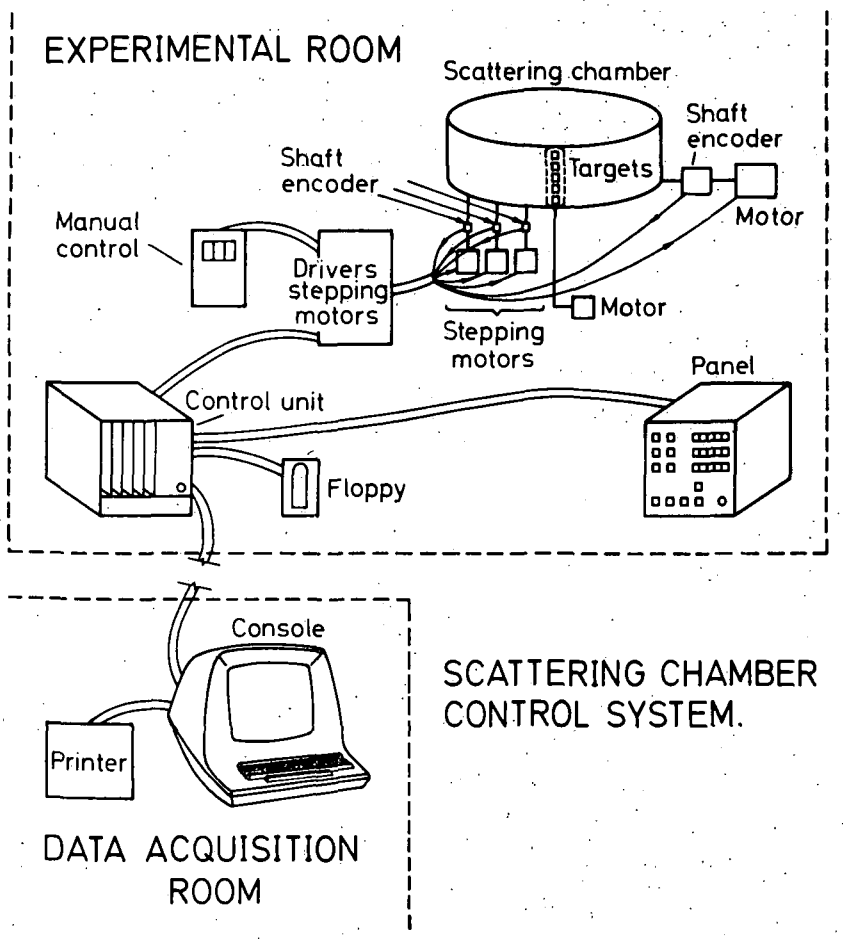

Fig. 9

A power unit drives the motors. Shaft encoders are used to accurately measure the position of the plates and the chamber.

The operation is fully programmable. A console located at the data acquisition room permits the operator to enter sequence of commands for programming.

There are three operating modes:

1. Position and time: in this mode each plate is positioned at a certain angle during a given time.
2. Position and charge: this case is similar to mode 1 with the exception that the measurement at each position finishes when a certain amount of charge is collected.
3. Position and external signal: in this case an external signal will trigger the plate to the next position.

In all these operating modes any target can be selected. In the experimental room, near the chamber, a panel allows a complete manual operation to ease the set-up of the experiments. A conversational language is used to facilitate programming.

At the moment the first prototype is being completed. The final version will be ready in mid 1982.

I.8 Scattering Chamber for Heavy-Ion Reactions

D.Otero, A.N.Proto, D.Nápoli and J.C.Rodríguez

An over view of the scattering chamber is shown in Fig.10. It consists

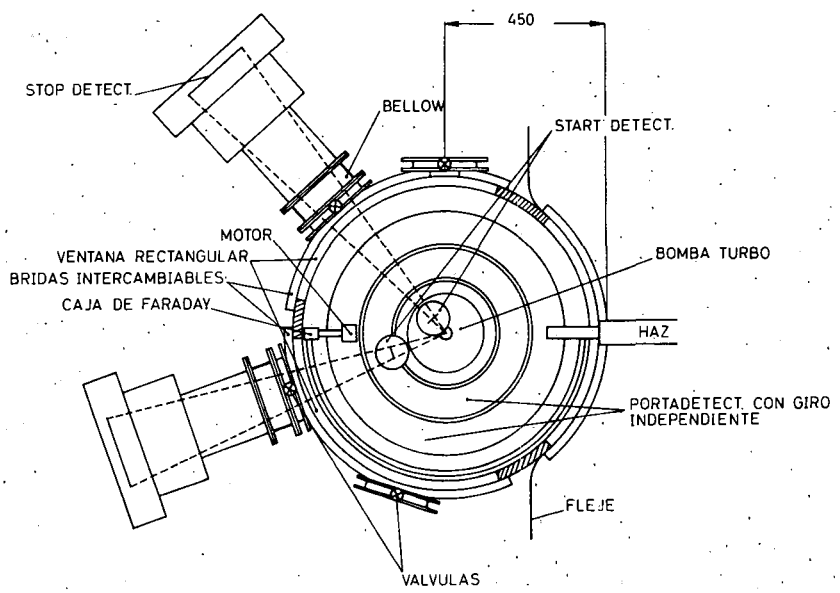

Fig. 10

of a main body of 680 mm diameter and two arms[1]) where large area detectors can be introduced for TOF measurements. The arms can rotate in the reaction plane by ± 43° continuously relative to the beam direction. Also the angle between the arms can be varied from 36° to 180° in steps of 5 degrees.

Inside the chamber two plates and an arc out of the reaction plane allow to use detectors inside the main body for Z, E identification and for evaporated particles determinations respectively. The targets (up to eight) are supported and moved from the upper part of the chamber.

The vacuum system is composed by three turbomolecular pumps (of 450 ℓ/seg). One is setted under the target, and the other two ones, on each arm.

The movements of the plates, the arc and the chamber as a whole are commanded authomatically from the control room (see I.7)

---

[1]) We thank The Weizmann Institute for the helpful information sended at the beginning of this project.

I.9 A CAMAC Based Control System for the Electromagnetic Isotope Separator (Nave Project)

D.Camín, J.Mónico, M.Satinosky, and S.Tau

Considering the new emplacement of the isotope separator close to the 20 UD Tandem, an entirely new control and monitoring system was conceived.

A simplified representation is shown in Fig 11. The system is built around a CAMAC serial highway driven by a microprocessor based autonomous crate controller.

As the ion source and its power supplies are 100 kV off ground potential a fiber optic link is used for the serial highway. This will assure proper isolation and very little wiring between the control console and the magnet-ion source areas.

At the control console one CRT terminal will permit to assign four parameters to a set of two assignable meters and two assignable knobs.

Also 24 lights and switches will provide direct control or monitoring on selected power supplies and auxiliary devices.

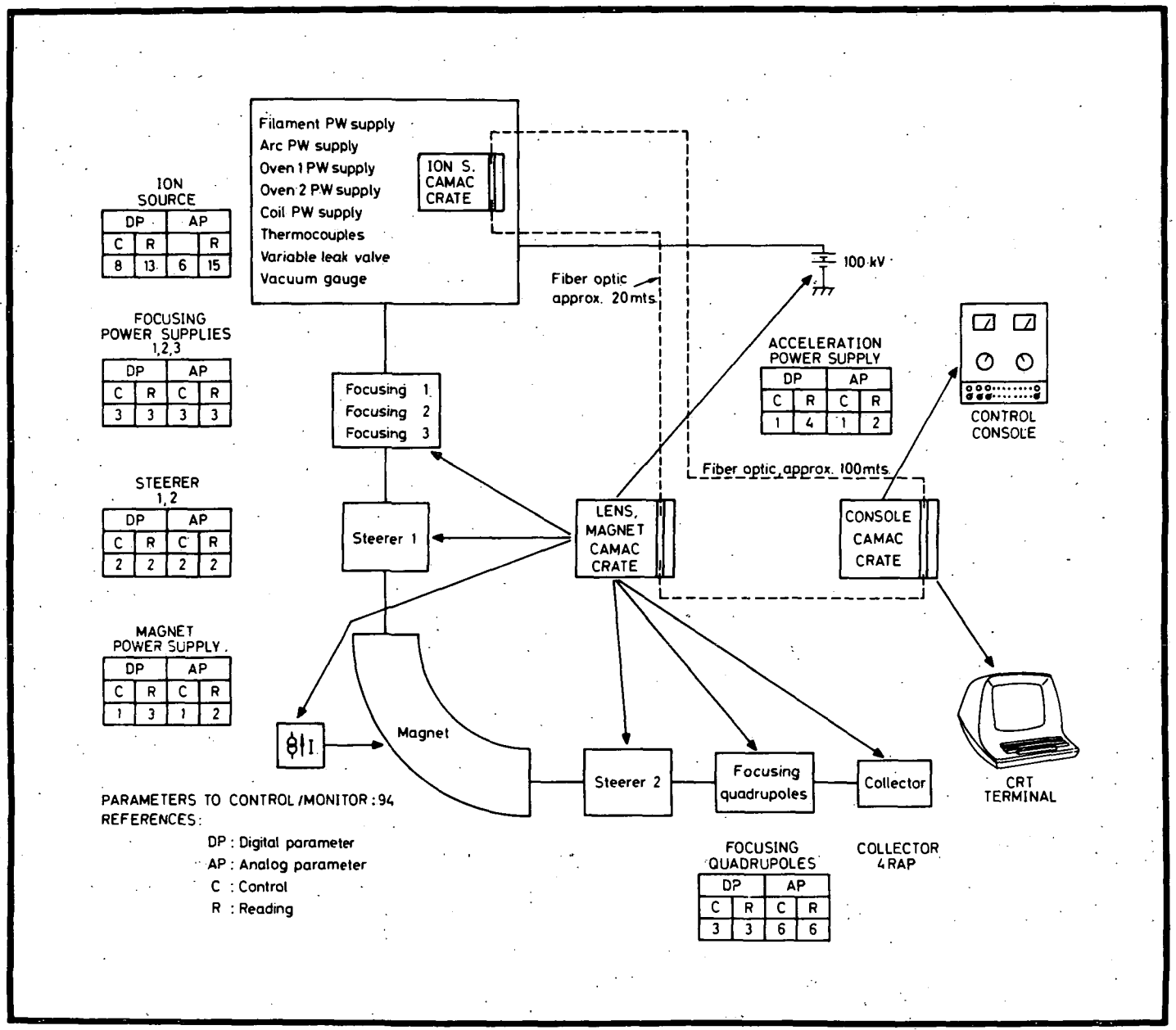
Filament PW supply
Arc PW supply
Oven 1 PW supply
Oven 2 PW supply
Coil PW supply
Thermocouples
Variable leak valve
Vacuum gauge
ION S. CAMAC CRATE
100 kV
Fiber optic approx. 20 mts
ION SOURCE
DP AP
C R R
8 13 6 15
FOCUSING POWER SUPPLIES 1,2,3
DP AP
C R C R
3 3 3 3
Focusing 1
Focusing 2
Focusing 3
ACCELERATION POWER SUPPLY
DP AP
C R C R
1 4 1 2
CONTROL CONSOLE
Fiber optic, approx. 100 mts
STEERER 1,2
DP AP
C R C R
2 2 2 2
Steerer 1
LENS, MAGNET CAMAC CRATE
CONSOLE CAMAC CRATE
MAGNET POWER SUPPLY
DP AP
C R C R
1 3 1 2
Magnet
Steerer 2
Focusing quadrupoles
Collector
CRT TERMINAL
FOCUSING QUADRUPOLES
DP AP
C R C R
3 3 6 6
COLLECTOR 4 RAP
PARAMETERS TO CONTROL/MONITOR: 94
REFERENCES:
DP : Digital parameter
AP : Analog parameter
C : Control
R : Reading

Fig 11

The hardware includes three CAMAC crates, 24 CAMAC modules, one control console and a CRT terminal. A printer and a floppy disk driver, for massive data storage, could be added if required.

CAMAC was choosen because it is an international standard for computer-orientated modular interface systems. Also it is used extensively in other local projects as de Data Acquisition System and the control system for the 20 UD Tandem. Software will be developed using the real time BASIC resident in the autonomous controller and the micropocessor assembly language (INTEL 8080).

A PROM operating system with file-organized software, editing and macro-assembly capability, will help to write the programs.

This facility is available on two CAMAC modules to be pluged in the console crate . Test with a simplified system will begin soon and it is expected to have a final version by the end 1982.

I.10 16 Inputs-16 Bit Digital Multiplexer for HP2116B Computer

A.Barragán and D.V.Camín

The old HP2116B computer will have a place in the Data Acquisition System of the TANDAR Project. In order to improve its input capability, the development of a 16 input digital multiplexer was decided.

A block diagram of the multiplexer is indicated in Fig. 12.

There are two buffers per each periferal device. The first set of buffers are loaded simultaneously when an enable signal is generated. This signal is provided by the computer.

The gate signal, also coming from computer, loads the second set of buffers freeing the first set to be loaded again.

An output bus built with open collector gates permits, under enable signal control, loading of the Input Register of the computer with the buffers content. This reading operation under computer control can be performed in two different modes:

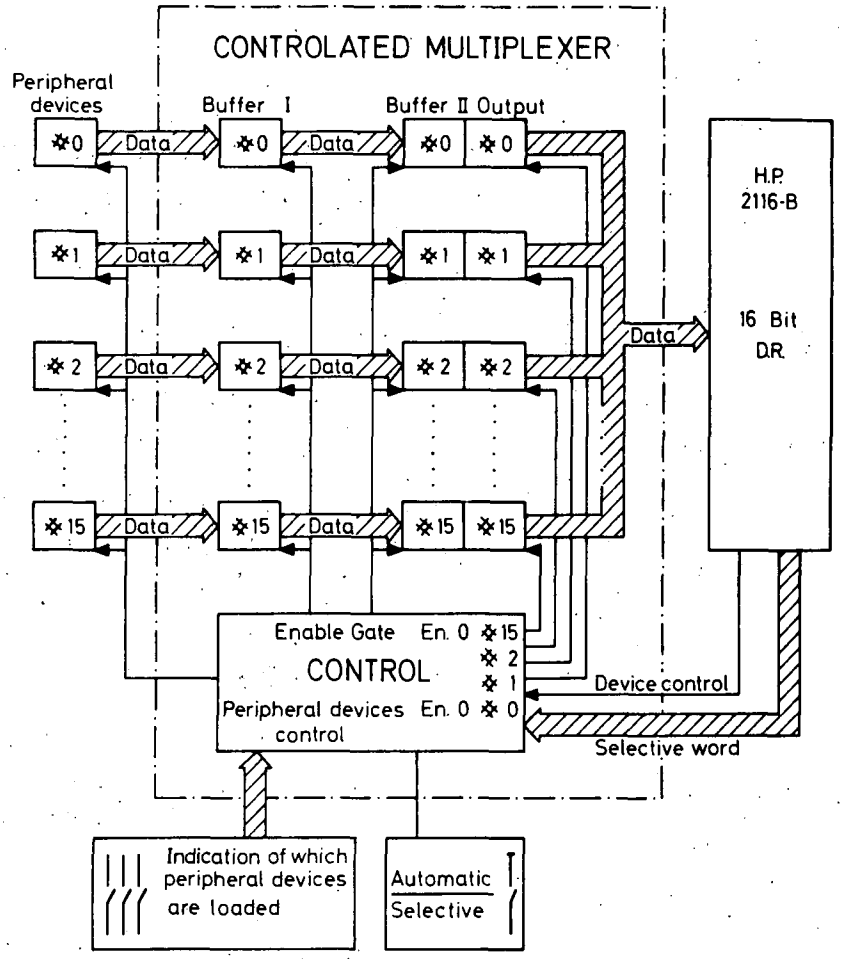

Fig. 12

1. Selective reading: the computer selects at random which buffer is read.
2. Automatic mode: all buffers deposit its content sequentially.

A special counting circuit was developed to skip those buffers corresponding to unconnected inputs. A set of 16 switches located at the front panel selects the inputs to be skipped. In this way time is saved as only buffers with significant content loads the computer.

I.11 Interfase for communication of a HP2116B and a PDP 11-34 computer

D.S.Camín and D.V.Camín

The use of the HP2116B computer in the Data Acquisition System of the TANDAR Project, demanded development of an interface to communicate with the PDP 11-34 used as front end computer.

The circuit connects output with corresponding input registers of both computers.

Optical isolation was used to avoid ground-loop problems.

The use of locally available optic-couples required special care in biasing them to transmit with good shape pulses of 1 μs width, keeping on with maximum delay design requirements. Fig. 13 shows de circuit diagram.

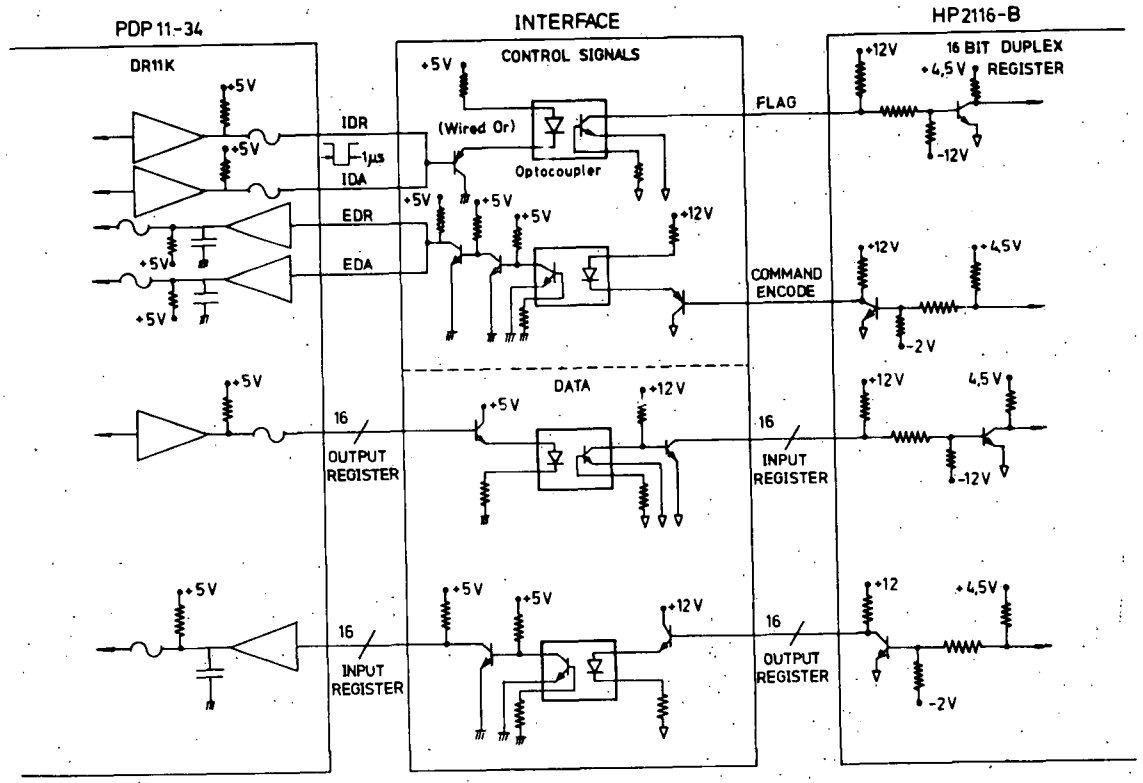

Fig. 13

I.12 Hardware for the Experiment Controller of the Data Acquisition System

E.Achterberg, C.A.Bolaños, D.V.Camín and J.E.Sinderman

The interface between the signals coming from the experimental rooms and the computer consists of a hardware system, a block diagram of which is given in Fig. 14.

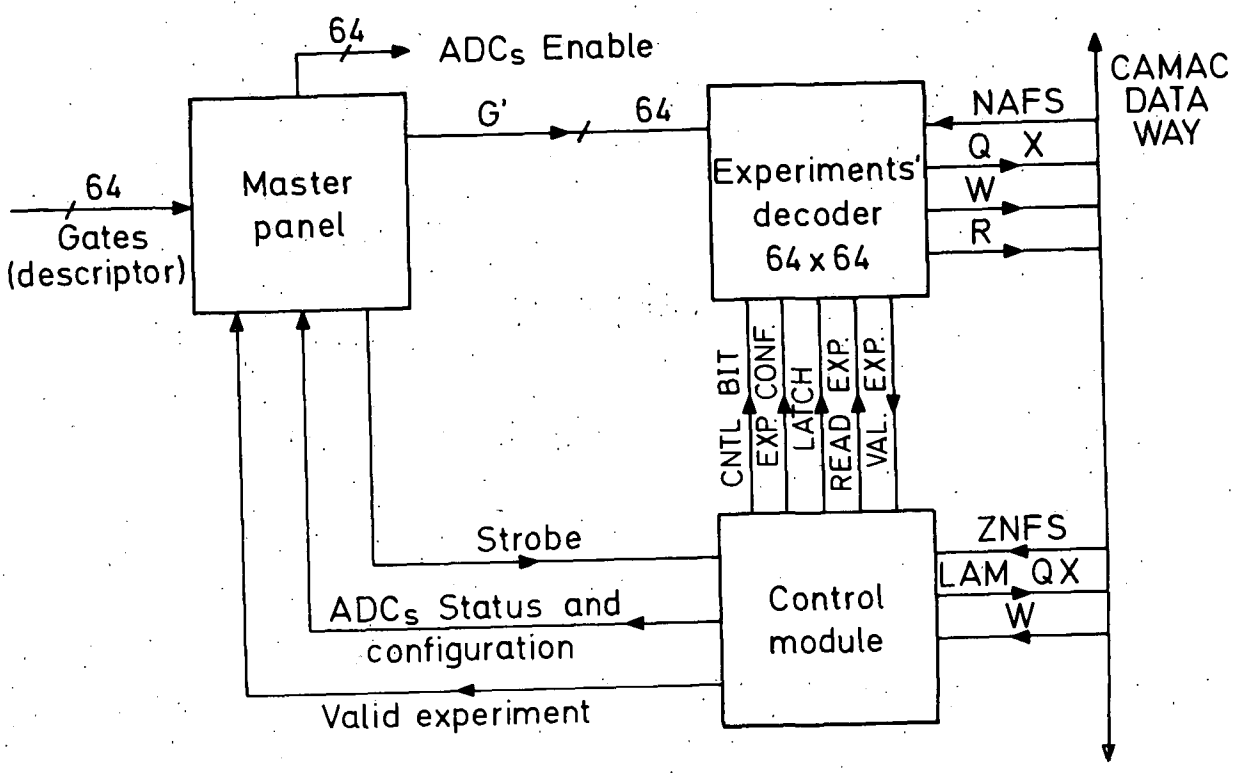

Fig. 14

This system is intended to "filter" the patterns of gate signals (descriptors) in order that only previously defined combinations (experiments) are analyzed by the computer.

Up to 64 gate signals can arrive at the master panel where a phasing process is performed. Once all the signals are in phase, they enter into the "experiment decoder". This unit is equivalent to a set of 24 remotely programmable coincidence/anticoincidence circuits, each

with 64 inputs. In its implementation, decoding with fast bipolar RAM's has been adopted.

In this way up to 24 different gate patterns can be detected. When one valid event (or experiment) is detected the experiment decoder, which has been built as a set of three CAMAC modules, generates a LAM which interrupts the computer. It also provides, via R lines, the information of which out of the 24 possible experiments has been detected.

Another important function is performed in the master panel: as soon as a "valid experiment" is detected, the ADC's involved with that experiment are enabled and further gate signals to them are blocked.

Once the computer has read the ADC's, it enables them again for a new conversion.

The control unit, built also as a CAMAC module, generates control signals and manages the selection of a master strobe signal, generates the LAM etc.

The reaction time of the experiment decoder is about 100 nanoseconds and so a fast counting rate can be achieved.

Provision has been made to easily expand both the number of gates and the number of experiments selected.

At the moment a prototype capable of receiving 16 gates and detecting 8 different experiments is being assembled.

Nuclear Physics

In Beam Spectroscopy
Radioactivity
Applied Nuclear Physics
Nuclear Structure
Nuclear Reactions
Instrumentation and Development

I. IN BEAM SPECTROSCOPY

I.1 In Beam Study of ^{86}Y

M. Davidson*, J. Davidson*, A.J. Kreiner and C. Pomar.

Until now ^{86}Y has only been scarcely studied[1]. Three low spin states were observed through the electron capture decay of ^{86}Zr, namely: 2^- (242.8 keV), 1^+ (271.9 keV) and (1^+) (883.9 keV). In addition a high spin isomeric state with $I^\pi=8^+$ at 218.3 keV and its gamma decay through an $I^\pi=5^-$ state to the ground state is known. Since the lowest lying single particle states are $2p_{\frac{1}{2}}$ and $1g_{9/2}$ for proton and neutron respectively (as seen in the ground states of neighboring odd Y and Zr), the ground state of ^{86}Y is expected to have spin-parity 4^- according to Nordheim's strong rule. This assignment was confirmed by Yamazaki et al[2] through a study of the EC+β^+ decay of ^{86g}Y. Low lying positive parity high spin states are likely to exist in doubly odd Y nuclei since the $\pi g_{9/2}$ excitation es known at low energies in odd mass Y isotopes. The structure of the $I^\pi=8^+$ metastable state in ^{86}Y was in fact interpreted by Kim et al[3] as a member of the $\pi g_{9/2} \times \nu^{-3} g_{9/2}$ multiplet. Recent experimental work has revealed several high spin states in ^{89}Y [Ref.4], ^{87}Sr [Ref.5], and ^{88}Y [Ref.6] originating in the (weak) coupling of $g_{9/2}$ protons and/or neutrons with the corresponding core excitations. These results as well as the lack of information concerning similar states in ^{86}Y gave the motivation for the present investigation through in beam gamma-ray spectroscopy techniques following the $^{85}Rb(\alpha,3n)$ reaction. Figure 1 shows a partial singles gamma-ray spectrum from this reaction at 50 MeV bombarding energy, where the excitation curve of the strong (already known) 208.1 keV line is observed to

reach its maximum. This transition is by far the strongest line of ^{86}Y and seems to collect 100% of the (α,3n) cross section. Another strongly competing reaction is the (α,2np) three particle channel leading to ^{86}Sr.

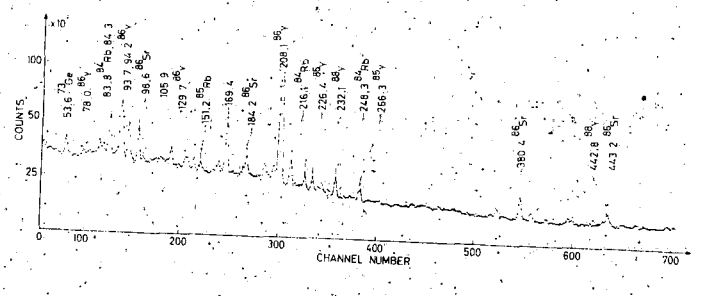

Figure 1:

Singles gamma-ray spectrum from the $^{85}Rb(\alpha,xnypz\alpha)$ reaction at 50 MeV. Lines are labeled according to their origin.

The level scheme proposed in the present work, and based on singles, gamma-gamma coincidence and angular distribution measurements, is shown in figure 2 . None of the transitions (except the 208.1 keV line) have been seen before. Perhaps the most interesting feature is the three-gamma-ray cascade formed by the 226.4, 1125.4 and 129.7 keV lines. All three show angular distributions with negative anisotropy which has been taken as an indication of dipole character. The lack of crossover transitions (which is a surprising fact) suggests an increasing spin sequence. The I=(9) level at 444.7 keV might be associated with the maximally aligned state of the $\pi g_{9/2} \times \nu g_{9/2}$ configuration. The next level in the cascade depopulated by the 1125.4 keV transition might represent the coupling of the state

discussed previously to the first excited 2^+ state of ^{86}Sr (a natural choice for a core). Since this state lies al 1077 keV it has the right energy to allow such an interpretation. However, a disturbing circumstance is the lack of a crossover transition from the (10) to the 8^+ state which should be of collective nature.

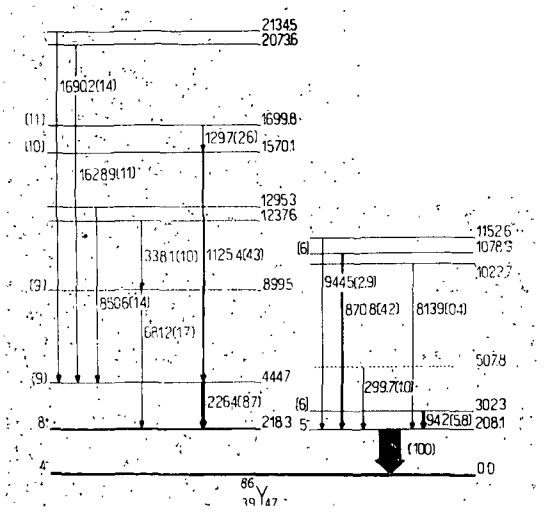

Figure 2

Level scheme for ^{86}Y proposed in the present work

---

* Departamento de Física, Facultad de Ciencias Exactas y Naturales, Universidad de Buenos Aires, Argentina.

1) Nucl. Data Sheets, Vol. 25, N° 4 (1978)553.

2) T. Yamazaki, H. Ikegami, and M. Sakai, University of Tokyo, Report INS32 (1961)

3) Y.E. Kim, D.J. Hoven, and J.M. Hollander, Nucl.Phys. 31 (1962)447

4) M. Davidson, J. Davidson, M. Behar, G. Garcia Bermudez, and M.A.J. Mariscotti, Nucl. Phys. A306 (1978)113.

5) S.E. Arnell, A. Nilsson, and O. Stankiewicz, Nucl. Phys. A241 (1975)109.

6) M. Davidson, J. Davidson, and M.A.J. Mariscotti, Nucl. Phys. A352 (1981)237.

I.2 In Beam Study of ^{79}Kr

M. Behar, A. Filevich, A.O. Macchiavelli and L. Szybisz*.

In the present work we have reinvestigated the ^{79}Kr, through the ^{78}Se(α,3n), by performing gamma singles, gamma-gamma coincidences, angular distributions and timing measurements using the DSAM technique. As a result a more complete level scheme was obtained -see figure 1-. The improvements over previous measurements are the following:

a) In the case of the negative parity bands precise energy and gamma intensity measurements of the cascades (some of them new), crossover and interband transitions have been established. These measurements allow us to determine the values of a number of parameters pertinent to a rotational model. In particular for the K=½ band the decoupling parameter a was found to be negligible and the quantity $[(g_K-g_R)/Q_0]^2$ remains constant within the experimental errors giving an average value of 0.45±0.05. For the K=5/2 band the corresponding $[(g_K-g_R)/Q_0]^2$ value is of order 10^{-3} and consistent with zero, which is in agreement with the measured g-factor for the K=5/2 bandhead. Therefore it is expected for this band a hindrance of the M1 cascade transitions.Due to this fact the crossover transitions are favoured and the 302.5 keV line shows a strong E2 admixture.

b) With respect to the positive parity states, we have shown conclusively that the 827.2 keV transition is in coincidence with the 19.2 keV line [as it was assumed but not proved by Clements et al.[1)]]. On the other side we have clearly identified the unfavoured $11/2^+$ and $15/2^+$ states. The lifetime of the 3146 keV level was measured and the result was $\tau \gtrsim 1.5$ ps, while the predicted value is τ=0.13 ps.

By applying the leading order theory an overall agreement is obtained for the negative parity bands, as well as in energy spacing and spins. For

the positive band it is necessary to include a Coriolis coupling calculation which again shows a general agreement. However from the results obtained in this work it appears that this band is only partially decoupled instead of being fully decoupled as suggested by Clements et al.[1].

---

* Dep. Física, Facultad de Ciencias Exactas, UNLP and Fellow of CONICET, Argentina

1) J.S. Clements, L.R. Medsker, L.H. Fry, Jr, and L.V. Theissen, Phys. Rev. C21 (1980)1285.

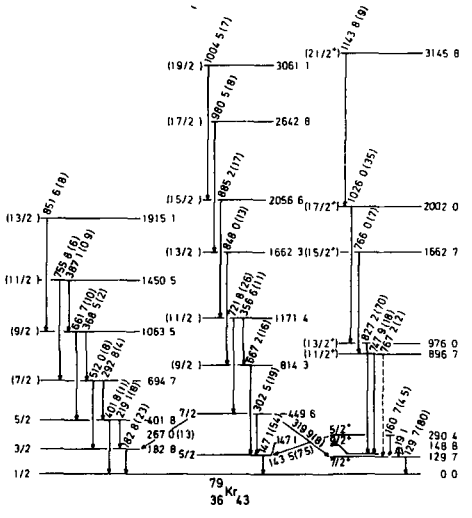

Figure 1

I.3 High Spin States in ^{49}Ti and the Empirical $(f_{7/2})^n$ Model

M. Behar, A. Filevich, G. García Bermudez, M.A.J. Mariscotti and E. Ventura.

The ^{49}Ti nucleus with two protons and one neutron hole outside the doubly magic ^{48}Ca constitutes a very good test for shell model calculations.

In this region rather complete $(1f_{7/2})^n$ calculations were performed by Kutschera et al[1]. They made definite predictions about level schemes and their properties for all the $42 \leq A \leq 54$ nuclei. In particular for ^{49}Ti the positions of levels with spins higher than 9/2 and the properties of their decay scheme are calculated. From the experimental point of view, despite extensive investigations through (d,p);(t,p);(n,γ) and (d,t), only low spin states have been reached. On the other hand Andersen et al[2] using the ^{50}V(t,α) reaction presumably reached high-spin levels but they were not able to make spin assignments.

Motivated by the model predictions and the lack of experimental information, we have used the ^{48}Ca(α,3n) reaction to populate high-spin states in ^{49}Ti.

The measurements were carried out using the Buenos Aires Synchrocyclotron from which an alpha particle beam is available. Excitation functions (in an energy range between 30 and 55 MeV), coincidence, angular distribution, and lifetime measurements were performed. From these experiments: a) the level sheme of figure 1 is obtained, b) lifetime limits of the highest lying levels have been deduced and c) mixing ratios of the gamma-ray transitions were extracted. The present results are compared with the calculations of Kutschera et al[1] and a very good agreement is obtained [figure 1 b) and ref.3], indicating that the high spin levels in ^{49}Ti which have been populated in the present reaction are essentially shell-model states very well described by the empirical $(f_{7/2})^n$ model

---

1) W. Kutschera, B.A. Brown and K. Ogawa Nuovo Cim. 112 (1978)1

2) S.A. Andersen, O. Hansen, L. Vistisen, R. Chapman and S. Hinds Nucl. Phys. A125 (1969)65

3) M. Behar, A. Filevich, G. García Bermudez, M.A.J. Mariscotti and E. Ventura, Nucl. Phys. A366 (1981) 61.

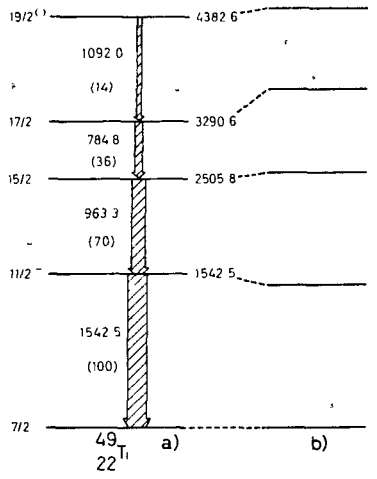

Figure I

I.4 High Spin States in the doubly odd nucleus $^{72}Br^{*}$.

G. García Bermudez, C. Baktash**, A.J. Kreiner, and M.A.J. Mariscotti.

High spin states of ^{72}Br were investigated using the ^{58}Ni (^{16}O,np) reaction in the 40 to 55 MeV bombarding energy range. The beam was delivered by the Brookhaven National Laboratory Tandem accelerator. The target was an enriched Ni foil of 1.5 mg/cm^2 backed with 8 mg/cm^2 of natural lead to stop the recoiling evaporation residues. Excitation functions of prompt gamma-rays and radioactive yields, measured with Ge(Li) detectors established 50 MeV as the most suitable beam energy to perform the rest of the measurements. A singles spectrum is shown in figure 1. Several cross bombardments (using the $^{40}Ca(^{35}Cl,x)$ and $^{58}Ni(^{19}F,x)$ reactions) as well as activity measurements were done to further strengthen the isotopic assignment.

Figure 1

Lines identified with dots belong to ^{72}Br.

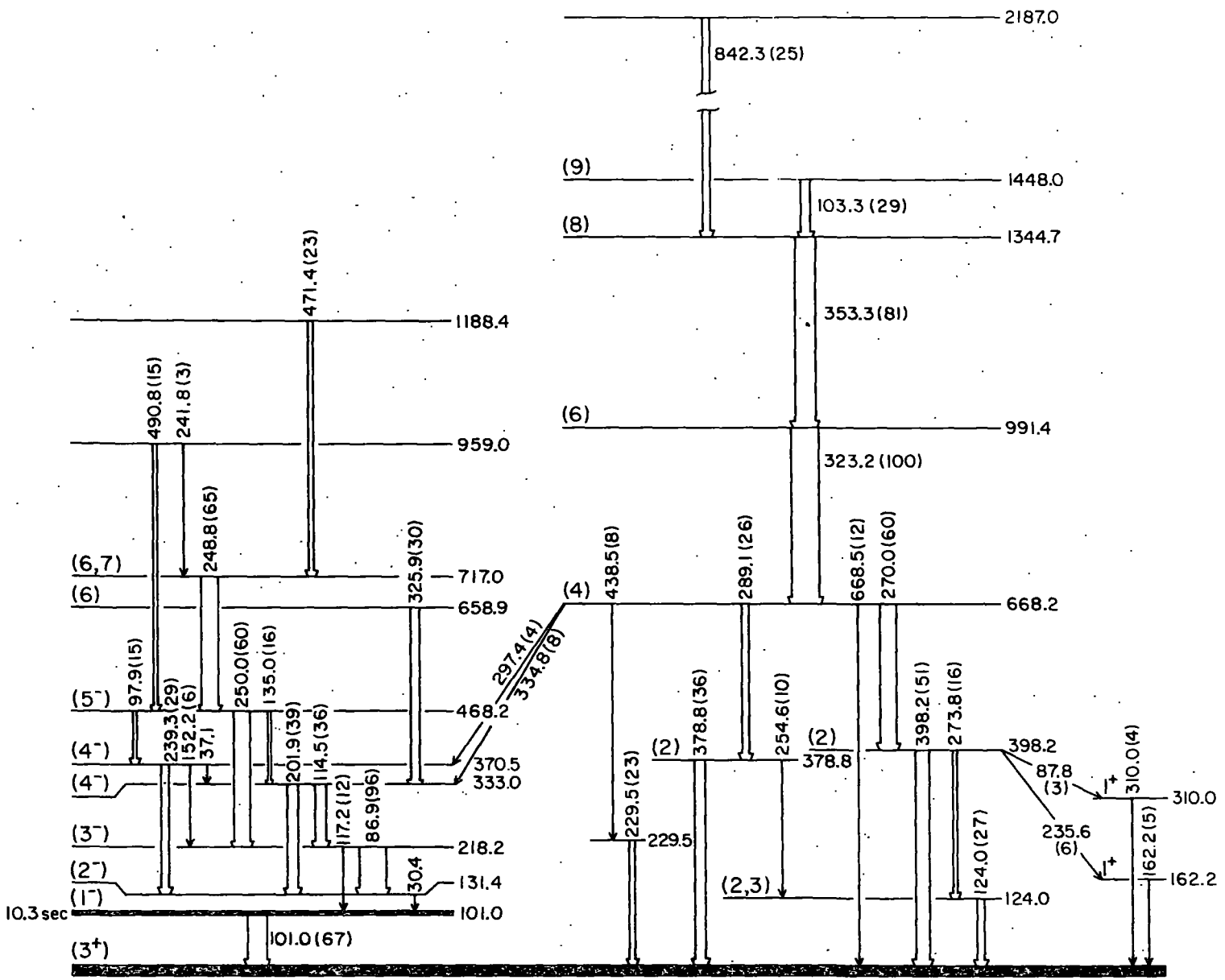

$^{72}_{35}Br_{37}$

Figure 2

The analysis of the gamma-gamma coincidence experiment revealed two groups of weakly connected gamma-rays which together with the angular distribution results leads to the almost completely new level scheme presented in figure 2.

A new isomeric state [$T_{1/2}$=10.3^{+}0.6] and I =(1^{-}) at 101.0 keV] and two sets of levels, most likely of opposite-parities, have been established in the present work.

In the heavier doubly odd Br isotopes with A=74, 76 and 78 ΔI=1 collective structures of $\tilde{\pi}\, g_{9/2} \otimes \tilde{\nu}\, g_{9/2}$ parentage have been identified[1]. No such band has been found in the present case but it is not unreasonable to think that states related to the above mentioned intrinsic excitation should also exist in ^{72}Br. Possible candidates are provided by some of the levels shown at the right hand side of figure 2. The new features of these levels as compared to those previously known[1] are, however, presently not well understood.

---

* Submitted to Phys. Rev.C

** Department of Physics, Brookhaven National Laboratory, USA.

1) G. García Bermudez, A. Filevich, A.J. Kreiner, M.A.J. Mariscotti, C. Baktash, E. der Mateosian, and P. Thieberger Phys. Rev. C23 (1981)2024.
M.Behar, A.Filevich, G.García Bermúdez, and M.A.J.Mariscotti, Nucl. Phys. A282 (1977) 331.
A.J.Kreiner, G.García Bermúdez, M.A.J.Mariscotti, and P.Thieberger, Phys. Lett. B 83 (1979) 31.
G.García Bermúdez, D.H.Abriola, M.Behar, M.C.Berisso, J.Fernández Niello, A.Filevich, and M.A.J.Mariscotti. J. Phys. G6 (1980) L89.

I.5 High Spin States in ^{94}Tc

M. Behar, A. Ferrero, A. Filevich, G. García Bermudez and M.A.J. Mariscotti.

The low lying levels of ^{94}Tc have been reasonably well identified. Previous experimental works[1] have established the existence of seven positive parity-states, six of them well described as members of the $[\pi(1g_{9/2})^3, \nu(2d_{5/2})]$ $I^\pi = 2^+ \ldots 7^+$ multiplet and two negative parity states, which have $[\pi(1g_{9/2})^4(2p_{1/2})^{-1}, \nu(2d_{5/2})]$ $I^\pi = 2^-, 3^-$ as their main configurations[2]

High spin states which arise from configurations like $[\pi(1g_{9/2})^3, \nu(2d_{5/2})]$ with seniority three, involving positive parity states up to 13^+ and those of seniority five $[\pi(1g_{9/2})^4(2p_{1/2})^{-1}, \nu(2d_{5/2})]$ which will lead to spin up to 15^- have not been previously observed. In nuclei belonging to the same region ($N \simeq 50$ and $Z \simeq 43$) levels of the above characteristics have been populated. In particular for $^{93}_{43}$Tc a number of positive parity states of I^π up to $21/2^+$ described as the coupling of the three $g_{9/2}$ protons, and at the same time negative parity states of I^π up to $25/2^-$ have been observed.

A similar situation occurs for the ^{91}Nb and ^{92}Nb isotopes and strikingly enough the stretched configurations $^{91}\text{Nb} \times \nu d_{5/2}$ give rise to almost all the observed level configurations in ^{92}Nb with remarkable parallelism to the corresponding ones, observed in ^{91}Nb.

Therefore it is of interest to investigate the ^{94}Te isotope and compare its level scheme with that of ^{93}Te. For this purpose we used the ^{93}Nb(α,3n) reaction between 30 and 55 MeV. From excitation functions, coincidences and angular distribution measurements the level scheme shown in figure 1 is obtained.

A search for isomeric states with lifetime longer than a few ns was performed. The natural 100 ns pulsing of the Synchrocyclotron was used to stop a TAC which was triggered by the gamma-ray signals from the gamma-ray detector. The 168.7 and 185.7 keV gamma-rays show in addition to a prompt distribution ($T_{1/2} \leq 5$ns) a flat background (around 10%) indicating that they are populated by an isomer with a halflife 50ns $\leq T_{1/2} \leq$ 10 s. This means that at least the isomer lies at an energy higher than 2420.7 keV. It is noteworthy that in the same region of the periodic table N≃50 Z=41 the Mo and Nb isotopes exhibit isomers with 40ns$\leq T_{1/2} \leq$40 s around 2.4 MeV as in the present case.

Shell model calculations of ^{93}Tc have been performed by several authors. In all the cases the first 38 protons and 50 protons are included in an inert core. Positive and negative parity states are due to the $[(2p_{1/2})^2(1g_{9/2})^3]$ and $[(2p_{1/2})^{-1}(1g_{9/2})^4]$ proton configurations respectively. These calculations reproduce fairly well the known experimental level scheme[4].

By comparing the results of the present experiment with those of ^{93}Tc one can observe that the stretched configuration for $^{93}\text{Tc} \otimes \nu d_{5/2}$ gives rise to all the high spin levels observed in the present experiment as is shown in figure 2 with the exception of the (10^-) 2234.9 keV level. It is likely that the 2234.9 keV level arises from $^{93}\text{Tc} \otimes \nu h_{11/2}$ configuration. This stretched weak coupling scheme seems to be a common feature in nuclei near the N=50 shell closure. It is observed in the even-even N=50 nuclei and the adjacent N=51 nuclei and also in the ^{91}Nb-^{92}Nb pair. The present result shows that this pattern also occurs for the ^{94}Tc-^{93}Tc.

---

1) D.E. Miraele and B.D. Kerm Nucl.Phys. A320 (1979)353 and ref.therein

2) G. Madueme and R. Arita Nucl.Phys. A297 (1978)347

3) J. Vervies Nucl.Phys. 75 (1966)17

4) B.A. Brown, P.B. Fossan, P.M.S. Lesser, and A.R. Poletti Phys.Rev. C13 (1976)1194.

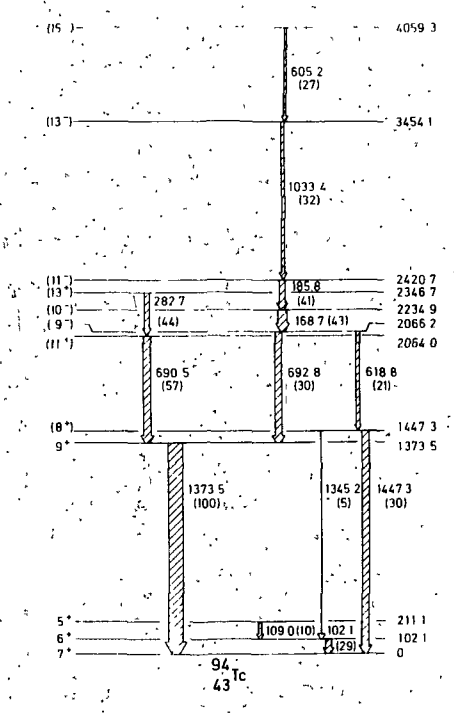

Figure 1

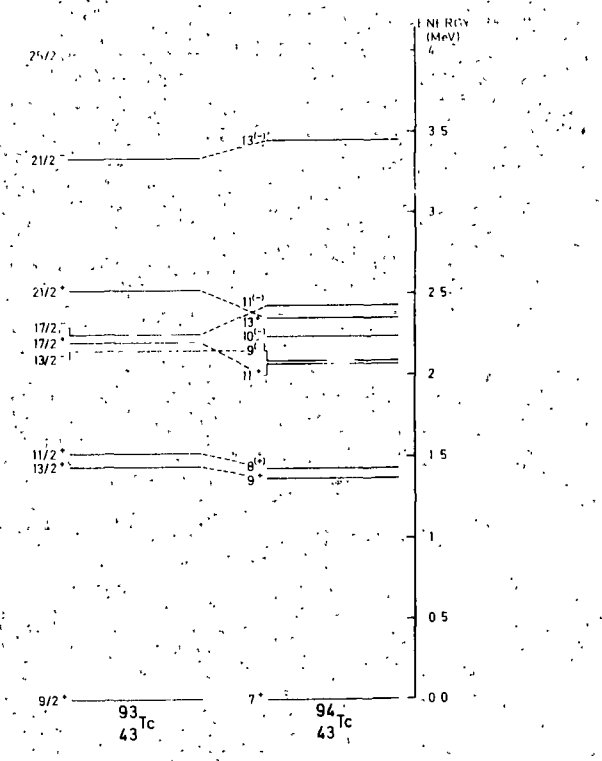

Figure 2

I.6 Investigation of the $\tilde{\pi}g_{9/2} \times \tilde{\nu}g_{9/2}$ Structure in ^{76}Br above $I^{\pi}=9^{+}$

M.A.J.Mariscotti, A.J.Kreiner, C.Baktasch*, E. Der Mateosian*, and P.Thieberger*.

Previous work[1,2,3] on ^{76}Br has provided information on a quasi-rotational band, built on the $\tilde{\pi}g_{9/2} \times \tilde{\nu}g_{9/2}$ configuration, up to $I^{\pi}=9^{+}$. At this spin value, (which corresponds to the maximum spin $I_M=j_p+j_n$ resulting from the coupling of the valence proton and neutron), a change in the usual odd-even level staggering has been predicted[3,4]. This prediction

has been shown[4] to be corrected in decays of other double odd nuclei, and it is related to the fact that for $I>I_M$ the energy of the nuclear system is incremented almost exclusively by increasing the state of collective rotation, while for $I<I_M$ the orientation of the valence particles plays the dominant role.

The present investigation was undertaken with the purpose of reaching higher levels ($I>I_M$) of the $\tilde{\pi}g_{9/2} \times \tilde{\nu}g_{9/2}$ system in ^{76}Br and test the prediction in this nucleus. To improve on the available work[1,2] done with 55 MeV alpha-particles, we have used the ^{62}Ni (^{16}O,np) reaction at E=55 and 65 MeV produced in the Brookhaven National Laboratory Tandem. The result of this and earlier work are summarized in figure 1. In addition to the previously known levels only evidence for a 10^+ and (11^+) state was obtained. Evidently there is strong side feeding populating this band at $I\sim 9-10$.

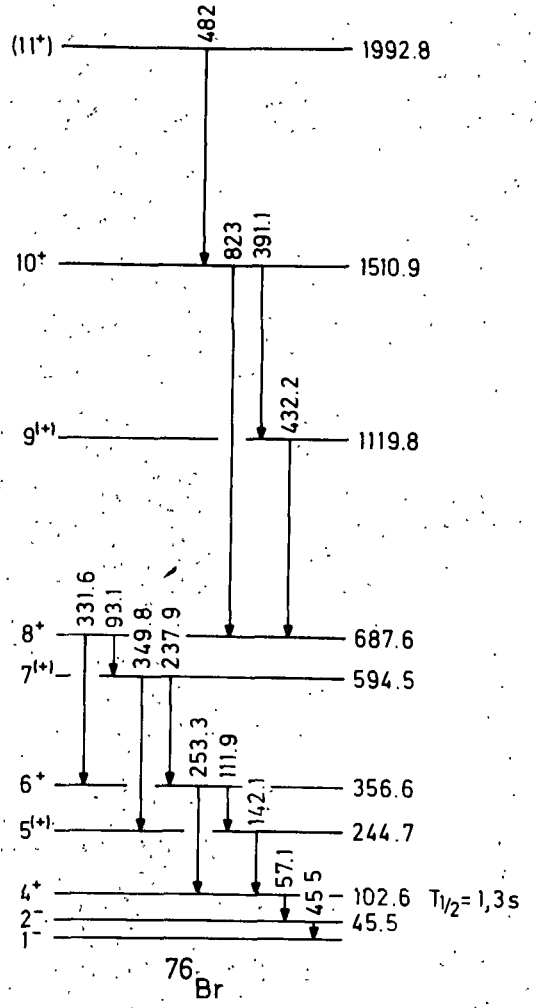

Figure 1

Figure 2 shows the level staggering in ^{76}Br deduced from the data in figure 1 and that corresponding to ^{74}Br from ref. 5. In the latter case, a change of phase at I=9 had already been pointed out[5]. For ^{76}Br, the present results also show a break, although a change of phase does not fully take place. This effect constitutes a novel property of the structure of doubly odd nuclei which is currently associated with the idea outlined above, and has been adequately reproduced by the calculations[3]. However, while the relative large spacings for the $I>I_M$ states are easily understood, the physical phenomenon giving rise to the repulsion of the I_M state from the rest of the multiplet needs further analysis.

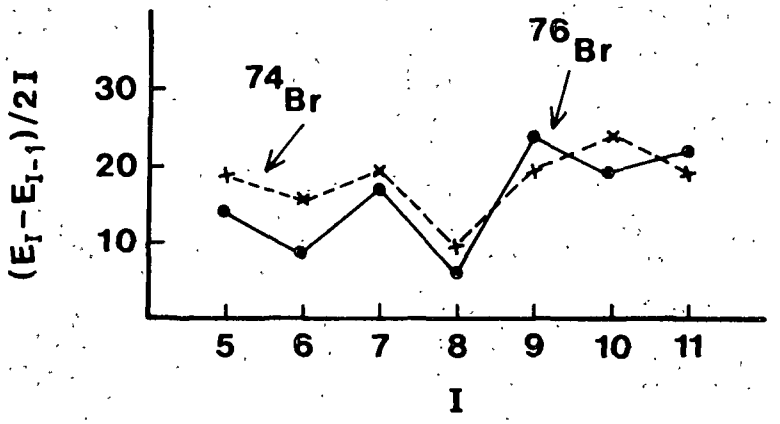

Figure 2

While carrying out this investigation, a study by J.C. Wells et al[6] came to our attention, which reports on levels of ^{76}Br populated through the ^{66}Zn(^{12}C,np). Our results are in agreement with theirs. In addition they report on several other side levels.

---

* Department of Physics, Brookhaven National Laboratory, Upton, USA.

1) M. Behar, A. Filevich, G. García Bermudez, and M.A.J. Mariscotti Nucl. Phys. A282 (1977)331.

2) W.D. Schmidt-Ott, A.J. Hautojärvi, and U.J. Schrewe Z. Physik A289 (1978)121.
A.J. Kreiner, G. García Bermúdez, M.A.J. Mariscotti Phys.Lett B83 (1979)31.

3) A.J. Kreiner and M.A.J. Mariscotti, Phys. Rev.lett. 43 (1979)1150.

4) A.J. Kreiner and M.A.J. Mariscotti, Journal of Physics G(Nucl.Phys) 6 (1980)L13.

5) G. García Bermudez, A. Filevich, A.J. Kreiner, M.A.J. Mariscotti, C. Baktash, E. Der Mateosian, and P. Thieberger Phys.Rev. C23 (1981)2024.

6) J.C. Wells, R.L. Robinson, H.J. Kim, R.O. Sayer, R.B.Piercey, A.V. Ramayya, J.H. Hamilton, C.F. Maguire, K. Kumar,R.W. Eastes, M.E. Barclay, and A.J. Caffrey Phys.Rev.C24 (1981)171.

I.7 In Beam Study of ^{97}Rh

A.O. Macchiavelli, M. Behar, A. Ferrero and A. Filevich

In the present work we have studied the excited states of ^{97}Rh through the reaction ^{96}Rn(α,2np). With this purpose we have performed singles and gamma-gamma coincidence experiments together with angular distribution measurements. As a result a preliminar level scheme has been constructed, which is shown in figure 1. No spin assignment have been performed yet since the analysis of the angular distribution data is in progress.

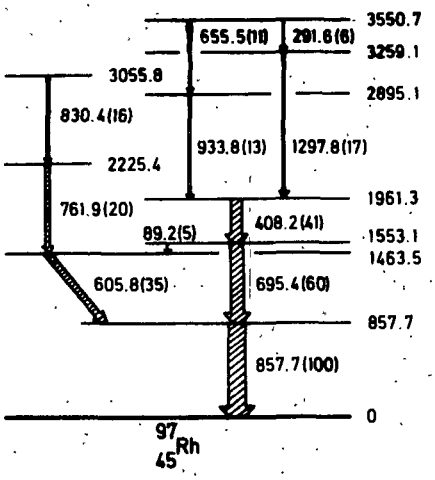

Figure 1

I.8 Possible Answer to the ^{100m}Rh Controversy

A.O. Macchiavelli, M. Behar, A. Filevich, and M.A.J. Mariscotti

The 4.7 min isomer in ^{100}Rh has been the object of several studies yielding contradictory results. These are summarized in figure 1 (a), (b) and (c). The isomer was first reported by Sieniawski[1] to lie at 339.5 keV with $I^{\pi}=(5^{+})$ and feeding the known (from the Pd decay) states at 74.8, 32.7 and 0.0 keV [figure 1 (a)]. A subsequent investigation by Kiselev et al[2] disproved the existence of a 264.7 keV isomeric transition and they proposed the scheme shown in figure 1 (b). The E3 multipolarity for the 74.8 keV isomeric transition of Kiselev et al was deduced from the gamma-intensity assuming perfect total intensity balance. This multipolarity was consistent with the previous assignment $I^{\pi}=5^{+}$ for the isomer.

In a third investigation, however, Babenko et al[3] measured conversion coefficients and inferred that the correct multipolarity of the 74.8 keV transition was M2 and not E3. This implies $I^{\pi}= 4^{+}$ for the isomer [figure 1 (c)]. This is the latest report available in the literature. It is at once evident that the existence of a 2^{+} state at 74.8 keV is inconsistent with this result since a prompt E2-transition to this state should destroy the isomerism.

We wish to point out in this note that a possible solution to this puzzle is that indicated in figure 1(d). Since the transition energy from the isomer to the 2^{+} state coincides with that from the 2^{-} to ground, the possibility of a double cascade involving two unresolved doublets exists, with such gamma-intensities that the combined multipolarities for each doublet gives an "effective" conversion coefficient which agrees with the experimental value of Babenko et al[3].

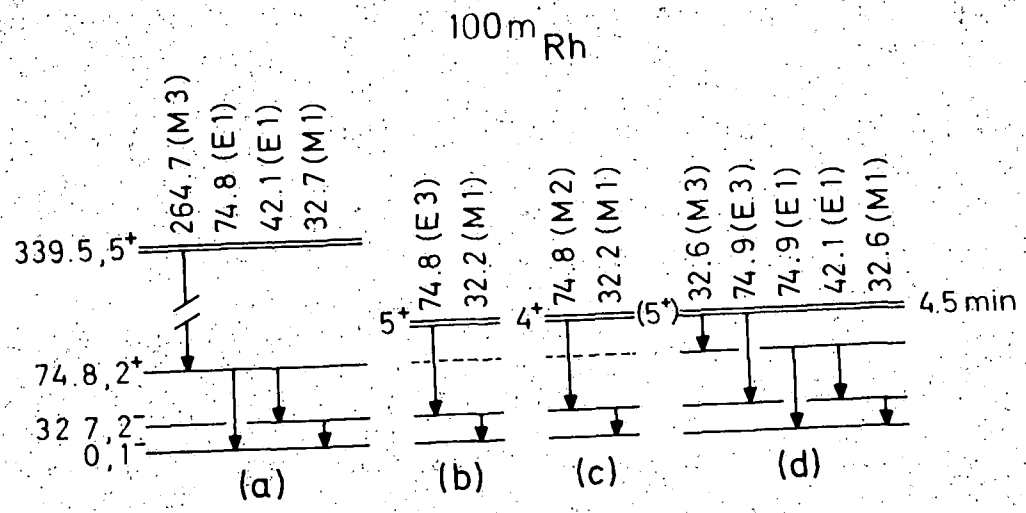

Figure 1

In order to check this explanation for the true nature of the ^{100m}Rh isomer we have carried out a series of measurements using the reactions $^{99}Ru(\alpha,2np)$, $^{100}Ru(\alpha,3np)$ and $^{100}Rh(d,2n)$ produced with the Buenos Aires Synchrocyclotron. The former two reactions also yield ^{100}Pd (which decays into ^{100}Rh) while the latter does not, so that a useful comparison of the respective spectra could be made. Spectra were measured on-and off-line with a high resolution X-ray Ge(Li) counter. No evidence for doublets was found in the analysis of the 74 keV peak and a limit of $\Delta E \leq 200$ eV was obtained. On the other hand the 4.5 ± 0.3 min decay shows, in addition to the 32.6 and 74.9 keV peak, a line at 42.1 keV. This result provides important evidence in favor of the hypothesis above. Unfortunately difficulties in obtaining adequate thin targets have prevented us until now from making an accurate determination of the intensity of the 32 and 42 keV peak. If this measurement yields the combined intensity values shown in Table I, full

consistency will have been achieved: the 32.6 keV peak will consist of an M1 and an M3 line, both yielding an effective conversion coefficient of 11. Similarly the two components, E1 and E3, of the 74.9 keV doublet yield an effective conversion coefficient of 10. These two values agree with the experimental data and at the same time are consistent with a 5^+ assignment for the ^{100m}Rh isomer.

TABLE I

E (keV)	multipole	deduced intensities gamma	deduced intensities total	effective conv.coeff deduced	effective conv.coeff meas
32.6	M3[b]	2×10^{-2}	150	11	8.1 3.0
	M1[a]	98	1008		
42.1	E1[a]	14	38		
74.9	E3[b]	18	970	10	12 3
	E1[a]	82	113		

a) Known
b) assumed
c) Ref.3

We are grateful to E. Achterberg for his help in performing accurate peak fitting analysis with the program ANPIK.

1) J. Sieniawski, Acta Phys. Polonica, B5 (1974)549

2) B.G. Kiselev et al, Izv.Akad.Nauk.Ser.Fizika 42 (1965)823

3) V.V. Babenko et al, Izv.Akad.Nauk.Ser.Fizika 44 (1980)1056

I.9 On Line Study of High Spin States in ^{100}Rh

M. Behar, A. Ferrero, G García Bermudez, A.J. Kreiner, A.O. Macchiavelli, M.A.J. Mariscotti and C. Baktash*

Up to now the information available on levels of ^{100}Rh was limited to that obtained from the ^{100}Pd (3.6 d) and ^{100m}Rh (4.7min) decays. Contradictory evidence has been reported for the latter, and a possible answer is provided in a separate communication of this Progress Report.[1)]

The on-line study was carried out with the Buenos Aires Synchrocyclotron and the Brookhaven National Laboratory Tandem by means of the reactions ^{99}Ru(α,2np) and ^{98}Mo(^{6}Li,4n), respectively. Excitation functions, gamma-gamma coincidences, lifetimes and angular distributions were measured. The results are summarized in figure 1. None of the levels shown were hitherto reported. The intensity balance shows that the decay of the residual nucleus feeds the (5^+) isomer in ^{100}Rh.[1)] A halflife of $T_{1/2}$=100 $\pm$ 10ns has been determined for the state at 111.9 keV above the isomer. The level scheme follows the generally expected pattern for a doubly odd nucleus, that is, a multiplet of states lying lowest, (steming from the different angular momentum couplings of the valence proton and neutron) and a sequence of levels with increasing spins and energy spacings roughly comparable to the collective excitations of the even-even core.

In the present case two sets of levels seem to coexist since states with spin values I=6,7 and 8 appear twice. A possible interpretation is that this is due to the existence of a dominant proton configuration $\pi g_{9/2}$, and

two competing neutron orbitals, $\nu d_{5/2}$ and $\nu g_{7/2}$. Calculations based on a two quasi-particle plus rotor Hamiltonian are in progress.

---

* Department of Physics, Brookhaven National Laboratory, Upton, USA.

1) A.O. Macchiavelli, et al., Paper I.8, this report.

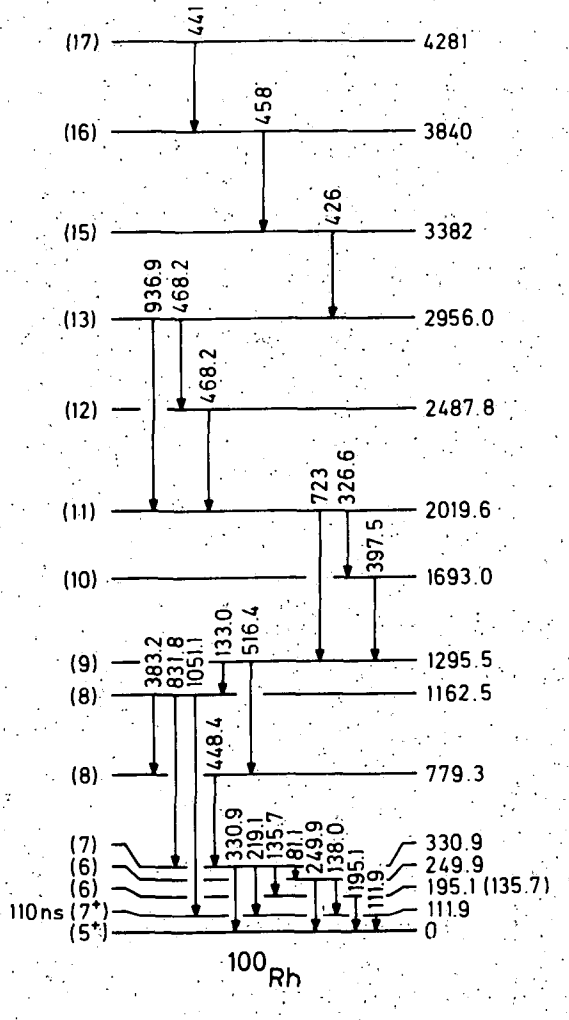

Figure 1

I.10 High Spin Structure of ^{75}Br and the (N,Z) Dependence of the Nuclear Deformation in the Br Region*

A.J. Kreiner, M.A.J. Mariscotti, C. Baktash**, E. der Mateosian**, and P. Thieberger**.

The nucleus ^{75}Br has been studied through the ^{62}Ni(^{16}O,2np) reaction. A 4.5 mg/cm^2 self-supporting enriched ^{62}Ni foil was irradiated with an ^{16}O beam from the Brookhaven National Laboratory Tandem Van de Graaff in the 45-70 MeV bombarding energy range. A positive and a negative parity band were established up to spin (25/2). A new low-lying isomeric $(9/2^+)$ state ($T_{1/2}$=39±4 nsec) at 220.6 keV excitation energy, almost certainly of $\tilde{\pi}g_{9/2}$ parentage, was found thus solving the longstanding problem of its location.

Suggestions were made that the $9/2^+(\tilde{\pi}g_{9/2})$ state should occur at very low excitation energy (or even be the ground state) in ^{73,75}Br due to an increasing deformation with decreasing neutron number. However, the appearance of a $9/2^+$ state as the band head for the $g_{9/2}$ system (as is the case in ^{77}Br) has to do with the tendency of the I=j=9/2,R=0 totally decoupled state to lie lowest for small prolate deformations and Fermi levels below the j shell[2] (i.e. the Ω=1/2 Nilsson orbit lowest in energy). For larger prolate deformations orbits with larger projections on the symmetry axis (Ω=3/2,5/2,...) come nearer to the proton Fermi surface thus generating states of smaller total angular momentum as the lowest states of the $g_{9/2}$ system.

The value of the deformation, β=0.31±0.02, for ^{75}Br extracted from the measured halflife of the $9/2^+$ state is in excellent agreement with the systematics obtained from neighboring even-even nuclei.

---

* Phys. Rev. C24 (1981)148. This work was sponsored by CONICET from

Argentina and the National Science Foundation,USA.
** Department of Physics, Brookhaven National Laboratory, Upton, USA.

1) E. Roeckl, D. Lode, and W. Pessara, Z. Phys. 226 (1974)123.

2) F.S. Stephens, Rev. Mod. Phys. 47 (1975)43.

I.11 Evidence for predicted level crossings in $\tilde{\pi} h_{9/2} \otimes \tilde{\nu} i_{13/2}$ bands in very neutron deficient doubly odd Tl isotopes*

A.J. Kreiner, C. Baktash**, G. García Bermudez, and M.A.J. Mariscotti.

High-spin bands based on isomeric states ($10 \leq t_{1/2} \leq 300$ nsec) have been found[1] over the last few years in doubly odd Tl isotopes in the A= 192-200 mass range (see figure 1). These bands represent the first examples of collective structures based on high-j excitations in doubly odd transitional nuclei and were successfully described as semidecoupled $\tilde{\pi} h_{9/2} \otimes \tilde{\nu} i_{13/2}$ systems using a two-quasiparticle plus rotor model[2]. They start with a set of transitions whose energies are small compared to energies in related bands of neighboring odd mass nuclei, i.e. $\pi h_{9/2}$ and $\nu i_{13/2}$ bands in odd Tl and Hg nuclei, respectively. The reason for this has to do with the fact that in doubly odd nuclei, where the intrinsic spin, J, is built out of two parts ($\vec{J}=\vec{j}_p+\vec{j}_n$), there is a multiplet associated with small core excitation (that with I=J and $|j_n-j_p| \leq I \leq j_n+j_p$). The fact that the lowest-lying state within this multiplet has a spin value of around 8 is related to the positions of proton and neutron Fermi levels, λ_p and λ_n, relative to the $h_{9/2}$ and $i_{13/2}$ Nilsson multiplets, respectively. The proton orbital is intruding from the next shell across the Z=82 closure and since the deformation is oblate, the Nilsson state with the largest projection on the symmetry axis (Ω_p=9/2) lies nearest to λp, giving rise to "normal" $\Delta I=1$

bands in odd Tl isotopes[3]. On the other hand, for N≳117 the Ω_n=1/2 member of the $i_{13/2}$ orbital lies close to λ_n, resulting in decoupled bands in odd Hg isotopes[4], in which $\vec{j}_n$ is approximately in a plane perpendicular to the symmetry axis. Hence, the energetically most favorable situation for the heavy doubly odd Tl isotopes is the perpendicular coupling of $\vec{j}_p$ and $\vec{j}_n$ which corresponds to J≳8. Higher-spin states in the multiplet (in principle up to I=9/2 + 13/2=11) are obtained by progressive alignment of j_p and j_n with respect to each other at the expense of intrinsic energy. In going to the neutron deficient side, however, λ_n starts penetrating the $i_{13/2}$ subshell and neutron quasiparticle states with larger-projections on the symmetry axis (Ω_n=3/2,5/2,...) become succesively lowest. The implication for the doubly odd system is that states with higher total angular momentum within the multiplet come down in energy. Eventually the state with I=9 will cross below the one with I=8 and subsequently I=10 below I=9. etc. For the observed structures in the Tl nuclei, which depopulate into long lived 7^+ states, this means that the character of the isomeric out-of-band transition will change from E1 to M2, E3, etc., thus giving rise to increasingly longer lifetimes.

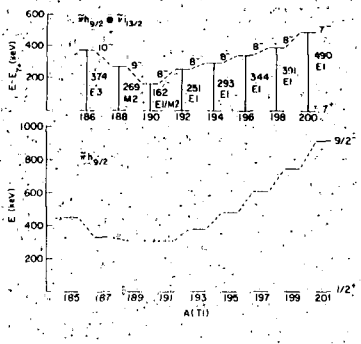

Figure 1

Systematics of excitation energies of the bandheads of $h_{9/2} \times i_{13/2}$ - and $h_{9/2}$ - structures in odd-odd and odd Tl isotopes respectively (Refs.1,3). The excitation energies in ^{189,191}Tl are not precisely known.

In order to verify these predictions, a study of the isotopes ^{186,188,190}Tl was undertaken using several (H.I.,xn) reactions: ^{168}Er(^{27}Al,5n) ^{190}Tl(E=130-160 MeV), ^{169}Tm(^{25}Mg,4n) ^{190}Tl(E=120 MeV), and ^{176}Hf(^{19}F,5n) ^{190}Tl(E=85-120 MeV; ^{169}Tm(^{24}Mg,5n) ^{188}Tl(E=115-135 MeV), and ^{159}Tb(^{32}S,5n) ^{186}Tl(E=160-165 MeV) and ^{155}Gd(^{35}Cl,4n) ^{186}Tl(E=155-170 MeV). Heavy ion beams were accelerated by the Tandem Van de Graaff at Brookhaven National Laboratory. The decays of the residual nuclei were studied using in-beam and off-beam gamma-ray spectroscopy techniques revealing the existence of bands similar to those found in the heavier Tl isotopes. Isomeric lines with transition energies of 161.9, 268.8, and 374.0 keV were identified in ^{190}Tl, ^{188}Tl and ^{186}Tl respectively. Some of their decay properties are shown in figure 1 providing striking confirmation of the predictions discussed above. Figure 1 also shows the neutron number dependence of the $\tilde{\pi}\, h_{9/2}$ band heads in neighboring odd Tl isotopes which appears to be similar to that of the $\tilde{\pi}\, h_{9/2} \otimes \tilde{\nu}\, i_{13/2}$ band heads, lending additional support for the present interpretation.

---

* Accepted by Phys.Rev.Lett. Worked performed under the auspices of CONICET, Argentina, and National Science Foundation, USA.

** Department of Physics, Brookhaven National Laboratory, Upton, USA.

1) A.J. Kreiner, M.A.J. Mariscotti, C. Baktash, E. der Mateosian, and P. Thieberger, Phys.Rev. C23 (1981)748.

2) A.J. Kreiner, Z. Physik A288 (1978)373.

3) J.O. Newton, F.S. Stephens, and R.M. Diamond, Nucl. Phys. A236 (1974)225

4) D. Proetel, D. Benson, Jr., A. Gizon, J. Gizon, M.R. Maier, R.M. Diamond, and F.S. Stephens, Nucl. Phys. A226 (1974) 237.

I.12 Structure in ^{200}Tl and the Odd-even Staggering in $\tilde{\pi}h_{9/2} \times \tilde{\nu}i_{13/2}$ Bands.*

A.J. Kreiner, M.A.J. Mariscotti, C. Baktash**, E. der Mateosian**, and P. Thieberger.

States of ^{200}Tl, populated through the ^{198}Pt(^{6}Li,4n) reaction at E=30 to 40 MeV, were studied using in-beam gamma-ray spectroscopy techniques. An almost completely new level scheme is presented comprising the $\tilde{\pi}h_{9/2} \times \tilde{\nu}i_{13/2}$ two quasi-particle band[1] which in this case is built on an $I^{\pi} = 7^{-}$ isomeric state ($T_{1/2}$= 4.8±0.2 ns) in contrast to $I^{\pi}=8^{-}$ for all the lighter doubly odd Tl sotopes studied up to now. These bands show an alternation of large and small transition energies, instead of a monotonic increase, with increasing angular momentum, a phenomenon which is called staggering. As far as this staggering is concerned the new data on ^{200}Tl provide a very interesting piece of evidence. In an attempt to characterize quantitatively the staggering a variable S is defined as $S=(l_1+l_3-2l_2)/(l_1+l_3+2l_2)$ where l_1, l_2, l_3 are the lowest three transition energies for the $\tilde{\pi}h_{9/2}$ bands in neighboring odd Tl isotopes and for the odd-odd cases they represent the transitions preceding the low energy multiplet[1]. We see that $1>S>-1$ (for $\Delta I=1$ bands) and it can be shown that S vanishes for any three consecutive transitions in a rigid rotor band. This variable is seen to behave in very much the same way in the bands of odd mass and doubly odd Tl nuclei with a tendency to disappear with increasing neutron number. This behavior strongly suggests that in these doubly odd nuclei the mechanism behind the staggering entails an interaction of the particles with the core rather than among the valence nucleons themselves.

---

* Phys.Rev. C23 (1981)748. Work carried out under the auspices of CONICET, Argentina and the National Science Foundation, USA.

** Department of Physics, Brookhaven National Laboratory, Upton, USA.

1) A.J. Kreiner, Z. für Physik A288 (1978)373.

I.13 High Energy Gamma-ray Decay of Evaporation Residues from (H.I.,xn) Reactions*.

J. Barrete**, M.T. Collins**, A.J. Kreiner, A.M. Sandorfi**, M.Al-Kofahi***, and S. Steadman***.

So called continuum gamma ray spectra from evaporation residues formed in compound nucleus (H.I.,xn) reactions have usually only been studied up to $\simeq$5 MeV (e.g. Ref.1). According to the customary view these spectra mainly consist of two parts. One, reaching up to $\simeq$2 MeV, composed of stretched E2 transitions may carry nuclear structure information (e.g. moments of inertia at very high spins). The other one is described as an E1 statistical component being a structureless exponential tail which merely reflects average level density properties of the emitting system. No attempts have been made to extract any structure information from this component except for a single measurement reported very recently[2]. There the continuum studies were extended up to $E_\gamma \simeq 30$ MeV and a very interesting discovery was made. Above approximately 10 MeV the gamma-ray spectra depart from a simple exponential behavior showing an excess intensity which reportedly reaches its maximum at around 15 MeV. The suggestion has been made that this excess is a consequence of structure in the E1 strength function due to the giant dipole resonance built on excited states. A major assumption of that work[2] has been that the detected high energy gamma-ray intensity is related to the decay of compound systems since no unambiguous identification of the reaction channels involved was made. We report here

results of an experiment specifically designed to overcome this difficulty. High energy gamma-rays ($E_\gamma \gtrsim 5$ MeV) produced in the ^{130}Te (^{34}S,xn) reaction at E_{Lab}=141 MeV were studied using a high resolution ($\Delta E/E$=5% at E_γ=20 MeV) 25 cm x 25 cm collimated NaI detector in coincidence with low energy transitions detected in five large volume Ge(Li) counters thus allowing the selection of particular reaction products. The presence of an excess intensity above the statistical component for $E_\gamma \gtrsim 10$ MeV was confirmed in both the ^{161}Er (3n) and ^{160}Er (4n) evaporation residues. Some representative NaI gamma-ray spectra are shown in figure 1. Another important point is that the enhanced gamma-ray strength does not present any structure of width comparable to or larger than the detector resolution. This resolution is sufficient to reveal any structure similar to that known for the giant dipole resonance built on the ground states of the well deformed residual nuclei under consideration.

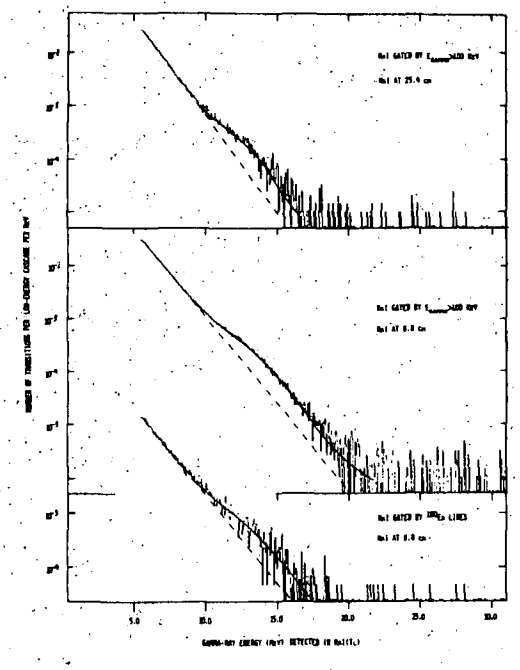

Figure 1

Gamma-ray spectra measured with a large volume NaI detector in coincidence with low energy transitions detected in Ge(Li) counters and normalized to the singles spectra in order to obtain the number of transitions per cascade. The upper part corresponds to a target-detector distance of 25.4 cm and was obtained in order to check for pile-up effect.

The present measurement enables us to study the cross section for production of high energy gamma-rays as a function of the reaction channel. For both the exponential statistical component and the excess strength at high energy, the number of transitions per cascade is a monotonic decreasing function of the number of evaporated neutrons (i.e. it is largest for the 3n channel, smaller for 4n, etc.). Another way of exhibiting this effect is by studying the relative intensity of the different channels in singles Ge(Li) spectra and in spectra where a coincidence is required with a gamma-ray ($E_\gamma \gtrsim 5$ MeV) in the NaI detector. Table I gives for the three reaction channels observed the relative intensities in singles and coincidence Ge(Li) spectra, the cross sections and the relative numbers of gamma-rays ($E_\gamma \gtrsim 5$ MeV) per cascade.

TABLE I

channel	I_γ singles (%±5%)	I_γ coinc. (%±5%)	σ (mb)	n_γ/cascade (rel.units±20%)
3n	4	16	13±3	1.2
4n	63	75	204±41	0.4
5n	33	9.5	107±21	0.1

This behavior can be interpreted in two ways:

a) The high energy gamma-rays ($E_\gamma \gtrsim 5$ MeV) come from regions in the E-I plane different from those from which the bulk of the cross sections come.

b) On the average the excitation energy above the yrast line is significantly larger the fewer the number of evaporated neutrons thus favoring higher gamma-ray energies.

The latter option would be in conflict with the standing opinion that the entry line in this type of rections runs more or less paralell to the yrast line and approximately one neutron binding energy above it independently of the channel. Nevertheless, in any event one would be probing regions of high excitation energy above the yrast line and an enhancement of the high-energy gamma-ray emission due to level density arguments[2] could be conceived.

Statistical model calculations performed with the program GROGI-F (ref.3) give a decrease in the absolute value of the slope in the gamma-ray spectra al E_γ increases. However this change appears to be too gradual to account for the data and would suggest that a major modification in the strength function and/or level density is required.

---

* Asilomar Meeting of the American Physical Society, October, 1981. Work done at Brookhaven National Laboratory.

** Department of Physics, Brookhaven National Laboratory, USA.

*** MIT, USA.

1) R.S. Simon, M.V. Banaschik, R.M. Diamond, J.O. Newton, and F.S. Stephens; Nucl. Phys. A290 (1977)253.

2) J.O. Newton, B. Herskind, R.M. Diamond, E.L. Dines, J.E. Draper, K.H. Lindenberger, C. Schück, S. Shih, and F.S. Stephens; Phys.Rev.Lett. 46 (1981)1383.

3) Modified version of GROGI 2 nuclear evaporation computer code including fission decay channel, H. Delagrange, CENBG 7707, Centre d'Etudes Nucléaires de Bordeaux-Gradignan.

I.14 Structure and Decay of the Highly Mixed $13/2^+$ States in ^{171}Er*.

A.J. Kreiner, P.D. Bond**, C. Baktash**, J. Barrette**, C.E. Thorn**, and M.T. Collins**.

The low-lying positive parity levels in neutron rich odd mass Er nuclei, which are due almost exclusively to the $i_{13/2}$ neutron orbital, are not well known. This situation, which is in sharp contrast with the well studied low-lying negative parity states, has been due to the lack of a mechanism to selectively populate high j single particle states. It has been recently shown, however, that there is a great selectivity to populate such levels for neutrons in heavy ion induced (^{16}O, ^{15}O) and (^{12}C, ^{11}C) reactions[1]. In particular the two lowest lying $13/2^+$ levels in erbium nuclei, nominally belonging to the $7/2^+[633]$ and $9/2^+[624]$ bands, were identified in that work. The systematic movement of these $13/2^+$ levels through the Er isotopes indicated that they would be nearly degenerate in ^{171}Er were it not for the Coriolis interaction. This presents the intriguing possibility to experimentally study two states which are as mixed in K as possible. In the present experiment the gamma decay of the lowest two 13/2 levels in ^{171}Er has been investigated using a particle-gamma coincidence technique, and confirmation is obtained that the earlier spin identification was correct. In addition, other members of the lower band ($7/2^+$) have been identified, the predominant modes of decay have been measured, and it is established that the band with larger $7/2^+[633]$ parentage lies lower than the one with greater amplitude of the $9/2^+[624]$ orbital, in contrast to an earlier conjecture[2].

Quasiparticle plus rotor model calculations have been made and compare well with the general features of both the particle and gamma-ray data.

---

* Accepted by Phys.Rev.C. Work done at Brookhaven National Laboratory.

** Department of Physics. Brookhaven National Laboratory, USA.

1) P.S. Bond, J. Barrette, C. Baktash, C.E. Thorn, and A.J. Kreiner, Phys.Rev.Lett. 46 (1981)1565.

2) B. Elbek, and P.D. Tjoem, DanskVid. Sesk. Mat.Medd 37 (1969)7.

I.15 Selective Population of High-j Orbitals in Er Nuclei by Heavy-ion-induced Transfer*

P.D. Bond**, J. Barrette**, C. Baktash**, C.E. Thorn**, and A.J. Kreiner.

In this work we report the use of two heavy-ion-induced stripping reactions to selectively populate high-spin particle states in deformed nuclei, specifically in ^{167,169,171}Er. The choice of the reactions studied here, (^{16}O,^{15}O) and (^{12}C,^{11}C), is based upon two factors. Their large negative Q values mismatch the incoming and outgoing grazing angular momenta so that small angular momentum transfers are strongly suppressed. The consequences of these kinematic conditions and selection rules which result from the transfered neutron in the projectile being $p_{1/2}$ for ^{16}O and $p_{3/2}$ for ^{12}C lead to a strong favoring of high-spin final states with spin $j_>$ ($j_f=l_f+1/2$) for ^{16}O projectiles, while high spin $j_<$ ($j_f=l_f-1/2$) and $j_>$ states are comparable for ^{12}C. The strong difference in the relative population of $j_>$ and $j_<$ final states for these two reactions is used to distinguish $9/2^-(h_{9/2})$ from $13/2^+(i_{13/2})$ states which the (α,^{3}He) reaction has difficulty doing from either strength or angular distribution measurements.

Targets of enriched ^{166,168,170}Er of 50-200 μg/cm^2 evaporated on thin C backings were bombarded with 120-MeV ^{16}O and 95-MeV ^{12}C ions from the Brookhaven National Laboratory tandem facility and outgoing ^{15}O and ^{11}C ions

were momentum analyzed by the quadrupole-triple-dipole spectrometer and identified in a position sensitive ΔE-E gas proportional counter. Typical resolutions for ^{15}O ions ranged from 100-150 keV and for ^{11}C from 80-120 keV.

Heavy-ion-induced transfer reactions on heavy nuclei have bell-shaped angular distributions, a shape independent of angular momentum trasfer. As a result a large fraction of the transfer yield can be subtended by the spectrometer at a single setting (typical solid angles used were 12 msr), a circumstance which made coincidence measurements with gamma-rays detected in Ge(Li) counters possible.

Through the strong selective population of known high-spin levels and the identification of previously unobserved high-j states in Er nuclei, this experiment has clearly demostrated that the unique features of heavy-ion-induced transfer make these reactions invaluable especially in spectroscopic studies of neutron rich nuclei which cannot be reached through the conventional (H.I.,xn) reaction.

---

* Phys.Rev.Lett. 46 (1981)1565. Work done at Brookhaven National Laboratory.

** Department of Physics, Brookhaven National Laboratory, USA.

I.16 $\tilde{\pi}g_{9/2} \otimes \tilde{\nu}g_{9/2}$ Structure in ^{78}Br

M. Behar, D. Abriola, A. Filevich, G. García Bermudez, A.J. Kreiner, M.A.J. Mariscotti, J.A. Pinston*, and D. Barneoud**.

Following the succesful description[1] of the correspondence found[2] between positive parity bands of $g_{9/2}$ parentage in ^{76}Br and ^{77}Kr, it is of

interest to search for the same excitations in ^{78}Br and to study to which extent they are related to levels in ^{79}Kr.

The existence of a $\tilde{\pi} g_{9/2} \times \tilde{\nu} g_{9/2}$ band structure built on the known 4^+ isomer in ^{78}Br was recently investigated[3),4)] and it is likely that some of the observed[4)] levels correspond to the lowest multiplet expected from this system. In order to gain more information on this band structure a search for higher states in ^{78}Br was performed. The ^{77}Se(α,2np) reaction produced with the 30 to 55 MeV alpha-beam of the BA Synchrocyclotron and the ^{76}Ge(^{7}Li,5n) reaction produced with the Grenoble isochronous cyclotron, were used in conjunction with conventional on-line gamma-ray spectroscopy techniques. The level scheme in the figure 1 summarizes the results. The levels up to 467.6 keV have already been reported[4),5)]. Of particular interest is the 904.1 keV transition which exhibits quadrupole character and compares well with the $(11/2^+)$ to $7/2^+$ spacing in ^{79}Kr. In order to check the assumption that the sequence of levels with I=4, (5),...(8),(9) and (10) in ^{78}Br corresponds to a $\tilde{\pi} g_{9/2} \times \tilde{\nu} g_{9/2}$ rotational like structure a calculation, similar to that performed for ^{76}Br (ref.1), has been carried out. The model involves a non-interacting quasiproton and neutron coupled to a rigid rotor. The neutron parameters were determined by fitting the positive parity band in ^{79}Kr. The deformation was taken as a mean value from that of the neighboring even-even cores. The main results of the calculation are: a) the $4^+,5^+,...8^+$ members of the lowest multiplet, corresponding to almost vanishing rotation, lie within 300 keV (in contrast to 600 keV in ^{76}Br owing to the smaller deformation); b) the 9^+ state is pushed up about 0.5 MeV above the 8^+ state; c) the predicted spacing between the 10^+ and 8^+ state is 0.9 MeV. These results are fully consistent with the data and hence provide evidence for the validity of the present interpretation.

---

* CEN, Grenoble, France.

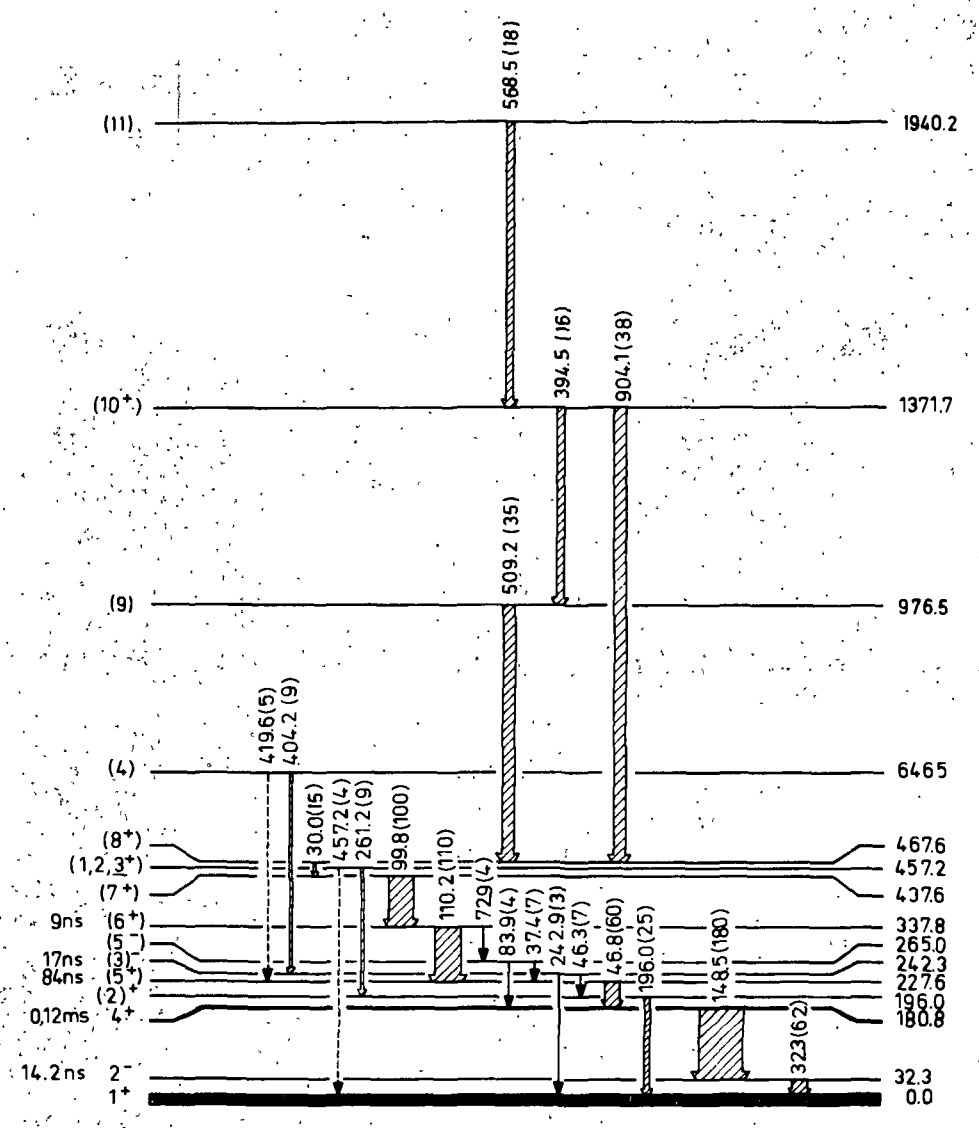
568.5 (18)
(11)
1940.2
394.5 (16)
904.1 (38)
(10+)
1371.7
509.2 (35)
(9)
976.5
419.6(5)
404.2 (9)
(4)
646.5
30.0(15)
457.2(4)
261.2(9)
99.8(100)
110.2(110)
729(4)
(8+)
(1,2,3+)
(7+)
467.6
457.2
437.6
9ns (6+)
(5-)
17ns (3)-
84ns (5+)
(2)+
0,12ms 4+
83.9(4)
37.4(7)
242.9(3)
46.3(7)
46.8(60)
196.0(25)
148.5(180)
323(62)
337.8
265.0
242.3
227.6
196.0
180.8
14.2ns 2-
1+
32.3
0.0
78
Br
35 43

Figure 1

** ISN, Grenoble, France.

1) A.J. Kreiner and M.A.J. Mariscotti, Phys.Rev.Lett. 43 (1979)1150

2) M. Behar et al. Nucl.Phys. A282 (1977)331, and A.J. Kreiner et al. Phys.Lett 83B (1979)31.

3) B.M. Kluger-Bell et al. J.Phys.G.Nucl.Phys. 5 (1979)827

4) G. García Bermudez et al. J.Phys.G.Nucl.Phys. (in press)

5) C.M. Lederer et al. Table of isotopes (1978), New York, J.Wiley and Sons, Inc.

I.17 Check on a Prediction for the Maximum Relative Cross Section of the $^{64}Zn(\alpha,n)$ Reaction.

M.A.J. Mariscotti, Solange de Barros*, L.T. Auler**

A few years ago a systematic study of relative cross sections for the various outgoing channels from the $^{64,66,67,68}Zn(\alpha,xnypz\alpha)$ reactions was reported[1]. These reactions were produced at bombarding energies between 30 and 55 MeV. In this energy interval the number of evaporated particles x + y + z ruoghly varies from 2 to 4.

The data obtained from these measurements were shown to follow a gradual behavior as a function of atomic mass, or equivalently, the degree of neutron deficiency of the target[1),2),3)]. Two parameters were studied: the energy E_{max} at which the excitation function reaches the maximum value and the relative cross section σ_{max} corresponding to this maximum.

In particular, the behavior of the latter quantity was described by a very simple phenomenological model. In view of the simplicity of this model and the relative success achieved in accounting for the data, it was of interest to check the predictions obtained outside the measured range. One possibility, provided by the low energy ciclotron of the Universidade

Federal do Rio de Janeiro, was to determine σ_{max} for the (α,n) reactions (i.e. x=1,y=0,z=0) on the same Zn isotopes, for energies $E_\alpha < 30$ MeV.

In the case of the ^{64}Zn target, several relative cross sections have been measured and fitted to the model[1], but only one for the (α,xn) group, namely that corresponding to x=2. Consequently the $^{64}Zn(\alpha,n)$ reaction provided an interesting test case, specially in view of the fact that its cross section is predicted to be more than 1 order of magnitude larger than that for the $(\alpha,2n)$ and comparable to the (α,np) reactions. Experimentally it was possible to carry out the measurement by irradiating a natural target and looking at the residual activity.

A stack of 5 mg/cm^2 foils of Zn, separated by sheets of Al of appropiate thicknesses was irradiated with the 28 MeV alpha-beam from the UFRJ cyclotron. The Al sheets were chosen so as to obtain Zn samples irradiated at several energies between 28 and 12 MeV in steps of 4 MeV.

In these measurements the (α,np) reaction was chosen as normalization. Known[1] to reach its maximum cross section at 28 MeV, the normalization was deduced from the intensity of the 1039 keV line from the $^{64}Zn(\alpha,np)^{66}Ga \xrightarrow{9.4h} {}^{66}Zn$ decay, after correcting for the halflife, crossover transitions and efficiency. The relative cross section of the (α,n) channel was in turn deduced from the gamma-intensity of the 167 keV line from the $^{64}Zn(\alpha,n)\ ^{67}Ge \xrightarrow{19min} {}^{67}Ga$ decay for each beam energy. The maximum cross section is obtained at 18 MeV and its value, relative to the (α,np) channel is

$$\frac{\sigma_{max}(\alpha,n)}{\sigma_{max}(\ ,np)} = 0.56 \pm 0.17 \qquad \text{for } ^{64}Zn$$

This value is in reasonable agreement with the predictions of the model; it represents about 20 times the previosly measured $\sigma_{max}(\alpha,2n)$, and

furnishes an additional evidence of the validity of the simple phenomenological model of ref.1.

This not only poses interesting questions as to the justification of the assumptions involved but also may estimulate its extension[3] to other regions of the Periodic Table and to be applied as a useful auxiliary tool in this type of spectroscopy work.

---

* UFRJ, Rio de Janeiro, Brazil.

** IEN, Brazil.

1) C. Pomar (thesis) unpublished, 1975 and C. Pomar and M.A.J. Mariscotti, 61st Meeting of Argentina Physical Society (Buenos Aires).

2) M.A.J. Mariscotti, R.M. Lieder, H. Beuscher, W.F. Davidson and A.Neskakis Z. für Physik A279 (1976)169.

3) M. Davidson, J. Davidson and M.A.J. Mariscotti Nucl. Phys A352 (1981)237.

I.18 Collective States in the Doubly Odd ^{72}Br Nucleus

G. García Bermudez, C. Baktash* and O. Kistner*

A recent study of the doubly odd nucleus[1], ^{72}Br, established a gamma-ray cascade of quadrupole transitions. The decay properties of this cascade suggest that these gamma-rays deexcite positive parity states. Positive parity $\Delta I=1$ bands had been found in ^{74,76}Br [Refs. 2,3]. The band in ^{76}Br has been described assuming two non-interacting quasiparticles, of $g_{9/2}$ parentage, coupled to a rigid rotor[4]. From the linear relationship between the level energy and I(I+1) which shows an effective moment of inertia similar to that of ^{74,76}Br (see figure 5, ref.1), it can be suggested that the ^{72}Br cascade could likewise be associated with the high

spin intrinsic $\pi g_{9/2} \times \nu g_{9/2}$ configuration. The purpose of this work is to explore further these similarities by measuring the lifetime of the levels of interest in order to determine the degree of collectivity involved.

Lifetimes were measured by the recoil-distance Doppler-shift technique. The nuclei were produced by the $^{58}Ni(^{16}O,np)$ reaction, provided by the Brookhaven National Laboratory tandem accelerator. The target was a stretched ^{58}Ni foil (99.9%) of 0.4 mg/cm^2 thickness and a thick piece of ^{208}Pb was used to stop the recoiling nuclei and the beam. The target-stopper distance was varied from 1 - 10,000 μm. Gamma-rays were measured with a Ge(Li) detector placed at 0° relative to the beam direction. The average recoil velocity (v_z/c) of the ^{72}Br nuclei as determined from the energy shift between the full Doppler shifted and unshifted gamma-ray was 1.58(5)%. An automated plunger device was used for these measurements which provided the capability of repeatedly cycling through a predetermined set of recoil distances, changing position every few minutes. In this way, systematic errors arising from drifts in the electronics and changes in the condition of the target due to the action of the beam were minimized. The cycling time was determined by gamma-ray counts derived from windows set on the 774.7 and 862.0 keV transitions, which deexcite levels of ^{72}Se. Several sets of measurements covering different flight distance intervals were performed. Due to background and interfering effect from other gamma-rays, most of the transitions were analyzed measuring the intensity of the unshifted peak with the exception of the 353.3 keV transition where measurements of the shifted peak were more favorable. The area of the unshifted transitions were corrected for solid angle, normalizing the data with the intensity of the Pb-xray observed from the moving stopper. A preliminary analysis of the data indicated that the lifetimes of the 1448.0, 1344.7, 991.4 and 668.2 keV levels ranged from 40 to 200 ps. Similarity in lifetimes, among these levels, made it necessary to analyze each level considering the influence of

Table I

Lifetimes and transition probabilities in ^{72}Br

State E_x(keV)	I	E (keV)	I_i	I_f	Branch (%)	(ps)	$\frac{B(E2)exp}{B(E2)w}$	B(E2)exp ($_{10}+1e^2fm^4$)
1344.7	(8)	353.3	(8)	(6)	100	126(28)	66(15)	117(26)
911.4	(6)	323.2	(6)	(4)	100	104(31)	125(37)	222(66)
668.2	(4)					206(80)		
		270.0	(4)	(2)	50.5	408(16)	78(31)	138(55)
		289.1	(4)	(2)	22	925(370)	25(10)	44(18)

delayed feeding from the higher levels as well as side feeding. For this purpose, the code MASTER[5] which describes the time evolution of the deexcitation process between many nuclear levels, was used. In table 1 the experimental transition probabilities for the 353.3, 323.2 and 270.0 keV transitions are reported. They show a strength ranging from 66 to 125 single particle units. This enhancement clearly indicates that these levels are highly collective and supports the previously noted similarities with the band structure found in the heavier isotopes ^{74,76}Br.

---

* Brookhaven National Laboratory, Upton, N.Y. 11973, USA.

1) G. García Bermudez, C. Baktash, A.J. Kreiner, and M.A.J. Mariscotti, Phys.Rev.C. March (1982).

2) G. García Bermudez, A. Filevich, A.J. Kreiner, M.A.J. Mariscotti, C. Baktash, E. der Mateosian, and P. Thieberger, Phys.Rev. C23 (1981)2024.

3) M. Behar, A. Filevich, G. García Bermudez, and M.A.J. Mariscotti, Nucl.Phys. A282 (1977)331; A.J. Kreiner, G. Garcia Bermudez, M.A.J. Mariscotti, and P. Thieberger, Phys.Lett 83B (1979)31.

4) A.J. Kreiner and M.A.J. Mariscotti, Phys.Rev.Lett. 43 (1979)1150.

5) H. Emling, GSI, Darmstadt 1979 (private communication).

I.19 Search for the Two Phonon Octupole Vibration in ^{208}Pb

W.F. Davidson*, W. Gelletly**, P. Hungerford+, W.R. Kane++, S. Kerr#, M.A.J. Mariscotti, K. Schreckembach# and D.D. Warner++

The nucleus ^{208}Pb is a suitable candidate for a search of two-phonon octupole states. An attempt to identify some of these states, in particular the 0^+ member of the multiplet, was made using the inelastic scattering reaction of Xe against Pb but the measurement was not sensitive enough[1]. In the present work, a different measurement with the same objective was undertaken: the detection of decay conversion electrons and coincidence gamma rays produced in the thermal neutron capture reaction on ^{207}Pb. Since the capture state has spin-parity 0^- or 1^-, population of 0^+ states in ^{208}Pb is expected. This reaction has already been studied[2,3,4]. Most of the total cross section (700mb) corresponds to the transition to the ground state; no more than 0.5% proceeds via other transitions and until now only the populations of the first 3^- and 2^+ states have been observed[2,3].

In spite of this limitation two types of experiments were programmed at the High Flux Beam Reactor of the Institute Laue-Langevin capable of reaching sensitivities of up to 30 μb. In the first one, a search for E0 conversion lines emitted by a 200 mg target of enriched ^{207}Pb in the energy interval of 3.5 to 6.1 MeV was performed by detecting electrons with the spectrometer BILL. Similar runs were also carried out with a ^{nat}Pb target. The results of these measurements are summarized in table I which lists the intensities of two peaks as seen with the enriched and natural targets. The expected ratio of about 3 is in good agreement with the measured relative intensities. Since these two peaks are very weak, the evidence for the existence of two E0 transitions in ^{208}Pb and hence, of two 0^+ excited states, is regarded as tentative. The 4882.0 keV line probably corresponds to the previously identified two-neutron pairing vibrational state[5]. The

energy 4904.9 keV does not correspond to any hitherto reported level in ^{208}Pb, so that if the peak identification is correct, this measurement constitutes preliminary evidence for a new 0^+ excited state in this nucleus.

In a second series of experiments a gamma-gamma coincidence arrangement was set up at the end of the high-flux filtered thermal beam port H22-F of the ILL Reactor. In this location a sample of 15 g of enriched (92.4%) ^{207}Pb, on loan from Oak Ridge, was exposed to a beam flux of about 10^8 cm^{-2} sec^{-1} for a net time of approximately 140 hours. Two 20% Ge(Li) counters were used. Table II summarizes the peaks identified in coincidence with the 3^- to 0^+ 2614.5 keV transition. None corresponds to the E0 lines in table I.

In conclusion, in spite of the fact that the anticipated high sensitivity was reached in the present experiments, the two-phonon octupole 0^+ excitation in ^{208}Pb could not be established. A summary of the results obtained is the following:

1) Tentative evidence for a new 0^+ state al 4904.9 keV in ^{208}Pb. The strength of the total E0 transition to the ground state is 45 b while the E3 transition to the 3^- state is less than 90 μb.
2) Observation of a weak E0 transition (30 μb) from a 0^+ state at 4882.0 keV which probably corresponds to the previously known two-neutron pairing vibration. The intensity of the E3 transition from this state to the 3^- is less than 80 μb.
3) Three two-gamma ray cascades in coincidence with the 3^- to g.s. transition and adding up to 4753.31 keV yield evidence for the population of three states in this reaction at 4253 (or 5726), 4934 (or 5047) and 3640 (or 6343) keV. Only the level at 4253 keV can be identified with a previously known one[6]. The present results favor a (2^+) assignment for this level. Since there is a strong peak at 4945.7 keV, due to C, in the electron spectrum, the possibility that the second combination is associated with an E0 transition of 4934 keV could not be elucidated; no

peak in the electron spectrum is observed at 5047 keV.

4) Tentative evidence for the population of the known[6] states at 3995 keV with a cross section of 130 μb, and 3.73 keV with a cross section of 260 μb.

The hospitality of the Institue Laue Langevin is warmly appreciated.

---

* Nationale Research Council of Canada

** University of Manchester

+ Technische Universitat Munchen

++ Brookhaven National Laboratory

Institute Laue-Langevin, Grenoble

1) P.R. Christensen, J.D. Garrett, O. Hansen, D. Hillis, O. Nathan, and F. Videbaek, unpublished, and S. Landowne, C.H. Dasso, R.A. Broglia and A. Winther, Phys.Lett. B70 (1977)292.

2) H.T. Motz, and A. Jurney, private comm. by H. Motz (see ref.3)

3) M.A.J. Mariscotti, W. Gelletly, and W.R. Kane, Phys.Rev. C5 (1972)178.

4) T. von Egidy, W. Mampe, B. Olma, and W. Kaiser, Z.Physik 236 (1970)440

5) J.R. Bjerregaard, O. Hansen, O. Nathan, and S. Hinds, Nucl. Phys. 89 (1966)337 and G. Igo, P.D. Barnes, and E.R. Flynn, Ann.Phys 66 (1971)60.

6) Table of Isotopes, 7th edition, C.M. Lederer et al, John Wiley and Sons, Inc., New York (1978).

TABLE I

Results of the search of EO lines in ^{208}Pb from the (n,e) reaction on ^{207}Pb and ^{nat}Pb

E_{trans} (keV)	EO conversion line intensity (μb)		Total EO intensity[a] (μb)
	^{207}Pb	^{nat}Pb	
4904.9 ± 0.8	15 ± 4	5 ± 2	45 ± 12
4882.0 ± 1.2	10 ± 4	< 3	30 ± 12
3500 - 4800			< 40
4800 - 5700			< 20
5700 - 6100			< 40

a. Total intensity includes internal pair production. Limits in the indicated energy intervals are quoted excluding the locations (± 15 keV) of background peaks due to photoelectron conversion of neutron capture gamma rays from the surrounding materials Zr, C and Al.

TABLE II

Gamma rays in coincidence with the 2614.5 gate other than the 4753.7 keV line

E_γ (keV)	I_γ[a] (μb)	Comments[b]
A) Pairs of gamma rays adding up to 4753 keV		
1025 ± 4	80 ± 40	DEP (4753) coincides with possible
(3729 ± 4)	?	3729 keV line. Intensity of 80 μb
(T:4754 ± 6)		less than DEP intensity error. Intermediate level at 3639.5 or 6343.5 keV.
1639 ± 4	370 ± 80	Intermediate level at 4253.5 or
3113 ± 3	330 ± 70	5727.5 keV. 4253 keV level and
(T:4752 ± 5)		transition to 3^- state are known (ref. 6)
2321 ± 4	260 ± 120	Intermediate level at 4935.5 or
2432 ± 4	160 ± 80	5046.5 keV. Strong C line in
(T:4753 ± 6)		e-spectrum would mask EO line at 4935.5 keV.
B) Single peaks		
567 ± 6	80 ± 60	
810 ± 4	80 ± 50	
1109 ± 6	260 ± 100	E_γ = Ekn(3.73) - E_{3^-}
1300 ± 4	160 ± 60	I_γ of DEP (2321) = $^3I_\gamma$(1300)/6
1383 ± 4	130 ± 80	E_γ = Ekn(3.995) - E_{3^-}
1939 ± 5	230 ± 150	
1983 ± 4	270 ± 90	E_γ = Ecs - Ekn(5.383, 2 or 3^-)
2090 ± 4	220 ± 80	I_γ of DEP(3113)= I_γ(2090)/2.
		E_γ = Ecs - Ekn(5.281, 0^-)
2213 ± 6	200 ± 100	
3277 ± 5	230 ± 110	Possible connection with 2^+ state
		No indication of 1471.4 keV transition between 2^+ and 3^- states with $I_\gamma > 40$

a. Intensities in μb are normalized to the observed 1200 μb cross section for the 4753.7 keV line in singles.

b. DEP, Ekn, Ecs and E_{3^-} denote double escape peak, energy of known level (ref. 6) energy of capture state and energy of 3^- state, respectively.

II. RADIOACTIVITY

II.1 ^{131}Sn Decay

H. Huck, M.L. Pérez, J.J. Rossi and H.M. Sofía.

The decay of ^{131}Sn has been studied at the Buenos Aires (IALE) on line isotope-separator facility as part of a systematic study of the short-lived Sn fission products and their daughters.

The ^{131}Sn level scheme was deduced from the gamma-ray energies and intensities, and gamma-gamma coincidence measurements.

Ground state half-lives were measured with a 95-cm^3 Ge(Li) detector using the spectrum-multiscaling technique for the intense gamma peaks between 250- and 1300-keV. The half-life for the 304-, 450-, 798- and 1226-keV gamma rays in the decay of ^{131}Sn, was determined to be 61$\pm$1s.

The level scheme proposed for the ^{131}Sn decay is shown in figure 1. It has been built using the experimental results and contains 67 transitions that carry 90% of the observed gamma intensity within a scheme of 36 levels.

The results can be discussed in terms of particle-core coupling calculations. The core (^{130}Sn) can be described microscopically as a collective two-hole state coupled to 0^+ (ground state) or 2^+ (first excited state). Thus, these states can be thought of as multipole pairing vibrations of the doubly magic ^{132}Sn. The theoretical predictions and the experimental data are compared in figure 2.

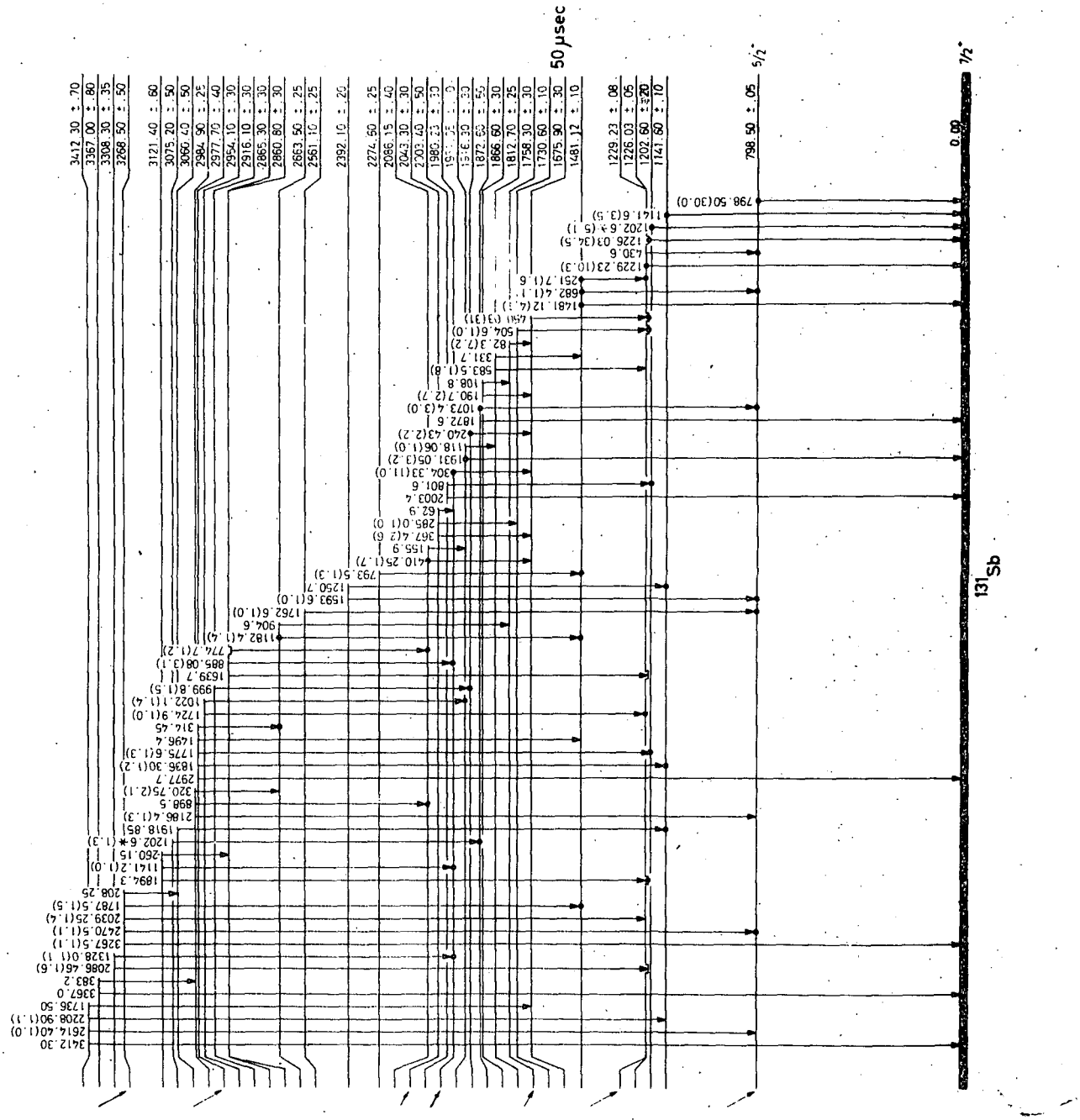

Figure 1

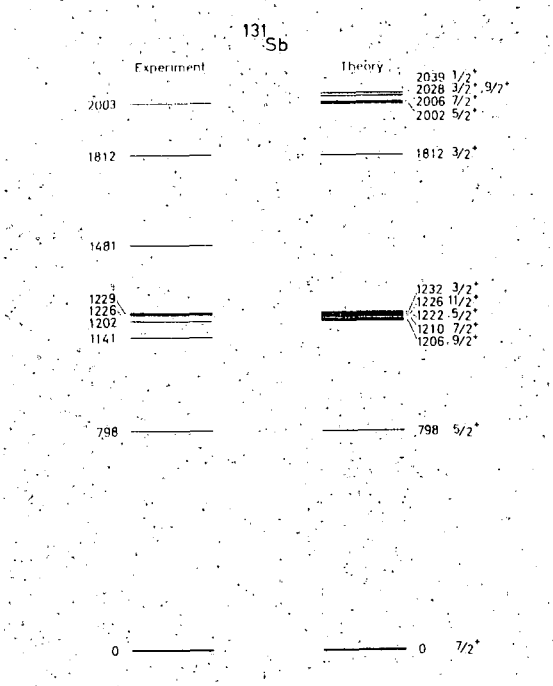

Figure 2

II.2 The ^{129}Sn and ^{129}Sb Beta Decays

H. Huck, M.L. Pérez and J.J. Rossi

Here we report results of measurements performed on the several ^{129}Sn and ^{129}Sb beta decays. These isotopes were obtained as ^{235}U thermal fission products, using an on-line electromagnetic isotope separator (IALE facility). Half lives and partial decays scheme for the ^{129}Sn (2.4 min) and ^{129}Sn (6.9 min) isotopes are established, leading to a level scheme for ^{129}Sb, for which the lowest lying levels are interpreted in terms of the coupling of single proton states to the collective ones based on the neutron holes.

In the ^{129}Sb decay a new half-life of 17.7 min has been found, besides the 4.4 h half-life reported previously. Its assignment to ^{129}Sb is supported by the results of growth-decay experiments on ^{129}Sb (17.7 min) and 129Te (69 min) activities. A partial decay scheme is also proposed, for which most of the levels are not seen in the $7/2^{+}$ ^{129}Sb g.s. decay, but some of them are supported by nuclear reaction results. This new half life has been missed up to now.

The gamma acitvity of the electromagnetically separated fission products was measured directly on-line by placing Ge(Li) detectors close to the focal plane of the isotope separator where a moving tape collector has been installed.

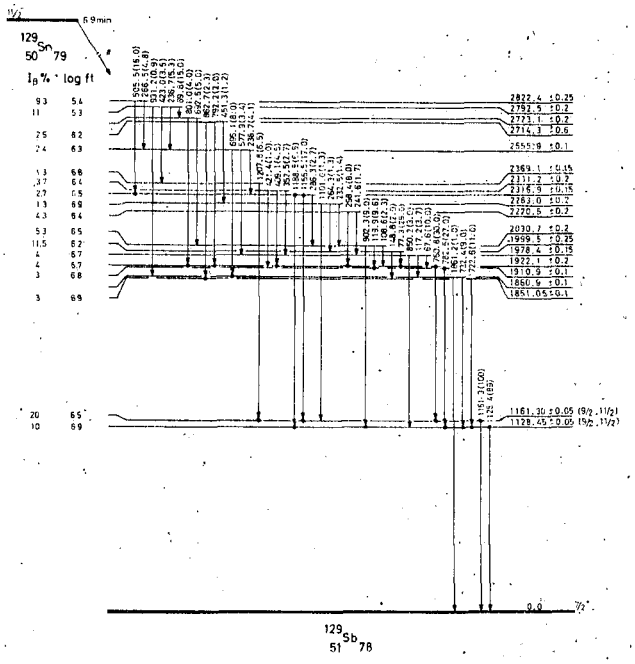

Figure 1

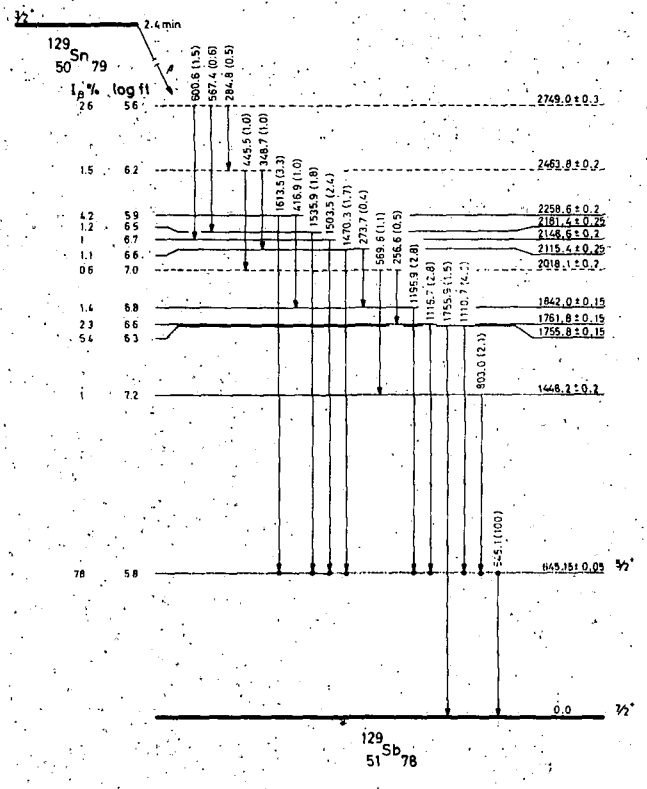

Figure 2

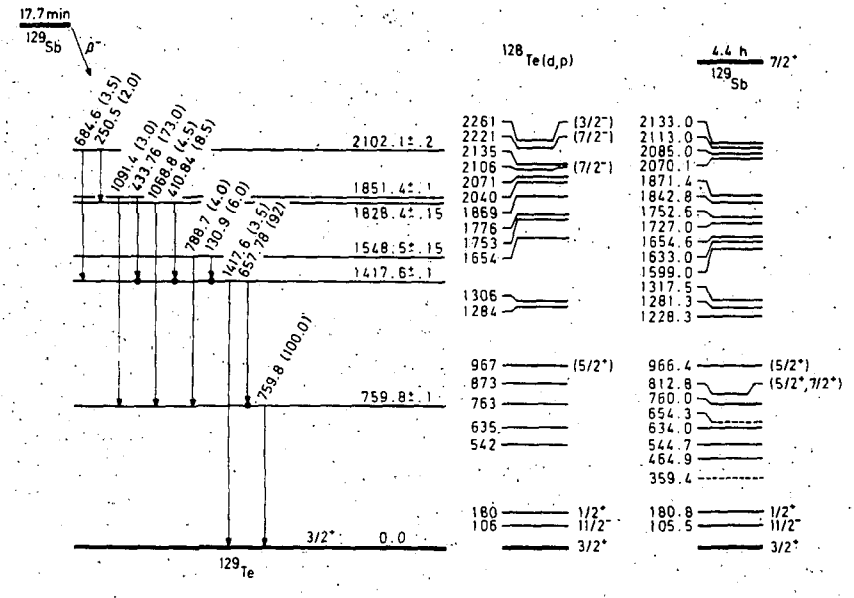

Figure 3

The ^{129}Sb energy levels can be interpreted as the ones generated by a proton interacting with a ^{128}Sn core. The latter can be studied as four neutron holes in the doubly magic ^{132}Sn. core, and its ground state described, in a very good approximation, as a two 0^+ boson state, where each boson is built as a coherent two hole state. In the same way, the first 2^+ excited state will be the one with one boson carrying angular momentum 2. The theoretical predictions and the experimental data are compared in figure 4.

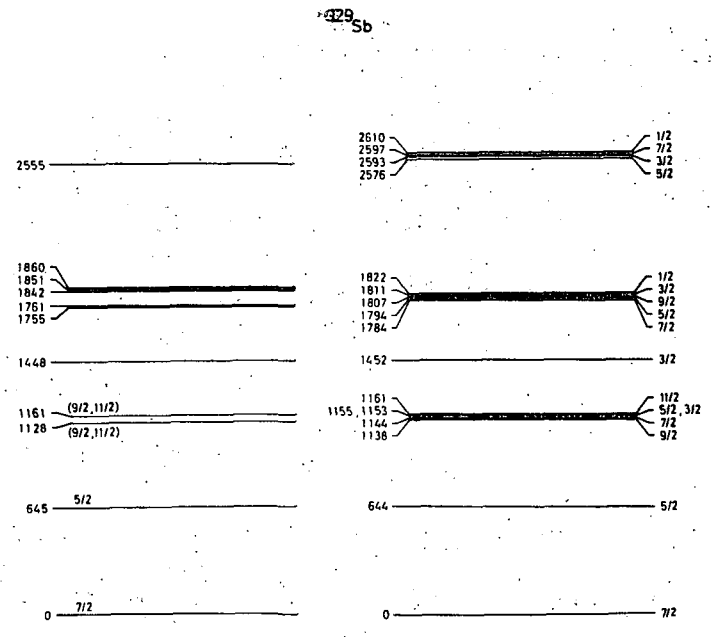

Figure 4

III APPLIED NUCLEAR PHYSICS

III.1 Study of Electronic Structure in Metals

D. Otero, A.N. Proto, and R. Romero*, A.H. Somoza* and M.D. Aycíriex*

The analysis of the Compton profile has been developed for the study of the electronic structure of metals.

As it is well known[1] the variation of the incident gamma-ray due to the compton scattering is given by:

$$E - E' = \frac{2}{mc^2} E E' \operatorname{sen}^2 \phi/2$$

Where E is the incident energy, E', the back scattered gamma-ray energy, m the electron mass, c, the velocity of light and ϕ the scattering angle. Besides to this systematic shift, there is a broadening of the back scattered gamma-ray, due to the Doppler effect. The broadening is given by:

$$\Delta E = 2 E p_z \operatorname{sen} \phi/2$$

Where p_z is the electron momentum along the incident direction. This electron could be in the atom core or could be a valence electron, and then this technique could be used as a complement of the positron annihilation studies (see Progress Report 3, 1978-1979).

To minimize the broadening due to the angular dispersion we develope an axial symetry set-up. A computer code to convolute the theoretical data with the detector resolution to allow the comparison of them with the measured distribution was also implemented. To check up the system, measurements on electrolitic cooper were made. The result is that the

electrons whose orbits are perturbed by the crystal lattice were the 4 s and 3 d.

---

* Department of Physic UNCPBA, Tandil, Argentina.

1) M. Cooper. Adv. in Phys. 20 (1971)453

III.2 Detrapping of Vacancies at ^{111}In in Quenched Silver+

C. Alonso Arias, M. Behar, A. Filevich, G. García Bermudez, E. Savino*, R.P. Livi** and F.C. Zawislak**.

The isothermal recovery of a quenched Ag foil doped with ^{111}In has been studied through the time defferential perturbed angular correlation technique. A nearest neighbor-vacancy configuration has produced a quadrupole interaction =166±3 MHz and a dettraping vacancy process has been detected with E_d=1.09 ± 0.05 . These results are discussed and compared with previous results[1] in the present paper+.

+ C. Alonso Arias, M. Behar, A. Filevich, G. García Bermudez, E. Savino, R.P. Livi and F.C. Zawislack to be published in Phys.Rev. B24 (1981)3162

* Departmento de Metalurgia, Comision Nacional de Energía Atómica

** Institute of Physic Universidade Federal Río Grande do Sul, Porto Alegre, Brasil.

1) L. Thomé and H. Bernas Hyp.Interact. 5 (1978)361

IV. NUCLEAR STRUCTURE

IV.1 Comparison of Upper and Lower Bounds Methods Using a Soluble Many Fermion Model.

M.C. Cambiaggio*, A. Klar**, F.J. Margetan**, A. Plastino* and J.P. Vary**.

Upper bounds, lower bounds and estimates based on moments are compared for the ground state energy of a soluble Hamiltonian due to Lipkin. The Hartree-Fock approximation, a coherent particle-hole method, a two-body density technique, the P and Q representatives formalism, moment methods with a Gram-Charlier expansion and moment methods in a Stieltjes-Tchebycheff bounding procedure are discussed and applied. We discuss features of the exact total eigenstate distribution since these pertain directly to two of the methods studied.

We show that lower bounds are of comparable quality with upper bounds and are no more difficult to obtain. No single bounding method is found superior over the entire range of parameters we study for the soluble Hamiltonian. However, in one region we find an upper bound from one method which coincides with the lower bound of another method, thus yielding the exact ground state energy. We also show that estimation methods based on the easily calculated first and second moments of the eigenvalue distribution are surprisingly accurate for a wide range of coupling parameters and number of active particles.

---

* Department of Physic, Facultad de Ciencias Exactas, UNLP, Argentina.

** Ames Laboratory, Iowa State University, Ames, Iowa, USA.

IV.2 The Effective Mass of Renormalized Fermions.

O. Civitarese, R.P.J. Perazzo, S.L. Reich and M. Saraceno

The single particle spectrum in the neighbourhood of the Fermi surface shows a systematic compression with respect to that obtained from an average, local and velocity independent central potential. This effect is sometimes described assuming that individual particles within nuclear mater behave as having an effective mass m^*.

In the present calculations we investigate the effective mass induced by the coupling of individual particles to the cooperative oscillations of the A-nucleon system. This coupling is evaluated within the formalism of the NFT and ref.1).

The kernel that plays the role of a non local, velocity dependent potential and whose ε-dependence and second order moment define the effective mass, is:

$$\mathcal{G}_{(x,x',\varepsilon)} = \sum_{m,m'} \varphi_m(x)\,\varphi_{m'}(x') \left\{ \sum_{m''s} \Lambda^2_{s,m''}\, D_s(s, s_{m''}) \right\} \quad (1)$$

$$D_s(\varepsilon, \varepsilon_{m''}) = \begin{cases} \dfrac{\theta_{m''}}{\varepsilon - \varepsilon_{m''} - w_s} + \dfrac{1-\theta_{m''}}{\varepsilon - \varepsilon_{m''} + w_s} & m, m' > m_F \text{ or } m\,m' < m_F \\ \dfrac{1-\theta_{m''}}{\varepsilon - \varepsilon_{m''} - w_s} - \dfrac{\theta_{m''}}{\varepsilon - \varepsilon_{m''} + w_s} & m > m_F,\ m'' < m_F \\ & \text{or } m < m_F,\ m'' > m_F \end{cases}$$

$$\theta_m = \begin{cases} 0 & m > m_F \\ 1 & m \le m_F \end{cases}$$

In eq(1) labels all possible collective modes and n the single particle orbits. The vertex function $\Lambda_{s,n''}$ account for the coupling between both degrees of freedom. If $\Lambda_{s,n''}$ where constant for all single particle states, the effective mass would be essentially constant in the interior of the nucleus and would approach the free value outside. Since levels close to the

Fermi surface are affected differently from those far away from it, the effective mass present an oscillatory behaviour in the interior, thus suggesting the relevance not only of the non locality of the density ρ but also of its particle-hole fluctuations.

The analysis of a realistic case such as ^{208}Pb, the effective mass ratio m^*/m is analized by decomposing it in the $\mathcal{E}$-mass[2] (determined by the residue of the Green's function at the one quasiparticle pole) and the k-mass[2] (determined by the expectation value of the second order moment of $\mathcal{G}$). In figures 1 and 2 are plotted the separate contributions to both masses as a function of the multipolarity of the collective modes (see ref.3 for details of the calculation) in which is clearly displayed the important role played by the low energy, strongly collective modes.

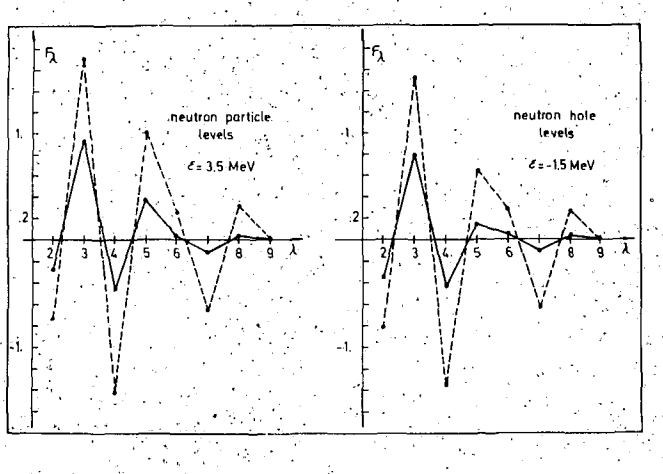

Figure 1

Figure 2

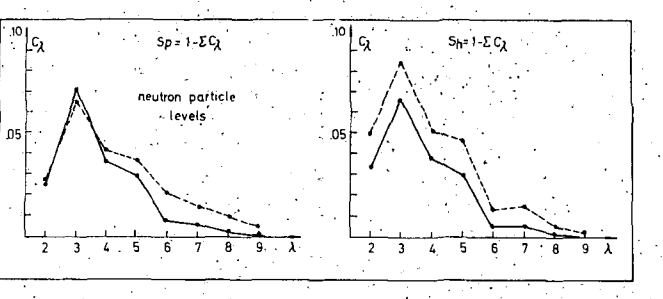

Both the energy dependence and the non local features show themselves very sensitive to the nature of the low energy nuclear collective motion. The former appears in the fragmentation of the one body transfer strength, while the second depends upon the particle-hole fluctuations of the density.

These two features hamper any refinement in the use of the concept of effective mass, for finite systems.

---

1) D.R Bes, G.G. Dussel, R.P.J. Perazzo and H.M. Sofía, Nucl.Phys A307 (1978)402

2) J.P. Jeukenne, A. Lejeune and C. Mahaux, Phys.Rep. 25C (1976)85

3) R.P.J. Perazzo, S.L. Reich and H.M. Sofía, Nucl.Phys. A339 (1980)23

IV.3 The Ground State of Deformed Nuclei as a Boson Condensate*

J. Dukelsky, G.G. Dussel and H.M. Sofía.

It is shown that the ground state of deformed nuclei can be consider as a condensate of two particle-bosons that have not a well defined angular momentum. Using a pairing plus quadrupole interaction it is shown that the existence of a condensate implies that the fermionic excitations have a physical structure similar to the ones obtained in a Nilsson plus BCS treatment. On the other hand, it is possible to obtain the structure of the boson (that forms the condensate) in terms of the fermionic excitations. From this structure we can evaluate the probability that the boson has angular momentum zero, two or any other. These probabilities are shown in the figure 1 for the rare earth nuclei using the same single particle energies and force strengths than Kumar and Baranger[1]. These results suggest that a description of deformed nuclei in terms of bosons having angular momentum zero and two may be meaningful.

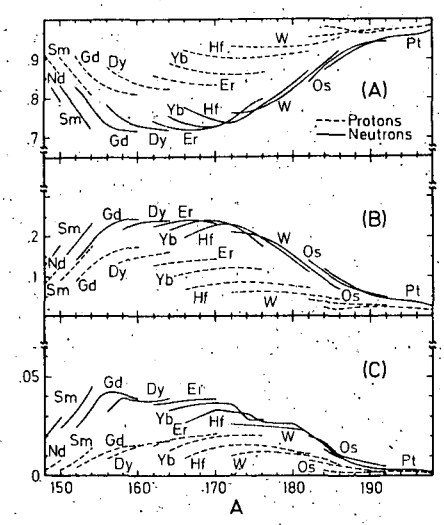

Figure 1

Probabilities that in the rare earth nuclei the P.S.A. boson has a given angular momentum. (A) probabilities for J=0, (B) for J=2 and (C) for J≠0,2. In the ordinate is shown the mass number and each of the lines corresponds to a different element. The neutron values are linked by a full line while the dashed line corresponds to protons.

---

* Work published in ref.2,3.

1) K. Kumar and M. Baranger, Nucl.Phys. A110 (1968)529

2) The amplitudes of s and d bosons in deformed nuclei. J. Dukelsky, G.G. Dussel and H.M. Sofía, Phys.Lett. 100B (1981)367

3) The ground state of deformed nuclei as a bosons condensate. J. Dukelsky, G.G. Dussel and H.M. Sofía, Nucl. Phys. A373 (1982)267.

IV.4 $\tilde{\pi}h_{9/2} \otimes \tilde{\nu}i_{13/2}$ Bands in Doubly Odd Tl isotopes including a Proton-Neutron Residual Interaction*

A.J. Kreiner.

The neutron number (or Fermi level) dependence of the $\tilde{\pi}h_{9/2} \otimes \tilde{\nu}i_{13/2}$ two quasiparticle collective structure is studied in presence of a residual proton-neutron (p-n) interaction. The bare p-n interaction is taken from the experimentally known $\tilde{\pi}h_{9/2} \otimes \nu^{-1}i_{13/2}$ multiplet in the particle-hole nucleus ^{208}Bi. This force has the following features. The matrix elements $\langle (j_p j_n^{-1})J|V_{p-n}|V(j_p j_n^{-1})J\rangle = V_J^{-1}$; $(\vec{J}=\vec{j}_p+\vec{j}_n)$ show small deviations ($\sigma \simeq 60$ keV) around a mean of about 150 keV for the J=5-10 states while the value for J=11 lies at 886 keV. In other words, it is more or less constant

for J=5-10 (smaller values of J do not play any role in the present discussion) and strongly repulsive for the maximally aligned state J=11 .

Since the interest lies in studying the behavior of the two quasiparticle system as a function of neutron number an expression for the effective p-n force has to be derived which incorporates the fact that the character of the quasineutron changes from hole-like to particle-like when the Fermi level, λ_n, moves across the $i_{13/2}$ subshell from top to bottom. This expression is:

$$V_J^{eff} = (u_{\Omega_m} u_{\Omega_p} u_{\Omega_{m'}} u_{\Omega_{p'}} + v_{\Omega_m} v_{\Omega_p} v_{\Omega_{m'}} v_{\Omega_{p'}}) V_J + (u_{\Omega_m} u_{\Omega_p} u_{\Omega_{m'}} v_{\Omega_{p'}} + v_{\Omega_m} u_{\Omega_p} v_{\Omega_{m'}} u_{\Omega_{p'}}) V_J^{-1}$$

where $V_J = \langle (j_p j_n) J \mid V_{p-n} \mid (j_p j_n) J \rangle$ is the particle-particle matrix element obtained from V_J^{-1} applying the Pandya transformation[1], u and v are the BCS amplitudes and Ω_n, Ω_p label different neutron and proton state. As λ_n penetrates the $i_{13/2}$ shell, the effective force and, in particular, the strong repulsion for J=11 becomes smaller and finally negligible due to the mixed p-h character of the neutron in the middle of the shell. This fact has a definite effect on the staggering (alternation of small and large transition energies along the bands) in the $\tilde{\pi} h_{9/2} \otimes \tilde{\nu} i_{13/2}$ structure. It implies that the staggering will change its "phase" along the isotopic chain, an effect which has not yet been observed. This circumstance casts some doubts on (a) the adequacy of the ^{208}Bi or a similar residual force, or (b) the applicability or accuracy of the model itself.

---

* Phys.Rev. C22 (1980)2570

1) S.P. Pandya, Phys.Rev. 108 (1957)1312.

IV.5 Isovector and Isoscalar Pairing Correlations in a Solvable Model

J.A. Evans*, G.G. Dussel**, E. Maqueda** and R.P.J. Perazzo**

We investigate the assumption that-alpha transfer enhancements are mostly linked to the isovector pairing interaction. We consider systems of even number of nucleons moving in several ℓ-shells of total degeneracy omega. We add, in the residual hamiltonian, a "deuteron" type of interaction to the usual T=1 pairing force,

$$H=-(1+x)(P^{+}.P)-(1-x)(D^{+}.D)$$

with

$$P^{+}_{\nu}=[a^{+}a^{+}]^{L=0,S=0,T=1}_{0\ ,\ 0\ ,\ \nu} \qquad \text{and} \qquad D^{+}_{\mu}=[a^{+}a^{+}]^{L=0,S=1,T=0}_{0\ ,\ \mu\ ,\ 0}$$

These operators, together with the number operator, the spin and isospin, and $W_{\mu,\nu}=[a^{+}a]^{0,1,1}_{0,\mu,\nu}$ are associated to the generators of the O_8 group[1]. We use this algebra to build the matrix elements of H. We consider a seniority-zero basis corresponding to the O_8 irreducible representation $(\Omega,0,0\ 0)$ and good N, S and T. In the pure pairing limit (x=1) we obtain isospin "rotational" bands following the T(T+1) law and the spin degree of freedom shows an almost "vibrational" behaviour. The roles of S and T are interchanged when x is replaced by -x. Each of the two channels present in H induce a kind of correlation that interferes destructively with the other. For x=0, H corresponds to the Casimir operator of SU_4.

In the figure we show, for $\Omega=6$, the square of the matrix element for a four (alpha-like) nucleon transfer together with two (T=1) two-nucleon transfers. These correspond to the two particle matrix elements in which the alpha-transfer shown would be factorized if only the pairing degree of freedom were present. They are seen to increase making full use of the correlations built by the pairing component of H. The maximum for x=0 is related to the fact that the alpha-transfer operator preserves the SU_4 symmetry.

We can conclude from our study and that of ref.2) that the alpha-transfer may present enhancements even when the pairing interaction is small and, thus, support the interpretation that it is, to a large extent, insensible to the two body correlations operant in nuclei.

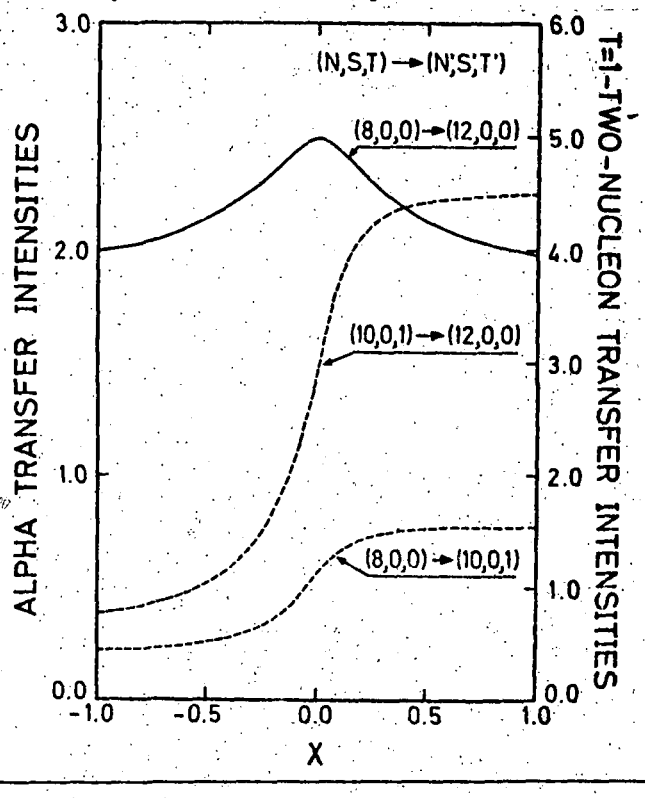

---

* School of Mathematical and Physical Sciences, University of Sussex, England.

** Fellow of the CONICET, Argentina

1) B.H. Flowers and S. Szpilowski, Proc.Phys.Soc. 84 (1964)673

2) O. Dragún, G.G. Dussel, E. Maqueda and R.P.J. Perazzo, Nucl.Phys. A167 (1971)529

IV.6 Core Polarization Effects in the ^{17}O Magnetic Form Factor

S.L. Reich and J. Vary*

The experimental magnetic form factor of ^{17}O has provided a strong challenge for microscopic theory[1,2]. Recently it has been shown, with more complete theoretical calculations[3], that there is substantial disagreement

over the entired range of the measured data. As part of a continuing effort to understand the origin(s) of this discrepancy we present here a perturbation calculation of the contributions arising from core polarization.

Within the Nucliar Field theory, shape oscillations of the ^{16}O core may be considered as independent boson degrees of freedom, coupled with the fermionic degrees of freedom of the odd neighbour through a particle vibration coupling

$$H_{pv} = -\sum_{\lambda\mu} K_\lambda(r)\, \alpha_{\lambda\mu}\, Y^*_{\lambda\mu}(r)$$

Where $K(r) = R\frac{dU}{dr}$ $(\lambda \geq 2)$

with U being the central one body posential.

And $$\alpha_{\lambda\mu} = \frac{i^{-\lambda}\beta_\lambda}{2\lambda+1}(C^+_{\lambda\mu} + C_{\lambda\bar{\mu}})$$

where β_λ is the usual collective model deformation parameter, and $C^+(C)$ phonon creation (annhilation) operators.

Up to second order in perturbation theory, the matrix element for a given magnetic transition, is given by the following diagramms.(figure 1). Where all possible time orderings, of the basic processes (A), (B) and (C) must be taken into account.

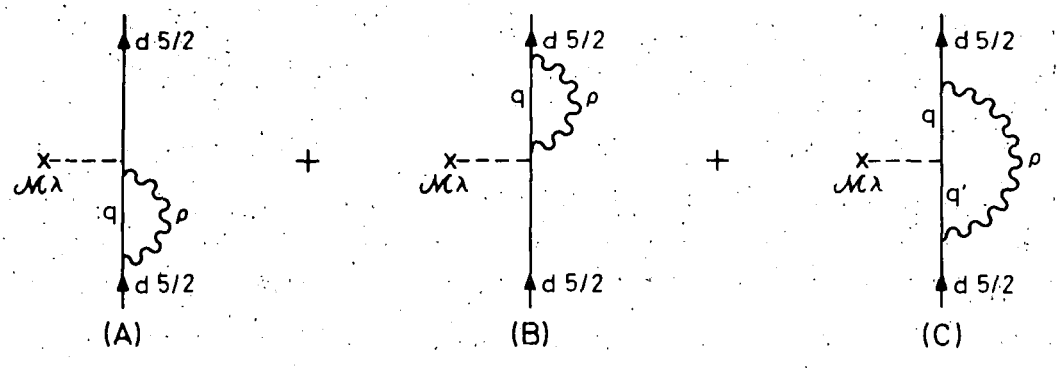

Figure 1

Renormalization of the matrix element $\langle d5/2 \| M(\mathcal{M}\lambda) \| d5/2 \rangle$ due to the particle vibration coupling

Preliminary results show that the enhancement for the M5 transition is bigger than for the M1 and M3 transitions. Results including a complete boson and fermion spectra are in progress.

---

* J. Vary Ames Laboratory , Iowa State University, Ames, Iowa, USA.

1) M.V. Hynes, H. Miska, B. Norum, W. Bertozzi, S. Kowalski, F.N. Rad, C.P. Sargent, T. Sasanuma, and W. Turchinetz, Phys.Rev.Lett. 42 (1979)1444

2) A. Arima, Y. Horikawa, H. Hyuga, and T. Suzuki, Phys.Rev.Lett. 40 (1973)1001.

3) R.J. MaCarthy and J.P. Vary, to be published

IV.7 The Fragmentation of the M1 Strength in ^{208}Pb

G.G. Dussel, R.P.J. Perazzo, S.L. Reich and H. Sofía.

The spreading width of a giant resonant state is determined in leading order through the coupling of that collective excitation with 2p-2h states. Since the latter can be interpreted as 2-phonon states, the lowest perturbative process describing this coupling is represented by the diagram of figure 1.

This procedure was used to evaluate the fractionation of the M1 strength in ^{208}Pb. A considerable experimental effort[1] has been devoted to the study of the 1^+(T=1) resonance in ^{208}Pb and still many ambiguities of the empirical data must be elucidated. The detailed knowledge of this state provides valuable information on the $\sigma\sigma$ channel of the residual nuclear interaction, allowing to estimate its strength and the B(M1). It is well known that only a small fraction of the M1 sumrule has been found, this fact being considered as an indirect evidence of the coupling to Δ-hole

configurations[2] at $\simeq$ 300 MeV of excitation energy. If we restrict to the nucleonic space we may consider this degree of freedom leaving two independent free parametes; the excitation energy W_1^+ and the vertex function Λ_0 that couples the 1^+ state to the single particle motion.

The states λ_1, λ_2 are RPA eigenstates of a residual multipole interaction with strength $K_{T=0}$, $K_{T=1}$ and K_{01} in the varios isopin channels. Both collective and non collective roots have been kept.

The value of the diagram of figure 1 is:

$$D = (-)^{J_3+J_2+\lambda_1+\lambda_0+1} \hat{\lambda}_1 \hat{\lambda}_2 \Lambda_0 \Lambda_1 \Lambda_2 M(J_1 J_2 \lambda) M(J_3 J_2 \lambda_2) \langle J_3 \| \sigma \| J_1 \rangle \times$$

$$\times \begin{Bmatrix} J_3 & J_2 & \lambda_2 \\ \lambda_1 & \lambda_0 & J_1 \end{Bmatrix} \langle 0 \| \lambda G(M1) \| \lambda_0 \rangle \frac{1}{\Delta\varepsilon}$$

$$\hat{\lambda} = \sqrt{2\lambda+1} \quad ; \quad M(J_1 J_2 \lambda) = \langle J_1 \| r^\lambda Y_\lambda \| J_2 \rangle i^{J_1+J_2-\lambda}$$

Where $\Delta\varepsilon$ is an energy denominator changing for each time permutation of the vertices of figure 1.

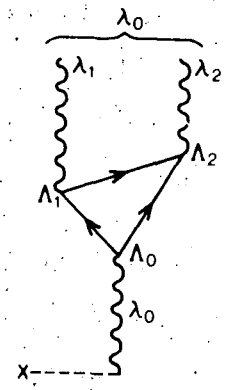

Figure 1

The M1 strength is transfered mostly to states with $\Delta\varepsilon \approx 0$, where D become so large that perturbation theory is not larger applicable. In these circumstances a diagonaligation is performed.

A tipical result is shown in figure 2. The fragmentation is exclusively due to the presence of a pair of 3^- or 5^- states, particularly when one of the two phonons involved is the corresponding collective root. The attenuation factor in the vertex Λ_0 that accounts for a transfer of strength

to the Δ-hole configuration causes no special redistribution of the strength that is localized at low energy.

Figure 2

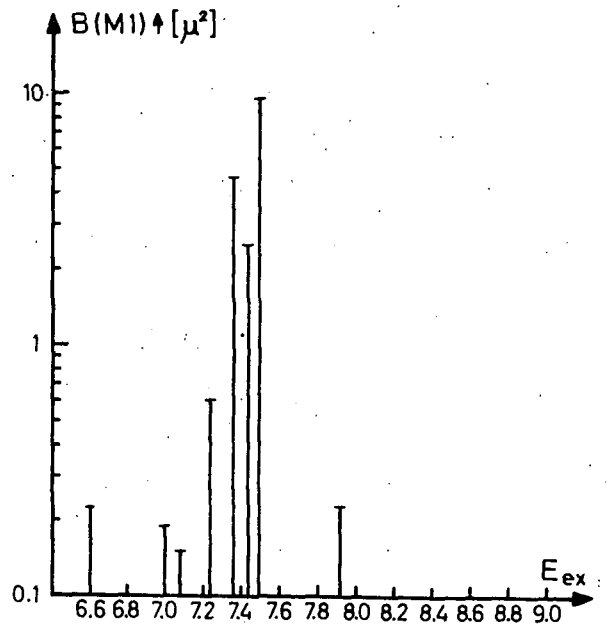

1) R.J. Holt, H.E. Jackson, R.M. Laszewski, and J.R. Specht, Phys.Rev. C20 (1979)93

2) A. Bohr and B.R. Mottelson, Phys.Lett. 100B (1981)10

IV.8 Perturbative Treatment of Rotating Fermion Systems

D.R. Bes, O. Civitarese, R. Liotta, M.T.A de Mehr and H. Sofía

In reference 1) a general procedure was developed which eliminated the infrared divergencies associated with perturbation theory in a deformed basis. Application of this procedure to the two-and three-dimensional rotors was carried out during the present period.

i) Two-dimensional rotors

The (exactly soluble) case of an even number of particles moving in a harmonic oscillator shell and coupled by quadrupole forces was studied in reference 2) using the formalism described in reference 1. The calculation

has been extended to the odd case, where again exact results are reproduced to the order of the perturbation which has been considered.

The formalism of reference 1) is applied to the description of the quasiparticle motion in many shells. The quasiparticles are considered as elementary (intrinsic) single particle modes of a system which rotates collectively (pairing modes).

The structure of the quasiparticle-pairing coupling terms and the structure of the pairing "rotational" mode is explicity discussed. Numerical calculations are performed for the case of the even Sn-nuclei.

ii) Three-dimensional rotors

The main difference with the two-dimensional case arises from the fact that the collective degrees of freedom cannot be eliminated from the effective Hamiltonian through path integration techniques. A possible solution is to work in the product space of the unified model

$$\Psi_{IKMm}(\phi, r_i) = D^{I}_{MK}(\phi)\ \chi_{iK}(r_i$$

with the effective Hamiltonian

$$H' = \lim_{D\to 0}[H + \frac{1}{2D}(I_v - L_v)^2 + \frac{Q}{6A}\sum_v \theta_v^2 + \frac{w}{2}\sum_n (1-\det(i[L_v,\theta_u]))^n/n]$$

Here I_v are collective angular momentum operators in the body fixed frame and L_v are their microscopic expressions in terms of particle variables. It is convenient to choose θ_v as the microscopic expression for the angular variable conjugate to L_v, at least to leading order in a small parameter Q^{-1}. They are conveniently chosen to be proportional to the components of the quadrupole tensor with vanishing expectation value, namely

$$Q_v \propto \sum_i (x_{v+1}\ x_{v+2})_i$$

The parameter Q is a (non-vanishing) expectation value of the quadrupole operator. The frequency

$$w = Q/(3AD)^{\frac{1}{2}}$$

is common to the three spurious modes and goes to infinity as $D\to 0$.

The "Coriolis" term $I_\nu L_\nu/D$ is of $O(Q^{\frac{1}{2}})$ and thus not sufficiently small from the point of view of the Q-dependence. It is eliminated (as well as the rotational term $(1/2D)\sum_\nu I_\nu^2$ by means of the transformation e^{iT} with

$$T = -\sum_\nu I_\nu \theta_\nu$$

Only the commutation of H and T contributes to the O(1) of the rotational energy, and the corresponding terms yield the Thouless-Valatin moment of inertia. However, the aim of the present approach is to go beyond this order. All terms in H' are necessary, for instance, in order to obtain the rotational energy to $O(Q^{-1})$.

The resultant effective Hamiltonian includes arbitrarily large residual interactions ($D \to 0$). These may be conveniently treated within the NFT formalism, which also allows to cast the results into a power series in Q^{-1}.

The procedure has been checked against the SU3 Elliot model. This model yields an exact rotational spectrum I(I+1), the excitation energies of the different band-heads and quadrupole matrix elements within a rotational band. These physical magnitudes are exactly reproduced to the order of the expansion in Q^{-1} to which our calculation is made[3]. This is at least an order of magnitude higher than the one corresponding to the semiclassical approximation (cranking model). Application to the realistic case of Mg^{24} is in progress.

---

1) V. Alessandrini, D.R. Bes and V. Machet, Nucl.Phys. B142 (1978)489

2) D.R. Bes, G.G. Dussel and R.P.J. Perazzo, Nucl.Phys. A340 (1980)157

3) D.R. Bes, O. Civitarese and H.M. Sofía, Nucl.Phys. A370 (1981)99

IV.9 The Nilsson-Bogolubov and the IBM Picture of Deformed Nuclei

D.R. Bes, R.A. Broglia*, E. Maglione** and A. Vitturi***

We try to answer the question of whether the Hilbert space subtended by the pair aligned model subspace, which is contained inside the particle-aligned model subspace, is large enough so that the properties of at least the ground state of a deformed nucleus are contained within it. The diagonalization of a pairing plus quadrupole Hamiltonian is carried out making use of the wavefunction

$$|\Psi\rangle = \prod_{\nu,m>0} (U_\nu(m) + V_\nu(m)\, a^+(\nu m)\, a^+(\tilde{\nu m}))|0\rangle. \qquad (1)$$

The states $|\nu\, m\rangle$ are eigenstates of Y_{20} with wigenvalue $q_\nu(m)$. In the aligned fermion model the quantities $U_\nu(m)$ and $V_\nu(m)$ are the standard BCS occupation parameters are (cf.ref.3)

$$U_\nu(m) = \frac{1}{\sqrt{1+\beta'^2 c_\nu^2(m)}} \quad , \quad V_\nu(m) = \frac{\beta' c_\nu(m)}{\sqrt{1+\beta'^2 c_\nu^2(m)}}$$

The calculations were carried out for the case of a j=41/2-orbital, for an equal number of neutrons and protons. The ratio $\Delta/\delta\varepsilon$ between the pairing gap Δ and the total energy splitting $\delta\varepsilon$ of the different magnetic substates of the j-shell has the realistic value of 0.1. The amplitudes c(m) are

$$c(m) = \Omega^{-\frac{1}{2}} \sum_\lambda \sqrt{2\lambda+1}\ \langle jm\ \lambda 0|jm\rangle\ \alpha_\lambda$$

Calculations were done for λ =0,2 and λ = 0,2,4 (figure 1)

The inclusion of pairs of fermions with $\lambda > 2$, although having small amplitudes, increases the relative importance of the D-pair with respecto to the S-pair and quadrupole polarize the nucleus. Using the SD part of the Nilsson plus BCS wavefunction (α_0 = 0.57 and α_2 = 0.77) to calculate the expectation value of the quadrupole moment, one obtains a result which is rather similar to that predicted by the Nilsson plus BCS model. Such calculation includes re-normalization effects arising from pairs of

particles coupled to higher values of j^{λ}, and have the drawback that they can be carried out only after the calculation in the full space has been done.

Similar results are obtained for the set of degenerate levels used in reference 1).

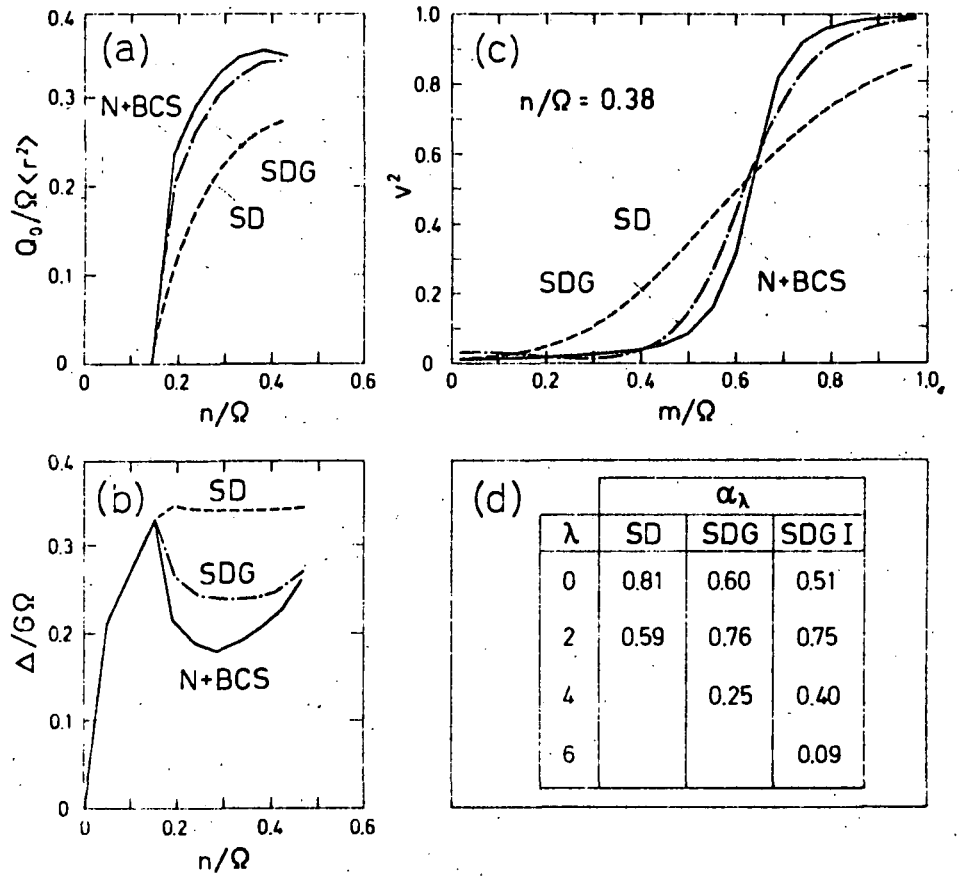

(d)

	α_λ		
λ	SD	SDG	SDG I
0	0.81	0.60	0.51
2	0.59	0.76	0.75
4		0.25	0.40
6			0.09

---

* Niels Bohr Institute, University of Copenhagen, DK-2100 Copenhagen, Denmark.

** Instituto Nazionale di Fisica Nucleare, Laboratory Nazionale di Legnare, Padova, Italy.

*** Instituto di Fisica Galileo-Galilei, University of Padova, and INFN, Sez. Padova, Italy.

1) T. Otsuka, Nucl.Phys. A368 (1981)244

IV.10 The Nucleus as a Condensate of Monopole and Quadrupole Pairing Vibrations*

R.A. Broglia[a)+], E. Maglione[b)+], H.M. Sofia and A. Vitturi[c)+].

It has been shown[1] that the aligned wavefunction, and the wavefunction obtained by restricting pairs of particles to be coupled to angular momentum zero and two as assumed by the quadrupole phonon model (QPM)[2] and by the interacting boson model (IBM)[3] are, for strongly deformed systems, rather different. They become identical in the vibrational limit and display different degrees of similarity for intermediate (anharmonic) situations[4]. To which extent this difference reveals itself in the predicted properties of the low-energy nuclear spectrum is an open question. In an attempt to clarify this point we have calculated the spectrum and the electromagnetic and two-nucleon transfer probabilities for some strongly anharmonic and transitional nuclei, in the framework of the nuclear field theory (NFT) version of the pair aligned model[5]. These calculations which are microscopic, depend on the strength of the pairing and particle-hole interactions. We find that for standard values of these parameters, the moment of inertia of both the beta- and the alpha-bands are too small.

While the main pattern of the phase transition observed in the Sm-isotopes is displayed by the model, major deviations are observed concerning the properties of the beta-vibrations, and in connection with the two-nucleon transfer strength associated with the 2^+ member of the ground state rotational band.

In spite of all these limitations, the simplicity brought by the Quadrupole Boson Model and by the IBM are attractive. The best example among the cases studied is the change in the spectrum and in the structure of the wavefunctions associated with the phase transition taking place around ^{150}Sm.

* These calculations were performed at the Niels Bohr Institute of Copenhagen-Denmark and at the Oak Ridge National Laboratory, USA. Nucl.Phys A375 (1982)217.

a) The Niels Bohr Institute, University of Copenhagen DK-2100 Copenhagen, Denmark.

b) Instituto Nazionale di Fisica Nucleare, Laboratory Nazionale di Legnaro, Padova, Italy.

c) Instituto di Fisica Galileo Galilei, University of Padova, and INFN, Sez.Padova, Italy.

+ Oak Ridge National Laboratory, Oak Ridge, Tennessee 37830, USA.

1) A. Bohr and B.R. Mottelson, Physica Scripta, 22 (1980)468.
R.A. Broglia, Invited talk to the Workshop on "Interacting Bose-Fermi System in Nuclei", Erice, June 12-19, 1980.

2) D. Janssen, R.V. Jolos and F. Dönau, Nucl.Phys. A224 (1974)43.

3) F. Iachello, in Interacting Bosons in Nuclear Phys. Ed. F. Iachello, Plenum Press, New York (1979)1, and reference therein.

4) T. Otsuka, Interacting Boson in Nuclear Physics, Ed. R. Iachello, Plenum Press, New York 1979, p. 93; J. Mc Grory, ibid p. 121.

5) D.R. Bes and R.A. Broglia, in Interacting Bosons in Nuclear Physics, Ed. F. Iachello, Plenum Press, N.Y. 1979 p.143.
R.A. Broglia, K. Matsuyanagi, H. Sofia and A. Vitturi, Nucl.Phys. A348 (1980)237.

IV.11 Nuclear Field Theory Treatment of Complex Nuclear Spectra*

R.A. Broglia[a], K. Matsuyanagi[b], H.M. Sofia and A. Vitturi[c]

The treatment of the interplay between collective and fermion degrees of freedom provided by the nuclear field theory[1] (NFT) is perturbative and graphical. Thus, no diagonalizations are to be performed but the different transitions as well as energies are to be calculated by summing up the corresponding graphical contributions to the order in $1/\Omega$ desired. The basis states are product states of the collective vibrational modes observed in

nature, i.e. surface modes, pairing vibrations, spin and isospin modes and of single particles.

The central feature of the NFT is that fermions and bosons are treated on par. Thus, the Pauli principle is properly taken care of at every order of perturbation.

In the present work we attempt to extend the scope of the NFT to deal with some non-perturbative situations, in particular with moderately anharmonic nuclear spectra. This is done by utilizing the result that particles moving in single-particle orbitals and interacting through a pairing and a quadrupole force display the main properties of rotational, vibrational and trasitional spectra. We also use the simplifying ansatz of the quadrupole phonon model [QPM; cf.refs.2),3)] and of the interacting boson model [IBM;cf.ref.4) and references therein].

The pairing-plus-quadrupole particle-hole model in a single j-shell in a basis of pairs of fermions coupled to $\lambda=0$ and $\lambda=2$, has a mapping onto a space of monopole and quadrupole paring phonons. It is possible to find a set of rules such that the mapped matrix elements can be calculated in the framework of the NFT. The model contains some of the features of transitional nuclei as well as the vibrational and, in some very approximate way, the rotational patterns. The model being fully microscopic, contains no free parameters, but the known strengths of the monopole and the quadrupole pairing forces as well as the strength of the quadrupole particle-hole interaction. The resulting fits cannot reproduce essential features of the nuclear system like, for example, the energy splitting between the pair of states 3^+-4^+, 5^+-6^+, etc., belonging to the quasi-γ-band. Because of the single j-shell approximation and thus the absence of pairing vibrational modes, the observed features of the quasi-γ-band are poorly reproduced.

The two obvious extensions of the model lie in the inclusion of many j-shell and in the treatment of odd nuclei. The first step would allow,

among other things, the introduction of a second monopole pairing boson (s'-boson) associated with the fluctuations of the pairing gap (pairing vibrations), and thus for a more realistic description of the β-vibrational modes.

---

* These calcutations were performed at the Niels Bohr Institute of Copenhagen, Denmark. Nucl.Phys. A348 (1980)237.

a) The Niels Bohr Institute, University of Copenhagen, DK-2100 Copenhagen, Denmark.

b) Kyoto University, Department of Physics, Kyoto, Japan.

c) Universitá degli Studi di Padova, Instituto di Fisica Galileo Galilei, Italy.

1) P.F. Bertignon, R.A. Broglia, D.R. Bes and R. Liotta, Phys.Reports 30C (1977)305 and references therein.

2) D. Janssen, R.V. Jolos and F. Dönau, Yad, Fiz. 22 (1975)965. (Sov. J. Part Nucl. 8 (1977)138).

3) G. Holzwarth, D. Janssen and R.V. Jolos, Nucl.Phys. A261 (1976)1

4) Interacting Bosons in Nuclear Physics, Ettore Majerana. International Science Series, ed. F. Iachello (Plenum, New York,1979).

IV.12 Two Correlated Quasiparticle States in the Principal Serie Approximation

J. Dukelsky, G.G. Dussel and H.M. Sofia.

The application of the Principal Serie Approximation (P.S.A.) to the description of the ground state and its comparison with the usual Hartree-Fock-Bogoliubov methods was presented in reference 1.

In the present work it is taken advantage of this knowledge to construct the two quasiparticle excitations in superconductive (non-deformed) systems. In the P.S.A it has to be distinguished between addition and

removing quasiparticles, corresponding to states in the systems with 2M+1 or 2M-1 particles. Hence, there are three sorts of two quasiparticles states in the system with M pairs of particles, one corresponds to one addition and one removal quasiparticles in the M pair system and the others correspond to two addition (removal) quasiparticles on the M-1 (M+1) pair system. It is then possible to construct three different sorts of bosonic excitations, one has a particle-hole character (for example the usual 2^+ collective state in spherical nuclei), and the others have a two particle (hole) structure.

The distinction between this two types of excitations in closed shell nuclei es quite clear because for those nuclei the concepts of particle and hole are well defined. Moreover, the admixture between both types of excitations, due to the ground state correlations, is of one order less than the R.P.A and it can be calculated perturbatively.

The situation is completely different in superconductive nuclei because it is found that the PS for the particle-hole and particle-particle Green functions are mixed in the leading order and must be treated together giving rise to a different R.P.A. equation for the description of the collective states[2]. In particular, there are two important points arising when both Green functions are mixed. The first one is that the number of states comes out correctly, while when both Green's functions are treated separately the number of states is twice as big at least. The second one is that the coupling between both collective states changes the values of the two particle transfer to excited states and its electromagnetic properties. The most striking difference is the change in the SME for $Q_{2\mu}$ and its EWSR. These changes will produce a rather large change in the inelastic scattering cross section of high projectiles, that are related to the SME of the mass

quadrupole operators. It must be noted that if the effective charges are evaluated microscopically there will also exist a big difference in the electromagnetic properties in both description.

---

1) G.G. Dussel and D.R. Bes, Nucl.Phys. A323 (1979)392

2) D.R. Bes, G.G. Dussel and J. Gratton, in Proc.Inter. Nuclear Physics Conference, Gattinbrurg, p.499, ed. R.L. Becker, Academic Press, N.Y. 1967.

IV.13 Separable Interactions and Excited States in Open Shell Nuclei*

J. Dukelsky, G.G. Dussel and H.M. Sofia.

Separable interactions have been widely used[1] in the description of nuclear collective and single particle excitations. The introduction of the pairing interaction[2] and the quadrupole-quadrupole[3] one, made possible to understand qualitative features of the low energy spectra of medium and heavy nuclei.

The concept of particle-particle (p-p) and particle-hole (p-h) collective degrees of freedom in double closed shell nuclei appears as a consequence of the existence of these two interactions.

$$H = H_{sp} + H_{tb} =$$
$$\sum_i \varepsilon_i C_i^+ C_i + \sum_{ijkl} V^J_{ij,kl} \left\{ [C_i^+ C_j^+]^J [C_k^- \bar{C}_l]^J \right\}_0^0 =$$
$$\sum_i \varepsilon_i C_i^+ C_i + \sum_{ijkl\lambda} Q^\lambda_{ij,kl} \left\{ [C_i^+ \bar{C}_k]^\lambda [C_j^+ \bar{C}_l]^\lambda \right\}_0^0$$

Where $C^+_{im_i}$ creates a particle in the state (i,m_i) while C_{k,m_k} transforms under rotations as (k,m_k).

The aim of this work is to study which are the relevants terms of the two body hamiltonian for an R.P.A. description of the bosonic excitations in open shell nuclei, where the concept of particle and hole disappears.

In this work are shown the following features:

1) The introduction of both types of interactions does not produce any double counting of processes up to the order of approximation utilized in the R.P.A.
2) The (p-p) hamiltonian can be obtained from the (p-h) one through a recoupling of the operators. This gives the contribution to the R.P.A. of all the λ (p-h) terms equivalent to a given J=I(p-p) term.
3) The sum of all the recoupling terms is of the same order and therefore their contributions must be included in a J=I RPA calculation.

To analize the consequences due to the simultaneous use of both interactions a calculation is done for the first 2^+ excited state of the S_n isotopes. There are two main consequences that appear from this calculation. One is the rather large increase in the two particle transfer spectroscopic amplitudes and the decrease of the matrix element associated with the electromagnetic transition to the first excited state. The other is the drastic decrease of the energy weighted sum rule for the operator Q. These two features may be considered as due to the almost complete disappearance of the backward amplitudes, and therefore the ground state correlations.

---

* Submitted to Phys. Lett.

1) A. Bohr and B. Mottelson, Nuclear Structure, Vol.2, W.A. Benjamin (1975)p.340.

2) A. Bohr, B. Mottelson and D. Pines, Phys.Rev. 110 (1958)936.
S.T. Belyaev, Matt. Fys. Medd. Dan. Vid. Selsk. 31 N°11 (1959)

3) J.P. Elliot, Proc. Roy. Soc. A245 (1958)128.

IV.14 A Reformulation of the Mode-Coupling Method[+]

R.J. Liotta[*], C. Pomar and B. Silvestre-Brae[**]

The Mode-coupling method[1] describes the nuclear spectra around closed-shell nuclei in terms of particle-hole and particle-particle correlated states. The method is simple and elegant but there are a few disadvantages in using it, mamely

i) the overcomplete set of basis states provides a number of spurious states which may not be easily disentangled from the physical states in a realistic calculation, where the basis has generally to be truncated (drawback shared by the nuclear field theory),

ii) the matrix that provides the energies is not hermitian and complex solutions may be obtained.

iii) It is not clear how to calculate the wave functions, for which arbitrary normalization conditions have so far been used[1].

In this work, we reformulate the mode-coupling method to avoid the three drawbacks mentioned above, while keeping the essential positive features of the model. The method is applied to the nucleus ^{91}Nb.

+ Lett. Nuovo Cim. 27 (1980)100

* Research Institute of Physics, S-104 05 Stockholm, Sweden.

** Institute des Sciences Nucléaires, Grenoble, France.

1) P. Ring and P. Schuck, Z.Physik 269 (1974)323.

IV.15 Multi-Step Shell-Model Treatment of Six-Particle Systems[+]

R.J. Liotta[*] and C. Pomar

The main achievement of models containing correlated states in the basis is that with only a few basis states a rather large amount of experimental data is explained.

In this work we extended the method given in reference 1) to analyse four- and six-particle systems outside closed-shell cores. The basic idea here is to use the two-particle spectrum components as building blocks to describe the four-particle system. Once the four-particle spectrum is obtained, we use this spectrum and that of the two-particle system as building blocks to describe the six-particle system. We found that the formalism turns out to be very simple. The equations that describe the six-particle are actually simpler than the corresponding equation for the four-particle system.

The method is applied to analyse the ^{204}Pb and ^{202}Pb spectra and (p,t) reactions[2]. Good agreement with experimental data is obtained. A liaison between this calculation and the pairing model is found and the importance of the Pauli principle upon the pairing vibrational states is attested.

+ Nucl. Phys. A362 (1981)137.
Phys. Lett. 92B (1980)229.

* Research Institute of Physics, S-104 05 Stockholm, Sweden.

1) Research Institute of Physics, Stockholm, Ann.Rep. 1978 p.68ff,and references therein.

2) W.A. Landford, Phys.Rev. 16C (1977)273.

IV.16 Structure of ^{203}Pb in Terms of ^{207}Pb and ^{204}Pb+

R.J. Liotta* and C. Pomar.

It was recently shown that the spectra of even lead nuclei can be described within a multi-step shell-model method (MSM). A nucleus calculated in a given step is used as a building block in sucessive steps[1]. An important feature of the MSM is that only very few states are required to get a good description of the final nucleous thus allowing drastic truncations of the original shell-model basis.

In this work we apply the MSM to the case of five holes outside the ^{208}Pb core (i.e.^{203}Pb) where a complete shell-model calculation would be a very difficult task.

It is found that most ^{203}Pb levels (up to 1.5 MeV) are very pure and only one MSM vector is necessary to described them. An important exception is the first state $\frac{1}{2}^-$ wich require at least three MSM bases vectors for its description. This is due to the fact that the state $|\, p_{\frac{1}{2}}\, 0^+_1; \frac{1}{2}^- \rangle$ is very much blocked by the Pauli principle. Very good agreement is obtained with the experimental energies in the first ten described states.

+ Accepted for publication in Phys.Lett.B

* Research Institute of Physics, S-104 05 Stockholm, Sweden.

1) R.J. Liotta and C. Pomar Nucl.Phys. A362 (1981)137.

IV.17 Graphical Multi-Step Shell-Model Calculation of Even Tin and Lead Ground States[+]

C. Pomar and R.J. Liotta[*]

In this work we intended to generalize the Multi-Step Shell-Model method[1] (MSM) for a system σ consisting of a number of s particles. We thus assumed σ partitioned in the subsystems μ and ν with number of particles m and n respectively, such that n is even and m=2. For this partition of the system σ we introduced a graphical procedure to evaluate the MSM dynamical matrix. We applied this equation to analize ground-state energies of spherical nuclei. This ground-state may be assumed to be proportional to only one MSM vector. Namely, $|\sigma=gs\rangle = N|\mu(gs)\otimes\nu(gs)\rangle$, where N is a normalization constant. Within this approximation we obtain

$$W_\sigma = W_\sigma(a) + W_\sigma(b) + W_\sigma(c)$$

Where $W_\sigma(a) = W_{gs}(2) + W_{gs}(n)$; $W_\sigma(b) = W_{gs}(n) - W_{gs}(2) - W_{gs}(n-2)$; $W_\sigma(c) = W_{gs}(4) - 2W_{gs}(2)$; and $W_{gs}(m)$ is the ground-state energy of the m-particle system.

In Table 1 we give both the experimental and calculated ground-state energies in the lead and tin regions. Taking into account the great differences between the zero order energies $W_\sigma(a)$ and the experimental values, one can well say that the agreement between theory and experiment is good. In the middle of the major shells, where the shell-model dimension is of the order of several millions, this agreement is excellent.

TABLE 1

	^{A}Sn (A = 132−n)				^{A}Pb (A = 208−n)			
n	W_σ(a)	W_σ(b)	W_σ(theor.)	W_σ(exp.)	W_σ(a)	W_σ(b)	W_σ(theor.)	W_σ(exp.)
6	37.380	----	39.240	38.796	43.035	----	44.463	44.246
8	50.946	1.416	53.292	52.722	58.353	1.211	60.278	60.170
10	64.872	1.776	67.578	67.159	74.277	1.817	76.808	76.570
12	79.309	2.287	82.526	82.146	90.677	2.293	93.684	93.470
14	94.296	2.837	98.063	97.737	107.577	2.793	111.084	110.950
16	109.887	3.441	114.258	114.008	125.057	3.373	129.144	128.610
18	126.158	4.121	131.209	131.117	142.717	3.553	146.984	146.820
20	143.267	4.959	149.156	149.162	160.927	4.103	165.744	165.690
22	161.312	5.895	168.137	168.129	179.797	4.763	185.274	185.000
24	180.279	6.817	188.026	188.200	199.107	5.203	205.024	----
26	200.350	7.921	209.201	209.260				
28	221.410	8.910	231.250	231.240				
30	243.390	9.830	254.150	-----				

Table I Theoretical and experimental[2] ground-state energies (in MeV) in the tin and lead regions. The number of active particles in n. The theoretical zero order energy W_σ(a) is given together with the correction W_σ(b). The contribution W_σ(c) is 0.930 MeV in Sn and 0.714 MeV in Pb. Some "experimental" data are actually estimated from systematic trends[2]. In this case, rather large errors (up to 1 MeV) may be encountered[2]. In addition, the binding energy of the core ^{132}Sn is only known within an error of 200 keV.

+ Accepted for publication in Phys.Rev.C.

* Research Institute of Physics, S-104 05 Stockholm, Sweden.

1) R.J. Liotta and C. Pomar, Nucl.Phys A362 (1981)137

2) A.H. Wapstra and K. Bos, Atomic Data and Nucl. Data Tables 19 (1977)175.

IV.18 Microscopic Description of Yrast States in Spherical Nuclei[+]

R.J. Liotta[*] and C. Pomar

It was recently shown that the ground-states of the even Tin and Lead isotopes can be described in terms of only one multi-step shell-model vector[1] (see also contribution IV.17). The validity of this approximation is essentially based in the fact that those states are isolated from the rest of the spectrum. It seems reasonable to extend this assumption to the case of the yrast states (that we call Θ_p) wich are also isolated from the rest of the spectrum. For these states we assume[2]

$$|\Theta_s\rangle = \chi(gs_2\,\Theta_n;\Theta_s)\; P^+(gs_2)\; P^+(\Theta_n)|0\rangle \qquad (1)$$

Where $P^+(\alpha m)$ is the m-particle creation operator of the physical state α_m. The amplitude χ plays, in the present approximation, the role of a normalization constant and gs_2 label the two-particle ground state. The approximation (1) would be valid as long as the norm of the vector $|\Theta_s\rangle$ is not negligible, i.e. as long as the Pauli principle is not very effective in blocking the state(1). But if the number of particles n is large enough the single-particle shells upon which the vector (1) is built would be filled and the approximation (1) would break down. This is what happens with the vector $P^+(\Theta_2)P^+(gs_n)|0\rangle$ in ^{202}Pb (for details see p.159 of reference 2)). This vector is much less important than the vector (1) because the states $|\Theta_2 \neq gs_2\rangle$ are very "pure" (i.e. they are described by very few shell-model configurations) in comparison with the normal pairing vibration $|gs_2\rangle$.

For the yrast states we obtain then from the multi-step shell-model dynamical equation[2].

$$W(\Theta_s) - W(gs_2) = W_1 + W_2$$

where $W_1 = (1 + \delta_{n4})(W(\Theta_n) - W(gs_2) - W(0_{n-2}))$ and

$$W_2 = (1 + \delta_{nh})(W(gs_4) - 2\,W(gs_2)).$$

$W(\alpha n)$ is the energy, refered to the "core", of the state αn.

Within the same approximation $W(gs_s)$ is calculated, such that.

With $E(\theta_s) = W(\theta_s) - W(gs_s)$ one finally obtains

$$E(\theta_s) = E(\theta_n) + \Delta E(\theta_n) \qquad (2.1)$$

$$\Delta E(\theta_n) = E(\theta_n) - E(\theta_{n-2}) \qquad (2.2)$$

i.e. the energy of the states θ_s would follow a monotonous variation with the number of particles n. If ΔE is negative (positive) in the beginning of the major shell $E(\theta_s)$ would decrease (increase) monotonously with the number of particles. This is indeed a tendency followed by all spherical nuclei. As an example (which is rather typical) we show in figure 1 the hole spectra in the lead region. Other examples are shown, e.g., in reference 3).

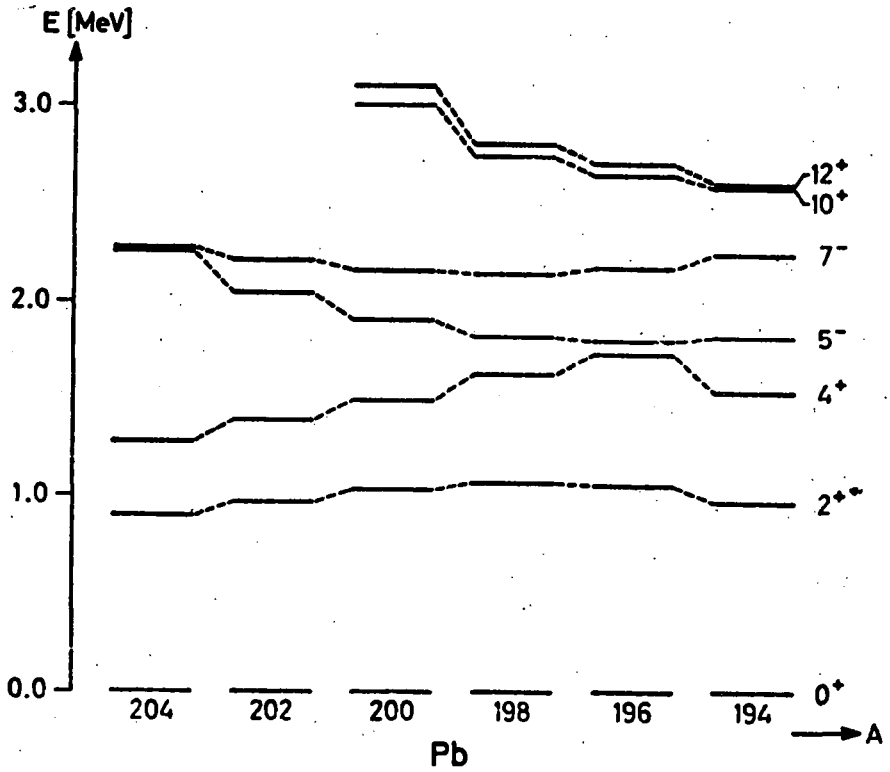

Figure 1: Experimental neutron hole spectra in the lead region

As mentioned above, eq.(2) cease to be valid when the single-particle shells that constitute the vector (1) are filled. For instance, the states 4^+ in figure 1 are built mainly upon the shells $p_{1/2}$, $p_{3/2}$, $f_{5/2}$. These shells

are filled in ^{194}Pb and therefore the tendency mentioned above is not followed in this nucleus. One may then apply eq. (1) starting from the other extreme of the major shell. Thereby the meaning of "empty" and "full" shells are interchanged and eq.(2) continue to be valid, in agreement with experimental data.

+ Submitted for publication to Physics Letters B.

* Research Institute of Physics S-104 05, Stockholm, Sweden.

1) C. Pomar and R.J. Liotta, Phys.Rev. (to be published)

2) R.J. Liotta and C. Pomar, Nucl.Phys. A362 (1981)137.

3) T. Lönroth, B. Fant, K. Fransson, A. Källberg and K.O. Pettersson, Phys.Scripta 23 (1981)774.
K. Fransson, Ph.D.Thesis, Stockholm University, 1981.

IV.19 A Graphical Procedure to Evaluate the Many-Body Shell-Model Equation: The Ground States of Spherical Nuclei+

R.J. Liotta* and C. Pomar

The graphical method introduced in reference 1) (see also above previous contribution) was generalized for any kind of particles of a system σ (i.e. the system σ can be partitioned in any number of blocks, each block containing any number of particles). In addition the overlap (or metric) matrix is also evaluated using the graphical procedure of reference 1) extended for this purpose.

The graphical procedure has been used to analize systems where proton and neutron degrees of freedom play a role. In particular it was studied nuclei with 4n particles outside the core such that those 4n nucleons were

2n neutron and 2n proton (n alpha-particles nuclei). Assuming that the ground-state for a nucleus with s=4+n nucleous outside a magic core can be written as

$$|gs;s\rangle = N_s \,|\, 4(gs) \otimes n(gs)\rangle$$

Where N_s is a normalization constant. Whithin this approximation we obtain

$$W_{\alpha_s} = W^{(0)}_{\alpha_s} + W^{(1)}_{\alpha_s} + W^{(2)}_{\alpha_s}$$

Where

$$W^{(0)}_{\alpha_s} = W_{\alpha_4} + W_{\alpha_m} \qquad (1.a)$$

$$W^{(1)}_{\alpha_s} = W_{\alpha_m} - W_{\alpha_4} - W_{\alpha_{m-4}} \qquad (1.b)$$

$$W^{(2)}_{\alpha_s} = W_{\alpha_8} - 2W_{\alpha_4} \qquad (1.c)$$

Where W_{α_m} labels the ground state of the m/4 alpha-particle nucleus.

In table 1 we show the calculated ground-state energies corresponding to ^{208}Pb plus alpha-particle nuclei. This is a good example of the breaking down of a pure MSM description when deformations set in. For spherical nuclei the calculated energies are in good agreement with experimental data.

N	Z	$W^{(0)}$	$W^{(1)}$	W (theor.)	W (exp.)	d
132	88	58.78	0.75	60.28	60.14	0.14
134	90	79.48	1.36	81.59	81.13	0.46
136	92	100.48	1.65	102.88	102.62	0.25
138	94	121.97	2.15	124.87	124.20	0.66
140	96	143.55	2.24	146.54	145.40	1.14
142	98	164.74	1.85	167.35	165.98	1.37
144	100	185.32	1.24	187.31	-	-

Table 1

Ground-state energies (in MeV), eq.(1) for ^{208}Pb as the core. The numbers N and Z indicate neutron and proton numbers, respectively. The contribution W_{α_s} (eq.1.c) is here equal to -0.75 MeV. The difference between theoretical and experimental values is d (eq.2).

In the well deformed nuclei (above A=228 in table 1) the contribution $W^{(1)}_{\alpha_s}$ does not increase regularly with A, as for spherical nuclei, and the energy difference between theory and experiment is more than 1 MeV.

A similar effect is seen in the tin region, as shown in table 2. For A > 148 one reaches a well deformed region and the contribution $W^{(1)}_{\alpha_s}$ shows an irregular dependence upon A. Another interesting feature emerging from table 2 is that when one crosses the magic number Z = 82, a sudden jump in

$$d = W_{\alpha_s}(\text{theor.}) - W_{\alpha_s}(\text{exp.}) \qquad (2)$$

is seen. This is because our MSM states contain only single-particles

N	Z	$W^{(0)}$	$W^{(1)}$	W (theor.)	W (exp.)	d
88	56	87.39	-0.09	87.21	87.80	-0.59
90	58	116.96	0.41	117.28	117.20	0.08
92	60	146.36	0.24	146.51	147.36	-0.85
94	62	176.52	1.00	177.43	177.30	0.13
96	64	206.46	0.78	207.16	206.60	0.56
98	66	235.76	0.13	235.80	235.34	0.46
100	68	264.50	-0.42	264.00	263.08	0.92
102	70	292.24	-1.42	290.73	290.07	0.66
104	72	319.23	-2.17	316.97	316.11	0.86
106	74	345.27	-3.12	342.05	341.88	0.17
108	76	371.04	-3.38	367.57	367.21	0.36
110	78	396.37	-3.83	392.45	391.49	0.96
112	80	420.65	-4.88	415.68	416 39	-0.71
114	82	445.55	-4.26	441.20	440.29	0.91
116	84	469.45	-5.26	464.10	462.60	1.50
118	86	491.76	-6.85	484.82	484.35	0.47
120	88	513.51	-7.41	506.01	505.38	0.63
122	90	534.54	-8.13	526.32	-	-

Table 2

As table 1 for the ^{132}Sn core. The contribution $W^{(2)}_{\alpha_s}$ is -0.09 MeV

components belonging to the major shell close to the original magic core. Actually, this feature may help to determine how "magic" is a given number N or Z. For instance, in table 3 we show the calculated ground-state energy

N	Z	$W^{(0)}$	$W^{(1)}$	W (theor.)	W (exp.)	d
76	58	-82.99	-0.01	-83.02	-83.31	0.29
74	56	-110.97	-0.32	-111.30	-111.49	0.19
72	54	-139.15	-0.53	-139.69	-140.36	0.66
70	52	-168.02	-1.20	-169.23	-169.94	0.70
68	50	-197.59	-1.92	-199.53	-199.31	-0.22
66	48	-226.96	-1.71	-228.69	-231.66	2.97
64	46	-259.32	-4.70	-264.03	-264.07	0.04
62	44	-291.73	-4.75	-296.49	-296.79	0.30
60	42	-324.45	-5.07	-329.53	-330.28	0.75
58	40	-357.94	-5.83	-363.79	-363.27	-0.51
56	38	-390.93	-5.33	-396.28	-396.32	0.04
54	36	-423.98	-5.39	-429.38	-430.82	1.44
52	34	-458.48	-6.84	-465.33	-465.87	0.54
50	32	-493.53	-7.39	-500.93	-501.66	0.73
48	30	-529.32	-8.13	-537.46	-540.09	2.63
46	28	-567.75	-10.77	-578.53	-	-

Table 3

As table 1 for the ^{146}Gd core. The contribution $W^{(2)}_{\alpha_3}$ is -0.01 MeV.

corresponding to the core[2] ^{146}Gd minus alpha-particle nuclei. The same jump seen in table 2 is here found for Z=50, N=68; Z=38, N=56 and Z=32, N=50. Strictly speaking, in this case our calculations would only be valid up to A=118, i.e. up to the point where one reaches the end of the original major shell. But the general tendency of the smooth variation of d versus A remains valid irrespective of the point where one stops the MSM process

given by eq.(1). Therefore, the abrupt change of d (A) in table 3 does not depend upon our way of calculating W_{ds}.

It is perhaps not very surprising to find in table 3 that the major shell filling 50 nucleons is so tightly closed. However, the nucleus $^{94}_{38}Sr$ was only recently found to be a "magic" nucleus[3),4)], although $^{88}_{38}Sr$ was already long ago considered a good hard core[5)].

It is worthwhile to point out that a standard shell-model calculation in the cases presented here would be virtually impossible. The shell-model dimensions in the middle of a major shell in medium and heavy nuclei is of the order of hundreds of millions.

We also found closed formulas for the different steps of the MSM. It would then be possible to solve the shell-model equations with the same degree of complexity, irrespective of the number of active particles. Thus, if drastic truncations are possible in general, as suggested by our present ground-state calculations and previous six-particle calculations in the lead region[6)], one may calculate systems for which standard shell-model calculations are impossible today.

+ Submitted for publication, to Nuclear Physics.

* Research Institute of Physics, s-104 05 Stockholm, Sweden.

1) C. Pomar and R.J. Liotta, Phys.Rev. C (to be published)

2) P. Kleinheinz, R. Broda, P.J. Daly, S. Lunardi, M. Ogawa and J. Blomquist, Z.Physik A286 (1978) 27.

3) P. Federman and S. Pittel, Phys.Rev. C20 (1979) 820.

4) F. Tondeaur, Nucl.Phys. A359 (1981)278.

5) B.F. Bayman, A.S. Reiner and R.K. Sheline, Phys.Rev. 115 (1959)1627.

6) R.J. Liotta and C. Pomar, Nucl.Phys. A362 (1981)137.

IV.20 The Decay of the T=1 Isospin Triplet in the A=12 System: IV. The energy dependence of the asymmetry coefficients $\alpha_{\beta^\pm}$ of the beta ray angular distribution in aligned ^{12}B and ^{12}N and the induced pseudotensor interaction.+

L. Szybisz* and H. Behrens**

The asymmetry parameters $\alpha_{\beta^\pm}$ of the beta ray emitted from aligned ^{12}B and ^{12}N are evaluated as a function of the energy. The agreement with experimental differential data is excellent for both $\alpha_{\beta^-}(W)$ and $\alpha_{\beta^+}(W)$. This work confirms, using available nuclear model information that no induced pseudotensor (IPT) interaction is required for a correct theoretical interpretation of the data. An upper limit for the IPT coupling constant f_T is determined from a simultaneous fit of $\alpha_{\beta^-}(W)$ and $\alpha_{\beta^+}(W)$.

+ L. Szybisz and H. Behrens, Z.Phys. A296, (1980)309.

* Departamento de Física, Facultad de Ciencias Exactas, UNLP, Argentina.

** Fachinformationszentrum Energie, Physik, Mathematik Karlsruhe, Eggenstein-Leopoldshafen, Federal Republic of Germany.

IV.21 Improved Limit on the Induced Scalar Interaction in Nuclear Beta-Decay+

L. Szybisz* and V.M. Silbergleit**

An improved procedure which allows to diminish by almost a factor 2 the upper limit on the induced scalar interaction obtained from a study of superallowed Fermi beta-transitions is reported. The new limit, $|f_S| \leq 0.6 \times 10^{-3} < f_M = 1.0 \times 10^{-3}$, support the CVC theory and the invariance of weak interactions under G-parity transformation.

+ L. Szybisz and V.M. Silbergleit, Z.Phys. A299, (1981)91.

* CONICET and Departamento de Física, Facultad de Ciencias Exactas, UNLP, Argentina.

** CONICET and Departamento de Física, Facultad de Ciencias Exactas y Naturales, UBA, Argentina.

IV.22 Crucial Influence of the Relativistic Form Factor Coefficients on the Determination of $f_{\hat{S}}$.+

L. Szybisz* and V.M. Silbergleit**

It is shown that the contribution of the induced scalar interaction through relativistic form factor coefficients is very important. It is found that this interaction affects the spectrum shape factor, to a first approximation, in the same way as the Fierz interference term, contrary to a previous assumption. A limit on the strength of $f_{\hat{S}}$ of order 1/M is set.

+ L. Szybisz and V.M. Silbergleit, G.Phys. G7 (1981)L-201.

* CONICET and Departamento de Física, Facultad de Ciencias Exactas, UNLP, Argentina.

** CONICET and Departamento de Física, Facultad de Ciencias Exactas y Naturales, UBA, Argentina.

IV.23 Hartree-Fock Theory in Exactly Soluble Models with a Finite Number of Particles[+]

M.C. Cambiaggio[*], A. Plastino[*], L. Szybisz[*] and M. de Llano[**]

A review is made of different exactly soluble models of a finite number of fermions, in order to study the properties of the Hartree-Fock approach, relating them to those of the exact Schrödinger solution. Particular attention is paid to the description of phase transitions.

+ Revista Mexicana de Física 27 (1981) 223.

* CONICET and Departamento de Física, Facultad de Ciencias Exactas, UNLP, Argentina.

** Instituto de Física, Universidad Nacional Autónoma de México, México.

IV.24 Constrained Hartree-Fock and Quasi-Spin Projection[+]

M.C. Cambiaggio[*], A. Plastino[*] and L. Szybisz[*]

The constrained Hartree-Fock approach of Elliott and Evans is studied in detail with reference to two quasi-spin models, and their predictions compared with those arising from a projection method. It is found that the new approach works fairly well, although limitations to its applicability are encountered.

+ Nucl.Phys. A344 (1980)233.

* CONICET and Departamento de Física, Facultad de Ciencias Exactas, UNLP, Argentina.

IV.25 Maximum Overlap, Atomic Coherent States and the Generator Coordinate Method+

G. Bozzolo*, M.C. Cambiaggio* and A. Plastino*

A version of the maximum overlap approach is presented, based on the generator coordinate method. Recourse is made to techniques developed with reference to atomic coherent states. Shape instabilities in quasi-spin two level models are studied.

+ Nucl.Phys. A356 (1981)48.

* Departamento de Física, Facultad de Ciencias Exactas, UNLP, Argentina.

IV.26 On the Possibility of Abnormal Occupation in ^{3}He and ^{4}He+

M.C. Cambiaggio*, M. de Llano**, A. Plastino* and L. Szybisz*

The possibility of abnormal occupation in the plane-wave Hartree-Fock ground state of Helium systems is studied with reference to several semiphenomenological potentials[1]. Some criteria have been established[2] which allow one to decide, on the basis of properties of the Fourier transform of the relevant two-body interaction, when such abnormal occupation may prevail energy-wise. All five Fourier transforms calculated in this work are definite positive and monotonically decreasing. Consequently, no abnormal occupation is possible, either in the Fermi or in the Bose case, according to the above mentioned theorems[2].

The possibility has also been investigated of finding, in the spirit of reference 3), a Slater determinant built up with Wannier-like single

particle wave functions which yields a lower energy than the corresponding plane-wave one. Only at high densities $\rho \geq 0.25$ A^{-3} one obtains lower energy per particle in the solid phase than in the fluid one, i.e., both for ^{3}He and ^{4}He a crystalline structure is preferred (at zero order) for densities outside the physical range.

+ Revista Mexicana de Física 28 (1981)91.

* CONICET and Departamento de Física, Facultad de Ciencias Exactas, UNLP, Argentina.

** Instituto de Física, Universidad Nacional Autónoma de México, México.

1) R.F. Bishop, H.B. Ghassib and M.R. Strayer, J.Low Temp.Phys. 26 (1977)669

2) M. de Llano, A. Plastino and J.G. Zabolitzky, Phys.Rev. C20 (1979)2418.

3) M.C. Cambiaggio, M. de Llano, A. Plastino, L. Szybisz and S. Ramirez, Nucl. Phys. A339 (1980)277.

V. NUCLEAR REACTIONS

V.1 On the Decay of Compound Nuclei Following Alpha-Particle and ^{12}C Induced Reactions*

S.J. Hjorth, A. Johnson, A. Kerek, W. Klamra, Th. Lindblad, S. Messelt, C. Pomar, O. Skeppstedt, L. Carlen, H. Ryde and M. Piiparinen.

Multiple coincidence rates have been measured(+) using a detector system consisting of Ge(Li) spectrometer and eight NaI(Tl) or eight liquid scintillators. Reactions induced by alpha-particles with energies of 51-55 MeV and 118 MeV ^{12}C ions are studied. The data are analysed to give the first and second central moments of the distribution of the number of gamma-rays feeding individual levels in the final nuclei. When these numbers are compared to spin distributions calculated with the statistical model code GROGI the relative importance of dipole and quadrupole deexcitation modes can be ascertained. In particular, in the $^{122}Te(\alpha,4n)^{122}Xe$ reaction the gamma-decay prior to the entry into the ground band is well described as a statistical process proceeding to 50% by dipole and 50% by quadrupole radiation. In the $^{166}Er(\alpha,4n)^{166}Yb$ and $^{192}Os(\alpha,4n)^{192}Pt$ reactions the relative amount of quadrupole radiation is larger and it seems that the dipole and quadrupole decay takes place via separate cascades. In the $^{164}Dy(^{12}C,7\text{-}8n)$ reactions the average multiplicity is independent of spin, suggesting that the nucleus forgets the spin of the entry state before the process enters into the ground band. In the $^{176}Yb(^{12}C,8n)^{180}Os$ reaction, finally, the nucleus definitely retains memory of the entry state during the decay. In this last case the multiplicity measurement is combined with a gamma-ray singles measurement to give an average excitation energy prior to

the alpha-decay and the average moment of inertia characterising the decay of the high-spin states.

---

* Z.Phys. A301 (1981)35

+ This experiment was performed of the Research Institute of Physics, 104 05 Stockholm, Sweden.

V.2 Chemical Potencial in Fission Processes

D. Napoli, D. Otero, A. Plastino* and A.N. Proto

The experimental features of fission processes are studied within the framework of the "surprisal" formalism[1], which is based on information theory. The advantage of this procedure lies in its ability to distinguish quite well the experimental facts from any "a priori" assumptions. For the fission processes our basic "a priori" assumptions are:

a) The scission configuration is represented by a binuclear system where the level density ρ_o on each well is that of a degenerate nuclear Fermi gas. Thus we can write,

$$\rho_o \sim \rho_L^o \rho_H^o \qquad (1)$$

with

$$\rho_{L,H}^0 \simeq U_{L,H}^{-2} \exp\left(\tfrac{1}{6}\pi^2 g_0 U_{L,H}\right)^{\frac{1}{2}} \qquad (2)$$

Where the subscripts L, H identified the light and heavy member of the dinuclear system, g_0 is the one particle level density at the Fermi energy ϵ_F, when the sum of the proton and neutron level density is considered and $U_{L,H} = U^*_{L,H} - E^{pair}_{L,H}$ is the internal excitation energy. As a first approximation we neglect the rotational energy dependence. We choose for the pairing energy $E^{pair}_{L,H} = \alpha\Delta$ where $\alpha = 0,1,2$ for odd-odd,

even-odd, or even-even nuclei and $\Delta = 12\ A^{-\frac{1}{2}}$. In general U_L is different from U_H and we do not postulate thermal equilibrium in the dinuclear system. This ρ_o is our "a priori" level distribution. Besides

$$\frac{1}{6}\pi^2\, g(\epsilon_F) \simeq \frac{1}{8} A(\mathrm{MeV})^{-1} \qquad (3)$$

b) The internal excitation energy is proportional to the mass of each member of the dinuclear system. The observed experimental data are the fission mass-yield distributions (figure 1) and we shall show that they are

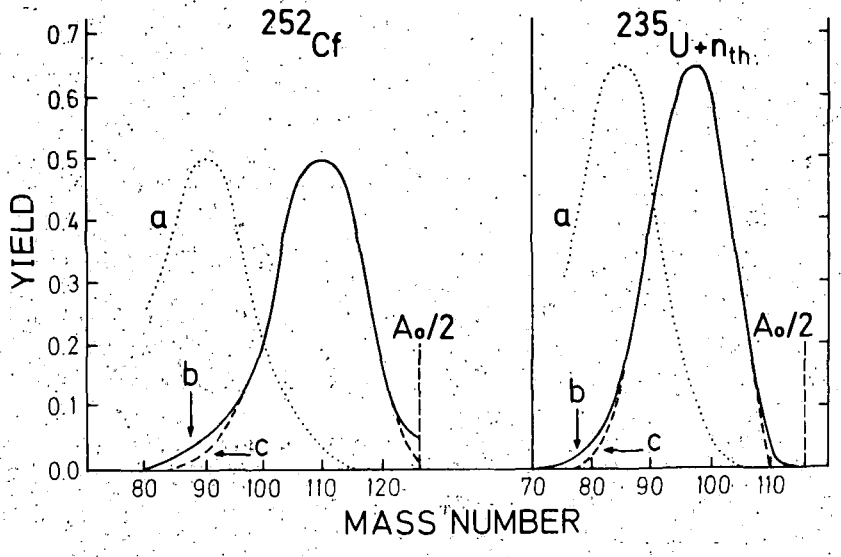

Figure 1

adequately described by choosing the mass number A as the relevant dynamical variable. The use of information theoretical methods implies the belief that the fission process envolves in such a way that the entropy of the final states is maximal, and constrained only by the appropiate dynamical variables. Our ansatz is that the mass-number is the most important one in this respect. To examine the departure of the observed distribution ρ from that expected on purely statistical grounds, i.e. ρ^o, it proves advantageous to introduce the concept of surprisal given by[1)]

$$-\ln \rho/\rho^o = \lambda A + \lambda_o \qquad (4)$$

Where λ_o ensures the proper normalization and λ is a Lagrange multiplier. From eq.(4) and taking into account the above assumptions the theoretical value of λ can be obtained by taking the derivative of the local entropy

deficiency at the mean value of the corresponding observable. In our case one finds:

$$\lambda_T = \left[\frac{1}{4}\left(\frac{A}{2U_L}\right)^{1/2} - \frac{2}{U_L}\right]\frac{\partial U_L}{\partial A_L} - \left[\frac{1}{4}\left(\frac{A_H}{2U_H}\right)^{1/2} - \frac{2}{U_H}\right]\frac{\partial U_H}{\partial A_H} + \frac{1}{4}\left(\frac{U_L}{2A_L}\right)^{1/2} - \frac{1}{4}\left(\frac{U_H}{2A_H}\right)^{1/2}\Bigg|_{A_L = \langle A_L \rangle}$$

Where $A_0 = A_L + A_H + \nu^*$ (6)

ν represents the neutron emision. Some results can be seen in figure 2.

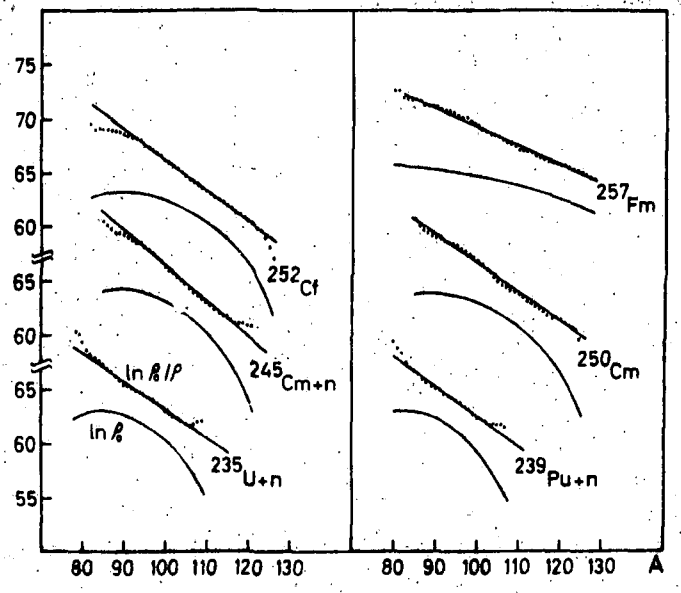

Figure 2

The expression for ρ can be factorized as follows:

$$\rho' = \rho_H \times \rho_L \qquad (7)$$

with

$$\rho'_{H,L} = \rho^0_{H,L}\, e^{\frac{\lambda}{2} A_{H,L}}\, e^{\lambda'_0} \qquad (8)$$

where λ'_0 is a renormalization constant. Besides

$$\frac{1}{T_{H,L}} = \frac{\partial \ln \rho'_{H,L}}{\partial U_{H,L}} \qquad (9) \qquad \text{and} \qquad \mu = \frac{\partial U_{H,L}}{\partial A_{H,L}} \qquad (10)$$

Then introducing (8) in (9) and (10) results that

$$\lambda = \Delta^R\left(\frac{\mu}{T}\right) - \Delta^0\left(\frac{\mu}{T}\right) \qquad (11)$$

This means that the Lagrange parameter is the difference between the $\frac{\mu}{T}$ of both fragments calculated in the real distribution $(\Delta^R(\frac{\mu}{T}))$ and the same magnitude but calculated on the "a priori" distribution $(\Delta^\circ(\frac{\mu}{T}))$ in this case the degenerate Fermi gas distribution. For the $\langle A_L \rangle$ the expression reduced to

$$\frac{\mu_H}{T_H} = \frac{\mu_L}{T_L} \qquad (12)$$

For the symetric case, instead

$$\mu_H = \mu_L \quad \text{and} \quad T_H = T_L$$

this means that exists thermal equilibrium. The results for ^{226}Ra (p,f)[2] are shown in figure 3.

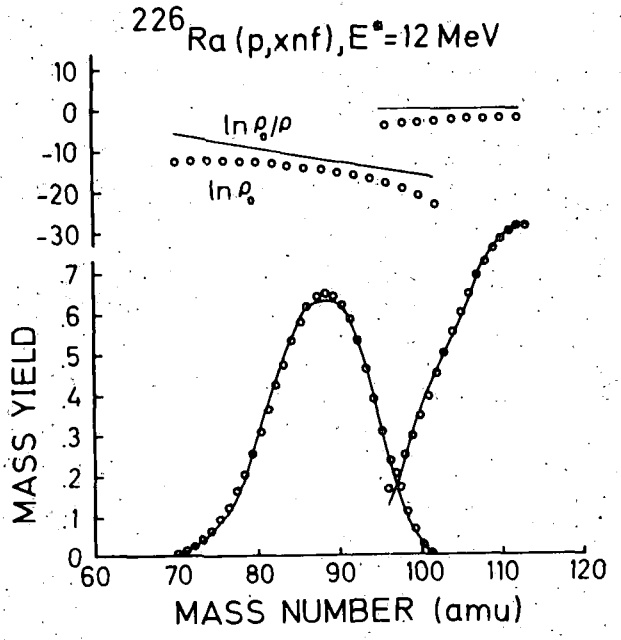

Figure 3

The μ/T values for several fissioning systems are shown in figure 4.

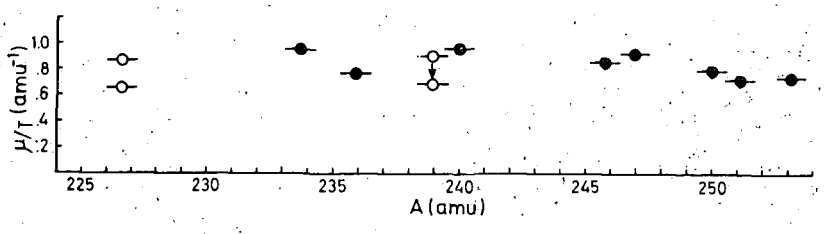

Figure 4

The chemical potencial μ, measures for this case, the amount of energy necessary to transfer one nucleon from one to the other member of the dinuclear system. The general behaviour of the μ/T is given by the degenerate Fermi gas nature of the nuclear matter, and by an additional contribution related to the mass-number, probably originated in shell effects. To explain the fine structure of the mass-yield curves further calculations explicitly including pairing-effects or local shell effects are being performed.

---

* A. Plastino, UNLP, Argentina and Research Council.

1) D. Otero, A.N. Proto and A. Plastino, Phys.Lett. B98 (1981)225 and reference therein.

2) A. Gayer and Z. Fraenkel Phys.Rev. C16 (1977)1066.

V.3 On the Heavy Ion Excitation of the Octupole Vibration in Deformed Nuclei.

O. Dragun and H. Massmann*

In the nuclear heavy ion research, one of the problems one is interested in solving is the transfer of nucleons to deformed nuclei. The coupled channel approach to this problem is very demanding in computer time and capacity, and this therefore makes one to look out for approximate ways of solving the problem.

Guidry et al.[1] are approaching the problem, for the backscattering case, using the so called classical S-matrix approximation. In that method one finds the classical trajectories for the relative motion of projectile and target, evaluates the phase (that is, counts the de Broglie wave

lenghts) along the trajectory, and also the amplitude for the tunneling of nucleons [in reference 1) they were studying the tranfer of a neutron pair] between the two (projectile and target)wells. Even though this method is very interesting, it does not allow to calculate differential cross sections.

In the present work we develope a modified DWBA approach, based on ideas presented in reference 2) and 3), which allows to solve the problem in an approximate way.

In reference 2) the multiple excitation of rotational states in deformed nuclei through Coulomb and Nuclear forces was considered. Letting the wave function (and therefore the phase shifts) depend on the angle θ' between the symmetry axis of the deformed nucleus and the vector $\vec{r}$ which joins the centers of the target and the projectile, a formalism was presented which allows to calculate the differential cross sections to different final states avoiding a coupled channel calculation.

Here we present a generalization of the method of reference 2) to other scattering processes in which together with the excitation of rotational states one has another process present which can be considered as a perturbation. In order to fix ideas we will consider here only the excitation of the $\nu = 0$ octupole vibration rotational band in even-even deformed nuclei. In order to get the differential cross sections, the DWBA expressions for the T-matrix will be used, but considering only the potential responsible for the excitation of the octupole vibration as the perturbative potential. All processes related to the excitation of the rotational states being included (in the spirit of reference 2)) in the distorted waves. Numerical calculations are in progress.

---

* Departamento de Física, Facultad de Ciencias, Universidad de Chile, Casilla 653, Santiago, Chile.

1) M. Guidry, T.L. Nichols, R.E. Neese, J.O. Rasmussen, L.F. Oliveira and R. Donangelo. Preprint NBI-80-28 (1980).

2) H. Massmann and R. Lippenheide, Ann. of Phys. 123 (1979)120.

3) J.O. Rasmussen and K. Sugawara-Tanabe, Nucl.Phys. A171 (1971)497.

V.4 Nuclear Surface Waves in Alpha-Particle and Ion-Ion Collisions

O. Dragun, A.R. Farhan*, E.E. Maqueda and H. Uberall**

Resonances in ion-ion scattering such as $^{12}C + ^{12}C$, $^{12}C + ^{16}O$ or $^{16}O + ^{16}O$ where they appear both experimentally and via optical model calculations have been earlier interpreted in terms of nuclear surface waves[1,2].

We have now carried out a study of the resonances which arise from an optical potential model for the $\alpha - ^{40}Ca$ system, and which become more distinct the smaller the absorption of the potential is chosen. Our resonances are obtained from partial-wave and transmission-coefficient plots, and when combined with the resonances found by Brink et al[3] via plots of the strenght functions, a unified picture emerges in which the resonances fall naturally into families in an ℓ vs.E diagram, each family corresponding to a given surface wave of the orbiting quasi-molecular system. From the dispersion curves, both Rayleigh and Whispering Gallery surface waves are found to be present in the $\alpha - ^{40}Ca$ system, with a preponderance of the R type, in contrast to what had been found for the $^{16}O - ^{16}O$ system[2]. The same analysis is applied to the experimental resonances in the $^{12}C - ^{12}C$ system, indicating the presence of a WG wave whose dispersion curve intersects the previously identified[1] R wave, and thus points to a perhaps more fundamental difference between the two types of surface waves in that case.

* Catholic University of America. Supported by Kuwait University.

** Catholic University of America. Supported by the National Science Foundation.

1) O. Dragún and H. Uberall, Phys.Lett. B94 (1980)24.

2) A.R. Farhan et al., Nuovo Cim. A57 (1980)205.

3) D. Brink et al., Nucl.Phys. A309 (1978)359.

V.5 Pair Exchange Reactions

D.R. Bes, O. Dragún, E.E. Maqueda and R.J. Liotta

Experiments involving the exchange of a pair of neutrons and a pair of protons between the target and the projectile have been recently performed[1]. The present study intends to stress the possibility of using pair exchange reactions like $(^{14}C, ^{14}O)$ as a new tool in nuclear spectroscopy, in order to excite, for instance, two-particle two-hole states, and thus obtain specific (and, in many cases, so far elusive) information about two-phonon states.

For the sake of simplicity of the final states we consider the reaction $^{208}Po(^{14}C, ^{14}O)^{208}Pb$. The calculation of the reaction has been made under the following simplifying assumptions: a) the reaction proceeds via a one-step process (DWBA); b) the responsible interactions is an effective zero range force between the centre of mass of the transferred diproton and dineutron; c) the relative coordinate in the initial and final channels is the same as the relative coordinate R between the two cores ^{206}Pb and ^{12}C (no recoil approximation); d) the transfer only takes place along the line joining the two cores (Buttle-Goldfarb type of approximation); e) the overlaps between initial and final intrinsic motion in the dinucleons are calculated using the same size parameter in both the lighter and heavier nuclei; f) the motion of the diproton and dineutron in the ejectile and projectile, respectively is obtained from a pure $(p_{1/2})^2$ configuration; g) the structure

amplitudes in the heavy systems are obtained using both TD-pairing and particle-hole states as building blocks. The largest cross section corresponds to the neutron pairing vibrational state at 4.86 MeV. The cross sections presented by the pairing two-phonon (and the 10.16 MeV four-phonon) states are predicted one order of magnitude smaller. However, the population of all states belonging to the pairing phonon family is considerably larger than the population of particle-hole phonon states. On the assumption that the normalization constant obtained at 51 MeV in the reaction $^{40}Ca(^{14}C,^{14}O)^{40}Ar$ can be taken to the Pb region at 250 MeV, we predict a peak differential cross section for the ground state transition of about 0.8 μb/sr.

Calculations either have been made or are in progress relaxing the assumptions listed before.

Similar considerations can be made for ^{48}Ca, using the $^{48}Ti(^{14}C,^{14}O)$ reaction and for ^{56}Ni and ^{146}Gd if one performs the reactions $(^{16}O,^{16}C)$ on ^{56}Fe and ^{146}Sm, respectively.

---

1) D.M. Drake et al., Phys.Rev.Lett. 45 (1980)1785.

V.6 Analysis of $(^{6}Li,d)$ and $(d,^{6}Li)$ Reactions in the Nickel and Tin Regions*

A. Vitturi[a)], L. Ferreira[b)], P.D. Kunz[c)], H.M. Sofia, P.F. Bortignan[a)] and R.A. Broglia[d)]

A central theme of nuclear structure is associated with the search for states that are specifically excited in four particle transfer reactions. The question we put in this work is whether the transfer of an "alpha particle" corresponds to a simultaneous excitation of a neutron and

of a proton pairing mode[1], or whether it excites a new nuclear elementary mode. In trying to answer this question we make use of recently obtained (^{6}Li,d) and (d,^{6}Li) data[2] in the Ni and Sn mass regions. To extract this information from the analysis of the experimental data a microscopic form factor is to be calculated which is a linear combination of four particle spectroscopic amplitudes. These coefficients contain all the nuclear structure information. The differential cross sections to be compared with the experiment can then be calculated in the framework of the distorted wave Born approximation (DWBA). To the extent that alpha modes exist, the results obtained in this way should display the main properties of the experimental spectrum. The effect of the other channels is expected to be a renormalization of the direct-channel differential cross section, as found in the case of the pairing modes.

In the present work we calculate a microscopic form factor which has an effective factorization of the four particle form factor in terms of the structure coefficient of the corresponding two particle transfer form factors. The results of our theoretical calculation are compared with the information obtained from two particle transfer processes.

The reactions analyzed in the Ni-mass region are the L=0 stripping processes:

^{58}Ni(^{6}Li,d)^{62}Zn(g.s)

^{56}Fe(^{6}Li,d)^{60}Ni(0^+;3.32 MeV)

^{56}Fe(^{6}Li,d)^{60}Ni(g.s)

and L=0 pick-up processes:

^{62}Ni(d,^{6}Li)^{58}Fe(g,s)

^{64}Zn(d,^{6}Li)^{60}Ni(0^+;3.32 MeV)

^{64}Zn(d,^{6}Li)^{60}Ni(g.s)

The structure of these states are construct utilizing the proton pairing vibration degrees of freedom as building blocks.

$$|g.s.(Zn)\rangle = |\Uparrow\rangle$$

$$|g.s.(Fe)\rangle = |\Downarrow\rangle$$

$$|g.s.(Ni)\rangle = \sqrt{\alpha}\,|0\rangle + \sqrt{\beta}\,|\Uparrow\Downarrow\rangle$$

$$|0^+ 3.32\ \text{MeV(Ni)}\rangle = \sqrt{\alpha}\,|\Uparrow\Downarrow\rangle - \sqrt{\beta}\,|0\rangle$$

Where alpha and beta for the different Ni isotopes were obtained from one proton pick-up reactions. The reactions analized in the Sn-mass region are

$$\text{Te}(d,{}^6\text{Li})\ \text{Sn(g.s)}$$

$$\text{Te}(d,{}^6\text{Li})\ \text{Sn}(0_1^+)$$

$$\text{Sn}(d,{}^6\text{Li})\ \text{Cd(g.s)}$$

for different target isotopes.

The proton part of the wave function is described in terms of addition (Te(g.s.)) and removal (Cd(g.s.)) pairing modes. Thus the excited 0^+ state in Sn is a two phonon pairing state described by the two phonon wave function Cd(g.s.) $\otimes$ Te(g.s.). The neutron part of the wave function is assumed to be of the BCS type.

The conclusions of this work is that it is possible to reproduce the main trends of the alpha-transfer L=0 transitions observed in the Ni and Sn-mass regions, in terms of a microscopic form factor and standard optical-model potentials, and in the framework of the DWBA.

The differential cross sections are very sensitive to the values of the frequency of the effective harmonic oscillator potentials where the 2π, 2ν correlated system moves before and after the transfer. The values that fit the data fulfill the following conditions:

a) The position of the last maximum of the microscopic form factors coincide with that of the standard macroscopic form factor.

b) The relative four particle cross sections associated with the pure configuration (j_π^2 (0), j_ν^2 (0)) are similar to the product of relative two-particle transfer cross sections associated with the configuration $j_\pi^2(0)$ and $j_\nu^2(0)$.

* These calculations were performed at the Niels Bohr Institute of Conpenhagen, Denmark.
Work published in reference 3) and 4).

a) Universita degli Studi di Padova, Instituto di Fisica Galileo Galilei, Italy

b) Instituto de Fisica, Universidade de Coimbra, Portugal.

c) Unversity of Colorado, Boulder, Colorado, USA.

d) The Niels Bohr Institute, University of Copenhagen, DK-2100 Copenhagen, Denmark.

1) D.R. Bes and R.A. Broglia, Nucl.Phys. A80 (1966)289.

2) O. Hansen et al., Nucl.Phys. A292 (1977)253.
N. Steim et al., Phys.Rev.Lett. 38 (1977)587.
J. Jänecke et al., Proc. Tokyo.Conf. p.358 (1977)

3) R.A. Broglia, L. Ferreira, P.D. Kunz, H.M. Sofia and A. Vitturi, Phys.Lett. B79 (1978)351.

4) A. Vitturi, L. Ferreira, P.D. Kunz, H.M. Sofia, P.F. Bertignon and R.A. Broglia, Nucl.Phys. A340 (1980)183.

V.7 Two Step Contribution to the Preequilibrium Regime.

A.O. Gattone, O. Dragún, A.M. Ferrero, H.M. Sofía.

A realistic estimation of the two-step process contribution to the preequilibrium regime for the (p,d) reaction is made.

We considered the two main reaction paths: an inelastic scattering of the incident proton followed by the pick up of a neutron (p,p',d) and the transfer reaction followed by an inelastic interaction of the exit deuteron (p.d,d'). In describing this two step reaction process we adopted the coupled reaction channel formalism.

It is quite natural to assume that when summing over a great number of actual nuclear states the interference terms between the one step, the (p.p',d) and the (p,d,d') processes average out in a large extent. Thus, the

calculation reduces to what is obtained by using a few representative intermediate and final states in which all the strength of an excitation energy range is concentrated. The two step differential cross section for a given final state J_F is written

$$\frac{d\sigma}{d\Omega}^{J_F}(E') = \sum_{L_{tr}, J_{tr}} \int \rho_{L_{tr}}(E'') S^{J_{tr}}_{E''} \frac{d\sigma}{d\Omega}^{J_c}(E'' E)\, d E'' \qquad (1)$$

Here L_{tr} and J_{tr}, (that are to be coupled to J_F) are the angular momenta transferred in the inelastic and neutron pick up steps, respectively, while E(E') is the projectile (ejectile) energy, and E'' is the intermediate proton or deuteron energy. $d\sigma^{J_F}/d\Omega(E'',E)$ is a purely dynamical factor that can be obtained from a coupled reaction channels code like CHUCK2. $\rho_{L_{tr}}(E'')$ plays the role of an spectroscopic density for the inelastic process and $S^{Jtr}(E'')$ is the spectroscopic factor for the transfer step. When summing over all final states the spectroscopic factor $S^{Jtr}(E'')$ is obtained through the pick up sum rule for (p,d) reactions. Furthermore, in actual calculations, the integral in(1) is replaced by a sum over appropiately chosen intermediate energy intervals $\Delta E''$.

Then

$$\rho_{L_{tr}}(E'')\,\Delta E'' = \sum_{E''-\frac{\Delta E''}{2}}^{E''+\frac{\Delta E''}{2}} \beta^2_{L_{tr}}(E'')$$

where β^2_{Ltr} is the strength due to particle-hole excitations and is obtained through an RPA formalism.

Numerical calculations were made for all the ejectile energy spectra in the $^{54}Fe(p,d)$ reaction at E_p=62 MeV. Due to the great number of representative states in the $^{209}Bi(p,d)$ reaction at E_p=62 MeV only two points of the spectra were calculated.

Preliminary results show that the contribution of (p,d,d') is appreciably greater than the (p,p',d) route, in agreement with results obtained in two step (p,t)[1] reactions, but in disagreement with the

assumptions made in reference 2). As a concluding remark, for excitation energies $E_x \gtrsim 20$ MeV it is necessary to include more than two-step processes.

---

1) W. Feix, R. Polaine, P.J. Van Hall, Poppema, Van Oosten, Klein, and Nijgh, Nucl.Phys. A363 (1981)333.

2) F. Hachenberg, H.C. Chiang, J. Hüfner, Phys.Lett. B97 (1980)183.

V.8 One Step Contribution of (p,d) Reactions in the Preequilibrium Regime.

O. Dragún, A.M. Ferrero, A.O. Gattone.

Recent studies[1,2] have awakened a controversy about the relative contribution of one and more than one step processes to the continuous energy spectra of reactions induced by light ions. For the (p,p') reaction, some authors find[1] that almost all the experimental strength between 10-20 MeV of excitation energy is exhausted by the one step contribution. For others[2], in turn, the contribution of two or more step processes should be considerably large in this range of excitation energy.

In this work, a realistic analysis of the one step pick up process for the (p,d) reaction on ^{54}Fe, ^{120}Sn and ^{209}Bi, at E_p=62, 39 and 29 MeV, is done. In terms of the well known DWBA theory, the cross section for the pick up of a neutron in an (nlj) shell is described by

$$\frac{d\sigma}{d\Omega}^{I_i \to \sigma I_f} = \frac{3}{2} \frac{D_0^2}{1.0 \times 10^4} \frac{S_{nlj}^{I_i \to \sigma I_f}}{2j+1} \frac{d\sigma_{nlj}^{DW}}{d\Omega}(E^*_{\gamma I_f}) \qquad [1]$$

where $E^*_{\gamma I_f}$ is the excitation energy of the final state. It is assumed that when summing over cross sections that correspond to excitation of a large number of actual nuclear states, the interference contributions involved in the individual cross sections average out to a large extent. Thus, the

summed cross sections is reduced to what is obtained by assumming that the states are described by a pure single particle shell model. Then

$$\sum_{\gamma I_f} \frac{d\sigma}{d\Omega}^{I_i \to \gamma I_f} = \frac{3}{2} \frac{D_o^2}{1.0\times10^4} \frac{d\sigma_{nlj}^{DW}}{d\Omega}(E_{nlj}) \sum_{\delta I_f} S_{nlj}^{I_i \to \gamma I_f} \qquad [2]$$

where $\sum_{\delta I_f} S_{nlj}^{I_i \to \gamma I_f} = \bar{n}_{nlj} = 2j+1$, is the pick up sum rule for (p,d) reactions, and E_{nlj} is an average energy representing all the states with the same I_f. Thus, the absolute values of the differential cross sections are obtained without any adjustable parameter. The optical parameters used were previously tested analysing (p,d) and (d,p) reactions leading to final states whose spectroscopic factors are very well known. In order to spread [2] in energy for every (nlj) transfered neutron a Gauss distribution with an appropiate halfwidth is choosen. Due to the number of (nlj) states considered, this halfwidth turn out to be an almost irrelevant parameter in the final calculation. In figure 1, the angular distributions for the $^{54}Fe(p,d)$ E_p=28.8 MeV, a), and $^{209}Bi(p,d)$ E_p=62 MeV, b) reactions are compared with the experimental results. In the first case, is clearly seen how the one step process exhausts all the experimental strength obtained after substracting the yield of deuterons evaporated from compound nucleus. In part b) the angular distribution for two energy bins is shown. From figure 2 can be clearly seen how it becomes necessary to take into account the contribution of multistep processes as the excitation energy increases. In conclusion, the one step process contribution exhausts the experimental yield over the first 5 to 8 MeV of excitation energy.

Substracting the theoretical calculation from the experimental spectra, the region where multistep processes turn to be dominant was obtained. From this spectra, an approximate linear dependence of the differential cross section with excitation energy, $d\sigma(m.s.)/dE \simeq CE_x$ can be deduced, where C is a constant depending upon the incident energy and in some extent on the mass.

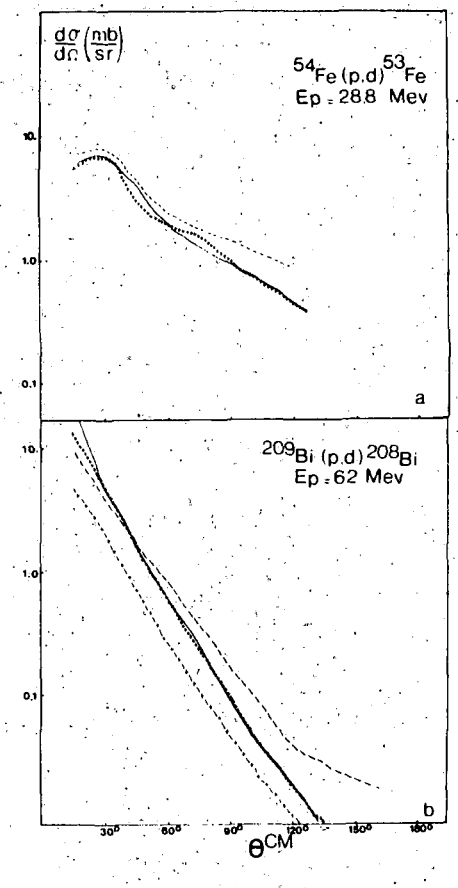

Figure 1

In part a) the calculated differential cross section in crossed line is shown; dashed line corresponds to the experimental cross section and the continuous one is the experimental minus compound nucleus cross section. In b) the experimental (continuous) and theoretical (crossed) differential cross sections in the energy range E_d^{CH} =50-57 MeV are shown; the dashed and dash-crossed line correspond to the experimental and theoretical differential cross section at E_d^{CH} =44-50 MeV.

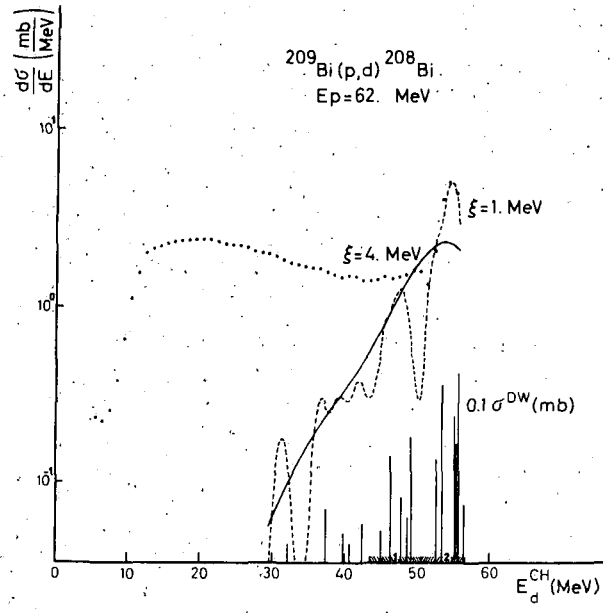

Figure 2

Calculated contribution of the one step (p,d) for halfwidth ξ =1 (dashed) and ξ =4 (continuous. Points show the experimental yield and the bars are the DWBA representative cross sections choosen. Angular distributions for region 1(2) are displayed in figure 1.b).

1) T. Tamura, T. Udagawa, D.H. Feng and K.K. Kan, Phys.Lett, B66 (1977)109. T. Tamura and T. Udagawa, Phys.Lett. B71 (1977)273.

2) G. Bertsch and S.F. Tsai, Physics Reports C18 (1975)127.

VI. INSTRUMENTATION AND DEVELOPMENTS

VI.1 Hyperpure Germanium Detectors Development

G. Martí, C. Gimenez.

The detector Group has initiated work to obtain HP Ge planar detectors. As a first development the Lithium diffused N^+ contacts have been made in Ge at different processing temperature. Subsequent resistivity measurements have been performed as a quality control. Also the P^+ contacts have tentatively been made by Al, Pd and Ni evaporation into the crystal surface. Satisfactory results are obtaining these contacts although an operative finished detector was not yet been produced.

Further work in these subject is being developped.

VI.2 The Design, Construction and Calibration of a Ge(Li) Polarimeter

A.O. Macchiavelli, G. Martí, C. Gimenez, J. Laffranchi and M. Behar.

The theory of a gamma ray polarimeter i.e. a detector sensitive to the linear polarization of gamma rays is described in reference 1). Basicaly it consists of a planar Ge(Li) detector in which one of the dimensions say the length L is greater than the thickness d (see figure 1). In this case it was designed by requiring 1st: $L/d \simeq 10$ to obtain high polarization efficiency, 2nd: volume detector (Area x d) would be about 1-2 cm^3 for having and appreciable relative detector efficiency for not extending so long the

measurements, 3rd: reasonable good total system resolution and Peak to Compton ratio.

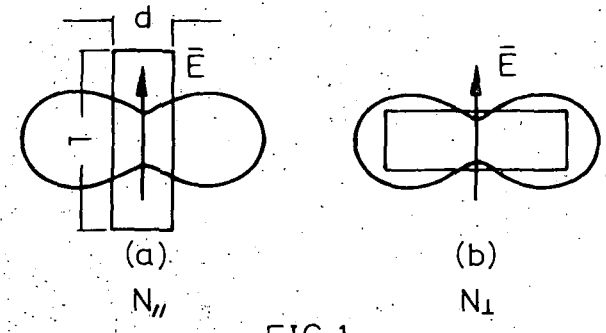

FIG.1

Principle of the planar detector used as polarimeter. E is the polarization vector.

Owing that the last two factors are very sensitives to the electronic noise and as it is proportional to detector capacity (C = 1,4 A/d pF) we had to choose a compromise between the requirements listed above and the available material.

The detector was made from a Lithium compensable p-Type Germanium block of 43 mm in diammeter and 8 mm of thickness and it was cut to obtain a 33x33 mm^2 square block. For (L/d) $\simeq$ 10 the intrinsic zone of the detector was defined in d=3 mm. From this value an aproximate theoretical capacity of 40 pF and $\simeq$ 1 cm^3 active volume was calculated (see figure 2).

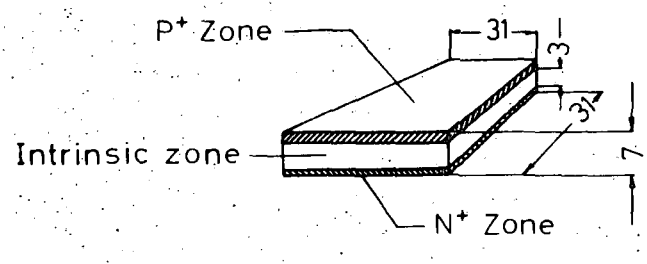

FIG.2

Planar detector used as polarimeter. Dimensions are in mm L/d=31/3 10

The detector was drifted following our usual techniques. The main drift was completed in 6 days at a constant voltage of 400 V and a low temperature drift (-25°C) was given during 6 days more until theoretical capacity was reached at ≃100 V. It was etched and mounted in a vertical cryostat as showed in figure 3. At 100 V it was totally depleted but it was operated at -480 V to minimize trapping, at this operating voltage a FWHM of 2,34 KeV, 6/1 Peak-to-Compton ratio and 0,5% relative efficiency were measured for the 1,33 MeV ray of ^{60}Co. For precisely determination of the position of the detector inside the cryostat several scanning measurements were carried out with a 122 keV gamma ray beam collimated (ϕ=0.5 mm).

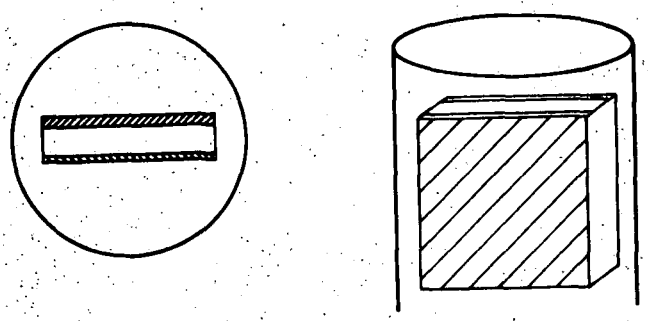

FIG.3

The detector mounted inside the cryostat.

For experimental measurements of the polarization efficiency we used fast and slow coincidences techniques between the polarimeter and a INa gamma ray detector. In the energy range of the experimental measurements (0.5 MeV-1.5 MeV) the polarization efficiency is aproximately constant (17%). This value is in good agreement with the results obtained in reference 2 for similar dimensions polarimeters.

1) Alpha-beta and gamma-ray spectroscopy, volume 2 1965, K. Siegbahn (Ed), page 1040-1044.

2) The electromagnetic interaction in nuclear structure, 1975, Hamilton (Ed) chapter XV, page 701.
A.E. Litherland, G.T. Ewan and S.T. Lam, Can.J.Phys. 48 (1970)2320.
M. Behar, K.S. Krane and R.M. Steffen, Nucl.Phys. A201 (1973)126.

VI.3 Ge(Li) Detectors Repairing and Maintenance.

G. Martí and C. Gimenez.

Detector I. Owing to an accident one of our X-ray Ge(Li) detectors remained for a week at room temperature. The main problem for making reparation is that the detector has the first amplification stage located inside the cryostat (Cooled F.E.T.) then it is impossible to evaluate leakage current and capacity characteristics for making a damage diagnostic.

It was evacuated during two hours to a pressure of 10^{-7} mbar inside the cryostat. The detector was able to operate at -300 V but total system resolution was very poor ($\simeq$ 12keV for 122 keV ^{57}Co gamma-ray).

We decided to make a clean-up drift inside the cryostat in despite of destroying FET owing to the high leakage current that would goes through it. The detector was warmed-up at room temperature with -200 V with simultaneously evacuation. When leakage current rises up to 40 mA (after 3-4 hours continuosly pumping) it was put into the cryostat filled with liquid nitrogen and then it was maintened two hours at a constant current of 30 mA with -400 V. Four hours later leakage current was measured giving a flat I-V characteristic from 0 to -1.500 V at a constant value of 50 pA. C-V characteristic was not measured.

The second stage of the repairing figure consisted in the FET exchange. The detector was warmed up again at room temperature with simultaneously

pumping and -200 V applied on it. When leakage current was about 40 mA power supply was switched off, cryostat was opened and carefully the original FET was replaced by a 2N-4416 selected low noise high quality FET. This operation took about 5 minutes from the cryostat was opened until it was closed again, finally it was re-evacuated during 2 hours but in this case no voltage was applied on the detector and the cooled finger was inmediately inmersed in liquid nitrogen.

The detector was checked at -1000 V (original operating voltage) and recovered its original FWHM resolution of 720 keV at 122 keV.

Detector II. Also owing to an accident one of our Ge(Li) detectors (ORTEC NS-0621) spend one week at room temperature. Leakage current and capacity looked very deteriorated showing lithium precipitation problems and some descompensation in the intrinsic zone. Two clean-up drifts inside the cryostat were carried out, that restered detectors original characteristics. The first was made at 50 mA with 600 V during two hours, the second was made at 3 mA with 1000 V during three days.

Because this detector was originally loaded in a vertical cryostat by the factory it made very difficult to use in the majority of nuclear experiments. As the operational characteristics (FWHM, peak to compton relation and efficiency) were very good we estimate convinient to exchange the crystal from the original vertical cryostat to an horizontal one. The complete exchange operation was made in approximately four hours and a half taking into account the time needed to warm the detector. After evacuation and subsequent cooling down at liquid Nitrogen temperature we noted a drastic leakage current deterioration. The detector was heated to room temperature dismounted, re-etched and loaded again. Then two clean up drifts inside the cryostat were made to restore descompensation. The detector was one day at 7 mA 1000 V and one day more at 3 mA with 1500 V. Operational

characteristics measured after the treatments were FWHM: 2.12 keV, peak-to-Compton relation 27/1 and relative efficiency 6% for the 1.33 MeV ^{60}Co gamma-ray.

VI.4 Manual for the Use of ASSEMBLER Functions and Routines Form the "Harwell Subroutine Library" Called by FORTRAN Programs in IBM/370 Operating System*.

A. Diaz Romero.

The aim of this manual is to show how to use the IBM Job Control Language to call ASSEMBLER routines and functions of the Harwell Subroutine Library from FORTRAN programs with particular emphasis on routines acting on the system clock or translating BCD, ASCII and UNIVAC FIELDATA codes into EBCDIC code.

---

* Internal report CNEA NT-2/81.

VI.5 FORTRAN Programs for the Use and Transmission of Literal Constants and Variables into Routines in IBM/370 Operating System.

A. Diaz Romero.

Facilities offered to the user of FORTRAN language by the utilization of string of characters, in the cases listed below, are explained and examples are given.

- Identification of the branch through which the program derived.

- Transfer the control of the program to labels and routines.
- Selective interruption or alteration of processing for a secuential data set.
- Use of I/O formats selected during the program execution.
- Printing of tittles or comments with variable formats produced during the program execution.
- Conversion of numerical character into integer or floating numbers.

Solid State Physics

Vibrational Spectroscopy
Crystal Structure and Phase Transformations
Mössbauer Spectroscopy
Theoretical Solid State Physics

I. VIBRATIONAL SPECTROSCOPY

I.1 Lattice dynamical calculations on azabenzene crystals : the distributed dipole model*

Z.Gamba and H.Bonadeo

Statical and dynamical properties of crystals of benzene and non-polar azabenzenes have been calculated using an intermolecular potential model which includes atom-atom and electrostatic interactions.

The molecular charge distributions are simulated with a distributed dipole model: their value and location are adjusted so as to reproduce the electrical multipolar moments obtained from ab initio calculations for this series of molecules. The simplest model, consisting in placing one dipole near the N atoms and another one on the line defined by the C-H bonds, reproduced well the azabenzene charge distributions.

This model also allowed a good fit of the observed crystals properties, which was impossible to obtain with the atom-atom potential alone. The model automatically includes the high order multipole moments which are usually neglected in molecule centered multipole expansions. It was found that the inclusion of these terms is fundamental for the description of the observed properties of this series of crystals.

The transferability of the intermolecular potential was checked successfully by calculating the properties of crystalline pyrimidine, a polar molecule, not included in the fit.

---

* J.Chem.Phys. 75, (1981)5059.

I.2 The lattice dynamics of acetylene

Z.Gamba and H.Bonadeo

Crystalline acetylene has two known phases: a high temperature cubic phase, stable between 133 K and the melting point (191 K) and a low temperature orthorombic phase, stable under 133 K.

In a recent paper, Filippini et al[1]) calculated the lattice dynamical properties of both phases; they used atom-atom intermolecular potentials

of several forms, and found that none of them reproduces the observed statical and dynamical properties of the two phases.

We have studied crystalline C_2H_2 using the atom-atom model plus electrostatic interactions calculated with a distributed dipole model. The most simple form of this model is, in the case of this linear molecule, to place two symmetrically opposed dipoles on the C-H bonds of acetylene; their value and position are adjusted to fit the quadrupole and hexadecapole molecular moments (the first two non-vanishing moments) calculated ab initio. With this simple model we cannot reproduce the observed crystal properties.

Hirshfeld and Mirsky[2]) have calculated electrostatic interactions in crystalline C_2H_2 representing the molecular charge distributions by charges, dipoles and quadrupoles localized at atomic nuclei; comparing the values of the first three non-zero molecular multipole distributions obtained with this model and our two dipole model, it was found that the value of the 2^6-pole obtained with the first one is about twice that of the other ones.

This led us to investigate the influence of this term. One possible way to do this is to place four (two independent) dipoles along the molecular axes, and to vary their magnitude and position so as to obtain different values for the 2^6-pole. It was found that as the 2^6-pole becomes larger, all problems presented in the refinement of atom-atom parameters tend to disappear; and for a given value of it, it is possible to calculate atom-atom parameters that, added to the electrostatic interactions, reproduce well the observed statical and dynamical properties of both phases.

With this parameter set it is possible to calculate real frequencies throughout the Brillouin Zones. These phonon dispersion curves and group symmetry considerations, led us to identify which phonons of both phases may be associated with the structural phase transition.

---

1) G.Filippini, C.M.Gramaccioli and M.Simonetta, J.Chem.Phys. 73(1980) 1376.

2) F.L.Hirshfeld and K.Mirsky, Acta Cryst. A35(1979)366.

I.3 Lattice dynamical calculations of the mean square amplitudes of crystalline biphenil*

H.Bonadeo and E.Burgos

Usually, atomic displacements of the atoms are interpreted in terms of molecular motions with the aid of the TLS model, which takes into account the molecular rotations and translations. However, when low-lying internal modes, which mix appreciable with lattice vibrations are present, the model must be appropiately extended. In the present work we present the formal extension of the method and apply it to the case of crystalline biphenyl, whose torsional motion provides a good example. We show that the mixing is very important especially in the calculation of the off-diagonal elements of the mean square displacement matrix, and that ignoring it leads to serious mistakes in the interpretation of experimental data. We have also calculated the mean square displacement matrix of crystalline biphenyl at two temperatures, using the Born S-matrix method, which proves to be an excellent approximation, and reduces the computer time by 1/5. The resulting amplitudes are in fair agreement with experiment, and show that the extremely high amplitude of libration about the long molecular axis may be satisfactorily explained without assuming a double-well shape for the torsional potential.

---

* Acta Cryst. A (in press).

I.4 Electrical multipoles and multipole interactions: compact expressions and a diagrammatic method*

E.Burgos and H.Bonadeo

The expressions for the calculation of high order multipoles and multipole interactions in cartesian coordinates tend to be extremely cumbersome. The 2^n-2^m interaction energy is

$$W_{n,m} = \frac{(-1)^n}{n!\,m!}\, q^A_{\alpha_1\ldots\alpha_n} f_{\alpha_1\ldots\alpha_n\beta_1\ldots\beta_m}(\bar{R}) q^B_{\beta_1\ldots\beta_m},$$

$$= \frac{(-1)^n}{n!\,m!\,(2n-1)!!\,(2m-1)!!} Q^A_{\alpha_1\ldots\alpha_n} f_{\alpha_1\ldots\alpha_n\beta_1\ldots\beta_m}(\bar{R}) Q^B_{\beta_1\ldots\beta_m} \qquad (1)$$

with

$$f_{\alpha_1\ldots\alpha_n\beta_1\ldots\beta_m}(\bar{R})=\left[\frac{\partial^{n+m}|\bar{r}+\bar{R}|^{-1}}{\partial r_{\alpha_1}\partial r_{\alpha_2}\ldots\partial r_{\beta_m}}\right]_{\bar{r}=0}=\frac{F_{\alpha_1\ldots\alpha_n\beta_1\ldots\beta_m}(\bar{R})}{R^{2(n+m)+1}},$$

and

$$Q_{\alpha_1\ldots\alpha_n}=\int_V \rho(\bar{r})F_{\alpha_1\ldots\alpha_n}(-\bar{r})\,dV,$$

where $Q_{\alpha_1-\alpha_n}$ is 2^n-pole moment, α_i, β_j are cartesian components and $\bar{R}$ is the radius vector joining the centers of charge distributions A and B.

The problem is to find compact expressions for the derivatives of $|R|^{-1}$. It is possible to define "permutation polynomials" of order m and degree k,

$$(R^k\delta^l)_{\alpha_1\ldots\alpha_m}=\sum_p R_{\alpha_1}R_{\alpha_2}\ldots R_{\alpha_k}\delta_{\alpha_{k+1},\alpha_{k+2}}\ldots\delta_{\alpha_{m-1},\alpha_m}$$

with $m=2l+k$, where the sum is extended over all different permutations of $\alpha_1\ldots\alpha_m$. It can be shown that

$$f_{\alpha_1\ldots\alpha_m}(\bar{R})=R^{-(2m+1)}\sum_{l=0}^{[m/2]}(-1)^{m-l}[2(m-l)-1]!!\,R^{2l}(R^{m-2l}\delta^l)_{\alpha_1\ldots\alpha_m},\qquad(2)$$

where $|m/2|$ is the integer part of m/2. From eq.(2) it is easy to obtain the functional form of f, F and Q. The diagrammatic method is based on the graphic representation of eq(1). We construct one center and m vertices corresponding to each component α_j of $(R^{m-2\ell}\delta^{\ell})_{\alpha_1\ldots\alpha_m}$. Each one of the m-2l components R_{α_j} is represented by a line joining the center with vertex α_j, and each $\delta_{\alpha_k\alpha_i}$ by a line joining vertices α_k and α_i. There is a one-to-one correspondence between the topologically distinct diagrams, with each vertex joined either to the center or to another vertex, and the terms in the r.h.s. of eq.(1). There are also relatively simple rules to obtain the corresponding coefficients. The graphs and results for a 2^6-pole are shown in Fig. 1.

$$F_{ijklmn} = 11!!\,(R^6)_{ijklmn} - 9!!\,R^2(R^4\delta)_{ijklmn} + 7!!\,R^4(R^2\delta^2)_{ijklmn} - 5!!\,R^6(\delta^3)_{ijklmn}$$

Fig. 1

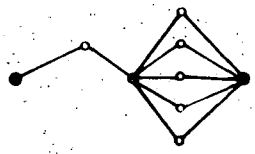

$$11!!\, Q^A_i R_i R_j R_k R_l R_m R_n Q^B_{jklmn}$$

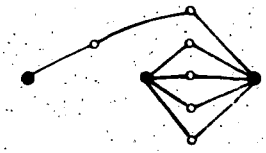

$$-\, 9!!\, R^2 Q^A_i R_j R_k R_l R_m Q^B_{ijklm} \times 5$$

$$W_{1,5} = \left[-11!!\, Q^A_i R_i R_j R_k R_l R_m R_n Q^B_{jklmn} + 5 \times 9!!\, R^2 Q^A_i R_j R_k R_l R_m Q^B_{ijklm} \right] \Big/ 1!\,5!\,1!!\,9!!\,R^{13}$$

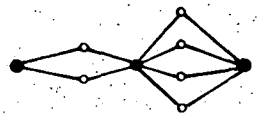

$$11!!\, Q^A_{ij} R_i R_j R_k R_l R_m R_n Q^B_{klmn}$$

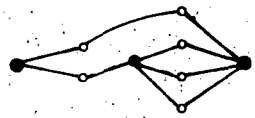

$$-\, 9!!\, R^2 Q^A_{ij} R_j R_k R_l R_m Q^B_{iklm} \times 8$$

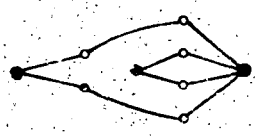

$$7!!\, R^4 Q^A_{ij} R_k R_l Q^B_{ijkl} \times 12$$

$$W_{2,4} = \left[11!!\, Q^A_{ij} R_i R_j R_k R_l R_m R_n Q^B_{klmn} - 8 \times 9!!\, R^2 Q^A_{ij} R_j R_k R_l R_m Q^B_{iklm} + 12 \times 7!!\, R^4 Q^A_{ij} R_k R_l Q^B_{ijkl} \right] \Big/ 2!\,4!\,3!!\,7!!\,R^{13}$$

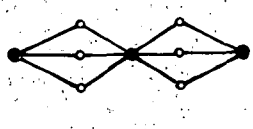

$$11!!\, Q^A_{ijk} R_i R_j R_k R_l R_m R_n Q^B_{lmn}$$

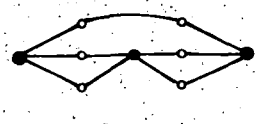

$$-\, 9!!\, R^2 Q^A_{ijk} R_j R_k R_l R_m Q^B_{ilm} \times 9$$

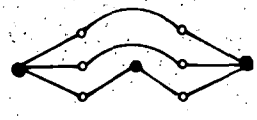

$$7!!\, R^4 Q^A_{ijk} R_k R_l Q^B_{ijl} \times 18$$

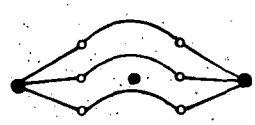

$$-\, 5!!\, R^6 Q^A_{ijk} Q^B_{ijk} \times 6$$

$$W_{3,3} = \left[-11!!\, Q^A_{ijk} R_i R_j R_k R_l R_m R_n Q^B_{lmn} + 9 \times 9!!\, R^2 Q^A_{ijk} R_j R_k R_l R_m Q^B_{ilm} - \right.$$
$$\left. - 18 \times 7!!\, R^4 Q^A_{ijk} R_k R_l Q^B_{ijl} - 6 \times 5!!\, R^6 Q^A_{ijk} Q^B_{ijk} \right] \Big/ 3!\,3!\,5!!\,5!!\,R^{13}$$

Fig. 2

The interaction energy results from a triple tensor product. It is possible to draw a graph which has in its center a diagram for F with n vertices to the left and m to the right of its center; on the left of it, $Q_{\alpha_1 \ldots \alpha_n}$ is drawn as a center with n lines, each linked to one left vertex of F; similarly, a diagram for $Q_{\beta_1 - \beta_m}$ is drawn on the right of F. Whenever two lines join, the corresponding indices are contracted, the resulting graph represents one term in the interaction energy. There are rules to calculate the corresponding coefficients, and the results for $n + m = 6$ is shown in Fig. 2. The method can be easily extended to any function of R, and can be used advantageously in connection with problems involving central forces.

---

* Mol. Phys. 44 (1981) 1

I.5 Frequency distribution in some disordered systems

A.Frigerio, N.Cohan, M.Weissmann and H.Bonadeo

We are interested in the study of vibrational spectroscopy of noble gas matrices impurified with low concentrations of alkali metal atoms.

We adapted the continued-fraction method in the form used in the calculation of density of electronic states by Cohan-Weissmann[1], to the calculation of density vibrational states. First we have tested the method in a disordered one dimensional chain of two-components. The comparison with numerical calculations of P.Dean[2] shows that the localized modes have correct frequency values and their band heights are in reasonable agreement with those of the exact results. The same agreement is valid for the spectra obtained by varying the concentration and the mass relation between the two components of the disordered alloys.

We then extended this method to a calculation on face centered cubic lattices, which is the structure of the systems we expected to measure with far infrared and Raman spectroscopy.

With the hypothesis of central forces and interactions between first neighbors sites only, we tested the program in the ordered case with the phonon density of the f.c.c. crystal.

In Fig. 1 the phonon density of states of the f.c.c. lattice[3] (full line) is compared with our results (dashed line) in a model of 365 atoms, which corresponds to a calculation with only eight exact moments.

Presently we are introducing the disorder in the masses and force constants, for systems such as Xe-Na, Ar-K, Xe-K, which we may be able to measure in our laboratory.

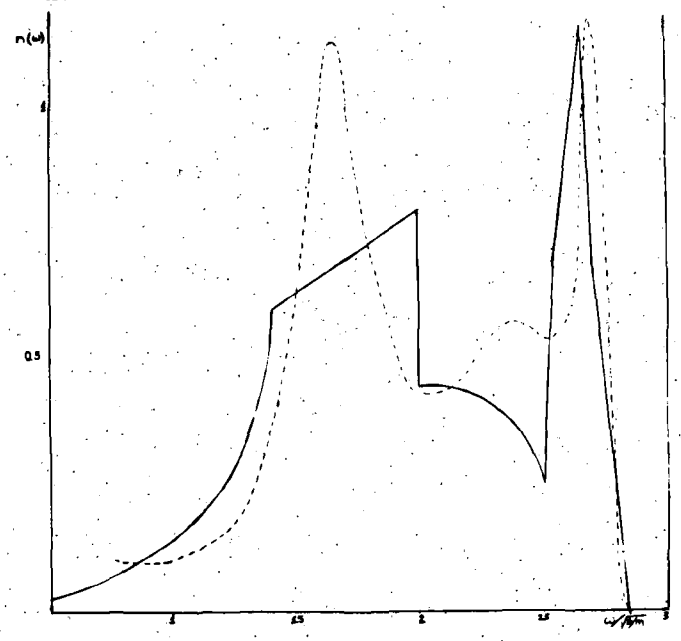

Fig. 1

---

[1]) N.Cohan and M.Weissmann, J.Phys.C: Solid State Phys.Vol 10(1977).

[2]) P.Dean, Reviews of Modern Physics, Vol 44, Nº 2 (1972).

[3]) J.J.Rehr and R.Alben, Physical Review B, Vol 16, Nº6 (1977).

I.6 A Cryostatic Cell for Raman and X-Ray Diffraction Work

E. Halac, N. Gutiérrez and H. Bonadeo

For studying the lattice vibrations of molecular crystals it is fundamental to obtain polarized Raman spectra. These allow the univocal assignment of the observed bands to the symmetry species of the crystal factor group, and therefore its comparison with those calculated using different models for the intermolecular forces. These spectra require the growth of single crystalline samples and the knowledge of the crystallographic axes orientation.

We are interested in the study of materials which are liquids at room temperature. This fact carries experimental difficulties due to the necessity of growing the single-crystals at low temperature, orienting them and obtaining its Raman spectrum, avoiding the manipulation of the sample.

We have constructed a cell which fulfils these requirements and is presently being applied to the study of Br_2 crystal.

The figure 1 shows a schematic drawing of the cryostat.

1) Exterior body
2) Liquid N_2 reservoir
3) Sample holder goniometer with two 30° perpendicular arcs.
4) Gear system for transmitting the moviments to the goniometer from the exterior.
5) Gear commands.
6) Mylar windows.
7) Glass window for the laser incidence.
8) Heater resistor.
9) Resistor passant.
10) Kovac passants for thermocuple.
11) Liq. N_2 inlet in horizontal position.
12) N_2 gas outlet.
13) XY displacement for centering in the Weissemberg chamber.
14) Vacuum connection.
15) Vacuum valve.

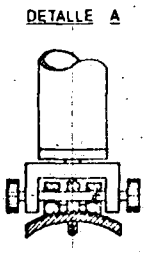

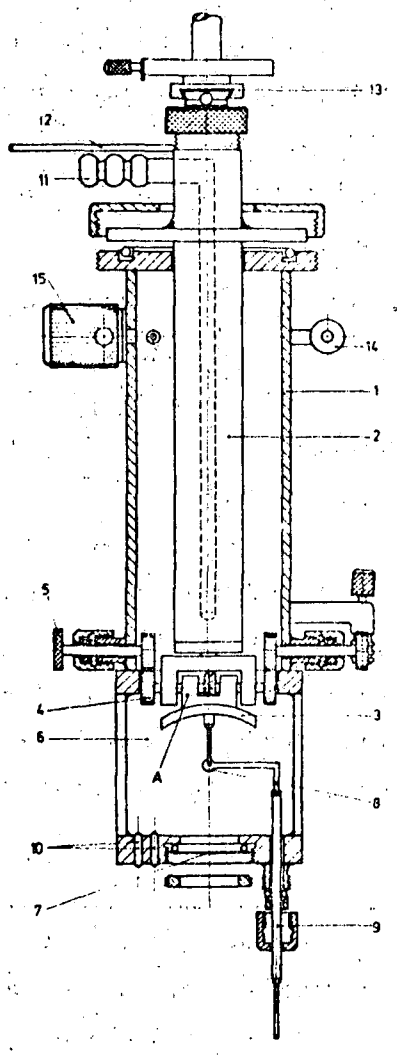

A sealed glass capillary tube contains the sample and is placed in the specimen holder of the goniometer head 3), which twines in the liq. N_2 reservoir 2).

After the cell has been evacuated, the growing of the crystal begins cooling gradually from one of its ends. The heater resistor 9) can be positioned at any height around the sample and allows the control of the thermal gradient.

Once the single crystal has been obtained, the cell is mounted in the Weissemberg chamber in horizontal position. Its axis is in coincidence with the turning one of the chamber. The Mylar windows 6) allow the alignment of the crystal and the incidence and scattering of X-rays in a complete turn of the cell. The sample orientation can be varied by means of the commands 5), each one transmitting the movement to one of the goniometer arcs by a gear system 4). The gears are mounted on passant axes with O-rings, in such a way that the vacuum is not altered during their turning.

Given the orientation of the crystallographic axes by means of the Weisserberg photographs, we can obtain the Raman spectra in polarized light. The cell is mounted in the spectrometer in different positions depending on the desired polarization. The glass window 9) allows the laser light. incidence.

CRYSTAL STRUCTURE AND PHASE TRANSFORMATION

II.1 X-ray characterization of gel grown $CaHPO_4 . 2H_2O$ and $PbHPO_4$ crystals†

F.Lefaucheux*, M.C.Robert*, E.Manghi and H.Arend**

The use of gel media offers in many cases a surprisingly efficient and simple crystal growth method for substances with a low solubility and a low thermal stability.

Two different gels have been used to grown brushite ($CaHPO_4.2H_2O$) and lead monetite ($PbHPO_4$).

1) Silica gel

2) Tetramethoxysilane gel (TMS).

The former compound is a biologically interesting material whereas the latter is an interesting ferroelectric.

Two main features characterize the crystals obtained:

- a high growth rate (up to 2 mm/day)
- a good quality.

As grown crystals have been characterized by X-ray Topography (Lang method). The defects observed on topographs are mainly gel inclusions and dislocations starting from these inclusions or from strained growth sector boundaries.

The dislocations density is higher for crystals grown from a silica gel than that obtained when TMS is used, both for brushite and lead monetite.

Reducing to 1.0006 the gel density for TMS 2%, large zones of the crystal are dislocation free. The correlation between the gel density and the dislocation density, can be explained by the reduction of entrapped particles.

The gel properties (e.g. viscosity) can be modified varying the temperature and in general more perfect crystals are obtained at lower temperatures. Experiments with $PbHPO_4$ performed in a TMS gel at 32 °C gives larger, thinner and more perfect platelets than those obtained at 40 °C. This material has a phase transition from a paraelectric to a ferroelectric phase at 37 °C, and good crystals can be obtained of both phases by changing the properties of the gel.

Solution grown crystals usually show growth bands which are related

to impurity segregation governed by convection currents.No typical growth bands are observed in gel grown crystals.

Their absence suggests that the gel behaves as a convection free medium.

---

† This work was developed at Lab. de Cristallographie, Univ. Paris VI, France (1980). Journal of Crystal Growth, 51(1981)551-556.

* Lab. de Cristallographie, Univ. Paris VI, France

** Lab. Solid State Physics, Swiss Federal Institute of Technology, Zurich, Switzerland.

II.2 Observation of ferroelectric domains in gel grown $Pb\ HPO_4$ crystals†

R. LeBihan**, M.Maussion**, F.Lefaucheux*, E.Manghi and M.C.Robert*

This material, an interesting ferroelectric with some promising properties for device applications undergoes a paraelectric-ferroelectric transition at 37 °C.

Among the studies devoted to ferroelectric properties of $Pb\ HPO_4$ only one[1]) gives some indirect information concerning the structure of ferroelectric domains: from the shape of hysteresis loops a multidomain state is assumed in this material.

Thus a direct visualization of these domains is needed.

The direct observation with scanning electron microscopy using a technique already described[2]) is a suitable and non destructive mean to study the structure of ferroelectric domains. This method has been applied to $Pb\ HPO_4$ single crystals grown in a TMS gel system[3]). In the secondary electron emission mode the domain boundaries are revealed on two natural facets which cut the polarization axis Ps lying on the (010) plane.

The domains are cylindrical, in both facets the observed domains sections are lenticular similar to those of TGS crystals ($\phi \sim 1 - 20\mu$).

As in the case of TGS, when several domains coalesce sections of irregular shapes can be observed.

The size and geometry of ferroelectric domains inferred from these observations are quite different from those proposed in another study by

X-ray Topography of the same material grown from a different gel[4]) under different conditions.

---

† This work was developed at Lab de Cristallographie, Univ. Paris VI, France (1980). Phys.Stat.Sol. (a) 64(1981)K5.

* Lab. de Cristallographie, Univ. Paris VI, France

** Lab. de Physique de Surfaces, Inst.de Physique, Univ. de Nantes, France.

1) L.Novak F.Smutny and J.Fousek, Czech. J.Phys. B27(1977)477.

2) R.LeBihan and M.Maussion, J.Phys. 33(1972)C2-2/5.

3) F.Lefaucheux, M.C.Robert, E.Manghi and H.Arend, J.Cryst.Growth 51 (1981)551-556.

4) B.Brezina and J.Horvath, J. Crystal Growth, 52(1981)858-863.

II.3 A Comparison between gel-grown and solution-grown crystals: case of ADP and KDP†

F.Lefaucheux*, M.C.Robert* and E.Manghi

The gel growth techniques have been developed for materials which are difficult to grow by other techniques, e.g. insoluble materials.

Very few studies have been devoted to gel growth of water soluble crystals which can be easily grown by classical solution methods.

In this study the growth defects in gel-grown ADP and KDP crystals are described and compared with those obtained in solution grown crystals.

The crystal defects are observed by X-ray Topography (Lang Method).

The growth-medium chosen was TMS gel which allows the preparation of ADP and KDP saturated gelled solutions.

Different techniques combining changes in temperature and diffusion in TMS gels yield crystals which are usually more perfect than those obtained by solution.

---

† This work was developed at Lab. de Cristallographie, Univ. Paris VI, France

* Lab. de Cristallographie, Univ. Paris VI, France.

II.4 Synthesis of $(AsO_4)_2H_2(UO_2)_2 \cdot 8H_2O$ using a gel method

E.Manghi and G.Polla

It has been shown[1]) that $(AsO_4)_2H_2(UO_2)_2 \cdot 8H_2O$ has two phase transitions:

Phase I	22°C	Phase II	-20°C	Phase III
Paraelectric Paraelastic	⟹	Ferroelectric Antiferroelastic	⟹	Ferroelastic

No X-ray crystal structure analysis could be performed on crystal of phases II and III as they can not be grown as single crystals from solution.

The stability range of phase II points to the gel method as particularly suitable to obtain good single crystals.

Differents conditions were tried, and the following two gave the best results:

1) 0,3 M aqueous solution of AsO_4H_3 was mixed with a 10% TMS aqueous solution; when this mixture has gellified in a test tube, a 0,5 M aqueous solution of $(N)_3O_2\ UO_2.6H_2O$ is carefully poured on the gel surface.
   After a week some crystals nucleate and after approximately one month they were removed from the gel.
2) The same procedure was followed but a 0,5 M aqueous solution of AsO_4H_3 was used.

The crystal habit is prismatic, quite different from micaceous crystals obtained from solution.

This difference in crystal habit allows one to carry out a series of experiments, which cannot be performed with mica-like platelets.

An example of the experiments carried out with these crystals using X-ray diffraction techniques is given in the next paper of this report.

---

[1]) Symmetry and phase transitions in $H_2(UO_2)_2(AsO_4)_2.8H_2O$.
M.A.R. de Benyacar and H.L.de Dussel, Ferroelectrics, vol 17(1978)469.

II.5 Ferroelasticity in $(AsO_4)_2(UO_2)\ H_2 \cdot 8\ H_2O$ †

H.L. de Dussel, L. S. de Wainer and M.A.R. de Benyacar

The ferroelastic character of phase II of HUAsH suggested by optical observations[1]) is analized.

The only ferroelastic specie[2]) compatible with the available data is 4/mmm F2/m (s). In order to describe the spontaneous strain tensors corresponding to the different orientation states it was necessary to study the lattice distortion at the transition, which has not been previously determined as precession photographs of the twinned crystal failed to show any departure from tetragonal symmetry. A new technique was used to obtain diffraction data in a powder diffractometer on polycrystalline samples oriented parallel: a) to $(h00)_T$ and b) to $(001)_T$.

The corresponding diffraction patterns showed in case a) $(h00)_M$ and $(0k0)_M$ and in case b) $(001)_M$ reflections of high intensity and which were almost free from all other types of reflections, so that no superposition of peaks is observed for any 2σ angle; nevertheless, in case a) unavoidable small deviations of some of the crystals were responsible for a few and weak (h01) reflections.

Thus, all the cell parameters of the monoclinic phase were determined at T=-12 °C.

$a = 7.15_2$ A $\quad b = 7.11_1$ A $\quad c = 17.55_4$ A $\quad \beta = 90.35 \pm 0.05$ °

The extinction rules determined the space group of this phase as $P2_1/m$ or $P2_1/c$.

Thus, the spontaneous strain tensor S_1 could be calculated

$$S_1 = \begin{pmatrix} -2.87 & 0 & 3.05 \\ 0 & 2.87 & 0 \\ 0 & 0 & 0 \end{pmatrix}$$

The other strain tensors are derived from S_1:

S_2 through reflection in $z_T = 0$

S_3 through rotation of $\pi/2$ along z_T

S_4 through rotation $-\pi/2$ along z_T

The observed domain walls are in agreement with those obtained using Sapriel's[3]) compatibility criteria.

Further investigations are in progress aiming at the obtention of the dimension and symmetry of the order parameter from the spatial

symmetry of phases I and II, using the theories of Toledano et al[4]).

---

† Part of this investigation was presented at the V International Meeting of Ferroelectricity, Penn,State, USA, August 1981.

[1]) M.A.R. de Benyacar and H.L. de Dussel, Ferroelectrics 9(1975)241.

[2]) K.Aizu, Phys.Rev. B2(1970)754.

[3]) J.Sapriel, .Phys.Rev. B12(1975)5128.

[4]) J.C.Tolédano and P.Tolédano, Phys.Rev. B21(1980)1139.

II.6 Study of domains and domain walls in ferroelastic $BiVO_4$ †

L.S. de Wainer, R.Baggio, H.L. de Dussel and M.A.R. de Benyacar

The domain structure of pure ferroelastic $BiVO_4$ has been studied by TEM and electron diffraction. Some preliminar results were described in CNEA NT-13/80.

Studies of the specimens in the electron microscope showed that when only parallel domains walls are present, a two fold splitting of the diffraction spots in the (001) plane is always observed, due to the presence of two orientation states.

The angle between the trace of the W'non-crystallographic domain walls and the (100) crystallographic direction was determined from electron micrographs. The measured value of 37.4° corresponds to the trace of a (1p0) plane with p=0 .78. Calculated values obtained using the formulas proposed by Sapriel[1]) and the cell parameters given by Sleight et al[2]) give for a crystal at T=40°C an angle of 36°C and p=0.72 in good agreement with our measured values.

When both sets of almost orthogonal domain walls appear, more than two beams contribute to the diffraction spots belonging to the (001) reciprocal planes. This multiple splitting can be explained if additional rotations necessary to bring domains into mutual contact along a permissible domain wall (PDW) are taken into account.

We impose the condition that the change of a vector parallel to a PDW, v=(1,p) must be the same in adjacent domains for each domain wall

$$\sum_j S_{1\,i_j v_j} = \sum_k S_{2\,i_k v_k}$$

As a consequence of this new compatiblity criterion each of the orientation states is splitted into two slightly rotated ones.

We obtained the spontaneous strain tensor of these four orientation states and analized the permissible boundaries between them.

---

† Ferroelectrics, 31(1981)121.

[1]) J.Sapriel, Phys.Rev. B12(1975)5128.

[2]) A.Sleight, H.Y.Chen, A.Ferreti and D.E.Cox, Mat.Res.Bull. 14(1979)1571.

II.7 Crystallochemical study of Apatites from subcutaneous calcifications

J.R.Matalón and M.A.R. de Benyacar

The main objective of this work was the study of the mineral phases present in subcutaneous calcifications.

The following techniques were used: X-ray powder diffraction for the identification of the mineral phases; infrared spectrophotometry for the identification of the functional groups, particularly $CO_3^{=}$ ions, and EDAX for the confirmation of the chemical composition and the determination of the Ca/P ratio. In all the samples the only mineral phase present is calcium carbonate - hydroxyapatite.

The calcified subcutaneous masses were observed as a white creamy fluid and as a granular material formed by white nodules a few tenths of mm. wide surrounded by a yellowish, soft, fibrous material. Besides the mineral phase, the presence of acid mucopolysaccharides was ascertained by a positive uronic acid carbazole reaction. Infrared spectra of untreated and heated samples showed different carbonate contents for the different patients and the presence of carbonate ions belonging to an A-B type carbonate-hydroxyapatite.

From these observations we conclude that the ratio of $CO_3^{=}$ ions replacing $PO_4^{=}$ groups (B type) and $CO_3^{=}$ ions replacing HO^{-} groups (A type) is not constant for all the patients, in good agreement with the variable Ca/P ratio obtained from EDAX for different samples. Our results are strikingly similar to those observed in dental enamels by K.Jonás et al (Phys.Chem.Minerals, 6(1980)55-60.

II.8 Idiopathic familial chondrocalcinosis due to apatite crystal deposition*

J.C.Marcos, M.A.R. de Benyacar, O.Garcia-Morteo, A.S.Arturi, J.A.Maldonado-Cocco, V.H.Morales and R.P.Laguens

The main objective of the work was the identification of calcifications of costal cartilage samples obtained by open biopsy from one member of a family with idiopathic familial chondrocalcinosis.

X-ray diffraction studies, energy dispersive analysis (EDAX) and infrared spectrophotometry of the sample demonstrated the presence of carbonate calcium hydroxyapatite. Radiologically, four out of the five patients has multiple intervertebral disc calcifications, mainly located at the nucleous pulposus area. Three of them also had periarticular calcific deposits associated with costal cartilage calcifications and degenerative changes in the small joints of the hands in two. None of these cases showed cartilage calcification in knees, symphysis pubis or triangular ligament of carpus. In the propositus an open biopsy of a second proximal interphalangeal joint showed, by optical microscopy, the presence of multiple calcified areas in the intercellular matrix and chondroid metaplasia with calcification of the matrix in the synovial membrane and capsule.

In this study no relation was found between HLA antigens locus A, B and C and this syndrome due to calcium hydroxyapatite crystal deposition.

---

* This work was carried out jointly by medical doctors from Instituto Gral San Martin, (La Plata); Instituto de Rehabilitación del Lisiado, (Buenos Aires); Universidad de La Plata, (La Plata) and members of the Solid State Physics Division, Physics Department, Comisión Nacional de Energía Atómica, (Buenos Aires)

II.9 Grain growth in ice

L.Levi and E.A.Ceppi*

Grain growth is studied in polycrystalline ice, obtained by rapid freezing doubly distilled water. The samples are formed by elongated grains of

200-300 μm mean width and 2-3 μm mean length. They are annealed at different temperatures, between 0°C and -10°C.

The results show that the mean length $\bar{l}$ is not affected by annealing while the mean width $\bar{w}$ increases with the annealing time t, so that grain growth may be represented by $\bar{w}(t)$. It is shown that, for large annealing times, $\bar{w}(t)$ tends to a limit value $\bar{w}_m$. This effect is related to the pinning action of air bubbles, always present in ice grown in contact with air, and the phenomenon is represented by using the equation

$$(\bar{w}_o - \bar{w})/\bar{w}_m + \ln((\bar{w}_m - \bar{w}_o)/(\bar{w}_m - \bar{w})) = (\bar{w}_o/\bar{w}_m)^2 Kt/\bar{w}_o$$

proposed by previous authors[1]) to interpret a similar behaviour observed in metals containing solid inclusions. Assuming $\bar{w}_m = d/f$, where d is the bubble diameter and f is the volume fraction of air dissolved in water, reasonable values are found for d.

It is shown that previous results of Jellinek and Gouda[2]) could be also interpreted by applying the same equation. Comparable values are consequently obtained for the rate factor $K = K_o \exp(-Q/RT)$, where Q is the activation energy for grain boundary mobility. It is found Q = 0.59eV. This value is compared with that of the activation energy for bulk self diffusion ~ 0.6 eV[3]).

Following the normal grain growth theory, it is concluded that, in this case, the phenomenon would be controlled by bulk diffusion of impurities, up to the very melting point.

The absence of a transition to a lower activation energy, usually observed for metals near the melting point[4]), is related to the low value of the grain boundary interface free energy of ice.

---

* CONICET and Servicio Meteorológico Nacional.

1) G.F.Bolling and W.C.Winegard, Acta Metall., 6(1958)253.

2) H.H.G.Jellinek and V.K.Gouda, Phys.Stat.Sol., 31(1969)413.

3) L.K.Runnels, Physics of Ice, International Symposium on Physics of Ice (1969)514. Plenum Press

4) C.J.Simpson, K.T.Aust and W.C.Winegard, Met.Trans., 2(1971)987-993.

II.10 Phase transitions in $8PbO.V_2O_5$

R.Baggio, L.Schmirgeld de Wainer, H.L. de Dussel, M.A.R. de Benyacar

$8PbO.V_2O_5$ undergoes a 2nd order phase transition at 155°C. The low temperature phase is ferroelastic[1]). We have studied this compound by means of optical microcopy, electron microscopy and diffraction, and X-ray diffraction from room temperature up to 900°C.

The compound was grown from the melt, as quasi-tetragonal platelets with the $|001|_{tet}$ axis normal to the plates.

At room temperature, two different types of domains are present: two sets of quasi-orthogonal needle-shaped domains already reported[1]) (hereafter named type a), and a set of bands at 45°C to the previous ones, sometimes ending in a sharp wall parellel to {100}(Type b).

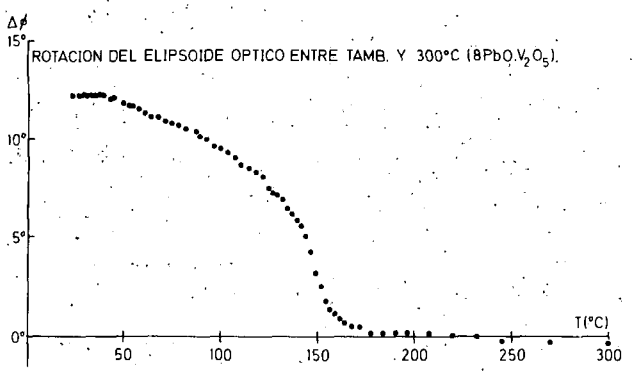

Fig. 1

Domains of type a can be moved under slight pressure (characteristic of a ferroelastic phase). Their extinction positions (and accordingly their optical elipsoids) are rotated 26°, at room temperature. On heating this angle ϕ decreases continuosly towards a limitting ϕ (Fig. 1 and 2) resembling the typical behaviour of the order parameter of a 2nd order transition.

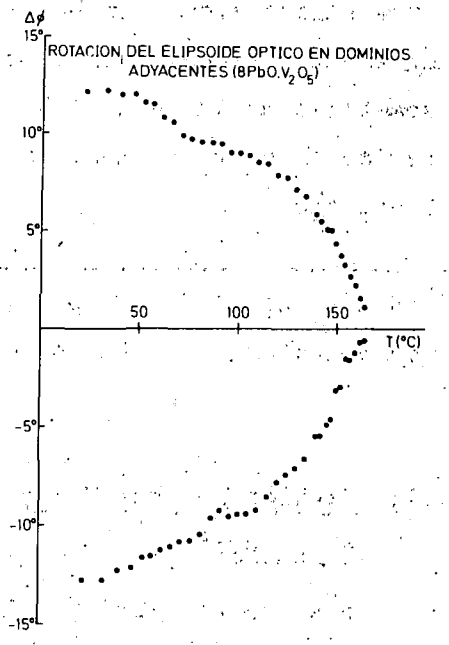

Fig. 2

A least squares fit of $(\phi - \phi_o)^{1/\beta}$ vsT (Fig. 3) with $1/\beta = 3.10$, showed a remarkable linear trend, and an extrapolated transition temperature T_o - 153°C in agreement with the values at which the domains are seen to vanish.

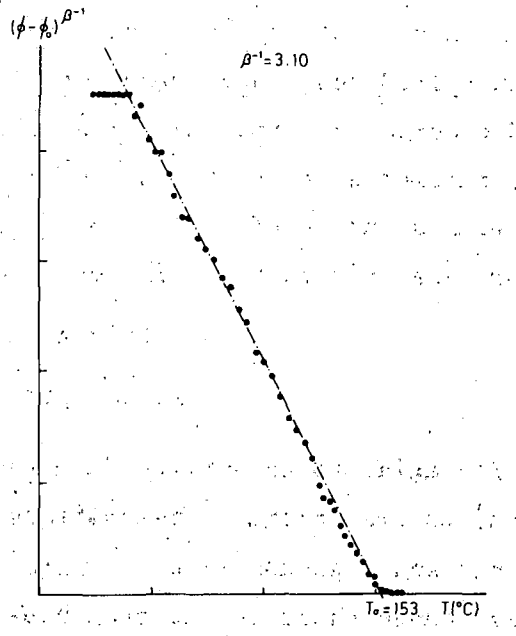

Fig. 3

Our X-ray and electron diffraction work show a monoclinic symmetry at room temperature, with the unique axis parallel to the pseudo-tetragonal one, in conflict with previously reported data. The rotation of the optical ellipsoid, however, supports our data.

On heating, domains of type b do not change up to 270°C,

when they dissapear in a dramatic transition, sometimes accompanied with cracking of the crystal.

The transition from can be crearly seen crossing the crystal and bringing about a sudden change of contrast. On cooling a thermal hysteresis sometimes as large as 100°C can be observed. These two facts characterize this transition, which has not been reported so far, as a first order one.

---

[1]) F.F.Dudnik and I.S.Kolesov, Sov.Phys. Solid State 22(4)(1980)700.

[2]) R. von Hodenberg, Ber.Deuts.Keram.Ges. 49(1972)243.

II.11 Problems in the X-ray study of copper-strontium formate octohydrate

P.K. de Perazzo, M.A.R. de Benyacar and H.L. Dussel

The study of properties of copper strontium formate octohydrate, hereafter CSFOH, was undertaken as part of a study of ferroic materials. This compound was chosen because of its probable similarities with copper formate tetrahydrate which undergoes an order disorder paraelectric to antiferroelectric first order phase transition at 236°K.

Although the crystal structure of copper formate tetrahydrate has been solved and can be described by alternative layers of copper formate and disordered water molecules perpendicular to c axis, there is no X-ray diffraction study of CSFOH. This compound was then crystallized from an aqueous solution of which blue colored good single crystals were obtained. From X-ray diffraction of these, cell parameters were determined.

$$a = 6.63\ \text{Å},\ b = 8.77\ \text{Å},\ c = 8.94\ \text{Å}$$

$$\alpha = 104°\ 21'\ \beta = 95°\ 57'\ \gamma = 88°\ 35'$$

The axial ratio derived from these data is in good agreement with that obtained from optical observations as mentioned by A. Winchell[1]) . Triclinic space groups P1 or $P\bar{1}$ are possible. X-ray irradiated (Cu/K) crystals change their colour from blue to black; in the irradiated crystals the presence of Cu^{+} ions has been detected by qualitative chemical tests.

Precession X-ray patterns of these irradiated crystals showed some weak reflections corresponding to an orthorhombic cell superimposed with the triclinic one, both having d_{010} parallel. The orthorhombic parameters are:

$$a = 6.79\ \text{Å},\quad b = 8.76\ \text{Å},\quad c = 7.26\ \text{Å}$$

$$\alpha = 90°,\quad \beta = 90°,\quad \gamma = 90°$$

We are now working with DSC (differential scanning calorimetry) on both samples, the untreated and the X-ray irradiated one to investigate dehydration under irradiation as a possible mechanism to explain the two cells.

---

[1]) A.N.Winchell, The optical properties of organic compounds, (1954)15

II.12 Aging of accreted ice*

F.Prodi** and L.Levi

There are relatively few results on grain growth in ice crystals, despite the interest of this material, mainly due to its abundance in nature. The comparison of the results obtained by Carte[1]), Roos[2]) and, more systematically, by Jellinek and Gouda[3]) suggests that the initial crystal structure of the samples may affect the behaviour of the phenomenon.

The study of ice accretions gives the possibility to investigate this phenomenon in polycrystalline structures characterized by a well defined texture and grain size distribution.

In the present work the effect of annealing has been studied in ice deposits grown in wind tunnel at different values of the air and deposit temperatures and consequently presenting different mean size and shape. Cross sections of the cylindrical deposits have been cut and replicated, as grown and after annealing, to determine the average cross section $\bar{\sigma}$, the mean maximum length $\bar{l}$ and width $\bar{w}$ and the orientation of the c-axis of the crystal grains.

Significant grain growth was observed even at the relatively low temperature of -19°C. The average grain cross section increased for nearly all deposits, but this was mainly due to the increase of the crystal width, while the length $\bar{l}$ varied slightly and in some cases even decreased with time. The grains were initially elongated but tended to assume compact final shapes.

The study of the c-axis orientation showed that the statistical distribution of the crystal orientation was not modified substantially by annealing, so that the initial sample texture could be usually recognized even after protracted storage of the samples, at a temperature $T < 0°C$.

These results may be of interest, for the interpretation of the hailstone structure, when these have suffered some degree of annealing before analysis.

The change of the crystal dimensions with annealing is interpreted in

terms of the grain growth theory.

---

* J.Atmos.Sci, 37(1980)1375.

** Laboratorio FISBAT, CNR, Bologna (Italia).

1) A.E.Carte, Bull.Observ. Puy de Dome, 3(1961)129.

2) D.V.D.S.Roos, J.Glaciol., 6(1966)411.

3) H.H.G.Jellinek and V.K.Gouda, Phys.Status Solidi, 31(1969)413.

II.13 Effects of the growth mode upon the crystal orientation in artificial and natural hailstone†

L.Levi, F.Prodi* and L.Lubart**

The c-axis orientation in cylindrical accretions and in oblate hailstone is studied and the results are discussed in relation to the hailstone aerodynamics. In the case of artificial accretions, frequency distributions are obtained for the angles between the projection of the c-axis into the plane of the normal sections of the cylinders and the radial direction (η), or the c-axis itself (θ) and for the total angle between the c-axis and the radial direction (ψ). In all deposits, grown in dry, wet or spongy regime, the distributions of η are shown to have a behaviour similar to that for the angle ψ, while the distributions of θ always show maxima for small angles, with no apparent dependence on the growth conditions . Two examples, corresponding to dry and wet regimes are given in Fig. 1 and 2 respectively.

A similar though less pronounced effect is shown by the c-axis orientation in natural hailtones cut through their equatorial plane. An interpretation of the phnomenon is proposed, relating the difference between the η and θ distributions to the body rotation about a spinning axis approximately normal to the airstream. The fact that the difference between the considered distributions is less pronounced in natural hailtones than in accreted cylinders is explaned as an effect of gyration of the hailtone rotation axis about the horizontal.

---

† J.Rech.Atmos., 14(1980)333.

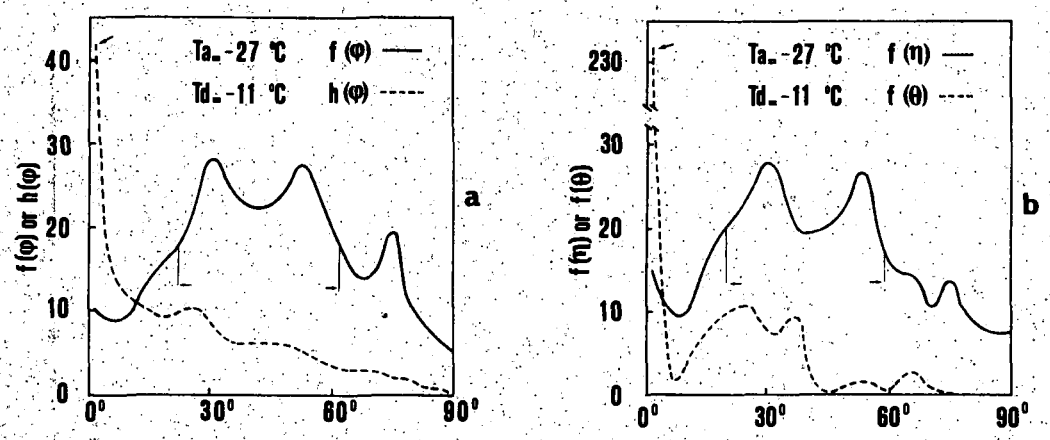

Figure 1

Frequency distributions of the η, θ and φ angles for a deposit grown in dry regime.

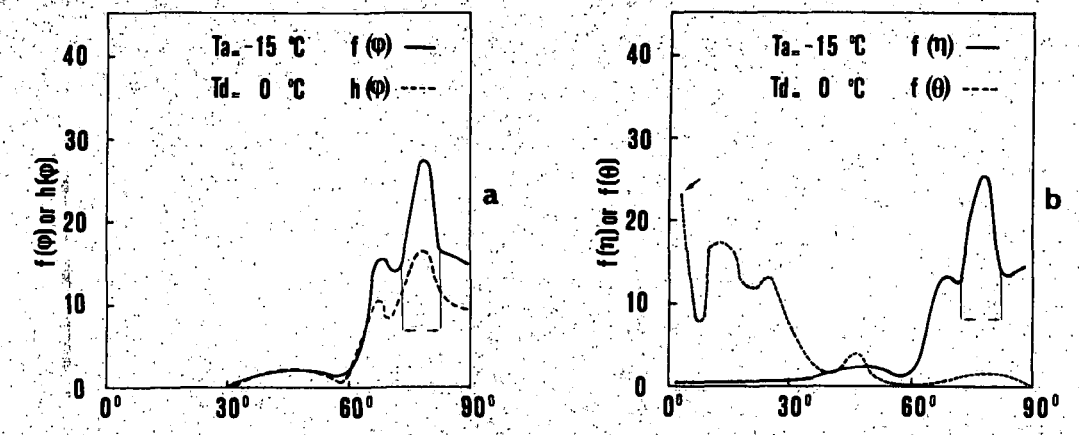

Figure 2

Frequency distributions of the η , θ and φ angles for a deposit grwon in wet regime.

* Laboratorio FISBAT-CNR, Bologna (Italia).
** Servicio Meteorológico Nacional.

II.14 Hyperfine bubble structures in ice grown by droplet accretion†

F.Prodi* and L.Levi

The air bubble distribution in ice grown by rapid freezing of supercooled water has been studied by Carte[1]), List and Agnew[2]) and Carras and Macklin[3]). It has been shown that the bubble size distribution depends on the freezing rate and that, in some cases, the ice takes a layered structure, formed by successive transparent and opaque fronts.

This "hyperphine air bubble structure" has been investigated in accreted ice to derive information useful in interpreting the growth history of natural hailstones. Cylindrical deposits have been grown in an icing wind tunnel in dry, wet and spongy conditions, in a wide range of air ($-27 \leq T_a \leq -10°C$) and deposit ($-15 \leq T_d \leq 0°C$) temperatures, at rotation rates of 0.25,1 and 4.4 Hz. Specific air bubbles features have been found, such as hyperphine fronts of various shape and characteristics, fan-like structures, non-periodical variations of ice opacity and protrusions of bubbly ice. The fronts which appear in dry regime are isochronous with growth and are equal in number to the rotations performed by the accreting cylinders; those in wet or spongy regimes are more separated and apparently independent of the number of rotations; they present bubbles of larger size and, sometimes, are interrupted by tiny radial segments of smaller bubbles. The bubble fronts and the other features described have been interpreted on the basis of simple mechanism related to the accretion process.

Most of the features observed in artificial accretions have also been identified in several hailstones for a given hailfall. It is shown that these features may help in interpreting the internal structure of hailstonesin combination with results of other analyses currently performed.

---

† J.Rech.Atmos., 14(1980)373.

* Laboratorio FISBAT-CNR, Bologna (Italia).

[1]) A.E.Carte, Proc.Phys.Soc., 77(1961)757.

[2]) R.List and T.A.Agnew, J.Atmos. Sci., 30(1973)1158.

[3]) J.N.Carras and W.C.Macklin, Quart. J.Roy.Meteor.Soc. 101(1975)127.

MÖSSBAUER SPECTROSCOPY

III.1 Influence of a $CuSO_4$ Treatment on Atmospheric Steel Rust Formation. A Mössbauer Spectroscopy Study†

C.Saragovi-Badler, I.A.Maier* and F.Labenski

Low alloy steel corrosion is still a not well known field. Particular interest is focused on the so-called weathering steels which show a remarkable resistance to atmospheric corrosion once a stable rust is formed, specially in SO_2 -containing atmospheres[1]).

Several analysis of alloying elements distributions in low alloy steels rust show an increase in copper and chromium concentration at the metal-oxide interface[1,2]), through some authors report a homogeneous distribution in the bulk rust with increasing concentration of alloying elements around pits and voids of the oxide layer. Accordingly, it was supposed that the presence of copper and sulphate produces a change in the composition and/or morphology of the corrosion products of low alloy steels which would be responsable of their good corrosion resistance. This conclusion was reinforced by results of experimental research on the influence of Cu^{2+} and SO_4^{-2} ions on the formation of iron corrosion products[3,4]).

Furthermore, studies of steel corrosion products morphology detected the formation of two different layers when observed by reflected polarized light[1]). In low alloy steels, exposed to the atmosphere for more than a year, an internal optically active layer was distinguished from an external optically active layer, while these two layers continued mixed in the rust of carbon steels, even after several years exposure. It was concluded that the internal optically isotropic layer would be responsable for the weathering steels corrosion rate decrease.

In the presente work, the initial copper and sulphate contents on the surface of low alloy and 1010 steels was increased by immersing in a $CuSO_4$ bath. By this method the copper content increment at the metal-oxide interface can be obtained earlier than by the atmospheric weathering process. The influence of this procedure on the weathering steel patina formation could be studied. Analysis of the so-treated carbon steel corrosion products would allow to determine if, at initial corrosion stages, the effect of the copper deposited on the steel surface is comparable to that produced by

copper as an alloying element in a weathering steel. The samples immersed in the $CuSO_4$ bath were exposed along with low alloy and 1010 steels blank specimens in an urban-industrial atmosphere.

Mössbauer spectroscopy was used for the analysis of the corrosion products[5]. This technique can give more information compared with other conventional techniques due to the fact it is a very suitable tool in the study of crystalline or amorphous iron oxides and hydroxides in bulk and in ultrafine particles (< 100 Å).

Our results show that there is larger proportion of α-FeOOH to γ-FeOOH and a greater amount of amorphous compounds in the external rust layers of weathering and 1010 steels. This fact is in accordance with the models proposed in [6]) and [7]) for atmospheric corrosion processes.

The present work also demonstrates that a copper deposit on low alloy steel and carbon steel surfaces produces a change in their atmospheric rusts composition: the amorphous or gel-like corrosion products present in rusts of blank plates of both steels, disappears.

Even though the effect of immersing the steel plates in a $CuSO_4$ bath can not be considered identical to the effect produced by the copper enrichment at the metal-oxide interface of a weathering steel exposed to the atmosphere, our results suggest that copper would not favour the formation of an amorphous protective layer on the metal surface.

---

† Accepted for publication in "Corrosion"

* CNEA, División Corrosión

1) L. de Miranda, Rapports Tech. du Cebel Cor, RT222, 125(1974)1.

2) R.Bruno, A.Tamba, G.Bombara, Corrosion, 29(1973)95.

3) T.Misawa, K.Hashimoto, W.Suetaka and S.Shimodaira, Proc. 5th Int. Congress on Met. Corrosion, NACE(1974)775.

4) K.Inouye, K.Ichimura, K.Kaneko, T.Ishikawa, Corros.Sci. 16(1976)507.

5) M.J.Graham and M.Cohen, Corrosion, 32(1976)432.

6) W.Meisel, J. de Physique C1, Suppl. Nº 1, 41(1980)C1-63.

7) K.Barton, Protection Against Atmospheric Corrosion, publ. J.Wileys & Sons, (1976) Chap.3.

III.2 A Fe^{57} study of corrosion process in Chrome-Magnesite bricks used in an arc furnace

C.Puglisi*, C.Saragovi-Badler and F.Labenski

The Mössbauer effect provides information concerning the local surroundings of the iron ion in any material.

This kind of information can be useful in the study of corrosion mechanisms in steelmaking refractaries.

In the present research we are making a post-morten study of Chrome-Magnesite bricks which were used in a steelmaking arc furnace. The aim of this work is to study which is the iron role in the corrosion process.

Chrome ores usually contain two constituents, the chrome grain and a gangue mineral (of the magnesium-silicate type). The chrome grains consist of a solid solution of spinel-compounds of the general formula R_3O_4. In chrome spinel the divalent ions are Mg^{2+} and Fe^{2+} and the trivalent ions Al^{3+}, Cr^{3+} and Fe^{3+}. It should be noted that the term chromite refers to the spinel $Fe\,Cr_2\,O_4$.

Samples of: raw material used in bricks manufacture form different factories, chrome minerals, and attacked bricks are being analyzed at different temperatures.

The experimental spectra obtained up to now, show peaks at the paramagnetic region only, for all the measured temperatures. The lack of magnetic structure points out that inverse spinel structure similar to that of magnetite is absent. The Mössbauer parameters corresponding to the paramagnetic region peaks indicate the presence of Fe^{2+} and Fe^{3+} ions. The Fe^{2+} ions would be in different tetrahedral sites as well as in the octahedral sites. The Fe^{3+} ions would be present in the tetrahedral and the octahedral sites.

We intend to pursue further studies of Chrome-Magnesite bricks using Mössbauer spectroscopy.

---

* INTI, Institute of Industrial Technology, Migueletes, Argentina.

III.3 Genesis of sandstone-type Uranium deposits at Sierra Pintada District, Mendoza, Argentina: A Mössbauer study contribution†

H.B.Nicolli*, F.Labenski, and C.Saragovi-Badler

The main problems related to the genesis of sandstone-type uranium deposits at Sierra Pintada district, western Argentina, have been studied in order to show the validity of the genetic model proposed.

The control factors in the uranium extraction from its sources, the uranium transport phenomena and the processes leading to the uranium precipitation in the host rock have also been discussed[1]). The latter depends on the distribution of the reduction agents, bacteria being the most important one. Bacteria development and activity are mainly regulated by the CO_2 partial pressure.

As the different pigments occurring in sandstone often reveal environmental changes, its identification is of great importance to define the main physico-chemical characteristics of the environment. As it is well known iron oxides are present in pigments. Taking into account that Mössbauer spectroscopy has become a very useful tool in the study of iron minerals[2]), in the present investigation this technique was used to identify the different iron oxides occurring in reddish, reddish-brown and reddish-violet coloured beds bearing high uranium contents.

Sierra Pintada, situated between 69°- 65°W and 33°- 39°S, is a 3500 km^2 geomorphological unit, a hilly strip with relatively smooth relief features

The Sierra Pintada uranium district is located in the Province of Mendoza, 35 km west of the town of San Rafael, Argentina. It consists of several uranium deposits and many anomalies in a 400 km^2 area. Up to the present it is the principal uranium district in Argentina. Its reserves are of the order of 16,000,000 tons of ore mineral of grades varying from 0.70 to 1.18% U_3O_8.

Samples measured using Mössbauer spectroscopy have been divided in four groups according to their common characteristics:

First Group: Samples 219/49; ee39022 and 219/116

According to Mössbauer spectroscopy results a mineral of the chlorite series with the Fe^{2+} ion in a distorted octahedral site and showing

inhomogeneities has been identified. A very small amount of Fe^{3+} is present only in sample 219/116. These samples correspond to beds of gray sandstones with a small degree of alteration. No contribution of uranium bearing solutions was observed (low radiometry and U_3O_8 values).

Second group: Samples 219/77 and 219/94

Mössbauer spectroscopy parameters show also the existence of minerals of the chlorite series. The Fe^{2+} ion is in a distorted octahedron and the amount of Fe^{3+} ion is somewhat greater than in the first group. Samples have been taken from grey to olive-grey coloured sandstone beds with a small degree of alteration. No contribution of uranium bearing solutions were observed (low radiometry and U_3O_8 values).

Third group: Samples ee39074 and 737/73

As in the previous mentioned groups minerals of the chlorite series are present but in this case the octahedral Fe^{2+} sites are very distorted. In sample 737/78, γ-$Fe_2O_3.H_2O$ is observed while in ee39074, the Fe^{3+} ion could be adscribed to a chlorite or to a γ-$Fe_2O_3.H_2O$. These samples correspond to light reddish or light reddish-brown sandstones which have been taken from altered beds where the occurrence of uranium ores was verified. The corresponding radiometry and U_3O_8 values are high.

Fourth group: Samples 219/64 and 219/102

In this case a mineral of the chlorite series is observed again with the Fe^{2+} ion in a distorted octahedral site. The Fe^{3+}/Fe^{2+} ratios of the chlorite point out that very important oxidation took place. Furthermore maghemite (or hematite) has been identified. These samples have been taken from reddish coloured sandstone beds with high degree of alteration in which the occurrence of uranium ores was observed (high to very high radiometry and U_3O_8 values.

Thus it can be seen that in the samples of the first two groups the sole iron mineral identified belongs to the chlorite series (with the Fe^{2+} site distorted) and with a rather low Fe^{3}/Fe^{2+} ratio. These results are concurrent with the fact the minerals of the horizons from which the samples were taken show a lower degree of alterations (weathering) and no contribution of mineralizing solutions.

On the other hand the samples from the last two groups show, in

addition to the chlorites (with the Fe^{2+} site very distorted), the occurrence of the γ varieties of ferric oxides. These results are in agreement with the fact that samples belong to horizons where the common sandstone minerals have been altered due to mineralizing solutions flowing as a free aquifer through the sandstone with incipient degree of diagenesis. These solutions modified the Fe^{3+}/Fe^{2+} ratio (>1) due to oxidation. In this environment, local reduction phenomena (biogenetic activity) which cause uranium precipitation were observed.

The experimental results confirm the hypothesis of the existence of physico-chemical phenomena in the depositional environment which mainly depend on the CO_2 partial pressure and which regulate the distribution of the reduction agents in it.

Consequently the biogenetic action (Bacteria development) was limited to the uranium host sandstone only at the upper levels of the free aquifer. There, the CO_2 partial pressure is lower, facilitating the bacteria development which produce a local reduction environment where uranium minerals precipitate.

At the same horizons, γ-$Fe_2O_3.H_2O$ (lepidocrocite) occurs since this variety precipitates only at low value of CO_2 partial pressure.

Lepidocrotite is unstable, and turns to maghemite which slowly becomes hematite. Thus the occurrence of these ferric oxides in the depositional environment are coincident with the highest uranium concentrations.

Satisfactory agreement was obtained between experimental data and the genetic model for sandstone-type uranium deposits at Sierra Pintada district.

---

† Submitted to "Chemical Geology"

* Comisión Nacional de Investigaciones Espaciales, San Miguel, Pcia.Bs.As.

[1]) H.B.Nicolli, M.A.Gamba, R.E.Ferreyra, 26th International Geological Congress (1980); Section Nº 13, Symposium 22 (13/0245)Paris(in press).

[2]) C.L.Herzenberg, D.L.Riley, Development in Applied Spectroscopy, (E.L. Grove, ed. Plenum Press) vol 8(1970)177.

THEORETICAL SOLID STATE PHYSICS

IV.1 Pseudo-spin formalism and the transition temperature of potassium ferrocyanide trihydrate

V.Massidda and E.Anda*

Ferroelectric transitions due to an order-disorder process in a double-well potential can be treated by the pseudo-spin formalism[1]). One of the most important quantities the theory allows one to calculate is the transition temperature T_c, which in the mean -field approximation satisfies

$$2\Omega/J_0 = \tanh\,(\Omega/2k_BT_c). \qquad (1)$$

Here Ω and J_0 are two parameters of the formalism: Ω is approximately equal to the energy difference between the first excited and the ground levels, while

$$J_0 = -4 \sum_j \langle i,+;\, j,+ |\, V_{ij} |\, i,-;j,-\rangle \qquad (2)$$

($|i,+\rangle$ and $|i,-\rangle$ are the ground and the first excited states, respectively, at site i).

If $2\Omega/J_0 \gtrsim 1$ eq.(1) has no solution for T_c, i.e. there is no phase transition. On the other hand, if $2\Omega/J_0 < 1$ the transition can be either of the soft-mode type (if $2\Omega/J_0 \lesssim 1$) or of the relaxational type (if $2\Omega/J_0 \ll 1$). In the latter case eq.(1) reduces to

$$T_c \simeq J_0/4k_B, \qquad (3)$$

so that the transition temperature is independent of Ω.

We have applied the pseudo-spin formalism to $K_4Fe(CN)_6.3H_20$ (potassium ferrocyanide trihydrate), using for the latter the model previously introduced by one of us[2]). According to this model, the "particles" undergoing the order-disorder process are the water molecules and the double well they see is due to their electrostatic interactions with the ions and with each other. The interactions V_{ij} (eq.2) are also of an electrostatic nature. In this way we are able to evaluate J_0 and to estimate the order of magnitude of Ω. We find $\Omega \simeq 10^{-4}$ eV and $J_0 = 0.083$ eV, so that $2\Omega/J_0 \ll 1$. Therefore we find that the transition should be of the relaxational type, in agreement with previous

authors[3]), and that T_c should not be affected by deuteration, as indeed is the case[4]).

Finally, from eq.(3) we obtain $T_c = 241$ °K, in excellent agreement with the experimental values (248.6 °K and 255.1 °K for the ordinary and deuterated material, respectively).

---

* Departamento de Física, Universidade Federal Fluminense, Niterói, Brasil.

[1]) R.Blinc and B.Zeks, Adv. in Phys. 21(1972)693.

[2]) V.Massidda, J.Phys.C11(1978)2865; see also CNEA NT-13/80, IV.5.

[3]) I.Savatinova and E.Anachkova, Phys.Stat.Sol. (b)84(1977)401.

[4]) S.Waku, K.Masuno and T.Tanaka, J.Phys.Soc. Japan 15(1960)1698.

IV.2 Identity relations for a certain type of lattice sums

V.Massidda

In a previous paper[1]) an expression was found for the potential in a crystal made of point charges with a uniform neutralizing background, shaped as a slab parallel to a given pair of crystal axes. Considering two slabs cut in different ways (parallel to the a and b or to the b and c axes respectively) and taking into account the dependence of the potential on the crystal shape, one can write down an identity in the following quantities: a, b, c (lattice constants), α, β, γ (crystallographic angles), j_a, j_b and j_c (fractional coordinates of the field point). From the mathematical point of view, this identity is not trivial because each side of it is not symmetrical in a, b and c, in α, β and γ, nor in j_a, j_b and j_c.

Now we have found a mathematical proof of this identity, showing that it actually is the sum of an infinite number of identities. The latter too have a physical meaning, since they represent the equality of the values of the potential in two slabs of a "crystal" made of straight lines parallel to the b direction bearing a sinusoidally varying charge density. The proof consists in applying Cauchy's theorem of residues to the function

$$F(z) = \frac{1}{U(z)}\, Q(j_a;\, 2\pi i z)\, \{Q[j_c;\, 2\pi\{CU(z) + i(\xi_{c,1} z + \frac{b}{a}\xi_{c,2} z')\}]$$

$$+ Q[1 - j_c;\, 2\pi\{CU(z) - i(\xi_{c,1} z + \xi_{c,2} z')\}]\},$$

where

$$Q[j;\, f(z)] \equiv \frac{e^{-jf(z)}}{1 - e^{-f(z)}},$$

$$U(z) = (z^2 - 2\cos\gamma\, z'\, z + z'^2)^{1/2}$$

and

$$C = \frac{c}{a}\,\frac{\cos\delta_c}{\sin\gamma}$$

(for the meaning of δ_c, $\xi_{c,1}$ and $\xi_{c,2}$ see ref.1).

The procedure can be generalized for application to similar lattice sums by choosing a different combination of Q-functions or a different U(z).

---

[1]) V.Massidda and J.A.Hernando, Physica 101B(1980)159; see also CNEA NT-13/80.

IV.3 Newton-Everett interpolation of continuous functions

J.A.Hernando

Interpolation needs are deeply rooted in almost all branches of physics because of the uncommonness of analytical solutions and the discrete nature of physical measurements.

If the calculations we are doing are very time consuming, it would be convenient to minimize these calculations and to interpolate whenever it would be possible, An important example is the solution of a non-linear integral equation such as those appearing in the statistical theory of liquids[1]). In such a case the first decision that must be taken is which integration method to employ. Roughly speaking, we have two kinds of methods: i) those in which the function to be integrated is calculated in a set of points evenly spaced (Newton-Cotes and Simpson's methods are the most widely known); ii) those in which the function to be integrated is calculated in a set of irrational abscissas (e.g. Gauss and Tchebysheff's methods). Integration methods of

the second group are, by far, faster and more accurate than methods of the first group. Therefore, it is clearly seen the convenience of implementing them in any iterative search of the solution to the integral equation. As a consequence, it is crucial to have an interpolation routine for evaluating the function to be integrated in the irrational abscissas needed. This routine must be such as not to spoil the advantages of these integration methods. We have done an interpolation routine that employs the finite differences formulae of Newton and Everett[2]).

The routine is designed to work with a continuous function defined in an evenly spaced set of points. The main purpose is to do the calculations in a quick and accurate form. The calculation is divided into two parts:

i) a calculation which depends exclusively on the points where the function is given and on the accuracy requested;

ii) a calculation dependent on the point where we want to interpolate.

The first calculations are done only once and then they are available for the following calculations. In the program it is assumed that the set of points where the function is defined is less or equal than 200. This can be easily changed.

If the function to be interpolated has a pathological behaviour, the results are strongly dependent on the size of the separation between functional values, so special care must be taken with this point. The average running time depends on the quantity of interpolation points calculated. However, it can be estimated to be of the order of 3 times the time needed for a double precision exponential.

---

[1]) J.P.Hansen and I.R.McDonald, Theory of simple liquids,Academic Press, N.York (1976).

[2]) Z.Kopal, Numerical Analysis (Chapman and Hall, London (1961).

IV.4 Internal Fields and Anti-ferroelectric ordering in Copper Formate tetrahydrate

J.Hernando, V.Massidda and P.K. de Perazzo

Copper formate tetrahydrate, hereafter CFTH, is an antiferroelectric crystal containing water molecules in its structure. Its antiferro-para electric phase transition is due to the reorientation of the water molecules[1]). Experimental evidence indicates that the motion involved in the mechanism of transformation is not due to tunneling or hopping of protons along the bonds[2]). The involved hydrogen bonds are rather weak, as suggested by their length (2.8 Å). Finally, the critical temperature is very little affected by deuteration. All these features are shared with potassium ferrocyanide trihydrate, recently studied by one of us[3]).

Continuing on this line, we are applying the electrostatic model of ref. 3 to CFTH. The electrostatic field at the water molecule sites and the Lorentz factor between the water molecules sublattices were calculated with PLATSUM2 program (see next report). The next step will be to find the orientation of the water molecules in the antiferroelectric phase by minimizing their electrostatic energy. This minimization will give the zero temperature configuration of the crystal.

---

1) N.Burger and H.Fuess, Ferroelectrics 22(1979)847.

2) M.Kay, Ferroelectrics 9(1975)171.

3) V.Massidda, J.Phys. C11(1978)2865; see also CNEA NT-13/80, IV.5

IV.5 PLATSUM2 : an improvement of the program PLATTSUM for evaluating lattice sums

J.A.Hernando and V.Massidda

The Fortran program PLATTSUM[1]) evaluates electrostatic lattice sums (e.g. the electric field of a point-multipole lattice) for a given field point and a given sublattice of source points. In practice, one

often needs the electrostatic quantities at several (N_1) field points, in a crystal whose unit cell contains several (N_2) sublattices. In such a case the PLATTSUM user must enter N_1N_2 data sets. However, all the needed information is contained in the coordinates of the field points and the source points (N_1+N_2). For instance, in our calculation with a rather simple crystal such as copper formate tetrahydrate (see preceding report) we have $N_1=16$, $N_2=44$, so that the difference between N_1N_2 and N_1+N_2 is considerable.

We have introduced a modification in the way the program processes the data set before starting the actual calculations. In the new version the user enters the minimal data set (N_1+N_2 coordinates) and directs the program to evaluate the required quantities created by the N_2 source points at the desired N_1 field points.

As the output contains the electrostatic quantities corresponding to N_1N_2 points, we have added an optional output channel. In this channel the results are tabulated in such a way as to be used as the input of another program without the need of further manipulation by the user.

---

[1]) J.A.Hernando and V.Massidda, Comp.Phys.Commun. 22(1981)13; see also Progress Report CNEA NT-13/80. IV.5 .

IV.6 Calculation of the internal field and its gradient in $Cs_2(TCNQ)_3$

J.A.Hernando and V.Massidda

The interpretation of the experimental results of Nuclear Quadrupole Resonance requires the knowledge of the electric field gradient created by the lattice charges of the crystal at the sites of the resonant nuclei. At the request of Dr. J. Murgich* we have evaluated the electric field and its gradient at the nitrogen sites in $Cs_2(TCNQ)_3$ due to the charges of the Cs ions and of the atoms of the TCNQ molecules. For the latter we have used the results of several authors[1,2]) referred to TTF-TCNQ and TMPD-TCNQ. The calculation was performed using the program PLATSUM2

(see preceding report).

According to the first results, the contribution of the lattice is at least one order of magnitude smaller than the experimental value. This is perhaps due to the fact that our calculation does not include the overlap and exchange contributions of the nearest atoms. This work will be continued in close collaboration with Dr. Murgich, with whom we will discuss several unsettled points of the above calculation.

---

* Centro de Química, IVIC, Caracas, Venezuela.

[1]) A.J.Epstein, N.O.Lipari, D.J.Sandman and P.Nielsen, Phys.Rev. B13 (1976)1569.

[2]) R.M.Metzger, J.Chem.Phys. 74(1981)3458.

IV.7 Effects of the lattice size and the symmetry of the renormalization transformation in the determination of critical indices

S.D'Elía and H.Ceva

The Monte Carlo Renormalization Group (MCRG) method[1]) is used to study the behavior of a two dimensional spin lattice in the ferromagnetic and tricritical fixed points.

Eigth spin interactions are considered: nearest neighbor (coupling constant K_1), second neighbor (K_2), three and four spin couplings (K_7 and K_4), as well as a uniform magnetic field (K_5). Moreover there are three staggered interactions: second neighbor (K_3), magnetic field (K_6) and three spin (K_8). These are all the interactions that can be fitted in a 2 x 2 lattice.

We studied three kinds of renormalization transformations:

(i) a transformation originally used by Nienhuis et al[2])

(ii) a transformation called NN, used by Nauenberg and Nienhuis[3])

(iii) a transformation illustrated in Fig.1. We show a 10 x 10 lattice with 4 rows and 4 columns added to implement periodic boundary conditions. Each white (black) renormalized spin is obtained by adding the 25 white (black) spins included in each tilted square.

In all cases, the renormalization transforms a N x N into a 2 x 2 lattice.

Case (i) does not conserve the symmetry of the original lattice; this shows up in our study as an increasing deterioration of the critical indices as N increases (i.e. a behavior opposite to the one expected apriori).

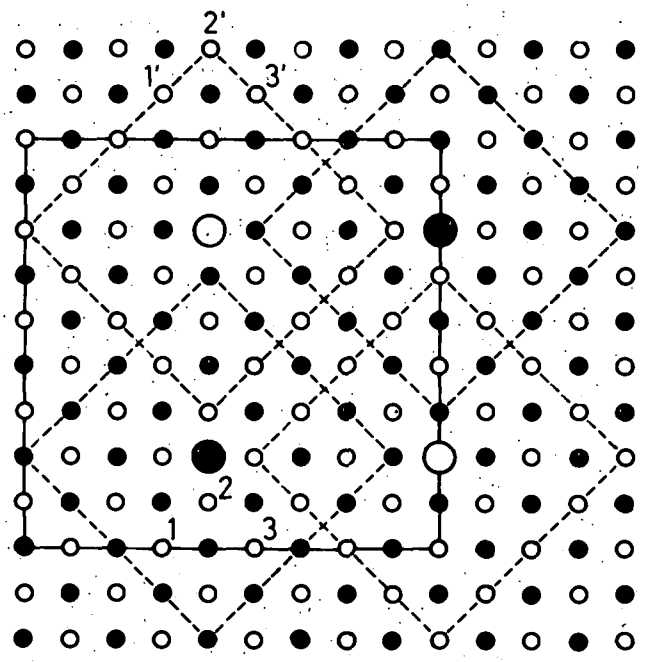

Transformation NN has no symmetry problems in the ferromagnetic fixed point; in this case all staggered interactions are set equal to zero, and both K_1 and K_2 are positive. Van Leeuwen has pointed out that it is not appropriate to study the tricritical fixed point with this transformation. We obtained very good ferromegnetic indices in the case of the transformation 18 x 18 → 2 x 2.

Results of the third transformation, both for the critical and tricritical points are good.

The size of the initial lattice was taken to be 4 x 4, 6 x 6, 10 x 10 and 18 x 18. Calculations are made in the final (2 x 2) lattice in two forms: using MCRG, and by considering all its configurations (i.e. this is an exact result). When both calculations are equal, the set {K} corresponds to a fixed point.

All cases show lattice size effects; in (ii) and (iii) the calculated indices improve with increasing lattice size.

---

[1]) R.Swendsen, Phys.Rev. B20(1979)2080.

[2]) B. Nienhuis, A.Sudbo and E.Hauge, Physica 92A(1978)222.

[3]) N.Nauenberg and B.Nienhuis, Phys,Rev.Letters 33(1974)944.

IV.8 Mixed-Valence in a single impurity: influence of the central potential†

L.M.Falicov*and H.Ceva

This work is concerned with the problem of characterizing the conditions under which a rare earth impurity (R.E.) in an otherwise normal substance will show intermediate valence (I.V.) behavior. Specifically, we assess the importance of the Coulomb interaction between the f-electrons of the R.E. and the matrix. This is done by comparing two situations: one in which there is, and one in which there is no Coulomb interaction.

The impurity is represented as a system with two configurations, $|D1\rangle$ and $|D2\rangle$, with energies E_1 and E_2 (when the R.E. atom is in D1 it has n f-electrons; in D2 it has n-1 f-electrons, and one d-electron more than D_1). Both configurations hybridize with the conduction band of the host, with strengths V_1, V_2.

The case with no Coulomb interaction is the simplest: the system consists of the states $|D_i\rangle$ and the band states $|k\rangle$, with density of states $E^{1/2}$. Hence the ground state can be written as

$$|\Psi\rangle = \alpha\,|D_1\rangle + \beta\,|D_2\rangle + \Sigma_k\,\gamma(k)\,|K\rangle$$

where the sum extends over the first Brillouin zone.

If $u \equiv |\alpha/\beta| \geq 1$, we define $R = u^2$. If $u<1$, then $R = 1/u^2$. A state will be called an I.V. state if $1 \lesssim R \lesssim 10$.

To include Coulomb interactions is more complicated. If the host is a metal, the situation is very involved because the f electron which "moves" back and forth between the impurity and the band is screened by the conduction electrons. Thus, it is a time-dependent many-body problem. We considered the case of a semiconductor, where the effect of Coulomb interactions is to introduce a set of hydrogen-like levels characteristic of the electron-hole pair produced when the f electron of the R.E. is promoted to the conduction band, leaving a hole in the impurity. This scheme is further simplified by noting that the hybridization between the hydrogen-like states and the original states D_i is important only near the R.E. atom. Thus we assume that the $|1s\rangle$ state

determines the main characteristics of the problem, and therefore replace the semiconductor-plus-impurity by a three states system: $|D1\rangle$, $|D2\rangle$ and $|1s\rangle$, with $E_{1s} = -(m/m_e)\,\varepsilon^{-2}$ 13.6 eV where ε is the dielectric constant, m the effective mass and m_e the electronic mass. The state $|D_i\rangle$ mix with strength V_i with the state $|1s\rangle$.

The ground state in this case is

$$|\Psi_{3L}\rangle = \alpha\,|D_1\rangle + \beta\,|D_2\rangle + \Gamma\,|1s\rangle$$

The change in the coefficient R (see figure) is taken as a meassure of the incidence of the Coulomb interactions in the I.V. problem. Information about the ground state as a function of the parameters E_1, E_2, V_1, V_2 has been obtained, and serves the purpose of characterizing the I.V. state.

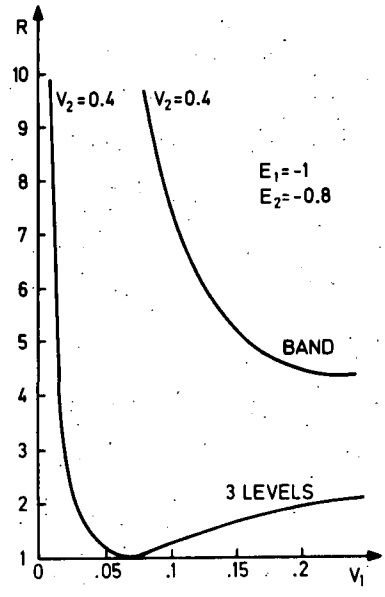

†

1)

IV.9 Charge transfer in structurally disordered systems

N.V.Cohan and M.Weissmann

In this paper we study the charge distribution in systems with structural disorder, both in the case of identical atoms and of alloys. Recent calculations[1,2]) have shown that even in disordered systems of identical

atoms the atoms acquire different charges due to the differences in the fields around them. Thus a charge distribution n(Q) can be defined, that gives the number of atoms with charges between Q and Q + dQ. Because the atoms have charges associated to them there is an electrostatic interaction among them which, we believe, will contribute to determine the optimum atomic configuration and charge distribution. In the present work we study this effect starting from a totally random distribution of atoms, we then calculate the corresponding charges on the atoms and subsequently relax the system by changing the atomic positions by an amount proportional to the electrostatic force on each atom. The most noticeable result is a considerable narrowing of n(Q).

When there is more than one type of atom, as in binary ordered alloys, there is usually a charge transfer form one type of atom to the other. If the alloys are disordered with either compositional or structural disorder (liquid and amorphous alloys) then the charge transfer obtained is not unique but our results show that there is a charge distribution for each type of atom. We also show that the effect of having two different atomic sizes in a random system leads to an electronic charge transfer towards the larger atoms. The differences in ionization potentials obviously produce charge transfers to the atoms with higher ionization potentials. Thus depending on the particular alloy, these two effects can produce charge transfers in the same or in opposite directions.

---

[1]) L.Guttman, W.Y.Ching and J.Rath, Phys.Rev. Letters, 44(1980)1513.

[2]) N.V.Cohan and M.Weissmann, J.Phys. C:Solid State Physics 12(1979) 1835.

IV.10 Chemisorption of ions on metallic surfaces

M.Weissmann and N.V.Cohan

We are beginning to study specific ionic adsorption of some simple negative and positive ions on metal surfaces used in electrochemistry.

Ionic adsorption of negative ions on the different surfaces of Ag has been studied experimentally in electrolytic solutions[1]. We intend to calculate the charge transfer and the chemisorption energy as a function of the distance to the surface. Some preliminary calculations with the iterative extended Hückel method[2] show that F^- is adsorbed at shorter distance than Li^+ and that its adsorption energy as a function of distance drops to zero much faster. At the optimum distance of adsorption F^- has transferred about 0.5e to the metal while Li^+ has acquired about the same electronic charge.

---

[1]) R.Parsons, Surf. Sci 101 (1980) 316.

[2]) N.V.Cohan and M.Weissmann, J.Phys.C: Solid State Physics 12(1979)1835.

IV.11 On the free energy of disordered alloys and the moment of the density of states

A.M.Llois and N.V.Cohan

Using a variational method[1]) we have calculated upper and lower bounds for the Helmholtz free energy F of a 1D tight-binding disordered alloy of the type $A_x B_{1-x}$ as a function of temperature, concentration and the number of exact moments of the density of states n(E) [2]). We have shown that the average of the upper and lower bounds calculated with very few exact moments is an excellent approximation to F. We have also obtained F using three different approximations to the exact density of states, which give similar values for the free energy F, and have shown that these values lie within the bounds of F that correspond to considerably higher number of exact moments than those provided by the approximation used for n(E).

In the table we show the results for F obtained using the three approximate methods for the obtention of n(E) and its upper and lower bounds for $x = 0.5$ and some values of kT. F_c is calculated with n(E) obtained using the method of prolongation by pseudoatoms[3]), with 5 exact moments. For the calculation of F_{AB}, n(E) is approximated by the method of

prolongation with atoms of type A and B[4]) and has 8 exact moments. F_k (k= 2,3,4) is calculated using a density of states obtained by a single continued fraction expansion where a_1, $a_2 \ldots a_k$, b_k were obtained from the first 2k exact moments of the alloy density of states. F_u^N, F_ℓ^N denote upper and lower bounds to F, respectively, taking N exact moments of n(E). W is the bandwidth.

TABLE

kT/W	1/40	1/8
Fc	- 2.234	- 3.139
F_{AB}	- 2.220	- 3.138
F_2	- 2.235	- 3.139
F_3	- 2.227	- 3.138
F_4	- 2.228	- 3.138
F_u^5	- 2.082	- 3.1255
F_ℓ^5	- 2.364	- 3.1579
F_u^9	- 2.188	- 3.1375
F_ℓ^9	- 2.266	- 3.1385
F_u^{13}	- 2.214	- 3.13789
F_ℓ^{13}	- 2.242	- 3.13792

[1])A. Trias, R. Ramirez and M.Kiwi, Phys. Rev. B15(1979)5877.

[2])A.M.Llois and N.V.Cohan, J.Phys.C: Solid State Phys. 13(1980)L1027.

[3])M.Weissmann and N.V.Cohan, J.Phys. C:Solid State Phys. 9(1976)473.

[4])N.V.Cohan and M.Weissmann, J.Phys.C:Solid State Phys. 10(1977)383.

K/Ar dating of some rocks from Marguerite Bay Argentine Antarctic Sector

R.O.Toubes

The gneisses from San Martin Island, homonymous Argentine Antarctic Base site in the Debenham Group, and several other rocks from the near Millerand Island in the Marguerite Bay, Antarctic Peninsula, Argentine Antarctic Sector, were dated.

The results are:

gneiss - San Martin Island	25 ± 5m.a.
rhyodacitic tuff - Millerand Island	108 ± 10m.a.
lamprophyre " "	113 ± 10m.a.
alkaline granite " "	114 ± 10m.a.
gneiss - San Martin Island	116 ± 10m.a.
rhyodacitic tuff - Millerand Island	126 ± 5m.a.
andesite	141 ± 10m.a.
gneiss - San Martin Island	465 ± 50m.a.

The first result is discarded and the other results are discussed and compared with data obtained by other authors:

Petrographis descriptions are included.

Geology of Bertrab munatak. Argentine Antarctic Sector

R.O.Toubes

An expeditive topographic-geology study of Bertrab munatak, Argentine Antarctic Sector, has been done. It is located at 77°44' South and 34°48' West. This work was made as a special collaboration with the Antarctic Department of the Army High Command, trough the Argentine Antarctic Institute on the ocassion of the foundation of General Belgrano II Army Base.

Because of the very difficult access, previous works have been limited.

The munatak is an outcrop of medium grained reddish gray granite, intrudded by conspicuous niolitic porfiry and spessartite veins over fault

plane, together with numerous quartz veinlets forming, ocasionally, amethyst druses.

All the rocks particularly the granite, show a strong jointing in two principal sets parallel to the veins.

The rocks age was not determined due to the generalized weathering but taking into account the dating of neighboring rocks (munataks Moltke and Littlewood) they should belong to the Precambrian.

Solar Energy

SOLAR ENERGY

I.1 Experimental and theoretical studies of concentrator systems

Solar Energy Applications Group*

The final aim of the program has been ajusted to heat fluids to 150-350°C using solar radiation concentrators, in order to provide industrial process heat and generate steam able to drive turbogenerators.

The two-dimensional optical analysis of cylindrical concentrators valid for any angle of incidence of the solar rays, developed earlier in the group, was generalized to non-ideal concentrators, which allows to take into account the possible errors in all of the significant concentrator parameters. This extended analysis was used to select the optimal parameters of a fixed-faceted-mirror solar concentrator (FFMSC) and to determine its construction tolerances. With these data, the construction of an "FFMSC industrial prototype" has been analyzed in detail, both technically and economically, following the lines of a French design based on the use of about 1 m long blocks mounted on two concrete ribbons.

As far as the two existing "FFMSC laboratory prototypes" are concerned, several modifications were introduced in order to improve the behavior of the complete system and preliminary measurements of the efficiency have been performed.

The comparative analysis of several storage systems appropriate to be used in combination with the concentrator systems being developed has been started, under contract, by the Department of Applied Chemistry of the Consejo de Investigaciones Científicas y Técnicas de las Fuerzas Armadas (Council of Technical and Scientific Research of the Armed Forces).

I.2 Low temperature thermal applications

Solar Energy Applications Group*

A 14-m^2 flat-plate solar collectors system to heat the water for the personnel showers at the Special Alloys Plant of the Atomic Energy Commission has been designed and its contruction has been supervised. The suppliers for the collectors were asked to submit efficiency curves for

---

* Work is performed by agreement between the Department of Physics and the Department of Prospective and Special Studies, following programs sponsored and controlled by the latter.

their products (measured according to international standards), a requirement not previously placed in Argentina. The system works on natural circulation and uses double glassed collectors.

The first stage of a contract with the Empresa Provincial de Energía de Córdoba (Energy Board of the Province of Córdoba) has been completed, It covered the technical assistance this institution required in the solar energy application and energy conservation fields during the implementation of an architectural design competition for its 2.000 m^2 administrative building to be erected in Villa Carlos Paz. The building will have special insulating requirements and warm water, heating and cooling will largely be supplied by solar energy conversion systems. The work has been performed with the collaboration of members of the Comisión Nacional de Investigaciones Espaciales (Space Research Commission) and of the Instituto Nacional de tecnología Industrial (Institute of Industrial Technology).

I.3 Photovoltaics

Solar Energy Applications Group*

A small fraction of the Division's effort has been devoted to start theoretical studies in solid state physics oriented to semiconductors, in order to provide an appropriate basis for future theoretical studies in photovoltaics.

The up-dating of an evaluation of the state of the art in photovoltaics, performed by the group in 1976, has been started.

Appendix

Staff

Publications

PERSONNEL OF THE PHYSICS DEPARTMENT

Research Staff

Abriola D.	on leave at State Univ.of N.Y.at Stony Brook,U.S.A.
Achterberg E.	
Baggio, R.	
Benyacar, M.	Head Solid State Physics Division
Berisso, M.C.	on leave at Univ. of Oxford, England.
Bes, D.	
Bonadeo, H.	
Burgos, E.	
Ceballos, A.	
Ceva, H.	
Dragún, O.	
Debray, M.	start oct/81, on leave at Univ.Georg-August, W.Ger.
Di Gregorio, D.	on leave at Oak Ridge National Laboratory
Dussel, G.G.	
Dussel, H. Lanza de	
Dukelsky, J.	
Etchegoyen, A.	on leave at Univ. of Oxford, England
Fernández Niello, J.	on leave at Sekt.Phys.Univ.Münich, W.Germany
Ferrero A.	
Filevich, A.	Head Experimental Nuclear Physics
Frigerio A.	
Gamba, Z.	
García Bermúdez, G.	
Gattone, A.	
Gil, S.	on leave at Univ. of Washington, Seattle, U.S.A.
Halac, B.	
Hernando, J.	
Huck, H.	
Kreiner, A.	
Labensky, F.	
Macchiavelli, A.	start oct/81 on leave at Law.Berkeley Lab.,U.S.A.
Manghi, E.	
Maqueda, E.	Head Theoretical Nuclear Physics Division
Mariscotti, M.	Chairman, Department of Physics
Massida, V.	
Moragues, J.	Head Solar Energy Group
Otero, D.	
Pacheco, A.	on leave at Law. Berkeley Lab., U.S.A.
Perazzo, P. K. de	
Perazzo, R.P.J.	
Pérez M.	
Pérez Ferreira, E.	Managing Director 20 UD Tandem Project
Pomar, C.	
Proto, A.	
Polla, G.	
Reich, S.	
Rossi, J.	
Saraceno, M.	

Saragovi-Badler, C.
Scheuer, W.
Schmirgeld de Wainer L.
Sofía, H.
Spina, M.E. — on leave at Univ. of Heidelberg, W.Germany
Toubes Spinelli, R.
Ventura, E.

Engineering Staff

Camín, D.
Fazzini, N.
Giménez, C.
González, H.
Martí, G.
Milberg, J.
Mónico, J.
Nicolai, J.
Requejo, R. — **Head of Engineering Division**
Ribarich, R.
Simoncelli, D.
Tau, S.
Tersigni, A.
Viero, J.

Research Staff associated to the Physics Department

Behar, M.
Cambiaggio, M.C.
Cohan, N.
Civitarese, O.
Davidson, M.
Davisdon, J.
Mehr, M.T.
Szybisz, L.
Waissmann, M.
Levi, I.
Llois, A.M.

Foreign Visiting Scientists

Acquadro, J.C.	Univ. of Sao Paulo, Brazil
Bayman, B.	Univ. of Minnesota, U.S.A.
Basset, A.	Univ. of Warwick, U.K.
Bennemann, K.	Free Univ. of Berlin, West Germany
Bjørnholm, S.	Niels Bohr Institute, Copenhagen, Denmark
Do Barros, S.	Fed. Univ. of Río de Janeiro, Brazil
Donangelo, R.	Fed. Univ. of Río de Janeiro, Brazil
Duek, E.	Univ. of N.Y. at Stony Brook, U.S.A.
Elder, M.	Scient. Research Council, Daresbury, U.K.
Eichler, J.P.	Univ. of Sao Paulo, Brazil.
Federman, P.	UNAM, Univ. Autónoma de México, Mexico.
Friedt, J.M.	Centre Recherches Nucléaires, Strasbourg, France
Galonsky, A.	Michigan State University, U.S.A.
Grempel, D.	Univ. of Maryland, U.S.A.
Liotta, R.J.	Research Instit. of Physics, Stockholm, Denmark
Macfarlane, M.	Univ. of Indiana, U.S.A.
Marcondes, H.	Univ. of Sao Paulo, Brazil
Massmann, H.	Univ. of Chile, Santiago, Chile
Mc Hyder, K.	Univ. of Oxford, U.K.
Pereira Malta, C.	Univ. of Sao Paulo, Brazil
Rao, N.	Univ. of Sao Paulo, Brazil
Stephens, F.	Lawrence Berkeley Lab., U.S.A.
Sieguel, E.	Univ. of Boston, U.S.A.
Szantos de Toledo, A.	Univ. of Sao Paulo, Brazil
Toledo Piza, A.	Univ. of Sao Paulo, Brazil
Toulouse, G.	Ecole Normale Superieure, Paris, France
Thieberger, P.	Brookhaven National Lab., U.S.A.

Research Students

Barragán, A.
Binda, A.
Bustos, C.
Camín, D.
De la Hera, P.
D'Elía, S.
Fendrik, A.
Mattalón, R.
Navarro, J.
Paganini, G.
Pakula, R.

Technical Staff

Antonuccio, F.
Bolaños, C.
Boretto, J.
Bergaglio, J.
Bustos, J.
Carmuega, M.T.
Cava, J.
Coralo, J.
Cordeyro, S.
D'Agostino, R.
Di Paolo, H.
Díaz Romero, A.
Garanzini, J.
Garay Ramos, E.
Grahmann, H.
Gutiérrez, M.
Ietri, B.
Kesque, J.
Laffranchi, J.
Lires, S.
Lolago, E.
Menéndez, E.
Miguez, C.
Montrasi, C.
Morales, A.
Orecchia, J.
Palacio, J.E.
Petragalli, I.
Prieto, J.
Professi, J.
Professi, M.
Ramírez, M.
Rendina, J.
Riso, J.M.
Rodríguez, E.
Rodríguez, J.C.
Rodríguez, L.
Rugilo, A.
Satinosky, M.
Schiavino, R.
Schevenels, L.
Vidallé, J.

Secretaries

Cáceres, A.
Ghiotti, B.

General Maintenance Staff

Barzola, G.
De Brasi, O.J.
Dieguez, R.
Gómez, D.
Piccini, G.
Soler, H.

PUBLICATIONS OF THE PHYSICS DEPARTMENT

Papers published or accepted during report period

Nuclear Physics

Level Structure of ^{82}Rb Studied trough the ^{81}Br(α,3n)Reaction
M.Behar, A..Filevich, G.García Bermúdez, M.A.J.Mariscotti and L.Szybisz
Nucl.Phys. A337(1980)253

Renormalization of Particle and Hole States in ^{208}Pb
R.P.J.Perazzo, S.L.Reich and H.M.Sofia
Nucl.Phys. A339(1980)23

Zero Order Crystallization in the Bethe-Fermi Homerwork and Electron Gas Problem
M.C.Cambiaggio, M.de Llano, A.Plastino, L.Szybisz and S.Ramires
Nucl.Phys. A339(1980)277

Constrained Hartree-Fock and Quasi-Spin Projection
M.C.Cambiaggio, A.Plastino and L.Szybisz
Nucl.Phys. A344(1980)233

Analysis of (^{6}Li,d) and (d,^{6}Li) Reactions in the Nickel and Tin Regions
A.Vitturi, L.Ferreira, P.D.Kunz, H.M.Sofía, P.F.Bortignon and R.A.Broglia
Nucl.Phys. A340(1980)183

Perturbative Treatment of Nuclear Rotations:Two Dimensional Case
D.R.Bes, G.G.Dussel and R.P.J.Perazzo
Nucl.Phys. A340(1980)157

Nuclear Field Theory Treatment of Complex Nuclear Spectra
R.A.Broglia, K.Matsuyanagi, H.M.Sofía and A.Vitturi
Nucl.Phys. A348(1980)237

Electric Field Gradients and Impurity Distributions in Doped-Noble Metals: A Systematic Study
I.J.R.Baumvol, M.Behar, J.A.H. da Jornada, R.P.Livi, K.W.Lodge. A.Lopez Garcia and F.C.Zawislak
Phys.Rev. B22(1980)5115

Detrapping of Vacancies at ^{111}In in Quenched Silver
C.Alonso Arias, M.Behar, A.Filevich, G.García Bermúdez, E.Savino, R.P. Livi and F.C.Zawislak
Phyc.Rev. B22(1980)

High Spin Band Structure of ^{192}Tl
A.J.Kreiner, A.Filevich, G.García Bermúdez, M.A.J.Mariscotti, C.Baktash, E. der Mateosian and P.Thieberger
Phys.Rev. C21(1980)933

Strength of a Multipole Residual Interaction
G.G.Dussel, R.P.J.Perazzo and S.L.Reich
Phys.Rev. C22(1980)292

The Self-Consistent Pseudopotentials in the Thermodynamic Limit
E.S.Hernandez, A.Plastino and L.Szybisz
Phys.Rev. C22(1980)299

Bands in Doubly Odd Tl Isotopes Including a Proton-Neutron Residual Interactions
A.J.Kreiner
Phys.Rev. C22(1980)2570

Evidence for a Predicted Change of Phase in the Level Staggering of Band in Doubly Odd Nuclei
A.J.Kreiner and M.A.J.Mariscotti
J.Phys. G:Nucl.Phys 6(1980)L13

High-Spin States in Br
G.García Bermúdez, D.Abriola, M.Behar, M.C.Berisso, J.Fernández Niello, A.Filevich and M.A.J.Mariscotti
J.Phys. G: Nucl.Phys. 6(1980)L89

Non-Axisymmetric Focusing Lenses for the Beam of a Mass-Separator
E.R.Duering, D.Otero and A.N.Proto
Nucl.Instr. and Meth. 169(1980)441

Multi-step Shell-Model Method: The Nuclei ^{204}Pb and ^{202}Pb
C.Pomar and R.J.Liotta
Phys.Lett. 92B(1980)229

Reformulation of the Mode-Coupling Method
R.J.Liotta and C.Pomar
Lett. Nuovo Cim. 27(1980)100

Investigation of Yrast States in Medium a Doubly Odd Nuclei
M.A.J.Mariscotti
Notas de Física, Mex. 4(1980)223

The RPA of Renormalized Fermions
G.G.Dussel, R.P.J.Perazzo and M.E.Spina
Nucl.Phys. A351(1981)12

Collective Excitations in ^{88}Y
M.Davidson, J.Davidson and M.A.J.Mariscotti
Nucl.Phys. A352(1981)237

Maximum Overlap, Atomic Coherent States and the Generator Coordinate Method
G.Bozzolo, M.C.Cambiaggio and A.Plastino
Nucl.Phys. A356(1981)48

Multi-Step Shell-model Treatment of Six-particle Systems
R.J.Liotta and C.Pomar
Nucl.Phys. A362(1981)137.

Nuclear Surface Waves in Alpha-particle and Ion-Ion Collisions
H.Uberall, A.Farhan, O.Dragún and E.Maqueda
Nucl.Phys. A362(1981)241.

High-spin States in ^{49}Ti and the Empirical $(f_{7/2})^n$ Model
M.Behar, G.García Bermúdez, A.Filevich, M.A.J.Mariscotti and E.Ventura
Nucl.Phys. A366(1981)61

Pickup Mechanism in (p,) Pre-Equilibrium Reactions
O.Dragún, A.Ferrero and A.Pacheco
Nucl.Phys. A369(1981)149

Perturbative Treatment of Nuclear Rotations:Three dimensional case
D.R.Bes, O.Civitarese and H.M.Sofía
Nucl.Phys. A370(1981)99.

Structure in ^{200}Tl and the Odd-even Staggering in $h_{9/2} \times i_{13/2}$ Bands
A.J.Kreiner, M.A.J.Mariscotti, C.Baktash. E.der Mateosian and P.Thieberger
Phys.Rev. C23(1981)748.

High Spin States in ^{74}Br
G.García Bermúdez, A.Filevich, A.J.Kreiner, M.A.J.Mariscotti, C.Baktash, E. der Mateosian and P.Thieberger
Phys.Rev. C23(1981)2024

Level Scheme of ^{140}Cs
D.Otero, A.N.Proto, E.Duering and M.L.Pérez
Phys.Rev. C23(1981)2691.

High-spin Structure of ^{75}Br and the (N,Z) Dependence of the Nuclear Deformation in the Br Region
A.J.Kreiner, M.A.J.Mariscotti, C.Baktash, E. der Mateosian and P.Thieberger
Phys. Rev. C24(1981)148.

The ^{131}Sn Decay
H.Huck, M.L.Pérez, J.J.Rossi and H.M.Sofía
Phys.Rev. C24(1981)

Crucial Influence of the Relativistic Form Factor Coefficients on the Determination of fs.
L.Szybisz and V.M.Silbergleit
J.Phys.G: Nucl.Phys. 7(1981) L201.

The Argentine 20 MV Tandem Accelerator Project
E.Pérez Ferreira, MA.J.Mariscotti, E.Ventura, A.Ceballos, N.Fazzini, A.Filevich, H.González, R.Requejo, R.Ribarich, J.J.Rossi, E.Achterberg, D.Camín, J.Nicolai and S.Tau
Nucl.Instr. and Meth. 184(1981)161.

Ion Source-Uranium Target Systems for the Buenos Aires ISOL Facility
H.Huck, J.Orecchia, M.L.Pérez, J.J.Rossi, A.Tersigni and J.Vidallé.
Nucl.Instr. and Meth. 189(1981)347.

Surprisal Approach in Cold Fission Process
D.Otero, A.Proto and A.Plastino
Phys.Lett. 98B(1981)225.

The Amplitude of s and d Boson in Deformed Nuclei
J.Dukelsky, G.G.Dussel and H.M.Sofía
Phys.Lett. B100(1981)367.

Pair Exchange Reactions
D.R.Bes, O.Dragún. E.E.Maqueda and R.J.Liotta
Phys. Lett. B 106B(1981)1.

Improved Limit on the Induced Scalar Interaction in Nuclear β-Decay
L.Szybisz and V.M.Silbergleit
Z.Physik A299(1981)91.

On the Decay of Compound Nuclei Following Alpha Particle and ^{12}C Induced Reactions
S.A.Hjorth, A.Johnson, A.Kerek, W.Klamra, Th. Lindblad, S.Messett, C.Pomar, W.Walus, O.Skeppstedt, Z.Sujkowski, A.Zglinski, L.Carlen, H.Ryde and H. Piiparinen
Z.Physik A301(1981)35.

Hartree-Fock Theory in Exactly Soluble Models with a Finite Number of Particles
M.C.Cambiaggio, A.Plastino, L.Szybisz and M. de Llano
Rev.Mex.Fis. 27(1981)223.

Geometry of the Time-Dependent Variational Principle in Quantum Mechanics
P.Kramer and M.Saraceno
Lecture Notes in Physics, vol 140 (Springer Verlag) , 1981.

Evidence for Predicted Level Crossings in $\pi h_{9/2} \times \nu i_{13/2}$ Bands in Very Neutron-Deficient Doubly Odd Tl Isotopes
A.J.Kreiner, C.Baktash, G.García Bermúdez and M.A.J.Mariscotti
Phys.Rev.Lett. (14 diciembre 1981).

Selective Population of High-j Orbitals in Er Nuclei by Heavy-Ion-Induced Transfer
P.D.Bond, J.Barrett, C.Baktash, C.E.Thotn and A.J.Kreiner
Phys.Rev. Lett. 46(1981)1565.

Técnicas de Fabricación de Detectores de Ge)Li) para Radiación Gamma
G.Martí and C.Gimenez
Energía Nuclear Nº 1(1981)47

Efecto de la Conductividad Sperficial en la Resolución y Eficiencia de Detectores Coaxiales de Germani-Litio
G.Martí and E.Caselli
Energía Nuclear Nº 3(1981)39.

The Nucleus as a Condensate of Monopole and Quadrupole Pairing Vibrations
R.A.Broglia, E.Maglione, H.M.Sofía and A.Vitturi
Nucl.Phys. A (in press).

The Ground State of Deformed Nuclei as a Boson Condensate
J.Dukelsky, G.G.Dussel and H.M.Sofía
Nucl.Phys. A (in press).

In Beam Studied of ^{78}Br
M.Behar, D.Abriola, A.Filevich, G.García Bermúdez, A.J.Kreiner and M.A.J.Mariscotti
Nucl.Phys. A (in press).

The ^{129}Sn and ^{129}Sb Beta Decays
H.Huck, M.L.Pérez and J.J.Rossi
Phys.Rev. C (in press).

Graphical Multi-Step Shell-Model Calculation of the Even Tin and Lead Ground States
C.Pomar and R.J.Liotta
Phys.Rev. C (in press).

Structure of ^{203}Pb in Terms of ^{207}Pb and ^{204}Pb
R.J.Liotta and C.Pomar
Phys.Lett. B (in press).

On the Possibility of Abnormal Occupation in ^{3}He and ^{4}He
M.C.Cambiaggio, M. de Llano, A.Plastino and L.Szybisz
Rev.Mex.Fis. (in press).

A Graphical Procedure to Evaluate the Many-Body Shell-Model Equations
R.J.Liotta and C.Pomar
Nucl.Phys. A (submitted to publication).

Comparison of Upper and Lower Bound Methods Using a Soluble Many Fermion Model
M.C.Cambiaggio. A.Klar, F.J.Margetan, A.Plastino and J.P.Vary
Phys.Rev. C (submitted to publication).

High Spin States in the Doubly Odd Nucleus ^{72}Br
G.García Bermúdez, C.Baktash, A.J.Kreiner and M.A.J.Mariscotti
Phys.Rev. C (submitted to publication).

Structure and Decay of the Highly mixed $13/2^{+}$ States in ^{171}Er
A.J.Kreiner, P.D.Bond, C.Baktash, J.Barrette, C.E.Thorn and M.T.Collins
Phys. Rev. C (submitted to publication)

Microscopic Description of Yrast States in Spherical Nuclei
R.J.Liotta and C.Pomar
Phys.Rev. C (submitted to publication).

Separable Interactions and Excited States in Open Shell Nuclei
J.Dukelsky, G.G.Dussel and H.M.Sofía
Phys.Lett. B (submitted to publication).

The Nilsson and the IBM Pictures of Deformed Nuclei
D.R.Bes, R.A.Broglia, E.Maglione and A.Vitturi
To be published.

SOLID STATE PHYSICS

On the Free Energy of Disordered Alloys and the Moments of Density of States
A.M.Llois and N.Cohan
J.Phys. C: Solid St.Phys. 13(1980)L1027.

Vibrational Spectra Packing Calculations and Crystal Structure of 1,2-diiodobenzene
C.Faerman and H.Bonadeo
Chem.Phys.Lett. 69(1980)91.

Intermolecular Potentials for Some Crystals of Heterocyclic Compounds Containing Nitrogen
Z.Gamba and H.Bonadeo
Chem.Phys.Lett 69(1980)525.

Decoration Patterns on Cleavage Surface of Ferroelectric Crystals
L.S. de Wainer, H.L. Dussel and M.A.R.Benyacar
Thin Solid Films 69(1980)351.

Mossbauer Spectra of Iron Containing Nafion Membranes
E.R.Bauminger, F.Labenski de Kanter, A.Levy, S.Ofer and C.Heitner-Wirguin
J. de Physique C1 41(1980)329.

Evidence for the Occurrence of a Universal Type of Iron Storage in Prokaryotic Cell: Bacteria and Mycoplasma
E.R.Bauminger, S.G.Cohen, F.Labenski de Kanter, A.Levy, S.Ofer, M.Kessel and S.Rotten
Bacteriology 141(1980)378.

The Planewise Summation Method for Triclinic Lattices
V.Massida and J.A.Hernando
Physica 101B(1980)159.

TEM Study of Domain Structure in Ferroelectric $BiVO_4$
L.S.Wainer, R.Baggio, M.A.R.Benyacar and H.L.Dussel
Electron Microscopy 1(1980)398.

Intermdiate-Valence Effects on the Phase Diagram of $NiS_{2-x}Se_x$
J.Mazzaferro, H.Ceva and B.Alascio
Phys. Rev. B22(1980)335.

Clustering of Ions in Cation Exchange Membranes: A Mössbauer Study
C.Heitner-Wirguin, E.R.Bauminger, F.Labenski de Kanter, A.Levy and S.Ofer
Polymer 21(1980)1327.

Study of Two Dimensional and Absorbed Microclusters by Molecular Dynamics
M.Waissmann and N.Cohan
"Oredering in Two Dimensions", ed. S.Sinha, North Holland (1980)327.

Aging of Accreted Ice
F.Prodi and L.Levi
J.Atoms.Sci. 37(1980)1375.

Crystal Structure of Droplets Frozen on an Ice Substrate after Low Speed Collision
L.Levi, O.B.Nasello and E.M. de Achaval
J.Crystal Growth 48(1980)121.

Hyperfine Bubble Structures in Ice Grown by Droplet Accretion
F.Prodi and L.Levi
J.Rech.Atmos. 14(1980)373.

Effects of the Growth Mode Upon the Crystal Orientation in Artificial and Natural Hailstones
L.Levi, F.Prodi and L.Lubart
J.Rech.Atmos. 14(1980)333.

A Study of the Initial Stage of the Accretion Process
O.B.Nasello, L.Levi, E.M.de Achaval and E.A.Ceppi
J.Rech.Atmos. 14(1980)

PLATTSUM: A Fortran Program that Evaluates Electrostatic Lattice Sums by the Planewise Summation Method
J.A.Hernando and V.Massidda
Computer Phys.Comm. 22(1981)13.

Study of Domains and Domain Walls in Ferroelastic $BiVO_4$
L.S. Wainer, R.F.Baggio, H.L.Dussel and M.A.R.Benyacar
Ferroelectrics 31(1981)121.

Pseudo-Spin Formalism and the Transition Temperature of Potassium Ferrocyanide Trihydrate
V.Massida and E.Anda
Ferroelectrics 34(1981)187.

Vibrational Spectra and Phase Transitions of Crystalline Bromoform
E.Burgos, E.Halac and H.Bonadeo
J.Chem.Phys. 74(1981)1546.

Electrical Multipoles and Multipole Interactions: Compact Expressions and a Diagrammatic Method
E.Burgos and H.Bonadeo
Mol.Phys. 44(1981)1.

X-Ray Characterization of Gel Grown $CaHPO_4.2H_2O$ and $PbHPO_4$ Crystals
F.Lefaucheux, M.C.Robert, E.Manghi and H.Arend
J.Crystal Growth 51(1981)551.

Observation of Ferroelectrics Domains in Gel Grown $PbHPO_4$ Crystals
R.Le Bihan, M.Maussion, F.Lefaucheux, E.Manghi and M.C.Robert
Phys.Stat.Sol(a) 64(1981)K5.

Lattice Dynamical Calculations of Mean Square Amplitude of Crystalline Biphenyl
H.Bonadeo and E.Burgos
ActaCryst. A(in press).

Lattice Dynamical Calculations on Azobenzene Crystals: The Distributed Dipole Model
Z.Gamba and H.Bonadeo
J.Chem.Phys. (in press).

SOLAR ENERGY GROUP

Concentrador Fijo a Espejo Facetado de la CNEA: Consideraciones Teóricas para el Diseño de un Prototipo Industrial
R.O.Nicolás and J.C.Durán
Actas de la 6a Reunión de Trabajo de la Asociación Argentina de Energía Solar (ASADES), Catamarca(1980).

Análisis Optico Bidimensional de Concentradores Cilíndricos no Perfectos
J.C.Durán and R.O.Nicolás
Actas de la 6a Reunión de la Asociación Argentina de Energía Solar (ASADES), Catamarca (1980).

Conversión de Energía Solar en Electricidad. Estado Actual de su Desarrollo
J.A.Moragues
Actas del Seminario sobre Conservación de la Energía Eléctrica (1980).

Generalization of the Two-Dimensional Optical Analysis of Cylindrical Concentrators
R.O.Nicolás and J.C.Durán
Solar Energy, 25(1980)21.

Aprovechamiento de la Energía Solar en la Argentina
J.A.Moragues
Actas de las Jornadas Nacionales de Energía, Santa Fe (1980)

Aspectos no Usuales de la Implementación en la Argentina de un Sistema Solar de Caletamiento de Agua
R.O.Nicolás, A.Rapallini and W.Scheuer
Actas de la 7a Reunión de Trabajo de la Asociación Argentina de Energía Solar (ASADES) Rosario, (1981) (in press)

Concentrador Fijo a Espejo Facetado de la CNEA. Estado de Avance y Desarrollo de un Prototipo Industrial
J.C.Durán, E.Mezzabolta, J.A.Moragues, R.O.Nicolás, W.Scheuer and C. Franciulli
Actas de la 7a Reunión de Trabajo de la Asociación Argentina de Energía Solar (ASADES) Rosario, (1981) (in press).

Papers Presented at Meetings and Conferences

A.P.S. Meetings, Washington, DC, U.S.A., April 21-24, 1980

A Nuclear Surface Wave Interpretation of Quasimolecular Orbiting in Heavy-Ion Collisions
A.Farhan, H.Uberall, O.Dragún and E.E.Maqueda

International Conference on Nuclear Behaviour at High Angular Momentum, Strasburg, France, April 22-24 1980

Multi-Step Shell Model Method
C.Pomar and R.J.Liotta.

International Conference on Ordering in Two Dimensions, Lake Geneve, Wisconsin, USA, May 28-30, 1980

Study of Two Dimensional and Adsorbed Microclusters by Molecular Dynamics
M.Weissmann and N.V.Cohan

VIII International Cloud Physics Conference, Clemont-Ferrand, France June 15-19, 1980

Hyperfine Bubble Structure of Ice Grown by Droplet Accretion
F.Prodi and L.Levi

Effects of the Grown Conditions upon the Crystal Orientation in Artificial and Natural Hailstones
L.Levi, F.Prodi and L.Lubart

A Study of the Initial Stage of the Accretion Process
O.B.Nasello, L.Levi, E.M. de Achaval and E.A.Ceppi

V International Conference on Hyperfine Interactions, Berlin, W-Germany July, 1980

PAC Study of the Interaction Between In-Rh and In-Pt in a Cu Matriz
I.J.R.Baumvol, M.Behar, J.A.H. da Jornada. R.P.Livi. K.W.Lodge and F.C. Zawislak

Electric Field Gradients Created by Impurities in the Noble Metals
I.J.R.Baumvol. M.Behar, J.A.H. da Jornada, R.P.Livi. K.W.Lodge, A. López García and F.C.Zawislak

Fourth Latin American Workshop on Self Consistent Theories of Nuclear Matter, Caracas, Venezuela July 7-18, 1980

Constrained Hartree-Fock and Quasi-Spin Projection
L.Szybisz

A New Approach to the Maximum Overlap Method
M.C.Cambiaggio

VII European Congress of Electron Microcopy, La Haya, Holland, August 1980

TEM Study of Ferroelastic BiVO4
L.S. Wainer, R.F.Baggio, M.A.R.Benyacar and H.L.Dussel

International Conference on Nuclear Physics, Berkeley, California USA, August 24-30, 1980

$\pi g_{9/2} \times \nu g_{9/2}$ Structure in ^{78}Br.
M.Behar, D.Abriola, A.Filevich, G.García Bermúdez, A.J.Kreiner and M.A.J.Mariscotti
LBL-11118 pag. 167.

Pick-up Mechanism in (p,α) Pre-Equilibrium Reactions Application to ^{93}Nb and ^{118}Sn, Ep=44,3 and 34,6 MeV
O.Dragún, A.M.Ferrero and A.Pacheco
LBL-11118 pag. 289.

Deformed Nuclei as a Boson Condensate
J.Dukelsky, G.G.Dussel and H.M.Sofía
LBL-11118, pag 356.

Have Alpha Transfer Anything to Do with the Pairing Force?
J.A.Evans, G.G.Dussel, E.E.Maqueda and R.P.J.Perazzo
LBL-11118, pag. 63.

Structure in ^{200}Tl and the Odd-Even Staggering in $\pi h_{9/2} \times \nu i_{13/2}$ Bands
A.J.Kreiner, M.A.J.Mariscotti, C.Baktash, E. der Mateosian and P.Thieberger
LBL-11118, pag. 783.

Multi-step Shell Model Method
R.J.Liotta and C.Pomar
LBL-11118, pag. 45.

Nuclear Rayleigh and Whispering-Gallery Waves Excitated in Heavy Ion Collisions
A.R.Farhan, H.Uberall, O.Dragún and E.E.Maqueda
LBL-11118, pag. 507.

3a. Reunion de la Sociedade Brasileira de Fisica, Cambuquira, Brasil, Agosto 31 - Sept. 4, 1980

Relato sobre el Tandem de CNEA
A.Ferrero and E.E.Maqueda

H.M.Sofía

Workshop in Nuclear Physics, Philadelphia, Pennsylvania, USA, September 1-3, 1980

A Quantum Mechanical Treatment of a Rotating Many-Body System
D.R.Bes

6th International Conference on Crystal Growth, September 1980

Growth Defect in Some Water Soluble Crystals Obtained by a New Gel Technique
F.Lefaucheux, M.C.Robert and E.Manghi

X Reunión de la Asociación de Tecnología Nuclear, Bariloche, Rio Negro, Argentina, November 1-5, 1980

Diseño, Construcción y Calibración de un Polarímetro para Radiación Gamma
A.O.Macchiavelli, G.Martí, C.Gimenez, J.Laffranchi and M.Behar

Annual Meeting of the Materials Research Society, Boston, Mass., USA, November 16-21, 1980

Isothermal Recovery of a Quenched Ag Foil
M.Behar, C.Alonso Arias, G.García Bermúdez, A.Filevich, E.Savino, R.P.Livi and F.C.Zawislak

Coloquio Latinoamericano de Física de Superficies, Universidad Federal Fluminense, Niteroi, Brasil, November 1-6, 1980

Adsorción Física y Dínamica Molecular
N.Cohan

Reunión Nacional de Física 1980, Bariloche, Rio Negro, Argentina, December 9-12, 1980

Estudio de Dominios y Paredes de Dominios en el Ferroelástico $BiVO_4$
L.S. Wainer, R.Baggio, H.L.Dussel and M.A.R. Benyacar

Orientaciones Permitidas de Dominios en Materiales Ferroelásticos
H.L.Dussel, L.S.Wainer, R.Baggio. M.A.R. Benyacar

Interacciones Electrostáticas en Cristales Moleculares Heterociclicos
Z.Gamba and H.Bonadeo

Estudio Mossbauer de Membranas de Intercambio Cationico
R.A.Bauminger, F.L. de Kanter, S.Ofer and C.Heitner-Wirguin

Estudio del ^{100}Rh a Través de la Reacción $^{99}Ru(\alpha,2np)$
A.O.Macchiavelli, M.Behar, A.Filevich, G.García Bermúdez and M.A.J. Mariscotti

Esquema de Niveles del ^{94}Tc
M.Behar, A.Ferrero, A.Filevich, G.García Bermúdez and M.A.J.Mariscotti

Estados de Alto Spin en ^{49}Ti
M.Behar, A.Filevich, G.García Bermúdez, M.A.J.Mariscotti and E.Ventura

Coeficiente de Asimetría α_β Correspondiente a la Distribución Angular de Rayos-β Emitidos por ^{12}B y ^{12}N Alineados
L.Szybisz and H.Behrens

Análisis de la Transición 2^- (0.692 MeV β^-)2^+ del ^{86}Rb
O.Rosso and L.Szybisz

Análisis de las Ocho Transiciones Beta Superpermitidas Mejor Determinadas Experimentalmente
V.A.Silbergleit and L.Szybisz

Tratamiento Perturbativo de las Rotaciones Nucleares. Descripción de Sistemas en Tres Dimensiones
D.R.Bes, H.M.Sofía and O. Civitarese

Modelo de Capas por Etapas Sucesivas Aplicado a Sistemas de Seis Particulas
R.Liotta and C.Pomar

Interpretación de Movimientos Orbitales en Sistemas Cuasi-Moleculares como Ondas de Superficies Nucleares
O.Dragún, A.R.Farhan, E.E.Maqueda and H.Uberall

Estructura de dos Cuasipartículas en Estados Colectivos de Núcleos Esféricos
J.Dukelsky, G.G.Dussel and H.M.Sofía

Amplitudes de Bosones s y d en Nucleos Deformados
J.Dukelsky, G.G.Dussel and H.M.Sofía

Distribución Angular de Particulas en Reacciones de Fusion Inducida por Iones Pesados
O.Civitarese

Contribucion de Procesos en una Etapa a Reacciones (p,d) en la Región de Pre equilibrio
O.Dragún, A.M.Ferrero and A.O.Gattone

Un Nuevo Método de Máxima Superposición
G.Bozzolo, M.C.Cambiaggio and A.Plastino

Sobre la Posibilidad de Ocupación Anormal en ^3He y ^4He
M.C.Cambiaggio, A.Plastino. L.Szybisz and M. de Llano

Método de Hartree-Fock con Vinculos y la Proyección de Cuasi-Spin
M.C.Cambiaggio, A.Plastino and L.Szybisz

Estudio de Mossbauer de Aceros de Baja Aleación
F.Labenski de Kanter, I.A.Maier and C.Saragovi-Badler

Multipolos Eléctricos e Interacciones Multipolares:Expresiones Compactas y Método Diagramatico
E.Burgos and H.Bonadeo

Sensibilidad del Ensanchamiento Doppler en Aniquilación de Positrones
M.D.Ayciriex, D.Otero, A.N.Proto, M.Pavioni, E.Romero and A.Somoza

Transiciones Orden-Desorden en Cristales Iónicos que Contienen Multipolos Reorientables. I. El Caso T=0°K
J.Hernando and V.Massidda

Transiciones Orden-Desroden en Cristales Iónicos que Contienen Multipolos Reorientables. II. El Caso T≠ 0°K
J.Hernando and V.Massidda

Microdensitometro Digital de Alta Velocidad
P.K. de Perazzo

Medición de Electrones de Conversión Interna en Isótopos Doblemente Impares del Tl
M.E.Debray, A.J.Kreiner, C.Pomar and J.M.Riso

Esquema de Niveles del ^{131}Sb
H.Huck, R.Pakula, M.Pérez and J.J.Rossi

Condición de Máxima Entropía en Procesos de Fisión Fria
D.Otero, A.Plastino and A.N.Proto

Renormalización de Masas Efectivas por Acoplamiento Dinámico con Vibraciones Multipolares
O.Civitarese, R.P.J.Perazzo and S.L.Reich

Diseño y Construcción de una Celda Criostática Raman Rayos-X
E.Halac and N.Gutierrez

V Pan-American Worhshop on Condensed Matter Theories. UNAM, Mexico, January 1981

Information Theory Approach in Cold Fission Process
D.Otero, A.Plastino and A.N.Proto

On the Possibility of Abnormal Occupation in ^{3}He and ^{4}He
M.C.Cambiaggio, A.Plastino, L.Szybisz and M. de Llano

APS Meeting, Baltimore, Maryland, USA, April 20-23, 1981

Nuclear Surface Waves in Alpha-Particle and Ion-Ion Collisions
A.R.Farhan, H.Uberall, O.Dragún and E.E.Maqueda

Fermi Level Induced Crossings within the $\pi h_{9/2} \times \nu i_{13/2}$ Structure in Doubly Odd Tl Nuclei
A.J.Kreiner, C.Baktash, E. der Mateosian, G.García Bermúdez, M.A.J. Mariscotti and P.Thieberger

IX International Conference on High Energy Physics and Nuclear Structure Versalles, France,July 6-10, 1981

Nuclear Surface Waves in Alpha-Particle and Ion-Ion Collisions
A.R.Farhan, H.Uberall, O.Dragún and E.E.Maqueda

V International Meeting on Ferroelectricity, Pennsylvania State University, USA, August, 1981

Synthetic Troegerite Phase II: Ferroelastic Character and Possible Point Groups
H.L.Dussel, L.S. Wainer, M.A.R.Benyacar and C.Sa

4a Reunión de la Sociedade Brasileira de Física, Cambuquira, Brasil, September 1981

Potencial Químico en Procesos de Fisión
D.Napoli, D.Otero, A.Plastino and A.N.Proto

Congreso de la Societa Italiana di Fisica, Pisa, Italy, October 1981

An Equation-of-Motion Treatment of Neutron-Proton Pairing Correlations
F.Andreozzi, A.Covello, A.Gargagno, E.E.Maqueda and R.P.J.Perazzo

Workshop in Nuclear Theory, International Centre for Theoretical Physics, Trieste, Italy, October 5-31, 1981

The Perturbative Treatment of Fermion System in Deformed Bases
D.R.Bes

Concluding Remarks on the Session About Models for Low Energy Spectrum
D.R.Bes

Pair Exchange Reactions
D.R.Bes, O.Dragún, E.E.Maqueda and R.J.Liotta

APS Meeting, Nuclear Physics Division, Asilomar,California, USA, October 28-30, 1981

High Energy γ-Ray Decay Evaporation Residues from (HI,xn) Reactions
J.Barrette, M.T.Collins, A.J.Kreiner, A.M.Sandorfi, M. Al-Kofahi and S.Steadman

Reunión Nacional de Física 1981, San Luis, Argentina, November 24-27,1981

Sistema de Control para el Acelerador Tandem 20UD Utilizando Micro-Computadora
C.Hinton, M.Mayers, C.Pauly, R.Rathmell and S.Tau

Distribución de Intensidades en el Plano Receptor de Concentradores Solares de Foco lineal
J.C.Durán and R.O.Nicolás

Teorema de Ehrenfest y Principio de Máxima Entropía
D.Otero, A.Plastino and A.N.Proto

Estado Actual del Montaje del Acelerador de Iones Pesados
N.Fazzini and H.Gonzalez

Sistema de Purificación y Trasvase de SF_6 para el Acelerador de Iones Pesados
N.Fazzini, H.Gonzalez, J.Nicolai, R.Requejo and S.Tau

Investigaciones en Tunel de Viento sobre la Congelación de Gotas que Impactan sobre un Sustrato de Hielo
O.B.Nassello and L.Levi

Crecimiento de Grano en Hielo
F.A.Ceppi and L.Levi

Comparación entre las Técnicas de Crecimiento Cristalino: Crecimiento en Gel y en Solución. Aplicación al Caso de A.D.P. y K.D.P.
E.Manghi, F.Lefaucheux and M.C.Robert

Indices Críticos: Efecto del Tamaño de la Red y de la Símetria de la Transformación de Renormalización
S. D'Elía and H.Ceva

Valencia Intermedia en una Impureza: Influencia del Potencial de la Celda
L.M.Falicov and H.Ceva

Transferencia de Cargas en Sistemas Desordenados
M.Waissmann and N.Cohan

Mezcla de Configuraciones en Modelos Solubles
M.C.Cambiaggio, A.Plastino and L.Szybisz

Interacciones Separables y Estados Excitados en Nucleos con Capas Abiertas
J.Dukelsky, G.G.Dussel and H.M.Sofía

Descripción Microscópica de Estados Yrast en Núcleos Esféricos
R.J.Liotta and C.Pomar

Esquema de Niveles del ^{79}Kr
M.Behar, A.Filevich, A.O.Macchiavelli and L.Szybisz

Contribución de Procesos en Dos Etapas en Reacciones de Preequilibrio
O.Dragún, A.M.Ferrero and O.A.Gattone

Estudio del Decaimiento Gama de Residuos de Evaporación a Altas Energias de Excitación
J.Barrette, M.Collins, A.J.Kreiner, A.Sandorfi, M.Al-Kofahi and S.Steadman

Reacciones de Intercambio de Pares
D.R.Bes, O.Dragún, R.J.Liotta and E.E.Maqueda

Comparación de Límites Inferiores y Superiores de la Energía del Estado Fundamental
M.C.Cambiaggio and A.Plastino

Equilibrio Termodinámico de Sistemas Nucleares
D.R.Napoli, D.Otero, A.Plastino and A.N.Proto

Dinámica de Redes en Cristales de Azatencenos: El Modelo de Dipolos Distribuidos
Z.Gamba and H.Bonadeo.

Teoría de la Información y Procesos Dinámicos Simples
V. La Mota, D.Otero, A.Plastino and A.N.Proto

Perfil Compton Estudiado con Simetría Axial
D.Otero, A.N.Proto, M.D.Aycíriex, R.Romero and A.H.Somoza

Decaimiento Beta de ^{129}Sn y ^{129}Sb
H.Huck, M.L.Perez and J.J.Rossi

Estudio por Difracción de Rayos X del Formiato de Cobre y Estroncio
P.K. de Perazzo and M.A.R. Benyacar

Fase Ferroelástica del Arseniato de Uranilo e Hidrogeno no Hidratado (HUAsH)
H.L.Dussel, L.S. de Wainer, M.A.R.Benyacar

Transiciones de Fase en $8PbO.V_2O_5$
R.Baggio, L.S. de Wainer, H.L. Dussel, M.A.R.de Benyacar

Internal Reports

CNEA-NT-19/80 Jornadas de Trabajo sobre "Aprovechamiento directo de la Energía Solar", Buenos Aires, octubre 1979.

CNEA-NT-20/80 W.Scheuer, Aprovechamiento de la Energía Solar.

CNEA-NT-22/80 J.A.Moragues, Conversión fototérmica de energía solar en electricidad.

CNEA-NT-27/80 III Nuclear Physics Workshop, Buenos Aires 7-8 April 1980.

CNEA-NT-2/81 A. Díaz Romero, Manual for the use of ASSEMBLER functions and routines form the "Harwell Subroutine Library" called by FORTRAN programs in IBM/370 Operating System.

Ph.D. Thesis

- Hugo A. Huck
"Estructura nuclear de núcleos cercanos al doblemente mágico ^{132}Sn",1981
Instituto Balseiro, Universidad de Cuyo, Bariloche, Río Negro, Argentina.

Licenciatura Theses

- Ana María Llois
"Estudio teórico de la energía libre de aleaciones desordenadas", 1981
Facultad de Ciencias Exactas y Naturales, Universidad de Buenos Aires, Argentina.

- Clotilde Sá
"Estudio por microscopía electrónica de la superficie de clivaje de la troegerita sintética ($H_2(UO_2)_2(AsO_4)_2.8H_2O$) en su fase I y fase II",1980
Facultad de Ciencias Exactas y Naturales, Universidad de Buenos Aires, Argentina.

- Mario Debray
"Implementación de una facilidad experimental para la espectroscopía en línea de electrones de conversión interna", 1980.
Facultad de Ciencias Exactas y Naturales, Universidad de Buenos Aires, Argentina.

- Augusto O. Macchiavelli
"Estados de alto spin del ^{100}Rh poblados por la reacción Ku((45MeV),2np), 1981.
Instituto Balseiro, Universidad de Cuyo, Río Negro, Argentina.

- Alberto H. Somoza
"Estudio de la estructura electrónica por perfil Compton", 1981.
Facultad de Ciencias Exactas, Universidad Nacional del Centro de la Provincia de Buenos Aires, Tandil, Argentina.

- Ricardo Romero
"Procesamiento de datos en perfil Compton", 1981
Facultad de Ciencias Exactas, Universidad Nacional del Centro de la Provincia de Buenos Aires, Tandil, Argentina.

- Daniel Nápoli
"Formalismo P.M.E. en procesos de fisión", 1981.
Facultad de Ciencias Exactas y Naturales, Universidad de Buenos Aires, Argentina.